CAPACI OCCASIO
FOUNDED 1894

SAIMM

JOURNAL OF THE SOUTHERN AFRICAN INSTITUTE OF MINING AND METALLURGY

VOLUME 118 NO. 10 OCTOBER 2018

United. Inspired.

We know your industry. Let us help you.
We were formed to be a stronger partner for you in mining, infrastructure and natural resources. By building on proven expertise, you can count on us to deliver the performance you need today and the technology to lead tomorrow.
Call us on **+27(0)11 821 9000**

Epiroc

epiroc.com/en-za

Advertorial

Epiroc showcases its Smart and Flexible automated drilling technology at Electra Mining 2018

Stand B26, Outdoor area 1

"Epiroc has always prided itself on taking the needs of the customers into account," says Hedley Birnie, Regional Business Line Manager of Epiroc's Surface and Exploration Drilling, the division that brings the legendary SmartROC and FlexiROC rigs to the drilling industry. "In listening to and understanding our customers' requirements, we have applied our many decades of experience to implement advanced digitalisation and automation technology in our products, adding tremendous value for the customers and differentiating Epiroc as a reliable productivity partner."

Equipped with leading-edge smart technology and featuring full drill cycle automation, Epiroc's SmartROC Down-The-Hole and Top Hammer drill rigs optimise the drilling and blasting experience from end-to-end, completely transforming the drilling procedure. Better planning, predictability, semi-autonomous drilling with improved drilling cycle accuracy, increased efficiencies, consistent operation and quality, extended machine availability and lifecycle, improved operational and maintenance costs, and reduced carbon footprint lead to sustainable productivity and profitability in mines, quarries and plants. "Most importantly, automation technology enables us to remove personnel from the work face, taking them out of harm's way, enhancing worker safety and performance," notes Birnie.

"We believe that the success of automation technology lies in a holistic approach and we therefore apply it across equipment, systems, operations and services," explains Birnie. "Everything starts with the planning and drilling of the holes. If done correctly, it will lower the total cost of the entire operation and Epiroc has the complete solution in the form of digitalisation and automation which perfectly complement each other."

Digitalisation in the form of ROC Manager and Surface Manager enables the creation of drill plans, drill patterns, hole angles and depths which are sent directly to the drill rigs from the planning office with GPS coordinates via a Wi-Fi network (or data stick for mines and plants that do not have a WiFi mesh or network over the pit).

Here, automation in the form of the Hole Navigation System (HNS) takes over and drilling can be performed according to the exact coordinates included in the drill plan providing accuracy on the X, Y and Z axes. HNS delivers a faster set-up, improves precision and reduces non-drilling time, fragmentation and explosive quantities. In addition, fewer people are required in the working area because there is no need for the manual marking of holes nor for the manual measuring of the drilled holes since this data can be retrieved from the Drill Quality Log File. HNS also minimises the risk of drilling in undetonated explosive material since the drill pattern coordinates are saved.

Using Rig Remote Access (RRA), the rig drills holes semi-autonomously and 'knows' to drill in the right place at the right depth, at the right angle and at the desired hole depth every time while drill tubes are added and extracted automatically. Using an option called single hole automation, also referred to as 'one touch', the rig can be set up in such a way that when all of the drilling plan parameters have been installed and the hole positions and depth are entered, the operator can select a hole on the plan. Then, with the press of one button, the operator can leave the drill rig to drill the hole in the correct place and to the correct depth after which rig will, on its own, extract all the rods back to the carousel and notify the operator that he may now select the next hole closest to his current position. This automation also allows for automatic overburden drilling.

During drilling, Measure While Drilling is performed and this data is logged and sent back to ROC Manager/Surface Manager for further analysis. MWD enables the rig to determine changes in the ground formation based on performance and penetration rate. Using Surface Manager, a 3-D model can be formulated showing the ground formation detailing the position of the ore layout within the inter-burden over-burden and waste partings.

The Rig Control System (RCS) on the SmartROC is a built-in auto-rod handling control system that helps to extend rig lifespan and subsequently improve uptime and availability by limiting extreme usage to safeguard the rig against operator abuse, and reducing wear on the rig as well as on consumables. A state of the art fuel saving device controlled by the RCS, can reduce the SmartROC's fuel consumption by between 15 and 25%, depending on ground conditions and the commodity being drilled.

BenchREMOTE, an additional option from Epiroc, is ideal for drilling in hazardous areas and near the high wall. The BenchREMOTE can be placed in an air-conditioned, vibration-, dust- and noise-free environment up to 100m away within the line of site of the drill rig from where the operator can safely and conveniently monitor progress. Furthermore, up to three SmartROC drill rigs can be operated from one BenchREMOTE base station. Information on up to ten drill rigs can be stored in the BenchREMOTE's memory so that if and when needed, the BenchREMOTE can be moved from one block or area to another and control the rigs in that area.

All the latest drill rigs from the Epiroc factory are now also fitted with CERTIQ, a web-based management control system that allows remote access to critical drill rig information in real time. In addition to critical warnings, the system also reports on fuel burn, idle time, tramming time, drilling or production time as well as standing time.

Epiroc's tried and trusted rig ranges such as the Power and FlexiROC offer a solution for those contractors and customers who do not have the need or the desire to have drill rigs with higher technology levels. The FlexiROC is available with CERTIQ, ROC Manager and Assisted Trouble Shooting.

Epiroc designs, maintains and supports all hardware and software and offers theoretical and practical aftermarket technical and operator training. The SmartROC and FlexiROC rigs are backed by extensive aftermarket support both locally as well as in Botswana, Mozambique, Namibia and Zimbabwe.

According to Birnie, some technology can be retrofitted to the SmartROC and FlexiROC. He points out that while automation technology is still fairly new to Southern Africa, mines and quarries are recognising that automation technology is crucial to a sustainable and profitable future. "We are seeing a noticeable increase in interest in our rigs and their automation features. We are investing heavily in R&D and constantly updating automation technology on our equipment to further our endeavour in ensuring the highest and most efficient rig performance possible while creating an ever safer and more productive operation and working environment."

For further information please contact: Kathryn Coetzer
Regional Communications Manager, T: +27 (0) 821 900, kathryn.coetzer@epiroc.com

Issued by Laverick Media Communications
Tel: +27 (0)11 0400 818 sonia@laverickmedia.co.za, www.laverickmedia.co.za

OFFICE BEARERS AND COUNCIL FOR THE 2018/2019 SESSION

Honorary President
Mxolisi Mgojo
President, Minerals Council South Africa

Honorary Vice Presidents
Gwede Mantashe
Minister of Mineral Resources, South Africa

Rob Davies
Minister of Trade and Industry, South Africa

Mmamoloko Kubayi-Ngubane
Minister of Science and Technology, South Africa

President
A.S. Macfarlane

President Elect
M.I. Mthenjane

Senior Vice President
Z. Botha

Junior Vice President
V.G. Duke

Incoming Junior Vice President
I.J. Geldenhuys

Immediate Past President
S. Ndlovu

Co-opted Member
R.T. Jones

Honorary Treasurer
V.G. Duke

Ordinary Members on Council

I.J. Geldenhuys
C.C. Holtzhausen
W.C. Joughin
G.R. Lane
E. Matinde
H. Musiyarira
G. Njowa
S.M Rupprecht
N. Singh
A.G. Smith
M.H. Solomon
D. Tudor
A.T. van Zyl
E.J. Walls

Past Presidents Serving on Council

N.A. Barcza
R.D. Beck
J.R. Dixon
M. Dworzanowski
H.E. James
R.T. Jones
G.V.R. Landman
C. Musingwini
J.L. Porter
S.J. Ramokgopa
M.H. Rogers
D.A.J. Ross-Watt
G.L. Smith
W.H. van Niekerk
R.P.H. Willis

G.R. Lane–TPC Mining Chairperson
Z. Botha–TPC Metallurgy Chairperson

K.M. Letsoalo–YPC Chairperson
G. Dabula–YPC Vice Chairperson

Branch Chairpersons

Botswana	Vacant
DRC	S. Maleba
Johannesburg	J.A. Luckmann
Namibia	N.M. Namate
Northern Cape	F.C. Nieuwenhuys
Pretoria	R.J. Mostert
Western Cape	L.S. Bbosa
Zambia	D. Muma
Zimbabwe	C. Sadomba
Zululand	C.W. Mienie

PAST PRESIDENTS

*Deceased

* W. Bettel (1894–1895)
* A.F. Crosse (1895–1896)
* W.R. Feldtmann (1896–1897)
* C. Butters (1897–1898)
* J. Loevy (1898–1899)
* J.R. Williams (1899–1903)
* S.H. Pearce (1903–1904)
* W.A. Caldecott (1904–1905)
* W. Cullen (1905–1906)
* E.H. Johnson (1906–1907)
* J. Yates (1907–1908)
* R.G. Bevington (1908–1909)
* A. McA. Johnston (1909–1910)
* J. Moir (1910–1911)
* C.B. Saner (1911–1912)
* W.R. Dowling (1912–1913)
* A. Richardson (1913–1914)
* G.H. Stanley (1914–1915)
* J.E. Thomas (1915–1916)
* J.A. Wilkinson (1916–1917)
* G. Hildick-Smith (1917–1918)
* H.S. Meyer (1918–1919)
* J. Gray (1919–1920)
* J. Chilton (1920–1921)
* F. Wartenweiler (1921–1922)
* G.A. Watermeyer (1922–1923)
* F.W. Watson (1923–1924)
* C.J. Gray (1924–1925)
* H.A. White (1925–1926)
* H.R. Adam (1926–1927)
* Sir Robert Kotze (1927–1928)
* J.A. Woodburn (1928–1929)
* H. Pirow (1929–1930)
* J. Henderson (1930–1931)
* A. King (1931–1932)
* V. Nimmo-Dewar (1932–1933)
* P.N. Lategan (1933–1934)
* E.C. Ranson (1934–1935)
* R.A. Flugge-De-Smidt (1935–1936)
* T.K. Prentice (1936–1937)
* R.S.G. Stokes (1937–1938)
* P.E. Hall (1938–1939)
* E.H.A. Joseph (1939–1940)
* J.H. Dobson (1940–1941)
* Theo Meyer (1941–1942)
* John V. Muller (1942–1943)
* C. Biccard Jeppe (1943–1944)
* P.J. Louis Bok (1944–1945)
* J.T. McIntyre (1945–1946)
* M. Falcon (1946–1947)
* A. Clemens (1947–1948)
* F.G. Hill (1948–1949)
* O.A.E. Jackson (1949–1950)
* W.E. Gooday (1950–1951)
* C.J. Irving (1951–1952)
* D.D. Stitt (1952–1953)
* M.C.G. Meyer (1953–1954)
* L.A. Bushell (1954–1955)
* H. Britten (1955–1956)
* Wm. Bleloch (1956–1957)
* H. Simon (1957–1958)
* M. Barcza (1958–1959)
* R.J. Adamson (1959–1960)
* W.S. Findlay (1960–1961)
* D.G. Maxwell (1961–1962)
* J. de V. Lambrechts (1962–1963)
* J.F. Reid (1963–1964)
* D.M. Jamieson (1964–1965)
* H.E. Cross (1965–1966)
* D. Gordon Jones (1966–1967)
* P. Lambooy (1967–1968)
* R.C.J. Goode (1968–1969)
* J.K.E. Douglas (1969–1970)
* V.C. Robinson (1970–1971)
* D.D. Howat (1971–1972)
* J.P. Hugo (1972–1973)
* P.W.J. van Rensburg (1973–1974)
* R.P. Plewman (1974–1975)
* R.E. Robinson (1975–1976)
* M.D.G. Salamon (1976–1977)
* P.A. Von Wielligh (1977–1978)
* M.G. Atmore (1978–1979)
* D.A. Viljoen (1979–1980)
* P.R. Jochens (1980–1981)

G.Y. Nisbet (1981–1982)
A.N. Brown (1982–1983)

* R.P. King (1983–1984)

J.D. Austin (1984–1985)
H.E. James (1985–1986)
H. Wagner (1986–1987)

* B.C. Alberts (1987–1988)

C.E. Fivaz (1988–1989)

* O.K.H. Steffen (1989–1990)
* H.G. Mosenthal (1990–1991)

R.D. Beck (1991–1992)

* J.P. Hoffman (1992–1993)
* H. Scott-Russell (1993–1994)

J.A. Cruise (1994–1995)
D.A.J. Ross-Watt (1995–1996)
N.A. Barcza (1996–1997)

* R.P. Mohring (1997–1998)

J.R. Dixon (1998–1999)
M.H. Rogers (1999–2000)
L.A. Cramer (2000–2001)

* A.A.B. Douglas (2001–2002)

S.J. Ramokgopa (2002-2003)
T.R. Stacey (2003–2004)
F.M.G. Egerton (2004–2005)
W.H. van Niekerk (2005–2006)
R.P.H. Willis (2006–2007)
R.G.B. Pickering (2007–2008)
A.M. Garbers-Craig (2008–2009)
J.C. Ngoma (2009–2010)
G.V.R. Landman (2010–2011)
J.N. van der Merwe (2011–2012)
G.L. Smith (2012–2013)
M. Dworzanowski (2013–2014)
J.L. Porter (2014–2015)
R.T. Jones (2015–2016)
C. Musingwini (2016–2017)
S. Ndlovu (2017–2018)

Honorary Legal Advisers
Scop Incorporated

Auditors
Genesis Chartered Accountants

Secretaries
The Southern African Institute of Mining and Metallurgy
Fifth Floor, Minerals Council South Africa Building
5 Hollard Street, Johannesburg 2001 • P.O. Box 61127, Marshalltown 2107
Telephone (011) 834-1273/7 • Fax (011) 838-5923 or (011) 833-8156
E-mail: journal@saimm.co.za

Typeset and Published by
The Southern African Institute of Mining and Metallurgy
P.O. Box 61127
Marshalltown 2107
Telephone (011) 834-1273/7
Fax (011) 838-5923
E-mail: journal@saimm.co.za

Printed by
Camera Press, Johannesburg

Advertising Representative
Barbara Spence
Avenue Advertising
Telephone (011) 463-7940
E-mail: barbara@avenue.co.za

ISSN 2225-6253 (print)
ISSN 2411-9717 (online)

SAIMM
JOURNAL OF THE SOUTHERN AFRICAN INSTITUTE OF MINING AND METALLURGY
VOLUME 118 NO. 10 OCTOBER 2018

Contents

SAIMM
JOURNAL OF THE SOUTHERN AFRICAN INSTITUTE OF MINING AND METALLURGY
VOLUME 118 NO. 10 OCTOBER 2018

Contents *(continued)*

UNDERGROUND COAL GASIFICATION

PAPERS OF GENERAL INTEREST

Underground Coal Gasification

On behalf of the South African Underground Coal Gasification Association (SAUCGA) I am delighted to present papers in this edition of the SAIMM *Journal*. The UCG edition showcases work by various researchers, through their respective institutions, highlighting the active and diverse research areas of importance to the SAIMM readership and to South Africa as a whole. The research work also supports the general consensus and drive towards cleaner and more sustainable mining technologies that are required for emerging countries that are endowed with coal resources. Some of the work reproduced here is the result of a number of workshops and important discussions held by SAUCGA members over the last few years. We are sincerely grateful to the SAIMM, the editorial board, and the reviewers for affording us this forum to communicate the pertinent issues relevant to UCG in the South African context.

The areas covered in this edition are loosely divided into the following categories: monitoring of UCG processes, thermodynamic modelling, and gas purification. Notably, there is a summary of the initial findings in the development of the SAUCGA roadmap. Most of the papers have multiple authors, indicating the strong collaboration propensity between industry and academia. It is hoped that this edition will encourage future discussions and collaborations and that more researchers, academics, policy-makers, funders, and UCG proponents will team up to make UCG a commercial reality.

The papers on monitoring cover groundwater monitoring as per standards laid out by existing legislation and propose fit-for-purpose monitoring standards for UCG operation, which can then be regulated and enforced. A second paper discusses the use of isotope techniques in hydrogeology to determine connections across groundwater systems and possible cross-contamination. An important result presented here is that at an existing UCG site the shallow and deep aquifers are not connected, and hence it is unlikely that the gasification zone could adversely impact shallow aquifers. Follow-on work is covered by another study, at a site that has completed a UCG trial, that looks at the geochemistry and leaching probability of products into groundwater. Acid-base accounting techniques have been used to predict the acid-producing capacity of a gasification zone in unburnt coal samples. This work is also supplemented by a stratification assessment towards a better understanding of diffusion effects within an underground cavity.

Thermo-equilibrium simulations have been studied to determine the mineral transformations in residual ash. The paper reports on the mineral transformations of potassium, aluminum, and titanium and the conditions for slag formation are identified. Another paper determines the thermodynamic limits of gasification processes using a ternary phase diagram based on the inherent chemical properties of the coal. Also covered is the possibility of using carbon dioxide as a reactant to produce synthesis gas, a topic that is also echoed by other authors. It is shown that carbon dioxide gasification is a practical solution to improve carbon efficiency and lowering the overall CO_2 footprint of a UCG process. Finally, a paper outlines a novel integration of known technologies using vortex tubes to develop an efficient process and equipment to purify syngas from UCG.

The SAUCGA hopes this edition provides a taste of future work that may emerge from research and practical efforts in the field of UCG in South Africa. It would indeed require the collaboration of many people to fully contextualize this multidisciplinary technology and to become the obvious choice for future clean coal industries.

S. Kauchali

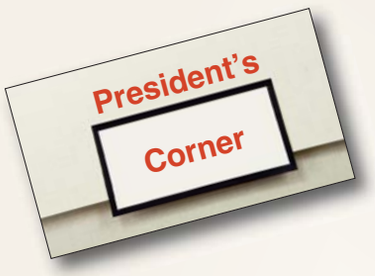

Safety, health, and the environment through the eyes of MineSafe

It is an honour for the President of the Institute to write the President's Corner note for the *Journal*, especially so when it is the first one after inauguration as President. It was indeed a great pleasure to present the story of research and development in the mining industry in South Africa in my Presidential Address at the AGM, and to be able to describe the journey so far that the Mandela Mining Precinct has travelled. The work of the Precinct has focused on the research and development of mining systems, of which health, safety and environmental topics are an essential component. What has become very clear, and flowing out of the Mining Phakisa in 2015, is the need for a collaborative approach in this research work.

No area of research is more demanding of collaboration and involvement of all stakeholders than that of safety, health, and environmental protection in mining, and the annual MineSafe conference and Industry Awards is an event that epitomizes the coming together of industry, labour, and the State.

MineSafe is one of the flagship events on the SAIMM Calendar, and this year's event, held from 29 to 31 August, built further on the success of previous conferences.

MineSafe is jointly organized between the SAIMM, and the Mines Professional Associations, in particular the Association of Mine Managers of South Africa, the South African Colliery Managers Association, and the Mine Metallurgical Managers Association. Of particular importance at this event is the level of participation by mine management, employees, and organized labour representatives from mine operational level to executive office-bearers, not only at the awards ceremony, but also at the technical presentations.

This year, the level of professionalism in the technical presentations was extremely high and the technical content, which addressed issues in safety, health, and environment, was exemplary.

In particular, papers focused on solutions to problems associated with geotechnical hazards facing miners, using techniques such as three-dimensional ground-penetrating radar, real-time monitoring of ground movement, and effective post-splitting of open pit highwalls. These advances in technology illustrate the importance of embracing the innovations in digitalization and data availability that allow not only improved operational control, but also predictive maintenance that can be applied not only to equipment, but also to the ground and its condition.

A focus on occupational health and safety addressed the need to deal with occupational health risks at source, to reach the aspiration of zero harm in health as well as in safety, instead of merely aiming for legal compliance.

In the area of environmental protection, advances in the treatment of polluted minewater were illustrated through the removal of heavy metals down to nanometre levels of treatment and filtration.

All of these areas were further backed up by well-considered and presented poster presentations, admirably showcased by their authors.

A critical theme of the event was the realization that none of these technologies or systems will realize their full value without the full engagement and support of the employees, their representative labour organizations, and the communities around the mines. This was emphasized throughout the conference, and in a powerful and at times emotionally charged keynote address on the awards day, backed up by a heart-rending industrial theatre presentation.

Safety, health, and the environment through the eyes of MineSafe *(continued)*

The awards celebrated the significant advances that have been made in mine health and safety since 1993, with some outstanding achievements that truly reflect that the aspiration of zero harm is reachable. However, statistics in 2017 and 2018 to date indicate that for the industry as a whole to reach these targets and the milestone targets, much work remains to be done. Not only is there more work to be done, but it is clear that this will only be achieved if the effort is truly collaborative and that engagement with all stakeholders is honest and transparent. Never more so has the clarion call of 'nothing about us without us' been so compelling.

So what does this mean for the future?

First, it means that research work that is aimed at improving health and safety must be coordinated and structured so as to achieve the goal of zero harm, by identifying solutions that will address current challenges, in a collaborative way. This involves coordination of effort between research institutions, universities, industry, the DMR, the Mine Health and Safety Council, OEMs, and organized labour. In terms of health, this coordination needs to extend beyond the mine fence by addressing the impact of the changing socio-economic circumstances of employees and communities. Meaningful engagement and dialogue are essential.

Secondly, in terms of MineSafe, it will be vital going forward that stakeholder involvement extends beyond attendance only, and that it involve engagement and participation in committees and presentations; best of all, in collaboration with other stakeholders.

Thirdly, the SAIMM should take a more active role, in providing platforms where constructive debates can be held to find collective solutions to reach our target of zero harm. This can be done through establishing innovative events such as 'Hackathons', debates, and breakfast events, as well as more traditional conferences, schools, and seminars.

As President, I commit to ensuring that the SAIMM will assist the Professional Associations to achieve this in a proactive way. These matters will become a part of the Technical Programme Committee agendas, and will help to forge closer relationships between the SAIMM, the Mines Professional Associations, industry, the Department of Mineral Resources, and organized labour.

Finally, congratulations to all the winners of the many prestigious awards for health, safety, and environmental performance at MineSafe 2018. In particular, the winners of the JT Ryan Awards, which went to AngloGold Ashanti Vaal River and West Wits Chemical Laboratories for surface operations, and Lonmin K3 Shaft UG2 Section for underground operations.

The Most Improved Mining Company award went to Lonmin.

The Institute recognizes these achievements as well as all the other worthy winners.

A.S. Macfarlane
President, SAIMM

Obituary

Philip Lloyd: Climate change sceptic who shared Nobel prize 1936-2018

Provocative and outspoken, he favoured fossil fuels, nuclear and teaching mathematics

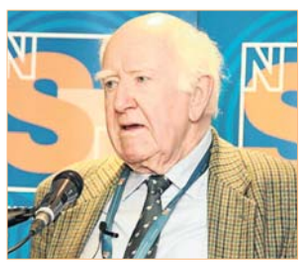

Caption—Philip Lloyd disputing evidence for climate change at a National Science and Technology Forum conference in 2017. Picture: NSTF

Philip Lloyd, who has died in Cape Town at the age of 81, was part of the UN Intergovernmental Panel on Climate Change (IPCC) team that shared the Nobel peace prize in 2007.

Ironically, he was something of a climate change sceptic and questioned the panel's impartiality.

He was a professor of chemical engineering at Wits University and a research fellow at the Energy Research Centre of the University of Cape Town (UCT), where his major interest was how people living in informal settlements could satisfy their energy needs without burning their homes down .

At the time of his death he was a professor of energy at the Cape Peninsula University of Technology, and consultant to the petrochemical industry.

He believed in fossil fuels and nuclear energy. He helped build the R11bn Mossgas project and was involved in SA's pioneering and world-acclaimed pebble bed modular reactor. He believed that the decision by the Mbeki government to pull the plug on the project was a blunder of note. As a result 'the baton was handed to the Americans who in essence are being gifted our technology and expertise', he said.

Lloyd was as formidably intelligent as he was cantankerous, outspoken and provocative.

On one occasion, the leader of the Campaign Against Nuclear Energy, who was also his next-door neighbour, had to save him from being bodily ejected from an anti-nuclear meeting.

He believed the cost and unreliability of wind and solar power made them unrealistic and ultimately unaffordable alternatives to fossil fuels and nuclear energy.

While a member of the UN panel on climate change, he found that the work of scientists was misrepresented by those involved in the policy-making process.

'What the scientists were saying was being translated into words I did not recognise as being the scientists' words,' he said. Many of the predictions of the climate change lobby were not coming true, he said, but scientists tended to gloss over this.

'There are scientists involved in this thing who are not necessarily unbiased,' he said, adding that he did not necessarily dispute climate change but did dispute the view of the IPCC and climate change lobby that carbon dioxide (CO_2) was to blame .

'The temperature change between 1920 and 1940, which is not regarded as being CO_2-driven, is very similar to the temperature change from 1970 to 2000, which the IPCC puts solely down to CO_2,' he said.

He also believed the information being used to determine the effects of climate change was too recent to form a good basis for conclusions.

Contrary to widespread reporting, he said, global temperatures were not rising excessively and there had been no recent indications of an acceleration in sea levels rising.

It was predicted that burning fossil fuels would cause an increase in hot weather, droughts, floods, violent winds, cyclones and sea levels.

'But when you dig out the evidence for these increases, you find remarkably little support for them,' he wrote.

'It has been warming for at least 180 years. Yes, it has become warmer, and glaciers are melting. But as the ice disappears on alpine passes, so footpaths appear that were last in use 800 years ago, when it was warmer than today.'

Most of the purported increases in extreme climate could barely be detected, he said.

Obituary *(continued)*

He believed the case for carbon taxes was more about populism than science, and that it was naive to put too much faith in predictive models .

"I seem to recall some recent models which proved beyond all doubt that Hillary Clinton would be the next president of the US".

He believed the "current panic about global warming will go the way of the 1970s panic about global cooling".

Lloyd was born in Sheffield in the UK on September 9 1936. He moved to SA with his family at the age of nine to escape the hardships of postwar Britain.

He won an organ scholarship to Diocesan College (Bishops) in 1949. He lost it when he ignored the 'DO NOT' signs, pulling out all the stops on the school organ for Bach's Toccata and Fugue in D Minor, which brought down the acoustic tiles from the chapel ceiling.

For his doctorate in chemical engineering at UCT he developed a uranium extraction process which is still in use.

He worked for the Atomic Energy Board which sent him to the Massachusetts Institute of Technology for a year.

On his return he worked for the then Chamber of Mines and helped develop a plan to rework mine dumps. As head of research at the chamber he led a team which devised a revolutionary underground processing plant to save having to bring all the ore to the surface.

In the '70s he was instrumental in starting Protec, an NGO offering higher-grade maths and science teaching to 1,000 black pupils every year.

Some 80% of black pupils who matriculated with higher-grade maths and science came through Protec.

With the arrival of democracy in 1994 it closed shop, believing there would be no need for it in a post-apartheid education system.

Instead, as Lloyd pointed out, a higher percentage of black students passed higher-grade maths and science before 1994 than after.

He frequently tackled his next-door neighbour, education minister Kader Asmal, about this.

Lloyd, who won the 'most outstanding young South African' award in 1976, was no mere swot.

He climbed mountains, skied, sailed and drove rally cars. He was the first South African to complete the 3,500km Monte Carlo rally.

He produced a never-ending stream of papers, articles and erudite letters to the editor until shortly before his death.

Philip had been a member of the Southern African Institute of Mining and Metallurgy for 50 years at the time of his death. He was regularly called upon to referee papers for the Journal and he was very forthright and constructive in his adjudications. At the AGM in 1972 he was awarded a gold medal for his paper 'The determination of the efficiency of the milling process' and not long before he passed away he donated the gold medal back to the Institute with the wish that the Institute sell the medal and use the money for education purposes. The proceeds from the sale of the medal are to be credited to the Institute's Scholarship Trust Fund.

He was divorced twice and is survived by three children. — Chris Barron.

Acknowledgement

This obituary was written by Chris Barron and published by the Sunday Times on 26th August 2018.

Welding – the Miracle Career

Johannesburg, 27 September 2018: For many years, the Southern African Institute of Welding (SAIW) has provided opportunities for young South African men and women to acquire the skills required in the welding and related inspection industries that enable them to obtain solid, well-paid jobs.

SAIW Executive Director Sean Blake says, 'Over 75% of our graduates find meaningful employment and this, in today's climate, is nothing short of miraculous'.

He adds that over and over, the SAIW sees how its training transforms people's lives as they get jobs in a host of industries that use welding. These include the oil and gas, construction, aeronautical, automotive, and shipping industries – in fact, almost any industry one can think of.

Over the years the SAIW has created innovative cross-industry initiatives that have improved the standards of South African welding. Since the introduction of its internationally recognized training programmes, the SAIW has also become the leading welder training organization in Africa, with branches in Johannesburg, Durban, and Cape Town, uplifting thousands of individuals through welding.

Take Houston Isaacs, for example. Schooled in Saldanha Bay, Houston always dreamed of a job using his hands. While employed as an operator at a well-known steel fabricator, his enthusiasm and dedication won him a bursary to train in welding at the West Coast TVET College. He completed his training in 2010, but jobs were scarce. That is, until he entered the SAIW Young Welder of the Year competition, in which he did brilliantly across all materials and welding techniques. A leading local gases and welding supplies company noticed his performance and immediately offered him employment.

Since then, Houston's life has changed. He says the future was uncertain until the SAIW put him on the welding map and that he will be forever grateful for the opportunity that the Institute gave him in life.

And welding isn't just for men either. Angel Mathebula's SAIW Foundation bursary enabled her to compete and secure employment as an IIW International Welder. 'We have many women on our courses and they often are the stars of the programmes. There is so much diversity in the welding and inspection world, there is room for anyone with the right credentials who is prepared to make the effort', says Blake.

The SAIW is an exciting place to learn welding. It is managed by the top professionals in the country. Its qualification and certification services are administered by SAIW Certification, an independent company that has been authorized by the International Institute of Welding (IIW) as an Authorised Nominated Body for the IIW Education, Training, Qualification, and Certification programmes. SAIW Certification also operates the SAQCC programmes for the certification of pressure equipment personnel as well as nondestructive testing (NDT) personnel.

The SAIW is holding an Open Day on 11 January 2019 to show young career seekers what it can do for them. Don't miss out on this opportunity, go to www.saiw.co.za and register. This could change your life.

B. Macheke
MoonDawn Media & Communications

http://dx.doi.org/10.17159/2411-9717/2018/v118n10a1

SAUCGA: The potential, role, and development of underground coal gasification in South Africa

by S. Pershad*†, M. van der Riet*†, J. Brand*‡, J. van Dyk*‡, D. Love*§, J. Feris*#, C.A. Strydom*°, and S. Kauchali*ᵡ

Synopsis

This paper offers an introduction to and strategic context for the other papers included in this special UCG edition of the Journal of the Southern African Institute of Mining and Metallurgy. South Africa is facing long-term energy security challenges, brought about by a myriad of factors that are somewhat unique or exacerbated in the global context. Underground coal gasification (UCG) is a process used to produce synthesis gas from coal *in situ*, that is, in the coal seam. UCG is an emerging, advanced clean coal technology that offers a potential solution for these challenges, as it can cost-effectively and cleanly liberate vast coal resources in the country that currently cannot be economically exploited using traditional mining technologies. One of the tasks of the South African Underground Coal Gasification Association (SAUCGA) is to advance the development of UCG in South Africa by compiling a technology roadmap. This paper presents the initial findings of the SAUCGA Roadmap (Draft), and contextualizes the technology opportunities and challenges, stakeholders, and provides a basis from which to progress further plans for technology development. Firm development plans and deadlines are not yet possible due to the reliance of the UCG Roadmap on the higher level South African energy policy and regulatory framework. However, the draft roadmap has taken the first step of identifying these policies and stakeholders, and should be seen as the seed from which this embryonic technology and industry can be further developed.

Keywords
South Africa, underground coal gasification, UCG, coal mining, SAUCGA, roadmap.

Introduction

South Africa's long-term energy security challenges include energy access and affordability, dwindling reserves of accessible bulk primary energy, mounting environmental concerns with all forms of energy generation (especially coal and nuclear), balancing the electricity grid by incorporating an increasing proportion of non-despatchable renewable energy sources, mounting environmental liabilities regarding defunct mining operations, and lastly but by no means less important, fluctuating exchange rates and energy commodity prices.

Correctly managed underground coal gasification (UCG) is an emerging, advanced clean coal technology that offers a potential solution for these challenges, as it has been shown to have the potential to cost-effectively and cleanly liberate vast coal resources in the country that currently cannot be economically exploited using traditional mining technologies.

The UCG opportunity arises in a period of energy transition, where utilizers of fossil fuels are under pressure to reduce emissions significantly to comply with international climate change commitments. In 2015 South Africa signed the Paris Agreement on climate change, which was developed under the auspices of the United Nations Framework Convention on Climate Change (UNFCCC). Furthermore, South Africa has a commitment to increasing the population's access to electricity, with one of the most significant hurdles being affordability. UCG technology offers potential solutions for these challenges. Research already completed and published by Eskom has highlighted this potential.

The South African Underground Coal Gasification Association (SAUCGA) is an independent, volunteer association established for the purpose of promoting the development of UCG in Southern Africa in the most appropriate, sustainable, and environmentally sound manner while recognizing the proprietary interests of participating bodies. It is thus fundamental for the efficient operation and ultimate value-add of SAUCGA to base its activities on a strategic planning document, which highlights the need for this roadmap that details a plan for UCG in South Africa, and therefore SAUCGA as well.

Furthermore, as with any emerging technology, strategic planning is essential to evaluate the current situation, what needs to be done now and in the future (bearing in mind the shifting goalposts), and the technology pathways to research and develop

* *South African Underground Coal Gasification Association, South Africa.*
† *Eskom Holdings SOC Ltd., South Africa.*
‡ *African Carbon Energy, South Africa.*
§ *Golder, South Africa.*
# *Cliffe Dekker Hofmeyer, South Africa.*
° *North-West University, South Africa.*
ᵡ *University of the Witwatersrand, South Africa.*

 ISSN 2225-6253. Paper received Apr. 2018; revised paper received July 2018.

the technology in order to meet likely scenarios. This roadmap is constructed around these key elements.

The roadmap seeks to gather stakeholder viewpoints and consolidate and provide a consensus pathway forward for the development of UCG in South Africa for the period 2016 to 2040, aligning with the South African Integrated Resource Development Plan 2010 (Department of Energy, 2010), the South African Coal Roadmap (Fossil Fuel Foundation, 2013), and the National Development Plan (National Planning Commission, 2010).

Other key strategic documents (such as the South African Coal Reserves and Resources Report, and the South African Gas Utilisation Master Plan, Integrated Energy Plan, and Integrated Resource Development Plan) will be considered as they are published.

The intent is for this roadmap to be updated regularly, and alignment with these documents will be undertaken as they are published. The following key assumptions need to be defined, to set the context of this roadmap.

- UCG has a definite role to play in South Africa's future. The underlying assumption is that it can be appropriately engineered and proven to meet evolving requirements.
- This roadmap assesses the period 2016 to 2040.
- This roadmap focuses on UCG application within South Africa, but may be expanded to include neighbouring countries in Southern Africa.
- The current economic, environmental and social paradigms are the basis for this roadmap, with projections drawn from reference studies.
- There will be no decline in South African market demand for electricity, liquid fuels, and chemicals, but demand will increase based on projections drawn from reference studies.

South Africa has developed an Integrated Resource Plan 2010 (Department of Energy, 2010) that projects that the energy mix will evolve in the period 2010 to 2030 to cater for a reduced role of coal (from about 89% in 2015 to 56% in 2030), replacement capacity, and growth in demand. This plan has been promulgated for the period 2010 to 2030, and IRP updates have been drafted with the most recent being the IRP 2016, which has undergone public comment and is still awaiting finalization. As such, the IRP 2010 remains the only promulgated IRP plan at present, and is therefore the country's reference resource plan. It is noted, that in the absence of a 2018 updated and accepted IRP, the assessment of UCG's potential capacity and role in comparison with other competing energy sources is difficult. It is also widely acknowledged that coal will play a significant, albeit reducing, role in South Africa's energy mix until 2050. UCG offers a better, cleaner coal usage alternative.

The IRP 2010 seeks to cap carbon dioxide emissions at 250 Mt/a. This cap therefore dilutes coal's predominance over the next decades, as seen in Figure 1. It must be noted, however, that coal will still play a significant role until at least 2050, and if the retirement of the ageing generating fleet is considered then new coal-fired generating capacity is going to be required. Given the environmental pressure, such capacity will need to be based on sustainable coal technology solutions, which include UCG. There are many coal-based technology options under development that could significantly reduce coal emissions, thereby displacing other energy resources by being able to compete in terms of emissions and cost.

UCG as a mining method

UCG is not a new technology. In fact, references to UCG can be found dating from the late 1800s, and the earliest US patented posting of UCG as an alternative mining method was filed in 1901.

The main difference between UCG and more conventional surface gasification projects is that in the latter, gasification occurs in a manufactured reactor, whereas the reactor for a UCG system is the natural surrounding geological formation (typically consisting mainly of sandstone or dolerite) containing unmined coal. In UCG, coal is gasified *in situ* and converted into syngas, which is then transported to the surface via a specially designed and drilled production borehole. The conversion of the coal to syngas is achieved through a partial combustion process controlled by the injection of oxygen (O_2) into the coal seam through an injection well.

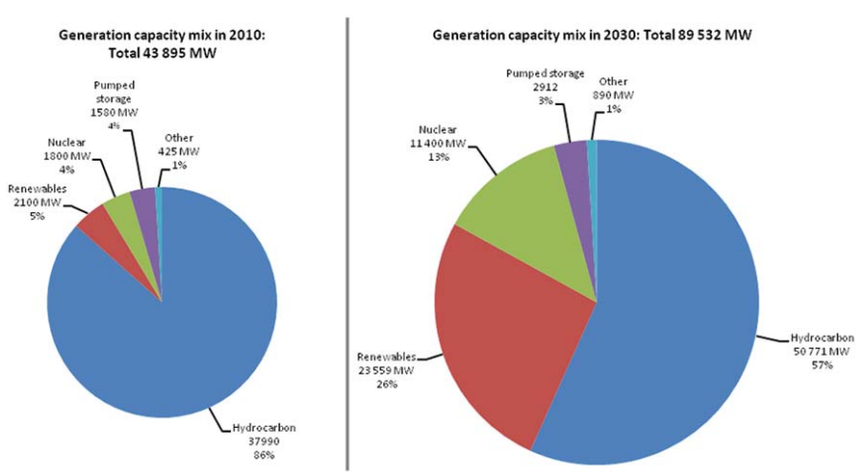

Figure 1—The size and mix of South Africa's power generation capacity, 2010–2030 (Department of Energy, 2010)

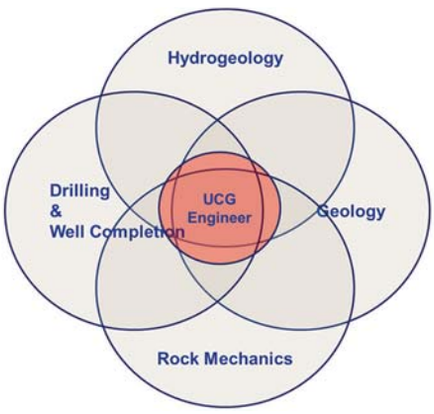

Figure 2—Key skills and disciplines involved in UCG-related underground activities (Pershad, 2016)

UCG principally requires mining and geoscience skills to be integrated in a multidisciplinary team to plan, design, operate, and rehabilitate a UCG gasifier, as illustrated in Figure 2. The core skills and sciences required are: geology; hydrogeology; rock mechanics; drilling and well completion; and UCG mining engineering and technology (which includes mining engineering, chemical engineering, and gasification expertise).

Process concept

UCG is similar to surface gasification, and is a chemical process that converts solid or liquid fuels into a clean combustible gas (synthesis gas or syngas) consisting of carbon monoxide (CO), hydrogen (H_2), methane (CH_4), and carbon dioxide (CO_2). The ratios of these components in the final product syngas depends on the chemical composition of the fuel (coal), the type of reactant (air, oxygen, CO_2, and steam) the ratios used in the process, and the operating conditions. Clean syngas can be used for synthesis of transportation fuels and chemicals, production of hydrogen, direct reduction of metal ores, electricity generation, or a combination of these.

The fundamental difference between UCG technology and surface gasification is that UCG enables coal to be gasified *in situ*. The conversion of the coal to syngas is controlled by the injection of oxygen into the coal seam through the injection well.

A borehole is drilled through the overburden down to the coal seam, which is then ignited. Oxygen or oxygen-enriched air is injected to feed the process and drive the gasification reactions that produce a syngas mixture. These gases are collected by the production borehole for utilization at the surface. UCG creates a cavity below ground filled with ash, the size of which depends on the rate of water influx from the water table, the heat content of the coal, the location and shape of the injection and production wells, and the thickness of the coal seam.

There are two main commercially available UCG methods. The oldest method uses alternating vertical wells for injection and production combined with reverse combustion linking to open up internal pathways in the coal. This process was used in the Soviet Union from the 1940s, and was later tested in Chinchilla, Australia and by Eskom in South Africa. The second method, which was developed in the USA in the 1980s, employs dedicated in-seam boreholes, drilled using directional drilling and completion technologies adapted from the global oil and gas industry. It incorporates a moveable injection point method known as CRIP (controlled retraction injection point) and generally uses air or oxygen-enriched air for gasification.

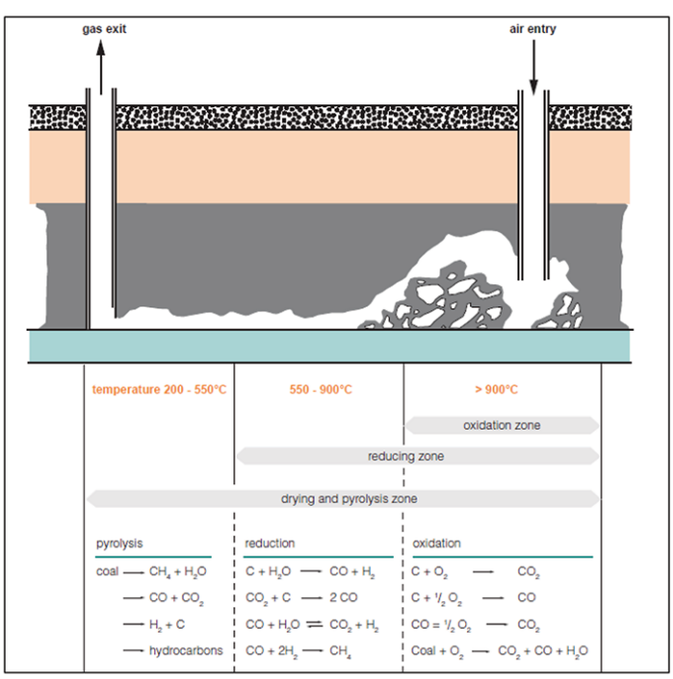

Figure 3—Basic UCG gasification reactions (Couch, 2009)

Gasification

A gasification process must satisfy chemical constraints based on the stoichiometry of the coal gasification reactions and the energy requirements to sustain these reactions. Gasification of char produced by the devolatilization process involves chemical reactions between primary reactants, *i.e.* carbon in the char, oxygen, and steam, as well as a number of reactions between primary and secondary reactants, *i.e.* CO, CO_2, and H_2. The basic gasification reactions are illustrated in Figure 3.

Advantages of UCG

UCG has considerable environmental benefits. The syngas is generated deep underground inside the coal seam, while the ash in the coal mostly stays in the seam. About 80% of the energy in the coal can theoretically be extracted as syngas, making UCG a very efficient mining process. At the same time, no persons are required underground, which offers safety benefits. UCG is not just more efficient and safer, but also offers the following advantages.

- UCG can be combined with large-scale combined-cycle plant to reach energy efficiencies exceeding 50% compared to the current 35% efficiencies obtained in subcritical pulverized fuel boilers.
- UCG produces less particulate emissions, thus the process requires minimal ash handling, and there is little or no leaching of trace elements from ash when operated correctly.
- UCG can monetize economically un-mineable coal that would otherwise be lost to the country's economy. Approximately only one-quarter of South African coal reserves are economically and technically recoverable with current conventional mining methods (Barker, 1999).
- UCG deployment can create new high-value jobs in the drilling, gas processing, and gas engine maintenance industries.
- UCG projects can be located in economically depressed areas of South Africa, often far from current mining areas.
- No chemicals are injected into the UCG process as only air and water are required for gasification.
- Fracking is not required and no fracking chemicals are injected to create the boreholes.
- The UCG syngas is already in a form that can be further monetized to liquid chemicals or fuels, or the syngas can be separated to obtain basic chemicals such as hydrogen, carbon monoxide, and methane.
- The form of sulphur present in the syngas allows for economic recovery of elemental sulphur (which can form part of the chemicals portfolio).
- Technologies for CO_2 removal (for future capture and storage) from the syngas are well matured.
- The UCG reactor can be operated to maximize methane production (if required by the market) with the rest of the syngas rich in CO-H_2 for further production of methane or other chemicals.

UCG in the global context (Blinderman, 2016)

A long period of UCG development, spawned by the energy crisis that started in 1973, was completed by the Rocky Mountain 1 trial in the USA in 1988 and the European UCG trial in Spain in 1992. Following several years of lull and uncertainty, the Chinchilla UCG project in Australia marked the beginning of new era of UCG development in Australia, New Zealand, South Africa, Europe, Canada and the USA. Spanning almost 20 years, this latest stage of UCG development was distinguished by a preponderance of privately funded projects with a significant share of the capital raised from stock markets.

It appears that this latest stage of UCG development has suffered considerably from the drop in fossil fuel prices in world markets, and from the commodity market slowdown. Whereas the reduced oil and natural gas prices seem to have affected new and existing UCG projects by decreasing the projected sale price of UCG products, the corresponding precipitous drop in coal price reduced the revenue streams of many UCG proponents to the extent that they could no longer invest in new UCG projects. An example of the latter was the 2012 shutdown of the Huntly West UCG pilot plant in New Zealand.

The economic slowdown led to the need for partnering with the Majuba UCG pilot project in South Africa, and reduced economic performance due to the suppressed energy prices in, for instance, North American markets led to closure of the Swann Hills and Parkland County UCG projects in Canada.

The other factor limiting UCG activity worldwide is the lack of preparedness of environmental regulations and misunderstanding and misinformation on UCG within some environmentally concerned communities, caused no doubt by the scarcity of factual information on UCG and confusion with fracking of oil shales. This regrettable state of public awareness may have contributed to the reluctance of local authorities to approve new UCG projects in several jurisdictions.

In the meantime, in many parts of the world where there is no sign of pending additional energy sources (including shale oil and gas), UCG development remains an imperative for supplying affordable energy and hydrocarbon feedstock for local industrial and retail markets. Examples of such locations are South Africa, India, and Pakistan.

It is therefore quite clear that a new stage of UCG development must be based on a solid foundation of specific and comprehensive regulation covering environmental protection, potential conflicts of ownership of mineral and petroleum rights, royalty regimes *etc.*

Many countries with large coal resources but which lack conventional oil and gas are now focusing on proposing detailed UCG regulatory frameworks. Among them are China, India, and South Africa. These efforts are spearheaded by appropriate governmental offices and there are indications that the regulations may be finalized within the next 2–3 years.

There are several UCG projects that are now being prepared in anticipation of pending regulations.

- In China, there are four proposed UCG projects targeting power generation, and supply of syngas to a

Fischer-Tropsch facility and a synthetic methane plant. Only limited information has been made available by the developers.

- In India, the central government has specified a pathway for government-owned corporations to develop UCG plants at a pilot scale. The coal blocks that would be allocated to these companies for UCG development have been identified; and work should start in earnest once the regulations are available.
- In South Africa, there are at least three projects that are now anticipating water use regulations governing 'unconventional' gas (*viz.* shale gas, coalbed methane, and UCG). They include the Majuba UCG partnership development by Eskom, the 50 MWe Theunissen UCG project by African Carbon Energy, and the Sterkfontein project developed by Oxeye Energy.

There are furthermore several UCG projects under way in jurisdictions where existing regulations appear to support UCG development. These areas include India, South and Central Australia, Indonesia, Alaska, Canada, and the UK.

Apart from UCG projects pursuing clear commercial outcomes, there a number of UCG projects that are conducted primarily for R&D purposes. These include the recently concluded European TOPS research project that considered technology options for coupled UCG and CO_2 capture and storage and HUGE, the Hydrogen Oriented Underground Coal Gasification for Europe project development largely by Polish researchers in Główny Instytut Górnictwa. The demonstration installation was built on the premises of CCTW Mikołów in the Underground Testing Range.

UCG in the South and Southern African context

Eskom Holdings SOC Limited (Eskom) has played a significant role in contributing to the research and development of UCG in the Southern African region by, among others, demonstrating the technical feasibility of the technology, as well as the potential economic feasibility of utilizing UCG technologies in exploiting un-mineable coal resources to produce syngas and other by-products for various downstream uses. These scientific findings are being prepared for publication.

Southern Africa still has significant coal resources, the majority of which are deemed uneconomic to mine due to depth or other technical or market factors. UCG offers a potential solution for accessing these abundant resources in a cost-effective and clean manner.

This technology opportunity arises in a period of energy transition, where fossil fuel users are under pressure to reduce emissions significantly to comply with international climate change commitments. In the local context, in 2015 South Africa signed the Paris Agreement on climate change, which was developed under the auspices of the United Nations Framework Convention on Climate Change (UNFCCC). Furthermore, South Africa has a commitment to increasing the population's access to electricity, with one of the most significant hurdles being affordability. UCG is a coal technology that offers potential solutions for these challenges.

In Southern Africa, Eskom has for the past 16 years taken a leading role in investing in the development of the first UCG facility in Africa (Pershad, 2016), based on the technology of Ergo Exergy Technology Inc. (Ltd).

Eskom's review of existing data and Majuba-specific tests led to the construction of a 5000 Nm^3/h pilot plant, which achieved ignition and first flaring of gas on 20 January 2007. From a research and development perspective Eskom demonstrated the following:

- The technology provides cost-competitive fuel for future power generation. It derives this fuel from local, unused coal resources shielded from international market forces.
- It has been qualitatively proven that the technology works, and is able to extract value from one of the most geologically complex coalfields in South Africa.
- There is a need to further quantify the performance of UCG technology, so that it can be optimized.

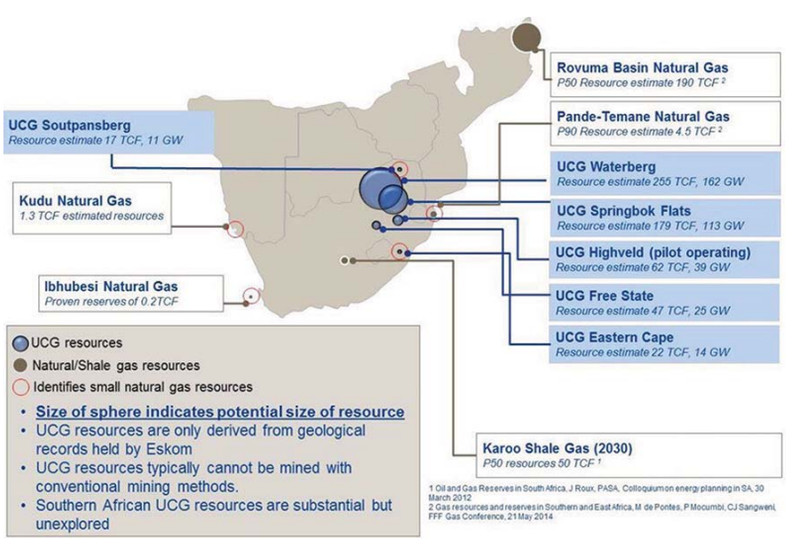

Figure 4—Map showing potential UCG sites in South Africa (Pershad, 2017)

- The Eskom Board supports the technology, but due to Eskom's current financial constraints a partner will be sought to further commercial development.
- Eskom will in parallel shut down and rehabilitate the initial Majuba gasifier as part of the original research intent.

Research already completed by Eskom has highlighted the technology potential. Eskom intends to complete the final stage of the research and prove the commercial viability of the technology in the next phase of development. The goal will be to achieve the same emissions footprint and cost as the supercritical pulverized fuel technology utilized in Eskom's new Medupi and Kusile power stations. The commercialization will coincide with the demand for new coal-fired generating technology, as per the Integrated Resource Plan (Department of Energy, 2010).

It must be noted that there are several different UCG technologies, apart from Ergo Exergy's technology, being utilized by other UCG developers.

The other proposed UCG projects in South Africa and to a lesser extent, the rest of the Southern African region (Mining Weekly, 2013) are African Carbon Energy and, more recently, Oxeye Energy, who are actively pursuing the potential application of UCG technologies in exploiting un-mineable coal resources in South Africa.

African Carbon Energy (Africary) is pursuing the development of a UCG facility in Theunissen, Free State Province. Africary intends to develop a UCG power generation facility which will form part of the Gas to Power Independent Power Producers Programme of the Department of Energy.

Oxeye Energy concluded a memorandum of understanding with Ergo Exergy for the potential development of a UCG facility for the generation of electricity. Oxeye is currently completing a conceptual study on the application of UCG technology in the Sterkfontein area, Bethal, Mpumalanga Province.

Figure 4 depicts the various potential sites for UCG in South Africa,, illustrating the significant potential.

Despite the concerted development of UCG in South Africa there are still major challenges holding back the commercial uptake of UCG technology. SAUCGA has identified these as follows.

- In South Africa, UCG was declared a controlled activity in 2015 by the Department of Water and Sanitation (DWS). The DWS has still to issue the water use license (WUL) control guidelines for applicants. Other unconventional gas sources such as shale gas and coalbed methane also face this regulatory hurdle.
- A core, critical, and widely accepted suite of energy framework policies for South Africa that would attract investors in mining, electricity, and energy. In this regard the revised Mining Charter, Integrated Energy Plan (IEP), Integrated Resource Plan (IRP), and Gas Utilisation Master Plan (GUMP) are eagerly awaited. These anchor policies will set the framework for projects and investments to be made with confidence and certainty.
- Electricity and energy demand growth synonymous with growing South African industrial and economic activity.
- To a lesser degree, the necessary skills and experience to advance a first-of-a-kind (FOAK) technology project through regulatory, project management, and financing systems that are created predominantly for known, off-the-shelf technologies. Similarly, risk management practices are not complementary to the evolution of embryonic technology, particularly where that technology development is at a larger scale, operating in the environment beyond laboratory scale, which requires licensing and permitting against an extensive body of knowledge that substantiates granting of licenses. This sets up a classic chicken-egg conundrum between the regulatory and R&D processes.
- The adverse environmental outcomes of some UCG projects around the world, and the corresponding public perception.

However, before the above issues can be addressed, stakeholder interest, engagement, and buy-in needs to occur in order to engage in a serious, concerted path of technology advancement and development. The current draft UCG roadmap is the first step in resolving these issues.

Industry knowledge suggests that countries such as Namibia, Botswana, and Mozambique have potential for the application of UCG technology to un-mineable coal resources.

Potential UCG applications in South Africa

Power generation

From 2007, South Africa faced a decade of electricity shortages due to a variety of reasons, and this has resulted in load shedding and a corresponding constraint on economic activity and growth. The electricity price has also increased significantly in the interim. There is now a theoretical overcapacity situation in 2018, as the Medupi, Kusile, and Ingula units are being commissioned. The excess capacity, however, has had the unintended consequence of allowing more time to review all primary energy sources and generating technologies.

In this regard, South Africa is unfortunately not blessed with conventional onshore natural gas resources and development of unconventional gas resources like shale gas and coal bed methane remains to be realized. While conventional natural gas offers a cleaner fuel for power generation, commodity price fluctuations present a risk to the South African economy.

South African is blessed with abundant coal resources, and the Integrated Resource Plan (Department of Energy, 2010) as well as the South African Coal Roadmap (Fossil Fuel Foundation, 2013) accounts for the continued use of coal in the electricity industry planning for the next 50 years.

In May 2015, the South African Department of Energy (DoE) further recognized the potential role that UCG-based power generation could play by requesting information on gas-based electricity generation capacities and time periods via a 'Request for Information'. Under this RFI, UCG was identified as a 'Gas' option, from the following definition:

Gas - Any of: (i) natural gas which occurs naturally underground (either from a conventional gas field or an unconventional gas field including shale gas and coal bed methane ("CBM")) or (ii) synthesis gas ("syngas")

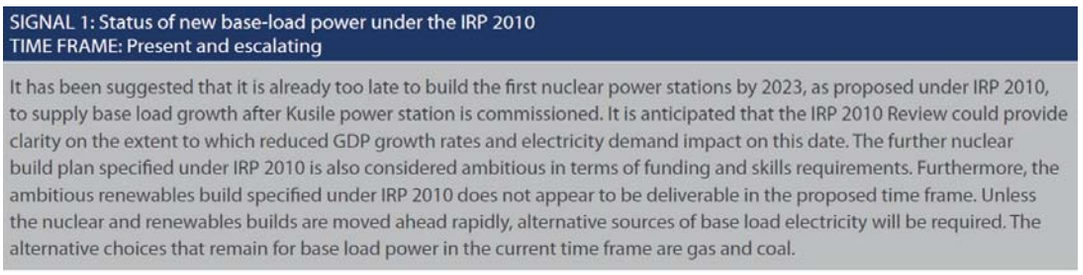

Figure 5—South African Coal Roadmap (Fossil Fuel Foundation, 2013) - Status of New Base Load Power Generation

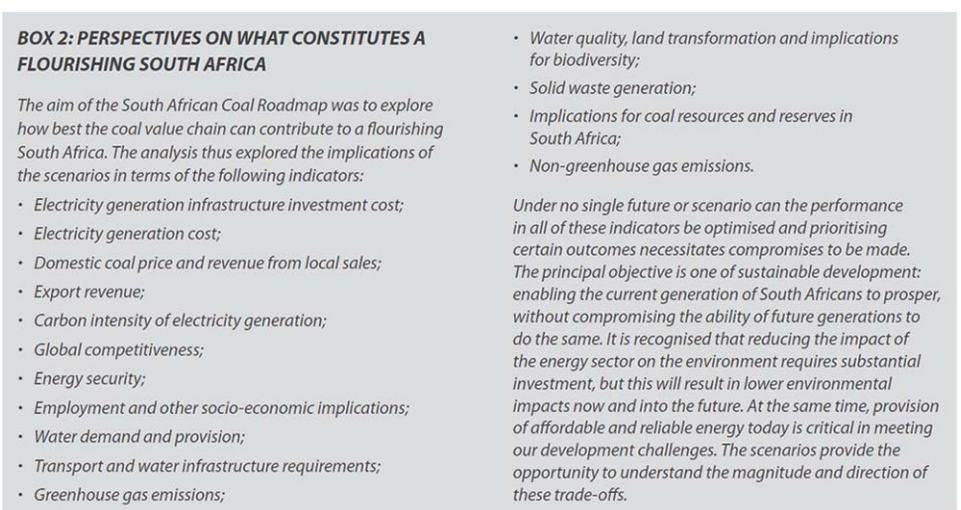

Figure 6—South African Coal Roadmap (Fossil Fuel Foundation, 2013) - Perspectives of a flourishing South Africa

including underground coal gasification ("UCG"), or conventional coal gasification as part of integrated gasification and combined cycle ("IGCC") gas technology or (iii) Liquefied Natural Gas ("LNG") or Compressed Natural Gas ("CNG") or (iv) liquefied petroleum gas ("LPG");

The South African Coal Roadmap (Fossil Fuel Foundation, 2013) considers the short-term signals illustrated in Figure 5, with respect for electricity generation under the IRP 2010.

The 'already too late' situation that was referenced to July 2013 can now be surmised as being very late in 2018. The Coal Roadmap goes further to describe the perspective on what constitutes a flourishing South Africa. From Figure 6, it is evident that electricity generation and infrastructure investment costs as well electricity generation costs are significant perspectives to be considered. UCG is a key technology that directly supports coal mining, and hence a flourishing South Africa.

The National Development Plan (National Planning Commission, 2010) explicitly identifies underground coal gasification technology under its Chapter 4 - 'Economic Infrastructure' (pages 163, 171, and 181) for the following South African context:

'South Africa needs to maintain and expand its electricity, water, transport and telecommunications infrastructure in order to support economic growth and social development goals. Given the government's limited finances, private funding will need to be sourced for some of these investments.'

'Policy planning and decision-making often requires trade-offs between competing national goals. For instance, the need to diversify South Africa's energy mix to include more renewable energy sources, which tend to be variable in terms of production, should be balanced against the need to provide a reliable, more affordable electricity supply.'

With specific reference to coal, UCG, and electricity, the NDP makes the following comment:

'Cleaner coal technologies will be supported through research and development and technology transfer agreements in ultra-supercritical coal power plants, fluidised-bed combustion, underground coal gasification, integrated gasification combined cycle plants, and carbon capture and storage, among others.'

It is thus evident that UCG for electricity generation in South African is in alignment with the IRP 2010 (Department of Energy, 2010), SA Coal Roadmap (Fossil Fuel Foundation, 2013), National Development Plan (National Planning Commission, 2010), and DoE gas industry intentions.

Critically, UCG for electricity generation in South Africa is under a clear, direct, and explicit developmental mandate.

Liquid fuels and chemicals production

The production of low-cost syngas may provide a lower cost route for electricity generation, but can also lead to the development of new lucrative chemical industries, with associated jobs and skills. A crucial factor for unlocking large-scale usage of UCG syngas will be the advancements made in catalysis for Fischer-Tropsch and direct syngas-to-olefins processes.

Key issues to be considered for plants producing liquid fuels and chemicals are:

- The quantity of nitrogen in the syngas and the need to include an air separation step prior to gasification.
- The pressure and temperature of the syngas, requiring addition compressors or heat exchangers for downstream conversions.
- Flexibility of the downstream conversion processes (syngas to liquid fuels/chemicals) to utilize a variety of syngas compositions derived from a UCG process – specifically the H_2:CO ratio required for downstream processes.
- Storage and transportation of the products, as well as handling of waste effluent (*e.g.* process water).
- The level of complexity (in plant configuration and operations) specifically for UCG sites that are physically far from service providers and markets.
- The need for, degree, and economics of gas clean-up for the protection of downstream catalytic processes. Generally, all processes for syngas conversion are catalytic in nature.

Polygeneration systems

With the South African coal-fired power sector facing potentially fatal challenges, it would be forward thinking to consider the possibility of producing not just power, but also a range of products from coal gasification. The products (in addition to electricity) may include cooling, heating, chemicals (hydrogen, CO_2, methanol, Fischer-Tropsch liquids, ammonia *etc.*). The possibilities of producing energy, fuels, and other products through a polygeneration system are shown in Figure 7.

UCG syngas derived from an air-blown gasifier is typically of low calorific value, between 3 and 5 MJ/m^3. This low calorific value gas, while reducing the capital cost of syngas production, leads to a number of issues.

Firstly, the lower energy content implies that compressing and long distance transportation is uneconomic, and secondly, the equipment for power generation is less available. The opportunity for liquid fuels and chemicals production (during minimum power demand) is therefore worth consideration. Here, the UCG reactors may operate at full capacity to produce syngas, and at off-peak electricity demand times the syngas can be diverted to a liquid fuels production plant. UCG thus offers the flexibility of producing multiple commercial products.

It is acknowledged that liquid fuel is considered to be a peaking fuel, enabling the power plant to operate during peak demand, with liquids produced during off-peak times. However, there is still a debate as to whether the liquid should be methanol or Fischer-Tropsch derived liquids (naptha and middle distillates). The advantage of methanol is that it is a single product of immense value as both a chemical and a fuel. However, the methanol reaction is thermodynamically equilibrium-limited, requiring high pressure and a large internal recycle.

Fischer-Tropsch synthesis, on the other hand, is not equilibrium-limited, and can operate with low partial pressures of hydrogen and carbon monoxide. The liquids produced can be tailor-made (via catalysis) to produce large amounts of naphtha and middle distillates that can be stored or used. Fischer-Tropsch products generally require further upgrading to be commercially acceptable by the market..

Environmental impacts of the UCG value chain

UCG takes place deep underground in unexposed coal seams (refer to Figure 8). A residue of slag, ash, and salts remains in the gasifier cavity in the coal seam. UCG is considered a cleaner energy source as the known effect on the environment is much less than that of the mining and combustion of thermal coal. It also generates far fewer greenhouse gas emissions compared to conventional coal mining. It has, however, various potential risks, among

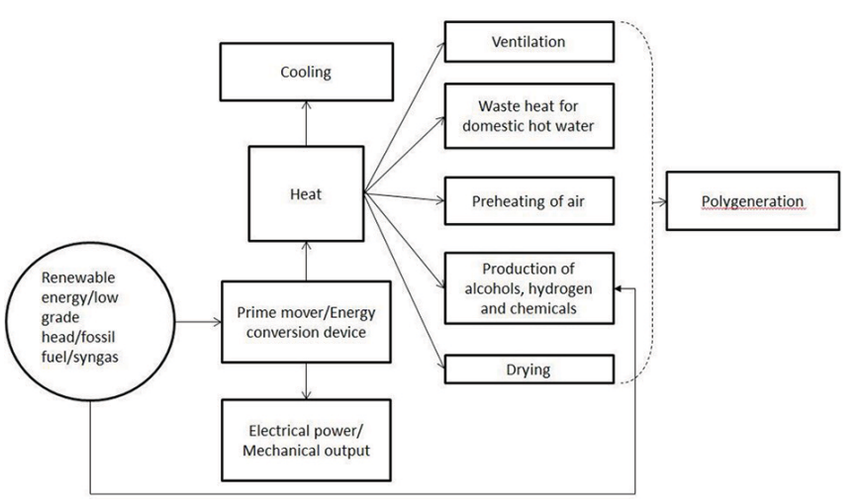

Figure 7—Pathways for polygeneration systems (adapted from Murugan, 2016)

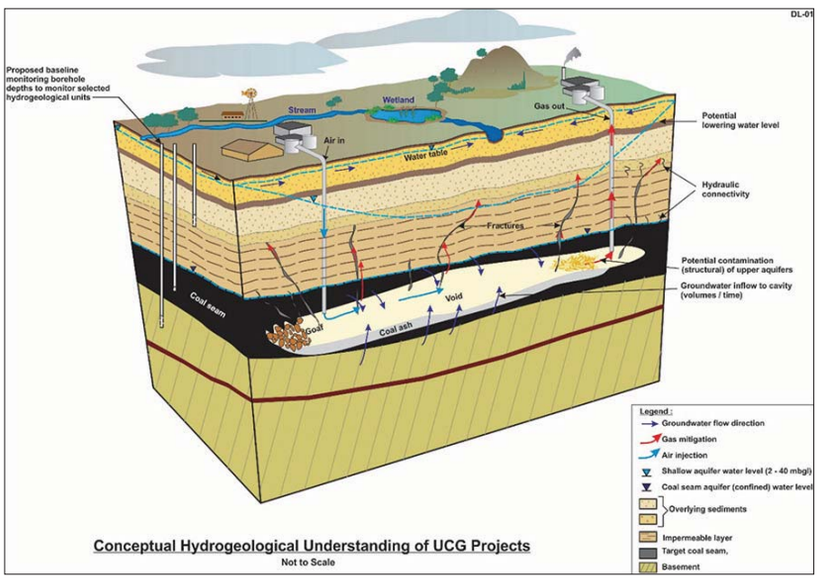

Figure 8—Schematic diagram of UCG (Love, 2016. © Golder Associates Africa 2015, reproduced with permission)

which the subsidence of the ground surface and potential groundwater contamination are the biggest concerns.

Groundwater consumption

The gasification reaction takes place underground within the gasification channel, within the underground cavity in the underground portion of the gasifier (Figure 8). The pressurized gasifier operates at high temperatures of 650°C to 1600°C. The process consumes water in the coal seam aquifer as well as moisture within the underburden and overburden layers, leading to a groundwater cone of depression. An external water source is not generally required for the UCG process, except in exceptional cases where very low groundwater levels are insufficient to meet the UCG water requirements.

Groundwater pollution prevention

Studies of (above-ground) gasification residues suggest that the residue is mainly an aluminium-calcium silicate slag with tars and unburnt coal minerals (Choudhry and Hadley, 1996; Ginster and Matjie, 2005). However very little information is available on the heavy organic chemistry of the residual ash and salts, with most environmental studies focusing on the light organic fraction present in the condensate, including phenols, benzene, methylbenzene (toluene), ethylbenzene, dimethylbenzenes (xylenes), and polycyclic aromatic hydrocarbons (Liu *et al.*, 2007; Smoli ski, *et al.*, 2012a, 2012b). The proportion of the light fraction remaining in the gasifier residue is also poorly understood.

The UCG process has two intrinsic source controls.

A proactive strategy, built into the design and proper operation of the UCG process.

- Vertical control: the gasifier must be below a suitable capping layer, for example an impermeable sill – this prevents loss of product and also contamination of any overlying aquifers.
- Vertical control: the gasifier operating pressure must be below the hydrostatic and lithostatic pressure at all times, so that the outward and upward 'push' of the operating gasifier pressure is counteracted by the downward pressure of overlying rock and water. Then pressurized water is not ejected upwards through solid rock and the groundwater flow direction is inwards towards the gasifier. Maintaining the gasifier pressure below hydrostatic and lithostatic pressure minimizes gas leaks from the gasifier and therefore ensures that minimal contaminants (phenol, benzene, *etc.*) leak out beyond the boundaries of the gasifier.
- Lateral control: the pressure gradient must be towards the cavity. A cone of depression caused by the gasification process consuming groundwater results in controlled ingress of groundwater used in gasification, and creates a pressure barrier against contaminant flow away from the gasifier, thus preventing egress of potential contaminants into the surroundings.

Reactive monitoring strategy (van der Riet et al., 2014; Love et al., 2014, 2015a, 2015b).

- Checking that there is no vertical migration of contaminants to shallow or upper intermediate aquifers.
- Checking that piezometric groundwater levels indicate that the cone of depression is being maintained and that the pressure gradient is in place.
- Checking that the operating pressure is below the hydrostatic and lithostatic pressure.
- Separation of the coal seam from the lower intermediate aquifers by *e.g.* a dolerite sill.

During shutdown, the gasifier is depressurized and the groundwater naturally present around the coal seam is allowed to gradually flood the cavity. This dissolves some of the ash and salts, and the more saline groundwater may affect downstream groundwater compositions by diffusion or by advection once the water table has stabilized and regional groundwater flow has resumed.

Table I

Groundwater zones in UCG and conventional mining (Love, *et al*., 2014b)

UCG zone during operations	Conventional mine equivalent	Conceptual basis	Monitoring purpose
Production	Underground mine workings or open pit - 'process water'	Operational area	Observe levels of 'process water' against operations summary
Process Control	Safety zone around mine workings or open pit	Buffer zone for early warning of any problems	Monitor for significant changes in early warning indicators
Compliance	External environment	Area expected to be unaffected by UCG operations	Compliance required with agreed water quality standards

The monitoring strategy indicated in Table I is therefore necessary.

Subsidence

Subsidence caused by UCG processes can impact on the groundwater flow and levels due to the potentially modified groundwater recharge. This may affect nearby users as recharge flows preferentially through the subsided area.

It must be noted, however, that subsidence in UCG is a design choice rather than a risk, as it aids the UCG process. The following aspects must be borne in mind.

- Many UCG sites are at considerable depth, with competent rock bodies above the gasifier and the confining layer. In such cases, gasifier operations can be designed so that the depth of goafing does not result in significant vertical movement in the overlying layers, and consequently no subsidence occurs on surface.
- Alternatively, a UCG operation may be designed to cause subsidence at the end of the life of the gasifier, so that this takes place in a controlled fashion, followed by remediation of the surface environment while the operator is still on site. The increased groundwater recharge in this scenario can be used to accelerate the gasifier shutdown and clean-up process.

Conclusions

The availability of coal and sustainable role of coal mining is widely recognized within the South African context by most stakeholders in several key policy documents such as the National Development Plan (National Planning Commission, 2010), the IRP 2010 (Department of Energy, 2010), and the draft IRP 2016 and IEP 2016. Furthermore, the status and developmental needs of the coal industry were proposed in the Coal Roadmap (Fossil Fuel Foundation, 2013).

UCG development was initiated by Eskom, under the auspices of the DPE with close involvement of the regulatory departments DMR, DoE, and DWS. There are now several new UCG developers with specific projects under way, which in turn have generated interest from numerous other affected parties. An embryonic industry is being born!

Furthermore, UCG as a technology has received explicit prominence in the country's future energy plans, and is noted for its potential key role in energy provision. This acknowledgement requires the formulation of a strategy for research, development, and commercial implementation of UCG.

At the request of the DoE and DMR, SAUCGA was established for the specific purpose of promoting the development of UCG in Southern Africa. This roadmap details SAUCGA's plan for UCG in South Africa, and lays out a strategy for SAUCGA as well. It records the current situational analysis locally and internationally; what needs to be done now and in the future; and the technology pathways to research and develop the technology in order to meet likely scenarios moving forward.

Pioneering studies by Eskom Holdings SOC Ltd, their licensor Ergo Exergy Technologies Inc., and other specialist consultants have proven that the technology can effectively exploit the geologically difficult Majuba coal resources, which had been declared un-mineable in the 1980s with conventional mining technologies. The Eskom project has furthermore proven UCG compliance with strict mining and environmental standards, and advanced the technology by developing control and mitigation measures which reduce potential underground contamination risks. The UCG mining operation can be considered within three zones, with the production zone in the centre, surrounded by a process control zone and the compliance zone. All three zones enable efficient control and monitoring of the process.

UCG has been developed by Eskom for power generation, but is equally suited to providing feedstock for the liquid fuels and chemicals industries, as well as a hybrid polygeneration industry.

UCG presents a more efficient method of mining the three-quarters of South Africa's coal which is considered to be uneconomic using conventional mining technologies, due to depth and other issues. UCG therefore significantly extends the country's coal reserves.

South Africa requires growth in energy-intensive and mining industries to unlock the natural resources in the country, and in so doing unlocking the associated wealth and creating employment opportunities. This urgent need incentivizes the development of highly efficient and environmentally sustainable technologies such as UCG.

Recommendations

1. UCG has been piloted and has been successfully proven in the local context, which indicates an opportunity to depart from traditional thinking and conventional technologies used for energy projects. In particular, UCG offers an opportunity to move forward to commercialization, with the close involvement of the regulatory authorities, NGOs, I&APs, and academia to fast-track learning, optimization, and policy formulation. It is recommended that UCG developers focus on actively ensuring such partnerships.
2. This brings with it the challenge of how to translate international experience and local R&D understanding into local policy certainty, to enable the birth of a first-of-a-kind technology (for South Africa). SAUCGA believes that UCG technology has reached a point where it now needs the guidance of:
   a. A technology department, such as the DST. This will enable the cohesion of the various stakeholders (advocated in the first point) under the auspices of one department that can unite the vision and goals for UCG technology. An excellent precedent has been set by the developmental role the DST has taken in the shale gas industry.
   b. A commercialization department, such as the DTI. This will enable the development of the financial and legal framework required to embrace a new technology.
3. Any technology involves risk, especially a new technology, for investors and regulators. SAUCGA proposes that government proceeds stepwise in regulating the industry, with for instance:
   a. A consultative permitting and licensing framework with the close involvement of regulatory staff in the projects, to monitor, advise, and learn. The regulatory prerequisites could ratchet up to the levels expected from known technologies, based on the performance of the preliminary UCG installations. This will alleviate the current chicken-and-egg scenario that has evolved with, for example the Water Use License, where technology uncertainty precludes any further development.
   b. Financial incentives (such as reduced royalties and taxes, or tax 'holidays') to encourage the nascent industry to grow.

Acknowledgement

The efforts and contributions of other SAUCGA members and collaborators in the compilation of the SAUCGA Roadmap must be commended. These are Dr R. Gumbi (Oxeye Energy), Professor F.B. Waanders (North-West University), Dr M Blinderman (Ergo Exergy), Mr E. Roberg (African Carbon Energy), and Ms T. Orford.

References

Barker, O.B. 1999. A techno-economic and historical review of the South African coal industry in the 19th and 20th centuries, Part 1. *Bulletin* 113. Department of Minerals and Energy.

Blinderman, M. 2016. *Personal communication* [Interview].

Choudhry, V. and Hadley, S. 1996. Utilization of lightweight materials made from coal gasification slags. *Proceedings of Advanced Coal-Fired Power Systems '96 Review Meeting*, Morgantown, WV. http://citeseerx.ist.psu.edu/viewdoc/download?doi=10.1.1.172.3837&rep=rep1&type=pdf

Couch, G. 2009. Underground Coal Gasification. CCC/151 ed. Clean Coal Centre, International Energy Agency, London:

Department of Energy. 2010. South African Integrated Resource Plan (IRP). Pretoria.

Exxaro Resources Limited. 2013.

Fossil Fuel Foundation. 2013. South African Coal Roadmap. Johannesburg.

Ginster, M. and Matjie, R. 2005. Beneficial utilization of Sasol coal gasification ash. *Proceedings of World of Coal Ash (WOCA)*, Lexington, KY, 11–15 April 2005. University of Kentucky Center for Applied Energy Research and the American Coal Ash Association. pp. 11–15.

Liu, S., Li, J., Mei, M., and Dong, D. 2007. Groundwater pollution from underground coal gasification. *Journal of China University of Mining and Technology*, vol. 17, no. 4. pp. 467–472.

Love, D. 2016. Towards closing the dirty water and carbon loops in cleaner UCG production. *South African Underground Coal Gasification Workshop*, Sandton.

Love, D., Aphane, V., van der Linde, G. and van Zyl, N. 2015a. Innovative approaches to predicting, mitigating and remediating groundwater pollution in UCG. SAUCGA, Secunda.

Love, D., Beeslaar, M., Blinderman, M., Pershad, S., van der Linde, G., and van der Riet, M. 2014b. Ground water monitoring and management in underground coal gasification. *Proceedings of the FFF Underground Coal Gasification (UCG) III Workshop*, Johannesburg, South Africa, 28 August 2014. Fossil Fuel Foundation.

Mining Weekly. 2013. Underground coal gasification holds promise. http://www.miningweekly.com/print-version/underground-coal-gasification-holds-promise-as-energy-source-sipho-nkosi-2013-08-19

Murugan, S. and Horack, B. 2016. Tri and polygeneration systems – A review. *Renewable and Sustainable Energy Reviews*, vol. 60. pp. 1032–1051.

National Planning Commission. 2010. National Development Plan 2030. Our future - make it work. Pretoria.

Pershad, S. 2016. UCG – Eskom's experience and future projects. South African Underground Coal Gasification Association, Sandton.

Pershad, S. 2017. UCG within the South African context : Eskom's experience to date. *Proceedings of the IEA Energy Efficiency and Emission Challenges Workshop*, Kruger Park.

Smoli ski, A., Sta czyk, K., Kapusta, K., and Howaniec, N. 2012. Analysis of the organic contaminants in the condensate produced in the *in situ* underground coal gasification process. *Water Science & Technology*, vol. 67. pp. 644–650.

Smoli ski, A., Sta czyk, K., Kapusta, K., and Howaniec, N. 2012. Chemometric study of the ex situ underground coal gasification wastewater experimental data. *Water, Air and Soil Pollution*, vol. 223. pp. 5745–5758.

Van der Riet, M., Beeslaar, M., Blinderman, M., Love, D., Pershad, S., and van der Linde, G. 2014. Groundwater monitoring and management in UCG. South African Underground Coal Gasification Association, Sandton. ◆

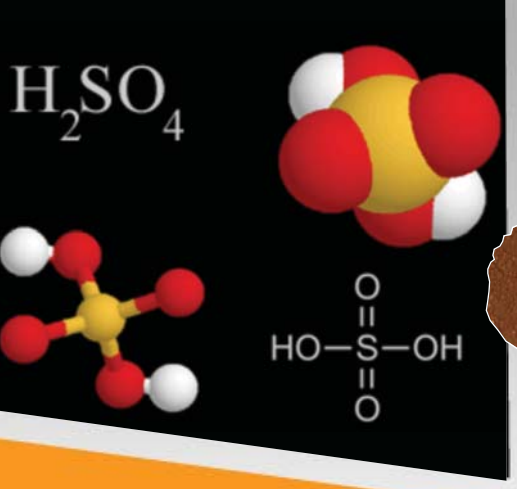

7th Sulphur and Sulphuric Acid 2019 Conference

11–12 March 2019 Conference

13 March 2019 Technical Visit

Swakopmund Hotel, Swakopmund, Namibia

BACKGROUND

The production of SO_2 and sulphuric acid remains a pertinent topic in the Southern African mining and metallurgical industry, especially in view of the strong demand for, and increasing prices of, vital base metals such as cobalt and copper.

The electric car revolution is well underway and demand for cobalt is rocketing.

New sulphuric acid plants are being built, comprising both smelters and sulphur burners, as the demand for metals increases. However, these projects take time to plan and construct, and in the interim sulphuric acid is being sourced from far afield, sometimes more than 2000 km away from the place that it is required.

The need for sulphuric acid 'sinks' such as phosphate fertilizer plants is also becoming apparent.

All of the above factors create both opportunities and issues and supply chain challenges.

To ensure that you stay abreast of developments in the industry, the Southern African Institute of Mining and Metallurgy invites you to participate in a conference on the production, utilization, and conversion of sulphur, sulphuric acid, and SO_2 abatement in metallurgical and other processes, to be held in March 2019 in Namibia.

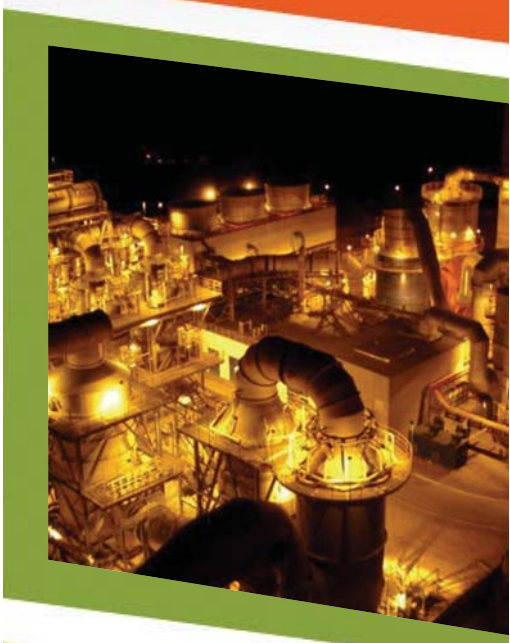

OBJECTIVES

- To expose delegates to issues relating to the generation and handling of sulphur, sulphuric acid, and SO_2 abatement in the metallurgical and other industries.
- Provide an opportunity to producers and consumers of sulphur and sulphuric acid and related products to be introduced to new technologies and equipment in the field.
- Enable participants to share information about and experience in the application of such technologies.
- Provide an opportunity for role players in the industry to discuss common problems and their solutions

WHO SHOULD ATTEND

The Conference will be of value to:

- Metallurgical and chemical engineers working in the minerals and metals processing and chemical industries
- Metallurgical/chemical/plant management
- Project managers
- Research and development personnel
- Academics and students
- Technology providers and engineering firms
- Equipment and system providers
- Relevant legislators
- Environmentalists
- Consultants

EXHIBITION/SPONSORSHIP

There are a number of sponsorship opportunities available. Companies wishing to sponsor or exhibit should contact the Conference Co-ordinator.

For further information contact:

Camielah Jardine
Head of Conferencing, SAIMM,
P O Box 61127, Marshalltown 2107
Tel: (011) 834-1273/7
Fax: (011) 833-8156 or (011) 838-5923
E-mail: camielah@saimm.co.za
Website: http://www.saimm.co.za

SAIMM
THE SOUTHERN AFRICAN INSTITUTE OF MINING AND METALLURGY

Conference Announcement

http://dx.doi.org/10.17159/2411-9717/2018/v118n10a2

Groundwater monitoring during underground coal gasification

by J.C. van Dyk*‡, J. Brand*, C.A. Strydom†, and F.B. Waanders‡

Synopsis

Underground coal gasification (UCG) is a fast-emerging, *in situ* mining technology that provides access to low-cost energy through the utilization of coal reserves that are currently not technically or economically exploitable by conventional mining methods.

Groundwater monitoring for conventional coal mining in South Africa is well established, with SANS, ASTM, and ISO standards for the specific environment, location, and purposes. South Africa's groundwater is a critical resource that provides environmental benefits and contributes to the well-being of the citizens and economic growth. Groundwater supplies the drinking water needs of large portions of the population, and in some rural areas it represents the only source of water for domestic use. Implementation of, and adherence to, groundwater monitoring standards are thus non-negotiable.

The groundwater quality management mission, according to the Department of Water and Sanitation in South Africa, is set in the context of the water resources mission and reads as follows:

'*To manage groundwater quality in an integrated and sustainable manner within the context of the NationalWater Resource Strategy and thereby to provide anadequate level of protection to groundwater resources and secure the supply of water of acceptable quality*.' (SABS, 2016).

In this paper we propose fit-for-purpose groundwater monitoring standards for a commercial UCG operation. It is important to proactively prevent or minimize potential impacts on groundwater through long-term protection and monitoring plans.

Keywords
Groundwater monitoring, underground coal gasification, national standards.

Scope of study / standard proposal

The purpose of this paper is to set out a National Standard Proposal to emphasize groundwater monitoring as one of the five strategies of the '*Policy and Strategy for Groundwater Quality Management in South Africa*' (Department of Water Affairs and Forestry, 2000) and to align it with the National Water Act, Act no. 36 of 1998 (Republic of South Africa, 1998).

The focus of this standard is directed solely towards groundwater monitoring during underground coal gasification (UCG). Groundwater in this context refers to water as sampled from dedicated monitoring wells around the targeted site, which will include the shallow aquifer referred to as groundwater, and water flow at the level of the underground gasifier, referred to as 'coal water'.

The period of monitoring will include:

1. Baseline monitoring before commissioning and start-up
2. Start-up and commissioning
3. Normal operation
4. Decommissioning or site closure
5. Monitoring after closure.

The proposal includes and will be limited to the following aspects:

- Groundwater
- Underground coal gasification (*in situ* coal mining)
- Monitoring boreholes
- Quality control,
- National standards
- Frequency of monitoring.

The proposal does not include:

- Technical specification of monitoring well design
- Monitoring well design and location (only general comments)
- Sampling methodology
- Pollution remediation
- Analytical standard per specific quality parameter
- Borehole location.

Background information

Groundwater monitoring for conventional coal mining in South Africa is well established, with specific SANS, ASTM, and ISO standards dedicated for the specific environment, location, and purposes. Coal mining can have a major impact on groundwater quantity and quality. Groundwater monitoring programmes are thus non-negotiable. The important aspect is to implement a fit-for-purpose monitoring programme for the specific technology,

* *African Carbon Energy, South-Africa.*
† *Chemical Resource Beneficiation, North-West University, South Africa.*
‡ *School of Chemical and Minerals Engineering, North-West University, South Africa.*
 ISSN 2225-6253. Paper received Mar. 2018; revised paper received Jun. 2018.

process, or site location. It is thus important to proactively prevent or minimize the potential impacts on groundwater through long-term protection and monitoring plans.

A successful monitoring program is one that (Barnes and Vermeulen,2007)

(1) Consists of an adequate number of wells, located at planned and strategic points
(2) Yields sufficient groundwater samples
(3) Follows a dedicated monitoring programme and quality control standard.

In order to have an efficient monitoring programme and to avoid unnecessary analysis and costs, it is also critical to determine upfront which parameters have to be monitored for the specific process and site conditions.

An overview of the coal industry in South-Africa, the future energy requirements, and a brief technical discussion on UCG, is presented to sketch the context of the proposed groundwater monitoring standard.

Utilization of coal in South Africa

Coal is globally the most widely used primary fuel, accounting for approximately 36% of the total fuel consumption for electricity production. In South Africa, coal provides approximately 77% of the country's primary energy needs (Figure 1). This is unlikely to change significantly in the next two decades, due to the lack of suitable alternatives. Globally and in South Africa, coal will continue to be the most important fossil fuel for energy production, and with the growing energy demand the demand for coal will increase (Time for Change, n.d.).

Coal is mined in South Africa by both underground and opencast methods, with approximately 37% of production from underground and 63% from opencast mining (Time for Change, n.d.).

Many of the South-African deposits can be exploited at extremely favourable costs, and as a result, a large coal-mining industry has developed (Department of Energy, 2012). The operations range from collieries that are among the largest in the world to small-scale producers. A relatively small number of large-scale producers supply coal primarily for electricity generation and synthetic fuel production. In addition to the extensive use of coal in the domestic economy, approximately 28% of South Africa's coal production is exported, mainly through the Richards Bay Coal Terminal, making South Africa the fourth-largest coal exporting country in the world.

Technologies to improve coal mining and extraction techniques have reached their peak, and according to rough predictions, there is still enough coal for the next 200 years if extraction continues at today's rate. This implies that in the near future the security of coal supplies will not be a concern. However, recovery of currently unmineable coal resources may be problematic in the long term because of the economic and ecological aspects of using this energy resource (Department of Energy, 2012). Coal utilization has always increased and forecasts indicate that in the absence of a dramatic change in policy, this trend will continue in the future. The IEA thus believes that greater efforts are needed by governments and industry to embrace cleaner and more efficient technologies to ensure that coal becomes a much cleaner source of energy in the future (YEA, 2017).

UCG is playing an increasingly important role as a cleaner and more environmentally friendly 'chemical mining' technique. This technique enables highly efficient utilization of the energy and chemical value obtained from the coal without the need for conventional mining operations, stockpiling, reclaiming, and transportation. The generation of mining wastes from overburden, discards, and ash is also avoided. Furthermore, the much-reduced underground infrastructure and elimination of the need for personnel to go underground makes UCG applicable to many deposits that would otherwise be unsafe to mine, unmineable, or sub-economic (Department of Energy, 2012). The 'UCG coal miners' are essentially 'chemical' miners, who work from the surface using drilling technology to access the coal resource and transform it into a recoverable reserve. The work environment is therefore more controllable, and safer. The shorter coal value chain from the resource in the ground to end-product enables UCG to produce lower cost energy than conventional mining.

As a practical illustration, a resource in the Free State area was reclassified from and Inferred Resource to a Measured Resource for UCG applications by Africary. An amount of 3.7 Mt (GTIS) was additionally classified as Measured, according to SAMREC (2009) and SANS 103020:2004, the South African guides to the systematic evaluation of coal resources and coal reserves. This serves as an example of utilizing a reserve that would be unmineable using conventional techniques, through applying the UCG process.

Underground coal gasification (UCG)

UCG is a gasification process used to produce gas from coal *in situ* (underground in the coal seam) by injecting air or oxygen, with or without steam, into the seam and extracting the product gas via wells drilled from the surface. UCG is a high-extraction mining method utilizing at least two boreholes (wells) that are drilled horizontally into the coal seam parallel to one another. Ambient air or air that has been enriched with oxygen is delivered to the coal seam via one or more boreholes (the injection wells) and the coal is ignited in order to start the gasification process. This may be thought of as a thermo-chemical mining process. The burning front results in high temperatures (>1000°C) that cause the coal ahead of the front to effectively reform into gas. Groundwater, augmented by water added to the injection borehole if necessary, reacts with the carbon in the coal to form a combustible gas mixture consisting mainly of carbon

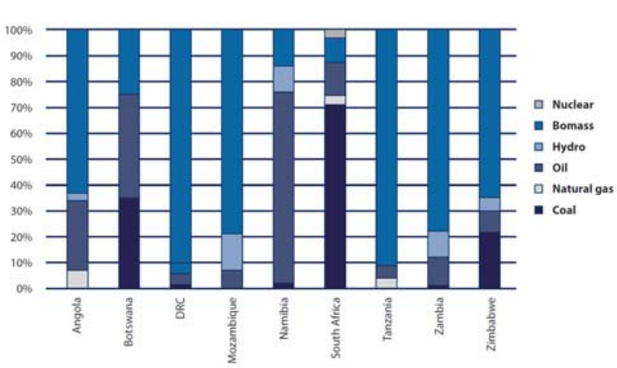

Figure 1—Coal utilization in Africa (Luckos, Shaik, and van Dyk, 2010)

monoxide (CO), hydrogen (H_2), and methane (CH_4). The resulting synthetic gas (syngas) can be used to produce electricity, as well as chemicals, liquid fuels, hydrogen, and synthetic natural gas (Sourcewatch, n.d.). These gases are then forced out through a second borehole (the production well). Ash and other remnants of the coal remain underground in the gasifier. The gasification of coal in this manner creates a reduced coal cavity below the surface, the size of which depends on the rate of water influx from the water table, the heat content of the coal, the location and specifications of the injection and production wells, and the thickness of the coal seam.

This coal reformation takes place at high temperatures, which are created by the gasification front, and high pressure, which is caused by the build-up of hot gases in the underground gasifier. It should be noted that the pressure in the gasifier will always be lower than the hydrostatic head of the groundwater at the depth of the coal seam, which will cause the groundwater to flow slowly towards the gasifier.

UCG has lower environmental and safety impacts than traditional coal mining and power generation. The technology eliminates mine safety issues, surface damage, stockpiles of overburden and discard coal, and solid waste discharge such as ash dumps, and has lower sulphur dioxide (SO_2), nitrogen oxide (NO_x), and particulate (PM_{10}) emissions.

The earliest recorded mention of the idea of underground coal gasification was in 1868. The first successful test was conducted by the Donetsk Institute of Coal Chemistry on 24 April 1934 at Lysychansk in the Soviet Union, where a local chemical plant began using the gas commercially in 1937. A number of UCG projects were established across the world after the Second World War, and UCG is now recognized globally as a technically and economically viable method of accessing deep, otherwise unrecoverable coal reserves, both on- and offshore. It has been estimated that UCG technology could effectively double the energy reserves obtained from the world's coal deposits (African Carbon Energy (Pty) Ltd , n.d.).

UCG presents certain environmental advantages over conventional coal mining. By not requiring mining, UCG can reduce the effects of issues such as acid mine runoff, mine safety, overuse of groundwater, and land reclamation. During gasification, approximately half of the sulphur, mercury, arsenic, tar, and particulates from the coal remain below surface. UGC syngas also has a higher hydrogen concentration than syngas produced on surface, giving it a potential cost advantage when used for electricity generation.

The basic UCG concept, together with the general gasification reactions (van Dyk, Keyser, and Coertzen2006; Luckos, Shaik, and van Dyk, 2010) is illustrated in Figure 2.

Groundwater monitoring at operating sites

Numerous articles on groundwater science, the impacts of industry on groundwater, and groundwater monitoring have been published and it is impossible to capture all information in this paper. However, the most critical and recent views in the literature related to groundwater and also to UCG are highlighted below.

According to Barnes and Vermeulen (2007), the coal industry impacts qualitatively and quantitatively on groundwater in two main areas:

1. Sulphur is one component in particular that contributes in a number of ways to changes in groundwater quality. When water and oxygen come into contact with a sulphide-bearing mineral such as pyrite, a reaction resulting in acid mine drainage occurs. Pyrite reacts with water and oxygen to form dissolved ferrous iron species, which with time increase the acidity of the water.
2. Deterioration of groundwater quantity is caused by the removal of water that has entered the mining operations. This result in a depression cone (decrease in hydraulic head) surrounding the gasification zone, causing dewatering of surrounding aquifers. The depression cone alters the natural flow of groundwater through the creation of paths of less resistance, which results in water entering the mining area.

In developing an analyses list, it is necessary to establish and define the objectives of the monitoring activity (*i.e.* baseline, construction, operational, closure, and post-closure monitoring). Conventional and UCG process-specific analyses techniques should be selected. The general chemistry of an aquifer may be used to monitor changes in the hydrogeological system surrounding a UCG plant. The monitoring of the mobility of chemical species, correlating recharge and flow zones with water quality, assessing the chemical equilibrium and kinetics of groundwater reactions, and developing contour maps and graphical plots are thus all needed to understand the flow and quality of the groundwater system. Monitoring programmes should include basic chemistry species analyses (especially important for ambient and compliance monitoring at larger sites that have the potential to be influenced by other contaminants), neighbouring facilities, and groundwater flow paths (Commonwealth of Pennsylvania, 2001).

Ahern and Frazier (1982) investigated changes in groundwater quality at various field test sites and in laboratory experiments. Their report summarizes more than 300 articles and 19 UCG field tests that were in operation or completed in the 1980s. The most significant findings and summaries related to UCG groundwater are highlighted.

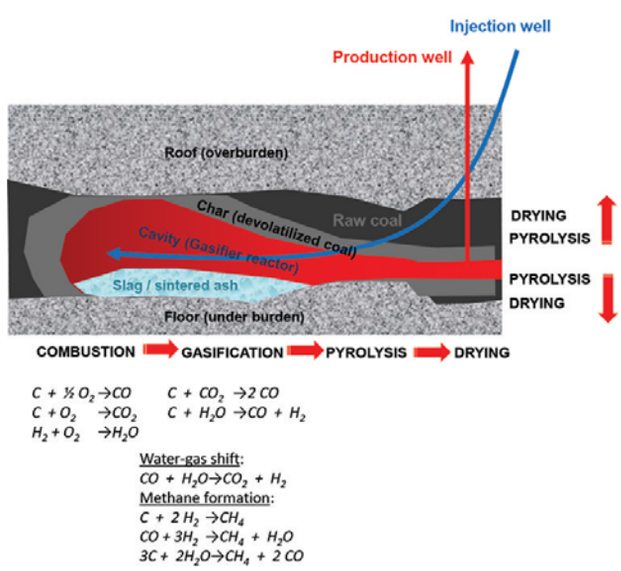

Figure 2—General concept of UCG

1. At the Hoe Creek I monitoring network, in the Powder River Basin, Wyoming, 11 wells were drilled into the coal aquifer. Water quality samples were taken during the burn, and 3 days, 83 days, 183 days and randomly over a 25-month period after the burn. Analyses for more than 70 inorganic and organic species were carried out. The following most significant changes were observed:
   a. Ammonium, boron, calcium, bromide, lithium, cyanide, magnesium, sulphate, potassium, and phenols showed at least a five-fold increase in the water in comparison to the baseline case, both within the burn zone and outside the zone.
   b. Other species reported to have increased in the water samples were barium, lead, organic carbon, and volatile organics.

   Most of the changes occurred within 10 ft (3 m) of the burn zone and independent of direction. Concentrations of several species increased over time at a monitoring well located 10 ft (3 m) from the burn zone, due to movement of contaminated groundwater out of the burn zone.
2. The Hoe Creek II monitoring network consisted of 14 wells drilled into the gasified coal cavity and overlying aquifer. Water quality samples were taken before the burn, during the burn, and at least five times up to 9 months after completion of the burn (Ahern and Frazier, 1982). The list of species at Hoe Creek II which increased in concentration in the groundwater closely parallels those measured at Hoe Creek I. The differences in concentration levels between the two sites can be attributed to differences in coal quality and rates of gasification.
3. Water quality data from the Hanna sites was obtained from the Hanna III test, which consisted of 12 wells drilled into the coal seam and overlying aquifer. Water quality was monitored before, during, and after operation (Ahern and Frazier,(982), and the main findings were summarized as follows:
   a. Conductivity and temperature increased over baseline values in both the coal aquifer and overlying water aquifer.
   b. Sodium and dissolved solids increased in all wells up to a period of 1 year after gasification.
   c. Sulphate and chloride ionic concentrations decreased in all wells.
   d. Aluminium concentrations increased to almost 100 times over the baseline values during the UCG operation, but rapidly decreased to the baseline values afterwards.
   e. Other elements and compounds that increased during gasification were boron, copper, iron, lead, zinc, calcium, ammonia, and sulphate compounds, in agreement with both Hoe Creek I and II findings.
4. Water quality tests were also reported for the UCG tests in Fairland, Tennessee Colony, and the Big Brown sites in Texas (Ahern and Frazier, 1982). At the Fairland monitoring network four wells were drilled into the coal seam, six close-in wells to the other aquifers and 40 wells at greater distances from the burn. The water quality was monitored before the experiment, at the end of gasification, and also one year after gasification. The main findings were:
   a. Concentrations of all monitored inorganic species increased during gasification, especially calcium, zinc, iron, hydrogen, magnesium, ammonium, manganese, sulphate, mercury, and boron.
   b. Phenols were the principal organic species produced, but high amounts of two- and three-ring polynuclear aromatic hydrocarbons were also observed, especially during gasification.
5. In the Huntley UCG pilot operations, New Zealand, the first and most important conclusion was that there were no detrimental effects on the groundwater in the Tauranga Group aquifer by either contamination or depletion. A spike in the dissolved organic carbon (DOC) was observed at the coal seam in one well during a period of high pressure, which reverted to background levels once the pressure was reduced. Monitoring wells further away showed no response. Although a wide range of chemical components were monitored, changes in DOC proved to be the most responsive indicator of the effects of gasification (Dobbs *et al.*, 2014).

Despite similar results from the different sites at which groundwater has been monitored and specific species showing general trends, it has to be stressed that a number of factors can influence these results. The following information on the specific site has to be taken into account regarding the effect of groundwater changes.

- Coal type—the coal rank may determine the type and relative amounts of chemical species produced during a UCG process; for example, liquid hydrocarbons, phenols, *etc.*
- Amount of coal gasified—this may be related to the amount of chemical species generated.
- Injection agent—the chemical composition of the atmosphere in which the coal is pyrolised may influence the types of chemical species formed.
- System pressure—this factor influences the distances which volatile species can move from the burn cavity during UCG operation.
- Burn cavity temperature—the temperature affects the mineralogy of the coal ash in the burn cavity and the leachability of constituents within the ash.
- Product gas composition—the composition, together with the cavity temperature, provides a measure of the ash leachability.
- Gas losses—gases produced by UCG cause changes in the chemical equilibrium and dissolution of certain species in the surrounding water.
- Roof collapse—a collapse of overburden into the cavity can introduce material of different chemical composition into the gasification hot zone and affect movement of chemical species.
- Interconnection of aquifers—interconnection through fracturing, roof collapse, ruptured borehole casing, or by other means can change groundwater movement and the movement of chemical species.

The water quality information gathered at UCG sites is not abundant, but appears to be adequate for developing a theory that explains similarities and differences in water

quality at various UCG sites. Some of the similarities and differences in water quality may be real, while others are only apparent. Real differences may result from different gasification techniques, different coal ranks, different hydrogeologies, or different baseline water quality.

Well location (not discussed in this paper) is site-specific and will differ for projects with different aims.

Proposed groundwater monitoring standard for UCG sites

Groundwater or borehole water is used without treatment for human and livestock consumption and other agricultural activities. Groundwater, as a natural source of water, cannot be directly required to adhere to the specifications of SANS 241-1, but it is recommended that any changes in water quality due to UCG activities must not decrease the quality to below the minimum standard stipulated in SANS 241-1 standard. The SANS standard is specifically cited to incorporate a standard with tighter restrictions. In summary, it is proposed that

- Baseline groundwater quality to be measured and monitored on a continuous basis
- SANS 241-1 to be used as standard to compare to the baseline quantity
- Minimum limits to be determined between a combination of (1) and (2) and the specification to be set at the determined quality values. Thus, if the baseline value for a specific property is higher compared to the baseline for drinking water as specified in SANS 241-1, then the baseline value will be set as standard; otherwise the standard stipulated in SANS 241-1 will be used.

The drinking water parameters according to SANS 241-1 shall comply with the physical, aesthetic, and chemical limits for lifetime consumption, as specified in Table I.

There are only a few chemical species in water that can lead to health problems as a result of a single exposure, except through massive accidental contamination of a drinking water supply. Moreover, experience shows that in many, but not all single exposures, the water becomes undrinkable due to unacceptable taste, odour, and appearance. Chemicals that cause adverse health effects include fluoride, arsenic, phenols, benzenes, and nitrate compounds. Human health effects have also been demonstrated in the case of lead (from domestic plumbing), while there is also concern regarding the potential extent of exposure to iron, manganese, selenium, and uranium. . These species should be taken into consideration as part of any risk assessment process (SABS, 2016).

The methods of analysis should be chosen to apply the necessary limit of quantification of SANS 241 and to be of the required accuracy and precision (SABS, 2016).

It is proposed that sampling of groundwater be conducted according to current SANS or ISO standards (Table II).

Laboratory quality control may be conducted according to the ISO 17025:2005 standard.

Table III summarizes the groundwater monitoring properties to be measured on each monitoring well (sentinel and compliance wells) on both the groundwater and coal water, as well as the measuring frequency.

The SANS, ASTM, or ISO standards listed in Table IV are recommended for the analyses as specified in Table III and serve as a guide, but overall laboratory quality control based on ISO 17025:2005 should be adhered to.

Conclusions

The importance of water and the environmental impact that specific operations may have on groundwater necessitate that standardized monitoring and rehabilitation programmes be adopted.

UCG is a fast-emerging *in situ* mining technology that can be used to exploit coal resources that are currently not technically or economically viable by conventional mining methods. As such it offers significant potential to increase the world's recoverable coal resources. The UCG plant operation, however, has to be performed in an environmentally responsible manner.

Table I

Physical, aesthetic, operational and chemical parameters of drinking water as specified in SANS 241-1

Water properties	Standard limit[a]	Water properties	Standard limit[a]	Water properties	Standard limit[a]
Free chlorine	≤5 mg/L	Nitrate as N	≤11 mg/L	Zinc as Zn	≤5 mg/L
Monochloramine	≤3 mg/L	Nitrite as N	<0.9 mg/L	Antimony as Sb	≤20 µg/L
Colour	≤15 mg/L Pt-Co	Sulphate as SO_4^{2-}	<500 mg/L	Arsenic as As	≤10 µg/L
Conductivity at 25°C	≤170 mS/m	Fluoride as F^-	≤1.5 mg/L	Cadmium as Cd	≤3 µg/L
Odour or taste	Inoffensive	Ammonia as N	≤1.5 mg/L	Chromium as Cr	≤50 µg/L
Total dissolved solids	≤1200 mg/L	Chloride as Cl^-	≤300 mg/L	Cobalt as Co	≤500 µg/L
pH at 25°C	≥5 to ≤9.7	Sodium as Na	≤200 mg/L	Copper as Cu	≤2000 µg/L
Cyanide as CN^-	≤70 µg/L	Manganese as Mn	≤500 µg/L	Selenium as Se	≤10 µg/L
Iron as Fe	≤2000 µg/L	Mercury as Hg	≤6 µg/L	Uranium as U	≤15 µg/L
Lead as Pb	≤10 µg/L	Nickel as Ni	≤70 µg/L	Vanadium as V	≤200 µg/L
Aluminium as Al	≤300 µg/L	Chloroform	≤0.3 mg/L	Bromodichloro-CH_4	≤0.1 mg/L
Total organic C	≤10 mg/L	Bromoform	≤0.1 mg/L	Dibromochloro-CH_4	≤0.06 mg/L
Phenols and benzenes	≤10 µg/L	Microcystin as LR[b]	≤1 µg/L		

a – The health-related standards are based on the consumption of 2 L of water per day by a person of a mass of 60 kg over a period of 70 years.
b – Microcystin needs to be measured only where an algal bloom (> 20 000 cyanobacteria cells per millilitre) is present in a raw water source. In the absence of algal monitoring, an algal bloom is deemed to occur where the surface water is visibly green in the vicinity of the abstraction, or samples taken have a strong musty odour.

Table II

SANS and ISO standards for sampling of mine and groundwater

Date : 2014-06-06 — *List of Standards and Abstracts* — Page No : 1 Of 2
Report Id : std_abs — TITLE : SANS Standards - Mine and Groundwater Testing — Requested By: EILEEN WEBB

SANS Number Int. Relatedness	SABS Number	Year	Edition	Status Code	Title	Abstract	Amend Code	Amend Number	Corr Number	Amend Ind	Amend Date
SANS 376 (ASTM D 2972:2003, IDT)		2005	1.00	ST	Standard test methods for arsenic in water	Specifies test methods that cover the photometric and atomic absorption determination of arsenic in most waters and wastewaters.					
SANS 5667-11 (ISO 5667-11:1993, IDT)	SABS ISO 5667-11	1993	1.00	ST	Water quality - Sampling Part 11: Guidance on sampling of groundwaters	Provides guidance on the design of sampling programmes, sampling techniques and the handling of water samples taken from groundwater for physical, chemical and microbiological assessment.	A	1		N	2006-02-16
SANS 5667-14 (ISO 5667-14:1998, IDT, Ed. 1)		2007	1.00	ST	Water quality - Sampling Part 14: Guidance on quality assurance of environmental water sampling and handling	Provides guidance on the selection and use of various quality assurance techniques relating to the manual sampling of surface, potable, waste, marine and ground waters.					
SANS 5667-18 (ISO 5667-18:2001, IDT, Ed. 1)		2007	1.00	ST	Water quality - Sampling Part 18: Guidance on sampling of groundwater at contaminated sites	Provides guidance on the sampling of groundwater at potentially contaminated sites. Is applicable to situations where contamination of the subsurface could exist as a result of downward migration of pollutants whose source is at the surface or just below it, and when the guidance in ISO 5667-11 (published in South Africa as an identical adoption under the designation SANS 5667-11) is inappropriate.					
SANS 6059	SABS SM 1059	2010	2.01	ST	Water - Mercury content	Specifies a method for the determination of the mercury content of water and wastewater by using atomic absorption spectrophotometry. The method is applicable to the determination of mercury in the concentration range 0,001 mg/L to 0,010 mg/L.	A	1		N	2010-04-23
SANS 10286	SABS 0286	1998	1.00	ST	Mine residue	Covers the disposal of mine residue in residue deposits. This residue includes all waste that is produced by a mine and that is defined as waste in terms of the Minerals Act, 1991 (Act 50 of 1991). Slimes dams, tailings dams, rock dumps, slurry ponds and discards and similar deposits all fall within the scope of this standard.					

Date : 2014-06-06 — *List of Standards and Abstracts* — Page No : 2 Of 2
Report Id : std_abs — TITLE : SANS Standards - Mine and Groundwater Testing — Requested By: EILEEN WEBB

SANS Number Int. Relatedness	SABS Number	Year	Edition	Status Code	Title	Abstract	Amend Code	Amend Number		Amend Ind	Amend Date
SANS 10299-1	SABS 0299-1	2003	1.01	ST	Development, maintenance and management of groundwater resources Part 1: The location and siting of water boreholes	Covers requirements for the location and siting of water boreholes. Whenever a borehole is considered for conversion to a water production borehole, the relevant clauses of this part of SANS 10299 shall apply.	A	1		N	2003-09-12
SANS 10523 (ISO 10523:2008, IDT, Ed. 2)		2012	1.00	ST	Water quality - Determination of pH	Specifies a method for determining the pH value in rain, drinking and mineral waters, bathing waters, surface and ground waters, as well as municipal and industrial waste waters, and liquid sludge, within the range pH 2 to pH 12 with an ionic strength below I = 0,3 mol/kg solvent and in the temperature range 0 °C to 50 °C.					
SANS 16590 (ISO 16590:2000, IDT, Ed. 1)	SABS ISO 16590	2000	1.00	ST	Water quality - Determination of mercury - Methods involving enrichment by amalgamation	Specifies two methods for the determination of mercury, one using tin(II) chloride and the other sodium tetrahydroborate as reducing agent. The methods are suitable for the determination of mercury in water, for example in ground, surface or waste water, in the concentration range 0,01 µg/L to 1 µg/L. Higher concentrations may be determined if the water sample is diluted.	A	1		N	2006-11-17

Table III

Frequency of measurement of important groundwater properties of importance

Property to monitor	Baseline period[a] (12 months)	Pre-gasification period[b]	Gasification[c]	Shut-down post-gasification[d]	After shut-down[e] (36 months)
Water level	Monthly	Daily#	Daily#	Daily#	3-monthly
pH value	Monthly	Daily#	Daily#	Daily#	3-monthly
Conductivity	Monthly	Weekly#	Weekly#	Weekly#	3-monthly
Total dissolved solids	Monthly	Monthly	3-monthly	Monthly	3-monthly
Total solids and loss on ignition	Monthly	Monthly	3-monthly	Monthly	3-monthly
Total alkalinity	Monthly	Monthly	3-monthly	Monthly	3-monthly
Calcium	Monthly	Monthly	3-monthly	Monthly	3-monthly
Magnesium	Monthly	Monthly	3-monthly	Monthly	3-monthly
Potassium	Monthly	Monthly	3-monthly	Monthly	3-monthly

Table III (Continued)

Frequency of measurement of important groundwater properties of importance

Property to monitor	Baseline period[a] (12 months)	Pre-gasification period[b]	Gasification[c]	Shut-down post-gasification[d]	After shut-down[e] (36 months)
Sodium	Monthly	Monthly	3-monthly	Monthly	3-monthly
Colour hazen unit	Monthly	Monthly	3-monthly	Monthly	3-monthly
Turbidity N.T.U	Monthly	Monthly	3-monthly	Monthly	3-monthly
Odour	Monthly	Monthly	3-monthly	Monthly	3-monthly
Carbonate Hardness	Monthly	Monthly	3-monthly	Monthly	3-monthly
Chloride	Monthly	Monthly	3-monthly	Monthly	3-monthly
Sulphate	Monthly	Monthly	3-monthly	Monthly	3-monthly
pH value	Monthly	Monthly	3-monthly	Monthly	3-monthly
Conductivity	Monthly	Monthly	3-monthly	Monthly	3-monthly
Total dissolved solids	Monthly	Monthly	3-monthly	Monthly	3-monthly
Total solids and loss on ignition	Monthly	Monthly	3-monthly	Monthly	3-monthly
Total alkalinity	Monthly	Monthly	3-monthly	Monthly	3-monthly
Calcium	Monthly	Monthly	3-monthly	Monthly	3-monthly
Magnesium	Monthly	Monthly	3-monthly	Monthly	3-monthly
Potassium	Monthly	Monthly	3-monthly	Monthly	3-monthly
Sodium	Monthly	Monthly	3-monthly	Monthly	3-monthly
Colour Hazen unit	Monthly	Monthly	3-monthly	Monthly	3-monthly
Turbidity N.T.U	Monthly	Monthly	3-monthly	Monthly	3-monthly
Odour	Monthly	Monthly	3-monthly	Monthly	3-monthly
Carbonate Hardness	Monthly	Monthly	3-monthly	Monthly	3-monthly
Chloride	Monthly	Monthly	3-monthly	Monthly	3-monthly
Sulphate	Monthly	Monthly	3-monthly	Monthly	3-monthly
Sulphite	Monthly	Monthly	3-monthly	Monthly	3-monthly
Settleable solids	Monthly	Monthly	3-monthly	Monthly	3-monthly
Nitrate	Monthly	Monthly	3-monthly	Monthly	3-monthly
Nitrite	Monthly	Monthly	3-monthly	Monthly	3-monthly
Fluoride	Monthly	Monthly	3-monthly	Monthly	3-monthly
Mercury	Monthly	Monthly	3-monthly	Monthly	3-monthly
Hexavalent chromium	Monthly	Monthly	3-monthly	Monthly	3-monthly
Total cyanide	Monthly	Monthly	3-monthly	Monthly	3-monthly
Phenolic compounds as phenol and benzenes	Monthly	Monthly	3-monthly	Monthly	3-monthly
Biochemical oxygen demand	Monthly	Monthly	3-monthly	Monthly	3-monthly
Chemical oxygen demand	Monthly	Monthly	3-monthly	Monthly	3-monthly
Total soluble solids	Monthly	Monthly	3-monthly	Monthly	3-monthly
Soap, oil and grease	Monthly	Monthly	3-monthly	Monthly	3-monthly
Sulphide sulphur	Monthly	Monthly	3-monthly	Monthly	3-monthly
Sulphide sulphur	Monthly	Monthly	3-monthly	Monthly	3-monthly
Free and saline ammonia	Monthly	Monthly	3-monthly	Monthly	3-monthly
Kjeldahl nitrogen	Monthly	Monthly	3-monthly	Monthly	3-monthly
Acidity/P-alkalinity	Monthly	Monthly	3-monthly	Monthly	3-monthly
Dissolved oxygen	Monthly	Monthly	3-monthly	Monthly	3-monthly
Oxygen absorbed (permanganate value)	Monthly	Monthly	3-monthly	Monthly	3-monthly
Residual/free chlorine	Monthly	Monthly	3-monthly	Monthly	3-monthly
Bromide	Monthly	Monthly	3-monthly	Monthly	3-monthly
Calcium carbonate saturated pH	Monthly	Monthly	3-monthly	Monthly	3-monthly
Free carbon dioxide	Monthly	Monthly	3-monthly	Monthly	3-monthly
Arsenic, selenium, titanium, aluminium, nickel, manganese, iron, vanadium, zinc, antimony, ead, cobalt, copper, total chromium, silicon, tin, zirconium, bismuth, thallium, beryllium, cadmium, boron, phosphorus as phosphate, uranium, molybdenum, barium, silver, thorium, lithium, (also Ca, Mg, K, Na)	Monthly	Monthly	3-monthly	Monthly	3-monthly

a – Period before commissioning, drilling or start-up. The current situation.
b – When drilling of wells will start and ignition of coal seam will take place.
c – Normal operating period of the UCG process and gasifier cavity.
d – Period of de-commissioning, cooling and shut-down of gasifier cavity.
e – The period after shut-down when the site is rehabilitated and gasifier cavity out of operation.
– Variation in pH and conductivity according to ISO 17025:2005 will enforce monitoring on a daily basis until the cause of variation has been resolved or quality is back to baseline values

Table IV

Available and recommended SANS, ASTM, and ISO standards to evaluate water quality

Property to monitor	Standard to be applied
pH value	SANS 5011
Conductivity	SANS 7888
Total dissolved solids	SANS 5213
Total solids and loss on ignition	SANS 5213 and
Total Alkalinity	ASTM D1067
Calcium	SANS 450, 6265 and 11885
Magnesium	SANS 6265 and 11885
Potassium	
Sodium	SANS 6050 and 11885
Colour Hazen unit	SANS 5198
Turbidity N.T.U	SANS 375 and 5197
Odour	No specific standard
Carbonate hardness	ISO 9963
Chloride	SANS 163-1 and 374
Sulphate / sulphite	SANS163-1 and 6310
Nitrate / nitrite	SANS 5210
Fluoride	SANS 163-1, 10359-1 and 10359-2
Mercury	SANS 6059
Hexavalent chromium	SANS 6054 and 11885
Total cyanide	SANS 4374, 6703-1
Phenolic compounds as phenol	SANS 6439
Biochemical oxygen demand	ISO 15705
Chemical oxygen demand	ISO 15705
Total soluble solids	ISO 21338:2010
Soap, oil and grease	ASTM D4281
Sulphide sulphur	ISO 6326
Free and saline ammonia	SANS 5217
Dissolved oxygen	SANS 6047
Residual/free chlorine	ISO 7393
Bromide	ISO 11206
Calcium carbonate saturated pH	SAN 50897
Free carbon dioxide	ISO 10523
Organic compounds, *i.e.* phenols and benzenes	ISO 16-128
Arsenic, selenium, titanium, Aluminium, nickel, manganese, Iron, vanadium, zinc, antimony, Lead, cobalt, copper, Total chromium, silicon, tin, Zirconium, bismuth, thallium, Beryllium, cadmium, boron, Phosphorus as phosphate, Uranium, molybdenum, barium, Silver, thorium, lithium, (also Ca, Mg, K, Na).	SANS 376, 11885, 379, 6054, 11885, 6170, 5203, 4374, 382, 5209, 6171, 377 and 383

Numerous studies have been published on groundwater science, the impact of industries on groundwater quality, and groundwater monitoring. Using some of these findings, it is important to develop a groundwater monitoring programme for UCG sites before the start-up of such an operation.

Groundwater monitoring in the South African mining industry for conventional coal mining is well established, with specific SANS, ASTM, and ISO standards dedicated for the specific environment, location, and purposes. The South African UCG and gas industries, however, are relatively unregulated at this stage. South Africa's groundwater is a critical resource. Utilization and implementation of groundwater monitoring standards are thus non-negotiable.

A National Standard has been proposed in this paper as a fit-for-purpose groundwater monitoring programme for commercial UCG operations.

Acknowledgements

Part of the research presented in this paper was hosted by the South African Research Chairs Initiative (SARChI) of the Department of Science and Technology and National Research Foundation of South Africa (Coal Research Chair Grant No. 86880).

Any opinion, finding or conclusion or recommendation expressed in this material is that of the author(s) and the NRF does not accept any liability in this regard.

In addition to the co-authors of this study, the following people and institutions are acknowledged for their inputs to this study.

- Dr Jennifer Pretorius, Senior Hydrologist, Golder Associates Africa (Pty) Ltd
- Michael Barnes, Hydrogeologist, Cabanga
- C. Bosman, Director CBSS Consulting
- Concepts, www.cabangaconcepts.co.za
- Sonia Maritz, Geologist, Shanduka Coal
- Johan de Korte, CSIR Consulting
- Lerato Mahalo, Standards SA
- R.J. Vreeswijk, Laboratory Manager, Buckman Africa
- J.F. Brand, CEO, African Carbon Energy
- Frikkie van Heerden, Buckman Africa
- Professor F.B. Waanders, North-West University
- Gerhard van der Linde, Associate, Divisional Leader – Groundwater, Golder Associates Africa (Pty) Ltd
- Dr Wietsche Roets, Department of Water and Sanitation
- Professor C, Strydom, North-West University
- Professor I. Dennis, North-West University

References

African Carbon Energy (Pty) Ltd. Draft EIA Report: underground coal gasification and power generation project near Theunissen. DEA Reference number: 14/12/16/3/3/2/558, EMS-9,22,23,3,4,5,26/13/11

Ahern, J.J. and Frazier, J.A. 1982. Water quality changes at underground coal gasification sites – A literature review'. Water Resources Research Institute University of Wyoming, Laramie, Wyoming.

Barnes, M.R. and Vermeulen, P.D. 2007. Guide to groundwater monitoring for the coal industry. Institute of Groundwater Studies, University of the Free State, Bloemfontein, South Africa.

Commonwealth of Pennsylvania, Department of Environmental Protection. 2001. Groundwater monitoring guidance manual. http://www.depgreenport.state.pa.us/elibrary/GetDocument?docId=7616&DocName=GROUNDWATER%20MONITORING%20GUIDANCE%20MANUAL.PDF%20

Department of Energy. 2012. Coal resources overview. Pretoria. http://www.energy.gov.za/files/coal_frame.html

Department of Water Affairs and Forestry. 2000. Policy and Strategy for Groundwater Quality Management in South-Africa. 1st edn. Pretoria.

Department of Water Affairs and Forestry. 2007. Best Practice Guideline G3. Water, Monitoring Systems, July 2007. http://www.dwaf.gov.za/Groundwater/Documents.aspx

Dobbs, R.M., Pearce, S.M., Gillard, G.R., Crampton, N.A., and Pattle, A.D. 2014. Deep groundwater characterisation and monitoring of a UCG pilot plant. Pattle Delamore and Partners, Christchurch, New Zealand.

IEA. 2017. International Atomic Energy, Paris. http://www.iea.org/topics/coal/

Luckos, A., Shaik, M.N., and van Dyk, J.C. 2010. Gasification and pyrolysis of coal. *Handbook of Combustion*. Vol. 4: *Solid Fuels*. Lackner, M., Winter, F., and Agarwal, A.K. (eds.). Wiley-VCH, Weinheim. pp. 325-364.

Republic of South Africa. 1998. National Water Act, Act No. 36 of 1998, 20 August 1998.

SABS. 2016. SANS 241-1:2011, Edition 1. South African National Standard, Drinking water, Part 1: Microbiological, physical, aesthetic, and chemical determinants. SABS Standards Division, Pretoria.

SAMREC. 2009. South African Mineral Resource Committee. The South African Code for Reporting of Exploration Results, Mineral Resources and Mineral Reserves (the SAMREC Code). 2007 Edition as amended July 2009. http://www.samcode.co.za/downloads/SAMREC2009.pdf

Sourcewatch. Not dated. http://www.sourcewatch.org/index.php/Underground_Coal_Gasification#Recent_UCG_Projects

Time for Change. (Not dated). http://timeforchange.org/prediction-of-energy-consumption

Van Dyk, J.C., Keyser, M.J., and Coertzen, M. 2006. Syngas production from South African coal sources using Sasol-Lurgi gasifiers. *International Journal of Coal Geology*, vol. 65. pp. 243-253.

Van Wyk, D. 2014. Competent Person's geological report including the recent drilling of the defined target area of Theunissen underground gasification project. African Carbon Energy, June 2014. ◆

http://dx.doi.org/10.17159/2411-9717/2018/v118n10a3

Conceptual use of vortex technologies for syngas purification and separation in UCG applications

by J.F. Brand*†, J.C. van Dyk*†, and F.B. Waanders†

Synopsis

Syngas from Africary's Theunissen underground coal gasification (UCG) project will be used for power production and synthesis of liquid fuels and commodity chemicals. However, some of the coal components, especially condensable water, oils, tars, inorganic trace elements, and a small fraction of fly ash and particulate matter, make their way to the surface via the production well and can cause adverse impacts on downstream processes. Africary's standard design incorporates a cold gas clean-up system that relies on relatively mature techniques based on highly effective wet scrubbers and acid gas removal (AGR) systems such as Rectisol®, but with the downside of low energy efficiency and waste water generation. In this paper, novel technologies for removing contaminants and species separation from the hot ($T > 300$°C) raw syngas are compared. Comparisons are made between supersonic gas separation (SGS), Ranque–Hilsch vortex tube (RHVT), vortex gradient separation (VGS), and inertia vacuum filtering (IVF), and a vortex-based gas separation concept is proposed for UCG applications.

Keywords

underground coal gasification, gas cleaning, supersonic gas separation, Ranque–Hilsch vortex tube, vortex gradient separation, inertia vacuum filter.

Introduction

Impurities in gasification feedstock (coal, biomass, waste, *etc.*), especially sulphur, nitrogen, chlorine, and inorganic mineral matter, often end up in the syngas and can cause adverse impacts on downstream processes. Africary's standard design incorporates a cold gas clean-up system that relies on relatively mature techniques based on highly effective wet scrubbers and acid gas removal (AGR) systems such as Rectisol®, Selexol® or aMDEA®; but with the downside of low energy efficiency and waste water generation.

Hot ($T > 300$°C) gas clean-up technologies are attractive because they avoid cooling and reheating of the syngas stream. Some available warm gas cleaning technologies include traditional particulate removal devices such as cyclones, candle filters, membranes, and molecular sieves. The warm gas desulphurization process technology developed by RTI LLC (2018) requires hot syngas to remove sulphur and has become commercially ready. Many other hot gas clean-up systems are still under development, given the technical difficulties caused by extreme environmental and operating conditions.

High-temperature syngas cleaning has been the focus of research for over three decades (Sharma *et al.*, 2008), but a scientifically proven and tested technology has not yet been commercialized. Significant improvements have been achieved with candle filters in the past few years (Prabhansu *et al.*, 2015); however, these conventional warm gas cleaning technologies have fundamental limitations due to the intrinsic material properties of candle filters that cause practical problems and lead to unacceptable availability.

Sharma *et al.* (2008) presented the status of syngas cleaning technologies for particulate removal systems and reviewed the practical problems and limitations faced by these gas cleaning systems. Recommendations were also made to overcome these fundamental limitations. Gas clean-up technologies can generally be classified according to the process temperature range: hot gas clean-up (HGC), cold gas clean-up (CGC), or warm gas clean-up (WGC). There is considerable ambiguity in the literature around the definitions, and Woolcock and Brown (2013) propose a more rigorous classification based on condensation temperatures of various compounds. CGC generally describes wet scrubbing processes (Balas *et al.*, 2014) that operate at near-ambient conditions, utilizing water sprays, and which result in exit temperatures that allow water to condense and the contaminants either being absorbed into the water droplets or serving as nucleation sites for water condensation (Woolcock and Brown, 2013). WGC is often assumed to occur at temperatures higher than the boiling point of water but which still allow for ammonium

* *African Carbon Energy, South Africa.*

† *Centre of Excellence in Carbon based fuels, School of Chemical and Minerals Engineering, North-West University, South Africa.*

 ISSN 2225-6253. Paper received Apr. 2018; revised paper received Jul. 2018.

chloride condensation. This typically implies a warm upper limit of temperatures of about 300°C. HGC typically occurs at temperatures higher than 300°C, at which it is still likely that several alkali compounds will condense (Hirohata *et al.*, 2008).

UCG has the potential to produce raw syngas at the production well on surface that is both hot and at pressure; ideal for the Fischer-Tropsch (FT) process, which preferably requires the clean syngas to be at temperatures of >250°C and pressures >25 atm. The preservation of both temperature and pressure during gas clean-up will greatly enhance the efficiency of the overall system. The syngas production pressure designed for Africary's Theunissen UCG project is 25 atm., based on hydrostatic pressure modelling, and the gas will reach the surface with a target temperature of 250–350°C.

In this study the aim is to address the fundamental limitations and practical constraints of existing hot particulate removal technologies. These systems generally suffer from poor availability caused by factors associated with tensile strength, the sealing system, thermal transient behaviour, corrosion, and residual ash accumulation (Hirohata *et al.*, 2008). These problems can be circumvented by introducing alternative hot gas separation and/or cleaning methods such as supersonic gas separation (SGS), Ranque–Hilsch vortex tube (RHVT), and vortex gradient separation (VGS) with inertia-vacuum filter (IVF). A vortex-based gas separation concept is proposed for UCG applications.

Description of Africary's UCG syngas content and contaminants

Contaminants generally include particulate matter (mineral particulates, trace elements, and char), water vapour, condensable hydrocarbons (oils and tars), sulphur compounds, nitrogen compounds, alkali metals (primarily potassium and sodium), and hydrogen chloride (HCl). The sulphur compounds and CO_2 are usually removed by various adsorption-based acid gas removal systems, but novel alternatives like the SST, RHVT, and VGS are proposed for the vortex tube concept for UCG applications.

The major syngas constituents and the predicted contaminants expected from the UCG production well are based on experimental work (van Dyk, Brand, and Waanders, 2014). The results are presented in Table I. Water, in the form of steam, is removed to dry the syngas by wash-cooling the gas to below its saturation temperature. This allows some condensable hydrocarbons like oils and tars to be removed with the water. Some of the water-soluble gases like ammonia are also removed during this process. The tars consist of condensable organic compounds and may vary from primary oxygenated products to heavier deoxygenated hydrocarbons and polycyclic aromatic hydrocarbons (PAHs) (Africary, internal modelling work).

Thermochemical conversion processes generate numerous tar species depending on the operating parameters, especially temperature, pressure, heating rate, type and amount of agent/oxidant, and residence time (Africary, internal modelling work). A UCG gasifier may yield 1 to 3% (mass basis) tar; however, regardless of the amount or type, liquid hydrocarbons like tar and oil are a universal challenge because of their potential to foul filters, lines, and equipment, as well as deactivate catalysts in downstream processes (Torres, Pansare, and Goodwin, 2007). Although eliminating all tar and oil is desirable, a more practical strategy is to simply remove sufficient liquid hydrocarbons at a temperature lower than the minimum temperature that the gas is exposed to downstream.

Inorganic compounds and residual solid carbon from the UCG production well constitute the bulk of the particulate matter. The inorganic content includes alkali metals (potassium and sodium), alkaline earth metals (mostly calcium), silica (SiO_2) and alumina (Al_2O_3), and other metals such as iron and magnesium (Africary, internal modelling work). Minor constituents present in trace amounts include arsenic, selenium, antimony, zinc, and lead (van Dyk and Keyser, 2014). Most nitrogen contaminants in syngas occur as ammonia (NH_3) with smaller amounts of hydrogen cyanide (HCN).

Coal from the Northern Free State Basin, South Africa, which will be used for the Theunissen UCG project, contains alkali and alkaline earth metals. The alkali metals are primarily potassium and to a lesser extent sodium, and are more problematic in syngas applications than alkaline earth metals due to their higher reactivity and potential to form substrates with halides like Cl and F.

Table I

The two types of raw syngas that can be produced from Theunissen UCG project (Africary, internal modelling work)

Streams	Raw gas 1	Raw gas 2
Components	**mol%**	**mol%**
H_2	34.5%	43.1%
CO	46.0%	27.5%
CO_2	7.3%	9.6%
CH_4	7.0%	12.4%
$C2H_4$	0.0%	0.0%
N_2	0.6%	0.6%
O_2	0.0%	0.0%
H_2O	4.4%	6.6%
H_2S + COS	0.2%	0.2%
Trace	**mg/h**	
Ba	1.3E-19	1.2E-19
Sb	1.4E+04	1.3E+04
Cd	2.5E-02	2.3E-02
Cr	7.4E-20	6.8E-20
Be	3.1E-07	2.8E-07
Pb	2.2E-02	2.0E-02
Mo	2.8E-14	2.6E-14
Cu	1.6E-17	1.5E-17
Co	8.4E-27	7.8E-27
Mn	1.2E-26	1.1E-26
Hg	9.2E+02	8.5E+02
Sn	9.5E+02	8.8E+02
As	7.6E-01	7.1E-01
Ni	1.0E-13	9.6E-14
Zn	7.4E-04	6.8E-04
V	5.8E-14	5.4E-14
Cl	1.4E+06	1.3E+06
F	2.1E+05	1.9E+05
Liquids	**kg/h**	
Tar	310	290
Oil	305	280
Naphtha	160	145

Common issues with particulate matter are fouling, corrosion, and erosion, which cause efficiency and safety concerns if not removed or addressed before syngas processing. For example, due to the inclusion of gas engines and compressors in the Africary Theunissen UCG plant, the particulate content must be reduced to below 1 mg/m^3. Particulate matter is classified according to aerodynamic diameter. For instance, PM10 denotes particles smaller than 10 µm, and PM1 particles smaller than 1 µm (Federal Remediation Technologies Roundtable, 2016). It is common practice to remove particulates of a certain size to below a given level, as indicated in Tables II and III.

Alkali compounds reaching the surface in the form of chlorides, hydroxides, and sulphates can cause substantial fouling and corrosion in downstream processes. Chlorides are the predominant halide in syngas, usually in the form of hydrochloric acid (HCl). Chlorine in coal occurs as alkali metal salts, which readily vaporize at the high gasification temperature and react with water vapour to form HCl. Substantial hot corrosion can occur, and reactions can also occur between HCl and other contaminant species in the gas phase, which can generate compounds such as ammonium chloride (NH_4Cl) and sodium chloride (NaCl) which cause fouling in downstream equipment upon cooling.

UCG syngas clean-up requirements for polygeneration

When a UCG plant is operated in a stable and correct manner, much less particulate and mineral matter is produced in the raw syngas compared to conventional gasification operations and only a small amount of particulate removal is required. However, the raw syngas may still contain a lot of moisture, tars, and oils, requiring removal. CGC relies on mature techniques, like wet scrubbers, that are decidedly effective but generate waste water and have poor energy efficiency and a large environmental footprint.

The level of cleaning that is required is based on the downstream consumer's technology requirements, fuel specification, and emission standards. For Africary's UCG polygeneration (power and diesel fuel) design, the cleaned syngas product specification is defined by the feed specification for the FT process vendor (Table II), and/or the gas engine vendor (Table III).

The liquid fuel products produced by the FT unit must follow the Euro-5 specification, as required by South African legislation, therefore removal of HCN, NH_3, Hg, Sb, Sn, sulphur compounds, metals, halogens (Cl and F), and several other trace components is required (Prabhansu *et al.*, 2015; correspondence with several FT process licensors). The syngas clean-up system must dry the raw syngas and effectively capture (> 99.9%) all the trace elements listed in Table I, as well as remove all particulate matter. It also needs to effectively separate (> 99.99%) acid gases like H_2S, COS, and CO_2 from the syngas, with an availability factor above 98%.

Separating at least 85% of all the H_2 and CH_4 from the raw gas 1 stream to augment the H_2:CO ratio of raw gas 2 stream is highly desired. As a second step, CO_2 separation from sulphur and capturing the sulphur either as organic or sulphuric acid will be desirable.

Cold gas clean-up – wet scrubbing

The cold gas clean-up (CGC) system is the predominant gas treatment technology chosen for UCG in combination with gas engines due to its proven reliability (Balas *et al.*, 2014). For the Africary Theunissen UCG process design, a cyclone in combination with a wet scrubber system can be implemented for power generation. The system will recirculate and cool water to remove the moisture, tar, oil, and particulates by wet scrubbing and may include lime dosing as sulphur adsorbent and pH control (National Lime Association, 2007; Wang, Pereira, and Hung, 2005).

Table II

Post clean-up syngas specifications for FT (Prabhansu *et al.*, 2015; correspondence with several FT vendors

Components/ properties	Limit value
Heavy metals	< 1 ppm_w
Silica	< 0.1 ppm_w
O_2	< 1 ppm_w
Halogens as H-X (HCl *etc.*)	< 5 ppb_w
Alkali metals	< 10 ppb_w
Soot/dust/solids	< 1 ppm_w
Tars and aromatic components	< 1 ppm_w
Nitrogen compounds, including NH_3, HCN, and amines	< 10 pp_{bc}
Sulphur (including H_2S and organic sulphur)	< 5 ppb_w
CO	> 30%
H_2 +CO	> 60%
Wet gas dew point	H_2O: saturated at syngas temperatures up to 50°C

Table III

Gas engine fuel gas specifications (Prabhansu *et al.*, 2015; Balas *et al.*, 2014; Scheibner and Wolters, 2002; correspondence with several gas engine vendors)

Components/ properties	Limit value
Sulphur	< 1 200 ppmv
Hydrogen sulphide equivalent	< 1 500 ppmv
Total sulphur compounds	< 57 mg/MJ or 2000 mg/10kWh
O_2	< 2% v
C4 and higher	< 2% v
H_2	< 40% of total LHV
Gas humidity	< 60%
Wet gas dew point	> 15°C below gas temperature
Silicon and siloxanes	< 0.56 mg/MJ or 0.2 mg/10kWh
Chlorine equivalent	< 3.5 mg/MJ or 400 mg/10kWh
Ammonia	< 1.5 mg/MJ or 55 mg/10kWh
Oils and tar	< 1.19 mg/MJ or 5 mg/10kWh
Particulate matter (soot, dust, ash)	< 1–3 µm and < 0.8 mg/MJ or 50 mg/10kWh
Calorific value (CV)	4.7–7.6 MJ/ Nm^3
Temperature	< 40°C
Pressure	< 200 $mbar_g$

To minimize the wet scrubbing thermal penalty for FT, Africary will utilize a dual-stage cooling process, whereby the syngas will be cooled to approximately 150°C in the first stage before being introduced to the warm gas desulphurization (WGD) system. A portion of this syngas will be used as the fuel gas stream and further wash-cooled in a second stage to 80°C. An additional trim water cooler will ensure that the fuel gas meets gas engine vendor requirements of < 40°C (Clarke Energy, 2016 personal communication). Wet scrubbing technology is considered the norm and state-of-the-art, as it deals with most of the condensable liquids and particulates. However, it only removes portions of the gaseous contaminants and does not perform any gas separation, and will therefore have to be used in conjunction with a separate acid gas removal (AGR) system. Further cooling of the syngas in the AGR system may reduce the temperature to as low as –62°C (the condensation point of chilled methanol) and the syngas must be heated afterwards.

Warm gas clean-up

Warm and hot gas cleaning technologies are attractive to avoid cooling and reheating of the gas stream as required for CGC. Existing technologies for gas cleaning at warm temperatures (< 300°C) include cyclones, candle filters (for removing solid contaminants), molecular sieve membranes (for gas separation), and sorbents (for removing sulphur-containing compounds (RTI LLC, 2018).

Molecular sieves

Carbon molecular sieve membranes are in development for the separation and purification of hydrogen from syngas. The potential benefits of high-temperature gas separation and membrane reactor processes are substantial; however, commercialization still remains elusive. A major technical barrier is the lack of robust inorganic membranes and full-scale modules that are suitable for use at the high-temperature and high-pressure conditions required (Parsley *et al.*, 2014). According to a supplier, hydrogen seems the most suited for gas separation with molecular sieves; however, the gas must be free from all sulphur-containing compounds, making it infeasible for raw syngas processing.

Candle filters

Despite decades of research with metallic filters (Sharma *et al.*, 2008), the materials have achieved only limited commercial success due to a natural correlation between porosity, mechanical strength, and thermal conductivity. Increasing the porosity of the material to increase the filtration area leads to a decrease in mechanical strength. This is a fundamental limitation for candle filters. An increase in the porosity increases both the filtering rate and surface area (m^2/g), but decreases the mechanical strength and thermal conductivity and accelerates the corrosion rate.

Significant improvements in candle filters have been achieved in the past few years (Prabhansu *et al.*, 2015); however, the reliability of these systems has never been successfully tested in a commercially integrated gasification-based system environment. From the literature (Swanson and Hajicek, 2002; Guan *et al.*, 2008), it is evident that most candle filters have operated for only a short period of a few thousand hours at 400°C, although they last much longer at lower temperatures of around 285°C (Scheibner and Wolters, 2002) in a coal gasification environment. Even the use of exotic state-of-the-art metals and ceramics has provided only limited success. The failure of candle filters after a short period of operation leads to an uneconomical plant availability factor and higher operating cost than for CGC and they are therefore not widely used.

Warm-temperature candle filter technology deals with most of the particulates; however, it removes only a portion of the contaminants and does not remove any condensable liquids or alkali metals, nor does it perform gas separation, and it will therefore have to be used in conjunction with a separate AGR and CGC wet scrubber system.

Hot gas clean-up

Supersonic gas separation

A theoretical approach by Sforza, Castrogiovanni, and Voland (2012) shows that supersonic gas separation (SGS) has promise as a robust method for hot separation of fuel species (CO, CH_4, and H_2) from H_2O, CO_2, and H_2S obtained from coal-derived syngas. They performed calculations based on general Lurgi-based gasification syngas input (31 atm., 450°C and 210 000 Nm^3/h) for a concept that performs segregation by condensation of some of the gases.

This process is illustrated in Figure 1. A particulate-free, hot, wet syngas enters a chamber with an arrangement of static blades or wings, which induce a fast swirl in the gas. Thereafter the gas stream flows through a Laval nozzle, where it accelerates to supersonic speeds and undergoes a pressure drop to about 30% of feed pressure. Supersonic isentropic expansion results in a rapid decrease of temperature (–80°C to –115°C) and pressure, leading to the sequential condensation (and/or solidification) of H_2O, CO_2, H_2S, NH_3, HCN, and COS, which form a fine mist including some liquid hydrocarbons (Secchi, Innocenti, and Fiaschi, 2016) like ethane, propane, and butane. The mist droplets agglomerate to larger drops, and the swirl of the gas causes cyclonic separation.

The dry gas, consisting of H_2, CO, N_2, CH_4, and Ar, continues through the separator, while the liquid phase, together with some slip gas (about 15% to 30% of the total stream), is separated by a concentric divider and exits the device as a separate stream. In the final section both streams are diffused back to subsonic conditions; the gas is slowed down and about 50% to 80% (Netušil and Ditl, 2012) of the feed pressure and temperature (depending on application) is recovered.

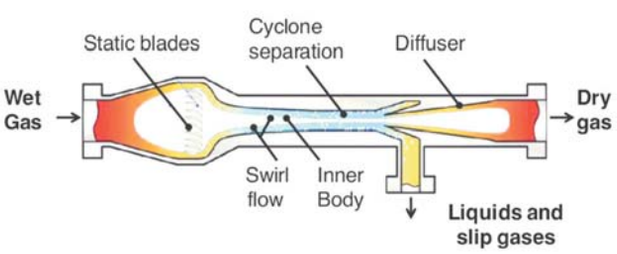

Figure 1—Schematic diagram of the supersonic gas separator for natural gas dehydration (Netušil and Ditl, 2012)

Such mechanical separators have no moving parts and a very small environmental footprint. However, the commercial use in drying natural gas from wells that inherently provide gas at very high pressures and modest temperatures is far different from the hot syngas cleaning proposal of Sforza, Castrogiovanni, and Voland (2012). In practice, the presence of any particulate matter in syngas travelling at supersonic speeds will result in a high probability of erosion, and further problems like hydrate plugging, flow rate inflexibility, and narrow turndown ratio (Haghighi, Hawboldt, and Abdi, 2015) have been reported. Furthermore, Netušil and Ditl (2012) stated that a 27.6% pressure loss is required for a separation efficiency of 90% moisture and > 50% for > 95% separation, showing diminishing returns for deep cleaning and recompression of the syngas might be required.

Condensing diverse gas mixtures into sizeable drops for accumulation and separation remains commercially untested, but Theunissen *et al.* (2011) proposed a rotational particle separator device to assist nucleation to reach the required size for cyclonic separation (> 15 µm).

Ranque–Hilsch vortex tube

The RHVT is a mechanical device with no moving parts that separates ambient temperature compressed gas into hot and cold streams. The gas emerging from the 'hot' end can reach temperatures of 200°C, and the gas emerging from the 'cold' end can reach –50°C. Pressurized gas is injected tangentially into a swirl chamber and accelerated to a high rate of rotation. A conical nozzle at the end of the tube allows only the outer shell of the compressed gas to escape at the hot end, while the remainder of the gas returns in a smaller inner vortex within the outer vortex towards the cold end.

The working principle (see Figure 2) can be approximated as follows (Xue, Arjomandi, and Kelso, 2013).

(1) The adiabatic expansion of the incoming gas cools the gas and turns its heat content into kinetic energy of rotation while the total enthalpy is conserved.
(2) The outer rotating gas flow moves towards the hot end outlet. The kinetic energy of rotation allows for friction and turns into heat by the means of viscous dissipation, and the temperature of the gas rises to higher than that of the incoming gas.
(3) A portion of the gas exits at the cold outlet and obeys the traditional notion (the Joule-Thompson effect) in that temperature drops with a decrease in pressure.
(4) Heat is transferred between the quickly rotating outer flow and the opposite, slowly rotating, smaller internal axial flow, allowing for heat transfer from the cold to the hot vortex. A zone of no mixing exists between the two, allowing separation based on temperature.

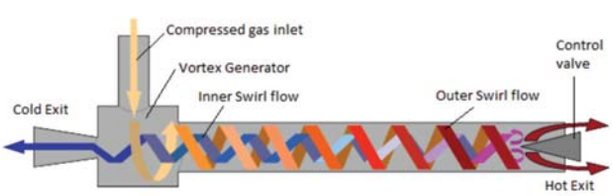

Figure 2—Flow structure inside a Ranque-Hilsch vortex tube (Netušil and Ditl, 2012)

The literature shows (Linderstrom-Lang, 1964, 1966) that partial separation of the components of a gas mixture occurs when it is passed through a RHVT. Marshall (1976) confirmed this effect using different gas mixtures and different sizes of tubes. He also studied the effect of reduced inlet and outlet pressures and found that if the outlet pressure is substantially below atmospheric, the separation factor is higher than the predicted correlation he derived (Marshall, 1976). This suggests that the performance can be improved by operating the vortex tube at vacuum pressure, which is also described further in the VGS technology description and indicates that the cut 'θ' at which the peak separation appears was generally at about 0.4, but varied for different settings between 0.2 and 0.6 (Wikipedia, 2018). This means that a RHVT can generally double the feed percentage of light species to the light side and double the heavy species to the heavy side. However, as a pure separation system the RHVT had poor performance and could only achieve an α value of approximately 1.025, indicating a very low separation efficiency. This led to more focused research on the heat separation capability of an RHVT than on the gas species separation capability.

In the late 1990s renewed interest in the technology was shown, with more focus on cryogenic air separation for space transportation and new work yielded a promising 80– 85% oxygen enrichment with a recovery in the 30–36% range (Binau, 1997), but also poor results using an oversized RHVT (Spracklen, 1998). Balepin, Rosshold, and Petley (1999) claimed that the best performance for air separation occurred with a 68% O_2 concentration, with a 38% recovery factor and highest concentration of 85–90% O_2 but with only a 7–10% recovery factor.

Kulkarni and Sardesai (2002) studied the application of a RHVT to enrich the methane concentration in gas from production wells. The experiments conducted on separating CH_4 from N_2 confirmed that gas separation does occur in a vortex tube. The inlet pressure was found to be the most dominant factor affecting separation, and the maximum separative power attained was $5.5 \times 10^{+7}$ kg.mol/min.

Farouk, Farouk, and Gutsol (2009) simulated temperature, pressure, mass density, and species concentration fields within the vortex tube and found that even though a large temperature difference was obtained, only minuscule gas separation occurred due to diffusion effects. An investigation of the correlations between velocity, temperature, and species mass fraction revealed that the inner core flow has a large Eddy heat flux and Reynolds stresses that adversely influence the gas separation efficiency. Dutta, Sinhamahapatra, and Bandyopadhyay (2011) supported this finding, and observed that although the separation of air into its main components (oxygen and nitrogen) occurred, the separation effect was very small and the process of species separation was driven mainly by Soret diffusion. It is, however, notoriously difficult to separate streams like air, where the components have very similar molar mass densities. The accurate measurement of O_2 and N_2 concentrations is also difficult to manage and may require specialized set-up and calibration conditions.

More recent research has indicated encouraging performance for a RHVT. Chatterjee, Mukhopadhyay, and Vijayan (2017) developed and published a one-dimensional

mathematical model that can compute mass transfer based on inlet pressure, temperature, inlet concentration and flow rate and outlet pressure, temperature, and flow rate. This model can be used for rapid design and simulation of species separation in an RHVT. The model considers simultaneous heat and mass transfer in a RHVT. A set of experiments was carried out with three vortex generators of different capacities to validate the mathematical model. Using the largest unit at a flow rate of 0.26 m³/s the oxygen concentration was boosted from the normal 21% to almost 28% for an $\alpha > 1.45$ with recovery in the 10–15% range. If this performance can be repeated with a feed stream containing species with large variation in molar mass, then the level of separation may well be in the commercial application range for a UCG flow scheme; where the pressure has to be let down anyway and a slight increase in temperature could easily be accommodated by the trim cooler.

Brand and Esterhuyse (2018) conducted similar experiments with air using a commercial RHVT. Their results, as shown in Table IV, indicate that separation of air occurred, but the calculated error of ±3% limits the accuracy of the measurement. Each sample was run twice, and the averages are reported in Table IV. The control sample of atmospheric air was run eight times, while a 95% confidence interval was used to determine an error of ±3%. The gas chromatograph used could measure the N_2 content of a sample with an accuracy of ±0.1%; however, O_2 and Ar were combined in a single measurement.

The first samples taken (C1 and H1 at 25% cold side flow) provide the expected O_2 decrease at the cold side (±0.5%) and increase of O_2 at the hot side of about 1.6%. However, the best results of about 2% increase in O_2 at the cold side of the RHVT and about the same increase of ±2% N_2 at the hot side in the second samples, using a smaller 10% flow at the cold flow orifice, was unexpected. This runs counter to the initial assumption that the heavier O_2 molecules will concentrate at the hot end while the lighter N_2 molecules will concentrate at the cold end.

Vortex gradient separation

A vortex gradient separator (VGS) has no moving parts, and a series of guide vanes/static blades induces a fast swirling vortex in the outer gas, surrounding a central core that passes thorough nozzles and diffusers that separate dirty flue gas or raw syngas into three streams (Chentsov, Beloglazov, and Korsakov, 2009). Figure 3 shows a schematic drawing of a VGS.

A dirty gas stream, comprising a mixture of gases, is fed into the inlet parabolic nozzle (1), consisting of sections 'α' and 'β', where the flow is accelerated and the outer gas tangentially accelerated by internal guide vanes/static blades (2). The outer gas flow is accelerated and rotated, while preserving its laminar flow structure by implementing a constant area change (dA/dL), and by steadily increasing the tangential and axial acceleration. The constants for area change are determined experimentally, depending on the gas stream properties (temperature, viscosity, density), but should not exceed Re 100 000. The gas then enters section 'δ', for laminar acceleration in a parabolic nozzle (3), again under constant area change. The gas then enters the vortex diffuser (4), where the rotation is accelerated, while the axial speed is decreased to perform initial separation. This separated gas is then again axially and tangentially accelerated in a paraboloid nozzle (5) and finally fed to a separation diffuser (6), a concentric divider where the stream is cut into light (7), medium (9), and heavy fractions (8).

The laminar vortex induces a higher pressure at the periphery, which allows heavy gas components such as sulphur dioxide to accumulate and collect in layers and the solid particles to coagulate in the centre (Figure 4) (Korsakov, 2010). Thus, it becomes possible to remove heavy acidic and toxic gas components with the simultaneous withdrawal of any suspended particles and vapour from a dirty gas source.

Chentsov, Beloglazov, and Korsakov (2011) described the gas dynamic flow formed in the VGS as 'fast rotating' with 'negatively-strained intermolecular bonds' with the following qualities. (1) The available kinetic energy (the molecular-kinetic motion of the gas molecules) is constrained. (2) The suspended particles transported by the gas are concentrated in the central zone of the channel in the form of a dust 'core'.

Table IV

Results for the RHVT air separation test (Brand and Esterhuyse, unpublished work)

Sample number	O_2 (mol.%)	N_2 (mol.%)	Total (mol.%)
Control (air)	22.3	75.9	98
C1	21.8	76.0	98
H1	23.9	77.0	101
C2	24.1	75.9	100
H2	22.8	77.6	100

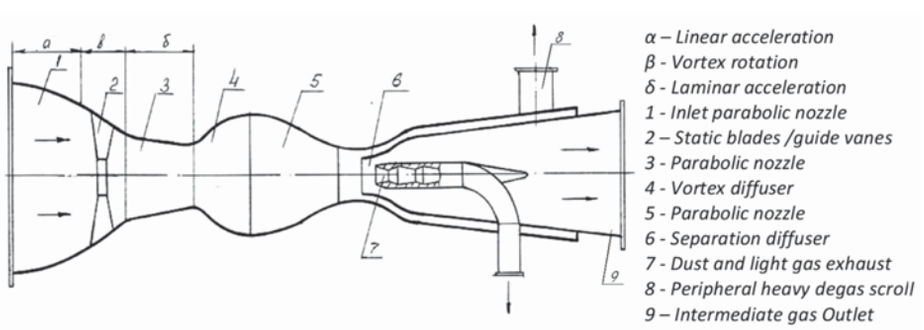

Figure 3—A typical vortex gradient separator (Chentsov, Beloglazov, and Korsakov, 2009)

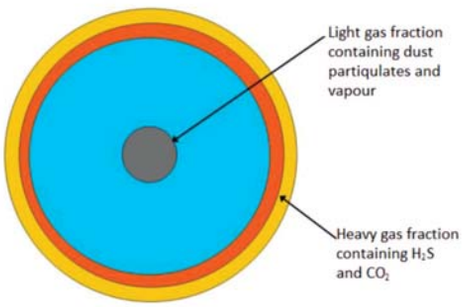

Figure 4—Cross-section of the gradient separator channel showing density variation (Korsakov, 2010)

Dust and aerosols are transported into the core from the rotating gas volume with the smaller size particles closer to the centre. (3) The VGS divides a gas mixture into its molecular components, based on their molecular weight and density, in the cross-section of the swirling channel, and the heavier gas components (like SO_2, CO_2, *etc.*) are distributed and collected in the peripheral zone.

In fluid dynamics, a negative pressure gradient, also called an *adverse pressure gradient* (APG), occurs when the static pressure increases in the direction of the flow. This is mathematically expressed as $dP/dx > 0$ for a flow in the positive x-direction. This is achieved by over-expanding a compressed gas into this 'negatively-strained' state. Gas in this state has many features that do not fit into the traditional molecular-kinetic theory, as the gas is basically flowing 'uphill' in the direction of the high pressure. This has an important impact on boundary layers, as increasing the fluid pressure is akin to increasing the potential energy of the fluid, leading to a reduced kinetic energy and deceleration of the gas while preventing laminar separation.

The principle observations associated with gas flow in an APG are (Korsakov, 2010):

1. In an APG, an axial gas flow accelerating in a converging nozzle *maintains its laminar structure* while transforming its potential energy into a laminar vortex.
2. If two streams containing dispersed dust particles in the 'over-expanded state' intersect, then the *particles transfer to the jet with the highest velocity*.
3. If a high-velocity gas stream travels over a large stationary gas volume separated by small slots, this *large stationary gas volume acts as a 'sump' for suspended particles*.
4. The *thermal conductivity of the gas rises sharply*. The thermal conductivity of air is usually 0.030–0.035 W/mK, but for air in a negative-stressed state it increases 10 000-fold to 340–420 W/mK. Rank's effect also becomes more pronounced, *i.e.* the effect of the temperature distribution over the channel cross-section, decreasing the temperature in the centre of the channel cooler while increasing it at the periphery.
5. The *heat transfer coefficient also increases* 100-fold (gas to the separator wall) from the usual range of 20–60 W/m^{2}K, to 2500–3000 W/m^{2}K.

The first two effects mentioned can be observed in nature where a 'dust devil' forms a funnel-like chimney that sucks dust particles into the centre of a vortex. A numerical simulation by Gu *et al.* (2006) based on an advanced dust-devil-scale, large-eddy simulation model verified that the horizontal inflow vortex could entrain solid particles and carry them into the vertical swirling wind field. Another trend identified was for the fine dust grains to rise along the inner helical tracks, while the larger dust grains were lifting along the outer helical tracks.

CFD modelling (Chentsov, Beloglazov, and Korsakov, 2011) shows the formation of a stable central vortex entering the separator nozzle. The peripheral rotation was estimated at around 3000 r/min, while the rotation around the core reaches 100 000 r/min.

The Russian student website Studopedia (n.d.) provides insights into the working principles of the VGS as follows. An APG provides an inertial seal by increasing the strain of the gas to provide a contracting laminar vortex. This allows the density of the stream to increase towards the centre axis and to exceed the relative particle density. This allows any particulates to float on the gradient flow surface, creating a constant dust layer in the centre of the VGS channel.

Arguably the most detailed description of the principles of the VGS was published by Moiseev *et al.* (2016a). The focus of this paper was on separating less than 0.5% methane from a mine ventilation gas flow by recovering the methane in concentrations of up to 80%. The authors further explain that the separation of the gas and dust flows within a VGS occurs towards the axial direction, due to the generation of several vortices including countercurrent flows, with sharp decreases in tangential velocity as can be seen in Figure 5. The CFD studies of a methane-dust-air mixture revealed the following features (see Figure 5) (Moiseev *et al.*, 2016a).

1. A near-axial flow is swirled around the central axis and moves along it in the shape of a twisting and narrowing core.
2. A peripheral flow is swirled around the central axis (in the shape of a spiral) and moves more slowly down the axis of the gradient separator, resulting in the presence of a counter-return flow.
3. Pulsation occurs due to the high tangential velocity and radial pressure drop, resulting in cooling of the central/axial gas flow and heating of the peripheral flow, thus providing for the simultaneous concentration of lighter components.
4. Thermal energy fluxes result due to micro-cooling cycles of radial turbulent flows.

Inertia vacuum filter

The same APG principles that are used to separate dust particles and light gases in the VGS can also be used as a filter mechanism to filter micrometre-sized particulates from a gas. Moiseev *et al.* (2016b) evaluated an inertia vacuum filter (IVF) for removing particles from coal mines ventilation air. The unit was designed to clean a volume of 200 000 Nm^3/h, using 500–570 kW/h. The particle removal efficiency was about 99.8% with the minimum size of the collected particles being 1 µm. In this device, gas containing dust particles is sucked/vacuumed through an accelerating nozzle (stream A in Figure 6).

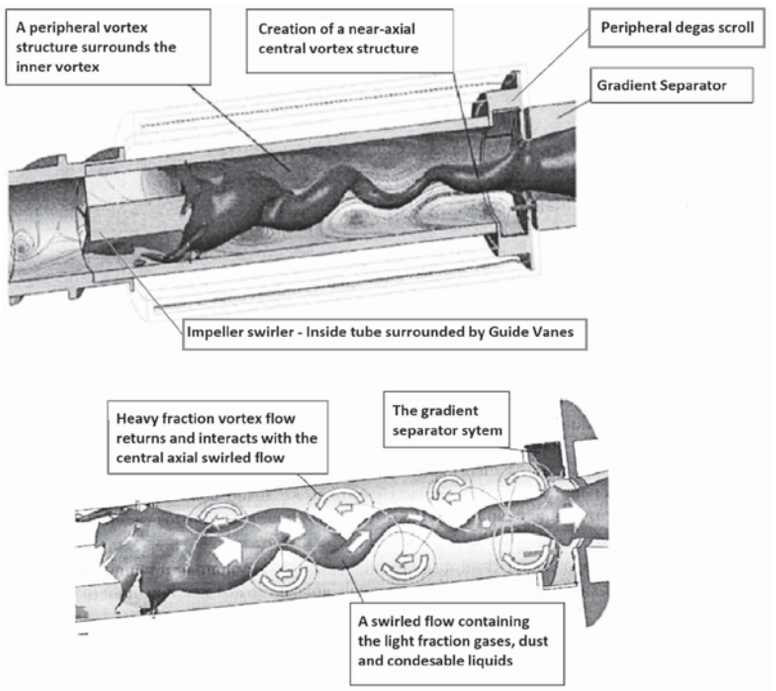

Figure 5—CFD model (Moiseev *et al*., 2016a) showing the same countercurrent vortex formation as described for RHVT (Dutta, Sinhamahapatra, and Bandyopadhyay, 2011)

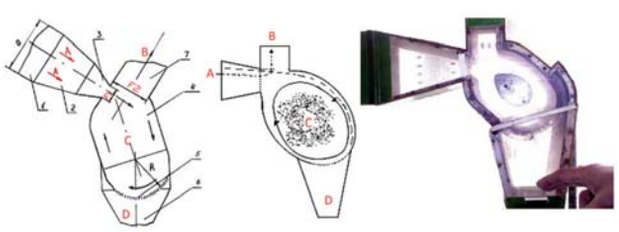

Figure 6—Schematic illustration of the principle of an inertia vacuum filter (Chenysov *et al*., 2009; Korsakov, 2010)

The area 'F1' of the accelerating nozzle is smaller than the cross-section of the exit 'F2' and the velocity of the gas increases and expands in this section as the gas goes into an AGP state. The dusty input stream passing through the cross-section of F1 has a greater velocity than the stream in the cross-section of F2 and therefore the particles in this stream also have a higher velocity (greater kinetic energy), which allows them to overcome the drag force of slower exiting stream B (as the suspended matter from the two intersecting jets will be captured by the jet that moves fastest). This allows for two jets of APG gas to intersect and for the output stream to permeate the inlet stream with its particles and for the suspended particles to become trapped inside the circulating stream C.

While the two-phase gas circulates inside the rotary chamber (4), it passes over a precipitation grille (item 5 in Figure 6). This process creates an aerodynamic trap whereby particles can enter the rotary chamber of the device, but cannot exit and eventually settle in the collecting chamber (6). The gas circling the rotary chamber also becomes a highly efficient filter, consisting of layers of gas acting as layers of filtering material. About 2–3% ultra-fine particles may accumulate in the rotating C stream, but eventually they also coagulate and fall into the collecting chamber.

Chentsov, Beloglazov, and Korsakov (2009) successfully tested a VGS combined with an IVF at the Ekibastuz coal power plant that removed fly ash with a particle size of 5–100 µm. The installation had a capacity of 15 000 m³/h and was equipped with measuring equipment with a measurement accuracy of ±0.1 g. Forty-five tests were carried out with up to –35 mbar vacuum, which achieved filtering of up to 99.25% of all particles, and with the latest upgrades operating at 99.99%. Korsakov (2010) stated that the installation had been in operation for 4 years. Chentsov and Barsukov (2011) also tested an IVF device was at the Pavlodar power station boiler. Here, the device placed between the second stage economizer and the air pre-heater achieved 65 to 70% dust removal down to 1 µm.

Characteristics of vortex separation for UCG

Several dusty and wet syngas clean-up technologies have been considered for raw (wet and dirty) UCG syngas at different implementation temperatures, and these are summarized in Table V.

The incorporation of HGC based on vortex gas separation with IVF may provide both particle separation and gas separation directly from a UCG production well. The advantages of such a hot, wet, and dirty gas clean-up system in combination with RTI's Warm Gas Desulfurization process can provide for efficient syngas clean-up for clean coal power generation. This process can further be combined with deeper acid gas removal, and control of the carbon to hydrogen ratio may allow the efficient blending of syngas produced by different UCG operating regimes to supply a cost-effective FT syngas for polygeneration operations.

Table V

Comparison of raw syngas clean-up technologies proposed for UCG

Temp.	Type	Advantages	Disadvantages
Cold	Wet scrubbing	Mature. State-of-the-art and widely used. Removes all liquids, tars, solids. Adsorbents can remove all acid gases to ppb level. Low pressure drop.	Expensive, generates waste water, and has poor energy and thermal efficiency. Reheating of syngas required. Large environmental footprint.
Warm	Cyclone	Cheap. Modest pressure drop. Works well to remove large particles.	Cannot remove ultra-fine particles or liquids. Prone to fouling. No gas separation.
	Candle filter	Can remove very-fine particles from dry gas.	Poor reliability. Cannot remove or tolerate tars and liquids. No gas separation. Expensive and uses exotic materials. Moderate pressure drop.
	Molecular sieve	Can separate clean gases. Can commercially separate H_2 and CO_2.	Very low sulphur tolerance. Requires very clean and dry gas.
Hot	RTI's WGD	Removes sulphur compounds at high temperature. Can tolerate and remove minor trace metals and particulates. Low pressure drop.	All liquids must be removed below the operating dew point. Cannot remove CO_2 or condensable liquids.
	SGS	Commercialized for NG separation. Removes acid gases to % level. No moving parts. Possible removal of liquids, tars, solids.	May be damaged by particles. Can foul quickly. Not experimentally proven on syngas.
	RHVT	Cheap. No moving parts. Modest separation of light species from heavy species. May provide cooling/heating option.	May be damaged by particles or liquids. Can foul quickly. Moderate pressure drop. May create additional cooling or heating demand. Very low separation factor and gas must be cascaded and recompressed for high separation values. Not commercially tested as a separation device.
	VGS	Removes all liquids, tars, solids. Separates light species from heavy species. Separates acid gases and light gases to % level. High separation factor. Commercially tested.	Modest vacuum compressor demand. Requires independent verification of published results.
	IVF	Can remove ultra-fine particles. Low pressure drop. Commercially tested.	May foul quickly from liquids. Modest vacuum compressor demand. No gas separation. Requires independent verification of published results.

Proposed UCG application

A conceptual novel UCG gas clean-up and separation unit design based on a VGS, cleaning raw syngas directly from the UCG production well is proposed. The concept will allow the hot and efficient separation of syngas into its useful components, together with partial cleaning for further gas utilization. As the UCG production well is pressurized the use of an axial flow pressure regulator will be required. This device must control the upstream flow in such a manner that the downstream compressors can vacuum the gas and allow the implementation of an APG of about 50 mm H_2O over the vortex separator and the filters. This modest vacuum requirement implies that the syngas well pressure is not reduced and that the power demand is kept relatively small compared to the total production plant requirements.

In a second step (see Figure 7) the incoming gas is separated and an initial vortex created by a stationary guide vane. The addition of a portion of recycled pure gas by a cyclone injector will impart significant tangential velocity to the outside of the incoming raw gas.

In a third step/chamber, the spinning gas will be allowed to intersect with the central dusty core (as described in the CFD studies), which will allow the transfer of dust to the central axial flow of light gases (mainly H_2 and CH_4), to be removed by the dust exhaust in the 'particle separation' step. This gas may be cooled with a steam-generating heat exchanger to protect the downstream vacuum compressors. Before the cooled gas is fed to the compressors it is passed through an IVF system or a CGC wet scrubbing system that will remove any condensable liquids and dust. This washed light fraction will be used for H_2:CO ratio control in the FT process.

In a fourth step the vortex speed is increased by internal guide vanes, which increases the pressure and density of the gases and allows the heavier molecular gases to move to the periphery, where they are removed by an inverted cyclone. The gas may be cooled to generate process steam and to protect the downstream vacuum compressors. Literature sources indicate that this heavy gas stream can be passed through a second-stage smaller VGS to separate the very heavy sulphur components from the CO_2. The sulphur components will be routed to a sulphur recovery plant and the CO_2 may be further processed on site.

The remaining cleaned gas (also called 'pure gas') is passed through the high-temperature booster-compressor, where a portion of the gas is recycled in the second step.

Although the proposed system may clean the syngas only partially it may still be reasonable to implement, as the removal of 99.9% of the particulates as well as acid gas will allow the use of smaller downstream equipment and guard beds instead of large process equipment.

Conclusions

The effectiveness and carbon efficiency of UCG can be improved by hot cleaning raw syngas directly from the UCG production well. The proposed vortex separation hot gas clean-up concept will allow for the removal of most of the particulates, together with the efficient separation of the syngas into its useful components, providing for acid gas removal and H_2:CO ratio control. The most important principle for vortex separation is the preservation of laminar flow allowed by the adverse pressure gradient. Other technical and economic advantages may include, but are not limited to:

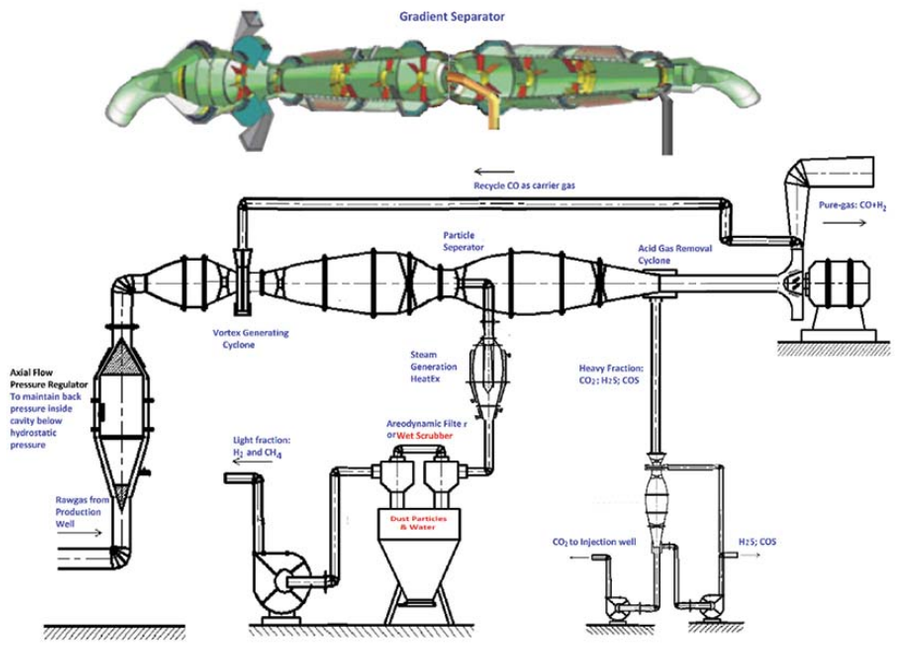

Figure 7—Diagram showing a proposal for hot gas clean-up of raw syngas from a UCG production well in several steps [adapted from Chenysov, Beloglazov, and Korsakov, 2009; Korsakov, 2010)

- Removal of most of the condensable water, oils, tars, fly ash, and particulate matter directly from the hot syngas, allowing hot gas processing and pressure boosting.
- Removal of most of the H_2S and CO_2, allowing for cheaper warm syngas desulphurization combined with guard beds, rather than low-temperature adsorption processes.
- Separation of H_2 from a second syngas stream for H_2:CO ratio adjustment before FT and negating the need for a CO-shift rector with a subsequent CO_2 avoidance.

The level of separation is in the commercial application range for the Theunissen UCG project as the syngas typically contains species with large variation in molar mass and the syngas pressure of the second stream used for power generation has to be let down anyway. Vortex separation specifically applied to a UCG process, is a practical solution to improve both energy efficiency and lower the CO_2 footprint.

The next steps and future work will include the modelling, design, and experimental testing of a VGS for both particulate filtering and gas separation efficiency.

Nomenclature

AGR	acid gas removal
APG	adverse pressure gradient
atm.	atmospheres / pressure ratio
CFD	computational fluid dynamics
CGC	cold gas clean-up
FT	Fischer-Tropsch
GC	gas chromatograph
HGC	hot gas clean-up
IVF	inertia vacuum filter
$N1$	mole fraction of heavier species at the inlet
$N2$	mole fraction of heavier species at hot outlet
$N3$	mole fraction of heavier species at cold outlet
PM2.5	< 2.5 µm particulates
PM5	< 5 µm particulates
PM10	< 10 µm particulates
Re	Reynolds number
RHVT	Ranque–Hilsch vortex tube
SGS	Supersonic gas separation
UCG	underground coal gasification
VGS	vortex gradient separation
WGC	warm gas clean-up
α	separation factor for light species between product and feed streams $= [(1 - N3) \div N3] \times [N2 \div (1 - N2)]$
θ	cut = molar flow in product stream (hot outlet) $\div N1$

References

Balas, M., Lisy, M., Kubicek, J., and Pospisil, J. 2014. Syngas cleaning by wet scrubber. *WSEAS Transactions on Heat and Mass Transfer*, vol. 9. pp. 195–204.

Balepin, V., Rosshold, D., and Petley, D. 1999. Progress in air separation with the vortex tube. *Proceedings of the 9th International Space Planes and Hypersonic Systems and Technologies Conference*, Norfolk, VA, 1–5 November 1999. NASA Langley Research Center, Hampton, VA. https://ntrs.nasa.gov/search.jsp?R=20000012624

Binau, N.J. 1997. Assessment of air separation technologies for the recovery of oxygen for use in hypersonic flight. MSc thesis, Montana State University, Bozeman, MT.

Chatterjee, M., Mukhopadhyay, S., and Vijayan, P.K. 2017. 1-D model for mass transfer calculation in vortex tube using heat and mass transfer analogy. *American Journal of Heat and Mass Transfer*, vol. 4, no. 1. pp. 1–24.

Chentsov, A.V., Beloglazov, V., and Korsakov, V. 2009. Methods for cleaning off-gas, based on gas-dynamic effects, not previously used in production.

(Сборник Докладов Второй Международной Конференции: «Пылегазоочистка-2009). Collection of reports of the Second International Conference 'Dust-Exposure', September 2009. pp. 62–66. http://www.multifilter.ru/pdf/news/intecheco2009ecolog_reports.pdf

Chentsov, A.V. and Barsukov, B.N. 2011. Gas dynamic methods - dry cleaning of waste gases. (Газодинамические Способы, Сухой Очистки Отходящих Газов). *Environmental Journal of Russia, Ecology and Technology*, vol. 4. pp. 40–44. http://bnbars.moy.su/vihr_statia/STATIA_1.pdf

Dutta, T., Sinhamahapatra, K.P., and Bandyopadhyay, S.S. 2011. Numerical investigation of gas species and energy separation in the Ranque-Hilsch vortex tube using real gas model. *International Journal of Refrigeration*, vol. 34. pp. 2118–2128.

Farouk, T., Farouk, B., and Gutsol, A. 2009. Simulation of gas species and temperature separation in the counter-flow Ranque–Hilsch vortex tube using the large eddy simulation technique. *International Journal of Heat and Mass Transfer*, vol. 52, no. 13–14. pp. 3320–3333.

Federal Remediation Technologies Roundtable. 2016. Remediation technologies, screening matrix and reference guide, Version 4.0. Air emissions/off-gas treatment/scrubbers. http://www.frtr.gov/matrix2/section4/4-60.html [accessed May 2018].

Gu, Z., Zhao, Y., Li, Y., Yu, Y., and Feng, X. 2006. A numerical simulation of dust lifting within dust devils—simulation of an intense vortex. *Journal of the Atmospheric Sciences*, vol. 63. pp. 2630–2641.

Guan, X., Gardner, B., Martin, R., and Spain, J. 2008. Demonstration of hot gas filtration in advanced coal gasification system. *Powder Technology*, vol. 180, no. 1–2. pp. 122–128.

Haghighi, M., Hawboldt, K.A., and Abdi, M.A. 2015. Supersonic gas separators: Review of latest developments. *Journal of Natural Gas Science and Engineering*, vol. 27. pp. 109–121.

Hirohata, O., Wakabayashi, T., Tasaka, K., Fushimi, C., Furusawa, T., Kuchonthara, P., and Tsutsumi, A. 2008. Release behavior of tar and alkali and alkaline earth metals during biomass steam gasification. *Energy & Fuels*, vol. 22, no. 6. pp. 4235–4239.

Korsakov, V.A. 2010. Alternative highly effective technological solutions, based on physical effects, not previously used in industry. (Научно-практическая конференция: «Инновационное предпринимательство: от идеи до внедрения»). *Proceedings of the Scientific and Practical Conference: 'nnovative Entrepreneurship: From Idea to Implementation*', 26–27 May 2010. pp. 22–30. http://omskmark.moy.su/publ/innovatica/marketing/2010_korsakov_v_a_alternativnye_vysokoehffektivnye/11-1-0-75 (accessed May 2018].

Kulkarni, M.R. and Sardesai, C.R. 2002. Enrichment of methane concentration via separation of gases using vortex tubes. *Journal of Energy Engineering*, vol. 128, no. 1. pp. 1–12.

Linderstrom-Lang, C. 1964. Gas separation in the Ranque-Hilsch vortex tube. *International Journal of Heat and Mass Transfer*, vol 7. pp. 1195–1206.

Linderstrom-Lang, C. 1966. Gas separation in the Ranque-Hilsch vortex tube - Model calculations based on flow data. Forskningscenter Risoe. Risoe-R, no. 135. Risø, Denmark.

Marshall, J. 1976. Effect of operating conditions, physical size and fluid characteristics on the gas separation performance of a Linderstrom-Lang vortex tube. *International Journal of Heat and Mass Transfer*, vol. 20. pp. 227–231.

Moiseev, V.A., Piletskii, V.G., Andrienko, V.G., Tailakov, O.V., and Chentsov, A.V. 2016a. The technological and design solutions for energy vortex gas separation of the ventilation and degasification emissions from coal mines using gradient separators. *Global Journal of Pure and Applied Mathematics*, vol. 12, no. 1. pp. 559–574.

Moiseev, V.A., Andrienko, V.G., Piletskii, V.G., Makotrenko, V.A., and Chentsov, A.V. 2016b. Technology of recovering mechanical impurities from ventilation and degasification emissions from coal mines. *Research Journal of Pharmaceutical, Biological and Chemical Sciences*, vol. 7, no. 5. pp. 397–402.

National Lime Association. 2007. Flue gas desulfurization technology evaluation - lime vs. limestone. Project Number 11311-001, Comparison Report 20070315 (March 2007). https://www.lime.org/documents/publications/free_downloads/fgdte_dry-wet-limestone2007.pdf [accessed May 2018].

Netušil, M. and Ditl, P. 2012. Natural gas dehydration. InTech. doi: 10.5772/45802

Parsley, D., Ciora, R.J. Jr., Flowers, D.L., Laukaitaus, J., Chen, A., Liu, P.K.T, Yu, J., Bonsu, M.S.A., and Tsotsis, T.T. 2014. Field evaluation of carbon molecular sieve membranes for the separation and purification of hydrogen from coal-and biomass-derived syngas. *Journal of Membrane Science*, vol. 450. pp. 81–92.

Prabhansu, M., Karmakar, K.R., Chandra, P., and Chatterjee, P. 2015. A review on the fuel gas cleaning technologies in gasification process. *Journal of Environmental Chemical Engineering*, vol. 3. pp. 689–702.

RTI LLC., 2018. Warm gas desulfurization process technology. https://www.rti.org/impact/warm-gas-desulfurization-process-technology [accessed May 2018].

Scheibner, B. and Wolters, C. 2002. Schumacher hot gas filter long-term operating experience in the nuon power buggenum IGCC power plant. *Proceedings of the 5th International Symposium on Gas Cleaning at High Temperature*, 17–20 September 2002. https://www.netl.doe.gov/File%20Library/Events/2002/gas%20cleaning%20at%20high%20temperature/1-05paper.pdf

Secchi, R., Innocenti, G., and Fiaschi, D. 2016. Supersonic swirling separator for natural gas heavy fractions extraction: 1D model with real gas EOS for preliminary design. *Journal of Natural Gas Science and Engineering*, vol. 34. pp. 197–215.

Sforza, P.M., Castrogiovanni, A., and Voland, R. 2012. Coal-derived syngas purification and hydrogen separation in a supersonic swirl tube. *Applied Thermal Engineering*, vol. 49. pp. 154–160.

Sharma, S.D., Dolan, M., Park, D., Morpeth, L., Ilyushechkin, A., McLennan, K., Harris, D.J., and Thambimuthu, K.V. 2008. A critical review of syngas cleaning technologies — fundamental limitations and practical problems. *Powder Technology*, vol. 180. pp. 115–121.

Spracklen, N.M. 1998. Preliminary investigation of the separation of a binary, two-phase hydrocarbon mixture using a commercially available vortex tube, MSc thesis, Montana State University, Bozeman, MT.

STUDOPEDIA. Not dated. Dry inert gas cleaning. (Газдарды құрғақ инерциялық тазалау аппараттары). Paragraphs 6.8 and 6.9. https://studopedia.org/1-9846.html [accessed May 2018].

Swansoen, M.L. and Hajicek, D.R. 2002. Hot-gas filter testing with a transport reactor gasifier. *Proceedings of the 5th International Symposium on Gas Cleaning at High Temperature*, 17–20 September 2002.

Theunissen, T., Golombok, M., Brouwers, J.J.H., Bansal, G., and van Benthum, R. 2011. Liquid CO2 droplet extraction from gases. *Energy*, vol. 36. pp. 2961–2967.

Torres, W., Pansare, S.S., and Goodwin, J.G. 2007. Hot gas removal of tars, ammonia, and hydrogen sulfide from Biomass gasification gas. *Catalysis Reviews - Science and Engineering*, vol. 49, no. 4. pp. 47–56.

Van Dyk, J.C. and Keyser, M.J. 2014. Influence of discard mineral matter on slag-liquid formation and ash melting properties of coal – A Factsage™ simulation. *Fuel*, vol. 116 (January). pp. 834–840.

Van Dyk, J.C., Brand, J.F., and Waanders, F.B. 2014. Equilibrium coal mineral matter simulation and slag formation during an underground coal gasification process. *Proceedings of the 6th International Freiberg Conference on IGCC & XtL Technologies, Freiberg*, Germany, 19–22 May 2014. TU Bergakademie, Freiberg. https://tu-freiberg.de/sites/default/files/media/professur-fuer-energieverfahrenstechnik-und-thermische-rueckstandsbehandlung-16460/publikationen/2014-17-2.pdf

Wang, L.K., Pereira, N.C., and Hung, Y.T. 2005. Desulfurization and emissions control. *Handbook of Environmental Engineering, Vol 2: Advanced Air and Noise Pollution Control*. Springer. pp. 35–95.

Wikipedia. 2018. https://en.wikipedia.org/wiki/Vortex_tube [accessed May 2018].

Woolcock, P.J. and Brown, R.C. 2013. A review of cleaning technologies for biomass-derived syngas. *Biomass and Bioenergy*, vol. 52. pp. 54–84.

Xue, Y., Arjomandi, M., and Kelso, R. 2013. The working principle of a vortex tube. *International Journal of Refrigeration*, vol. 36. pp. 1730–1740. ◆

HMC 2019
HEAVY MINERALS 2019

The Southern African Institute of Mining and Metallurgy
in collaboration with The Zululand Branch are organising

The Eleventh International

HEAVY MINERALS CONFERENCE

'Renewed focus on Process and Optimization'

5–6 August 2019—Conference

The Vineyard, Cape Town, South Africa

ABOUT THE VENUE

The Vineyard is nestled on an eco-award-winning riverside estate, overlooking the eastern slopes of Table Mountain and conveniently located on the edge of the city. A short distance from the hotel in any direction allows you to easily explore some of the world's top tourist destinations.

August and September in the Western Cape is flower season. Explore the Cape's unique 'fynbos' floral kingdom at the world-famous Kirstenbosch Botanical Gardens, where one of the many attractions is the staggering aerial tree-canopy walkway.

A short distance from the hotel is the Constantia Winelands, which affords guests the opportunity to discover classic vintages and Cape Dutch homesteads, and within a five-minute walk is the well-known retail centre, the upmarket shopping precinct of Cavendish, with exclusive local and global outlets, travel agencies, foreign exchange outlets, and more.

CONFERENCE THEME

This series of heavy minerals conferences has traditionally focused on the industries associated with ilmenite, rutile and zircon. There are many other economic minerals which have specific gravities such that they may also be classed as 'heavy minerals'. The physical and chemical properties of these other minerals result in them being processed by similar technologies and sharing similar markets with the more traditional heavy minerals. In this conference we focus on optimization of mining, processing, and recovery.

CONFERENCE OBJECTIVE

This series of conferences was started in 1997 and has run since that date. The Conference alternates between South Africa and other heavy mineral producing countries. It provides a forum for an exchange of knowledge in all aspects of heavy minerals, from exploration through processing and product applications.

This is a strictly technical conference, and efforts by the Organizing Committee are aimed at preserving its technical nature. The benefit of this focus is that it allows the operators of businesses within this sector to discuss topics not normally covered in such forums. The focus on heavy minerals includes the more obvious minerals such as ilmenite, rutile and zircon; and also other heavy minerals such as garnet, andalusite, and sillimanite.

WHO SHOULD ATTEND

- Academics
- Business development managers
- Concentrator managers
- Consultants
- Engineers
- Exploration managers
- Geologists
- Hydrogeologists
- Innovation managers
- Mechanical engineers
- Metallurgical managers
- Metallurgical consultants
- Metallurgists
- Mine managers
- Mining engineers
- New business development managers
- Planning managers
- Process engineers
- Product developers
- Production managers
- Project managers
- Pyrometallurgists
- Researchers
- Scientists

Contact: Yolanda Ndimande, Conference Co-ordinator · Tel: +27 11 834-1273/7
Fax: +27 11 833-8156 or +27 11 838-5923 · E-mail: yolanda@saimm.co.za · Website: http://www.saimm.co.za

Conference Announcement

SAIMM
THE SOUTHERN AFRICAN INSTITUTE OF MINING AND METALLURGY

http://dx.doi.org/10.17159/2411-9717/2018/v118n10a4

Acid-base accounting of unburned coal from underground coal gasification at Majuba pilot plant

by L.S. Mokhahlane, M. Gomo, and D. Vermeulen

Synopsis

Underground coal gasification (UCG) is an unconventional mining method that converts coal *in situ* into a fuel gas that can be used for electricity generation. Residue products from UCG have the potential to leach into surrounding groundwaters. The geochemistry and leaching dynamics of these products are explored in this study. The products include char, ash, and the heat-affected zone in the surrounding rocks. Core samples from the pilot plant at Majuba are the first ever to be recovered from a UCG cavity in Africa, and they give key insights into the geochemistry of the gasification zone. Mineralogical and chemical analyses were performed on the samples, and acid-base accounting (ABA) was used to predict the acid-producing capacity of the gasification zone, particularly for char samples. Some of the char contained pyrite, although not all samples were acid-producing as determined by the ABA analysis. The ABA results showed that some of the unburned coal has moderate levels of sulphur, which could be the driving medium for acidic conditions. The ABA analysis indicated that water in contact with the gasification zone would eventually have a pH lower than 7, which could lead to acid rock drainage. These results form part of a preliminary investigation into the geochemistry of the reaction zone, post gasification.

Keywords

underground coal gasification, residue products, geochemistry, acid-base accounting.

Introduction

Underground coal gasification (UCG) is an unconventional mining method that converts coal *in situ* into a fuel gas that can be used for industrial purposes, including electricity generation. The gasification process leads to the formation of a cavity composed of char, rubble, and void space (Bhutto, Bazmi, and Zahedi, 2013). Residue products from UCG have the potential to leach into groundwater. These products include char (devolatilized coal), which can generate acid rock drainage (ARD). ARD is caused by the oxidation of sulphide minerals, which acidifies the leachate, thus increasing the solubility of some environmentally toxic metals (As, Cd, Hg, Pb, Zn, *etc.*) (Bouzahzah *et al.*, 2015).

The main source of ARD is oxidation of sulphide-bearing minerals due to interactions with oxygen, water, and microorganisms (Simate and Ndlovu, 2014; Kefeni, Msagati, and Mamba, 2017; Bouzahzah *et al.*, 2015). Although ARD occurs naturally, it can be enhanced by mining activities that escalate exposure of sulphide minerals to water, air, and bacteria (Simate and Ndlovu, 2014). At the Majuba pilot plant, the unburned coal remaining in the cavity has been in contact with groundwater since the gasifier was shut down in 2013. It is possible that in a commercial UCG plant, most of the coal will be consumed and no unburnt coal will be left in the cavity. Most of the sulphur will be converted to H_2S during the gasification process and transported with the syngas to surface, where it can be removed and captured as elemental sulphur.

The Majuba pilot gasifier was extinguished by injecting water from the surface into the gasification zone. This method of quenching depends on the hydrogeological conditions, as highly permeable strata may not need assisted quenching. Post gasification, the groundwater level will eventually rebound and water will begin to flow through the cavity (Liu *et al.*, 2007); this, however, depends on the permeability of the surrounding strata and extend of the UCG workings. The geochemical interactions in the cavity have the potential to generate ARD, especially if the sulphide quantities are adequate for acid generation. Equation [1] shows the reaction for oxidation of pyrite, which leads to acid generation:

$$2FeS_2(s) + 7O_2(g) + 2H_2O(l) \rightarrow 2Fe^{2+}(ag) + 4SO_4^{2-}(aq) + 4H^+(aq) \quad [1]$$

This reaction produces ferrous iron, sulphate ions, and acid. The ferrous iron can further be oxidized to ferric iron by the following reaction:

$$4Fe^{2+}(s) + O_2(g) + 4H^+(aq) \rightarrow 4Fe^{3+}(aq) + 4SO_4^{2-}(aq) + 2H_2O(l) \quad [2]$$

* *Institute for Groundwater Studies, University of the Free State.*

 ISSN 2225-6253. Paper received Apr. 2018; revised paper received Jul. 2018.

In environments with low oxygen concentrations, Reaction [2] will occur only when the pH reaches 8.5 (Simate and Ndlovu, 2014). The UCG cavity post-gasification is likely to be a low-oxygen environment, unlike in conventional mining where the coal seam is in contact with the atmosphere in open pit mining and some underground mines. While oxidation of sulphide minerals contributes to the acidity of rock drainage, dissolution of carbonate minerals plays a role in neutralizing the acid *via* the following reaction:

$$CaCO_3(s) + H^+(aq) \rightarrow 3HCO_3^-(aq) + Ca^{2+}(aq) \quad [3]$$

The dissolution rates of dolomite and magnesite are much slower than that of calcite (Lapakko *et al.*, 1999). Acid generation is hence a dynamic process that needs monitoring over a long period of time.

The potential for acid generation from strata disturbed by mining activities is regulated by guidelines from the South African's Department of Water Affairs and Sanitation (Best Practice Guideline G4: Impact Prediction, Department of Water Affairs and Forestry 2008). The guideline uses the source-pathway-receptor model for its risk-based approach to impact prediction. Underground mine voids are identified as potential risk sources for water bodies. Underground coal gasification creates a cavity or void that contains residue products such as ash, char, and the heat-affected zone in the surrounding rocks. According to the G4 guideline, all these products will have to undergo geochemical assessment, including evaluation of the risk of acid generation and the potential for leaching of metals.

There are two types of laboratory tests that can be used for the prediction of acid rock drainage – static and kinetic tests. Static tests include acid-base accounting (ABA), which is relatively quick and simple to carry out while the kinetic tests, such as leaching tests, usually take longer to complete. Kinetic tests also require larger samples and are usually carried out to determine the leachate quality and long-term ARD risk. Acid-base accounting is described by Sobek *et al.* (1978) as predictive tool that accounts for the balance between the acid-producing potential (AP) and the neutralizing potential (NP) of geological material; the difference is calculated as the net neutralizing potential (NNP). The acid-producing material is generally the sulphide minerals (Equation [1]), while the acid-neutralizing minerals are carbonate minerals such as calcite, dolomite, and magnesite (see Equation [2]). Dissolution of some silicate minerals such as anorthite can also neutralize acid. However, silicates dissolve more slowly than their carbonate counterparts (Lapakko *et al.*, 1999).

In UCG, ARD has the potential to weaken the infrastructure around the gasification zone as the production and injection wells are installed using cement and steel casing. The geochemistry of the surrounding aquifers can also be altered as metals become more soluble in acidic conditions, ultimately leading to ARD into the surrounding strata. The objective of this paper is to explore the leaching dynamics and geochemistry of the unburned coal from the UCG process.

Site location and geological setting

The Eskom UCG pilot plant near Majuba power station in Mpumalanga Province, South Africa, has completed phase 1 of gasification. This is the first UCG plant in Africa and had already produced fuel gas and successfully co-fired this gas with coal in a pulverized coal boiler at Majuba power station by 2010 (Pershad, Pistorius, and van der Riet, 2018). Gasification has ceased and verification drilling has commenced into the gasification zone. Verification boreholes are wells that are core-drilled into the gasification zone to establish the extent of gasification with the aim of retrieving core samples containing residue products. The verification boreholes were sited at strategic locations within the gasification panel. G1VTH1 was the first verification borehole to be drilled, and its location is shown in Figure 1.

The targeted coal-bearing formation for gasification is the Gus seam in the Vryheid Formation of the Ecca Group. The Gus seam varies from 1.8 to 4.5 m in thickness and at the Majuba UCG site it is found at a depth of around 280 m. Other coal seams encountered in the area are usually laterally impersistent and serve as marker seams – they are not targeted for gasification. Coal has a lower density than the Karoo sediments (alternating sandstones and shales), as seen in the wireline log in Figure 2. The sharp density spikes from the top to bottom of the log represent the Eland, Fritz, Alfred, and Gus seams respectively. The main economic Gus seam is thicker than the other seams, with alternating sequences of bright and dull coal. The bright coal has a lower density than the dull coal. The coal zone also contains several thin (5–20 cm) laterally impersistent bright coal layers (the Eland and Fritz coal seams) above the Gus seam, which are used as marker seams (de Oliveira and Cawthorn, 1999).

Methodology

G1VTH1 was percussion-drilled from surface to 200 m, and then core-drilled to just below the targeted Gus seam (286 m). The core samples were placed in trays and fragments of the recovered char from the Gus seam were taken (red blocks in Figure 2) for acid-base accounting. No ash was recovered, and this might be due to soft materials being washed away during drilling, as core drilling uses fluid circulation to remove the cuttings from the core barrel.

Acid-base accounting is a predictive tool used to assess the acid-producing capacity of coal mines and rock waste, in which the acid-neutralizing potential (*NP*) and acid-producing potential (*AP*) of rock samples are determined and the difference, the net neutralizing potential (*NNP*), is calculated as follows:

$$NNP = NP - AP \quad [4]$$

The *AP* is based on the theoretical oxidation of all sulphur in the sample to sulphuric acid. The total sulphur in the samples was determined using a LECO sulphur analyser. The *AP* is generally expressed in kilograms of $CaCO_3$ per ton of material. The conversion factor is 31.25 kg $CaCO_3$ per ton, *i.e.*:

AP = sulphur content (%) × 31.25 kg $CaCO_3$ equivalent per ton.

The dissolution of acid-neutralizing minerals such as carbonates contributes towards the *NP*. Hydrochloric acid is used to sufficiently digest these minerals and the *NP* is expressed in kg $CaCO_3$ per ton, but it can also be converted into acid-neutralizing capacity (ANC, expressed as kilograms H_2SO_4 per ton) by multiplying the NP by 0.98.

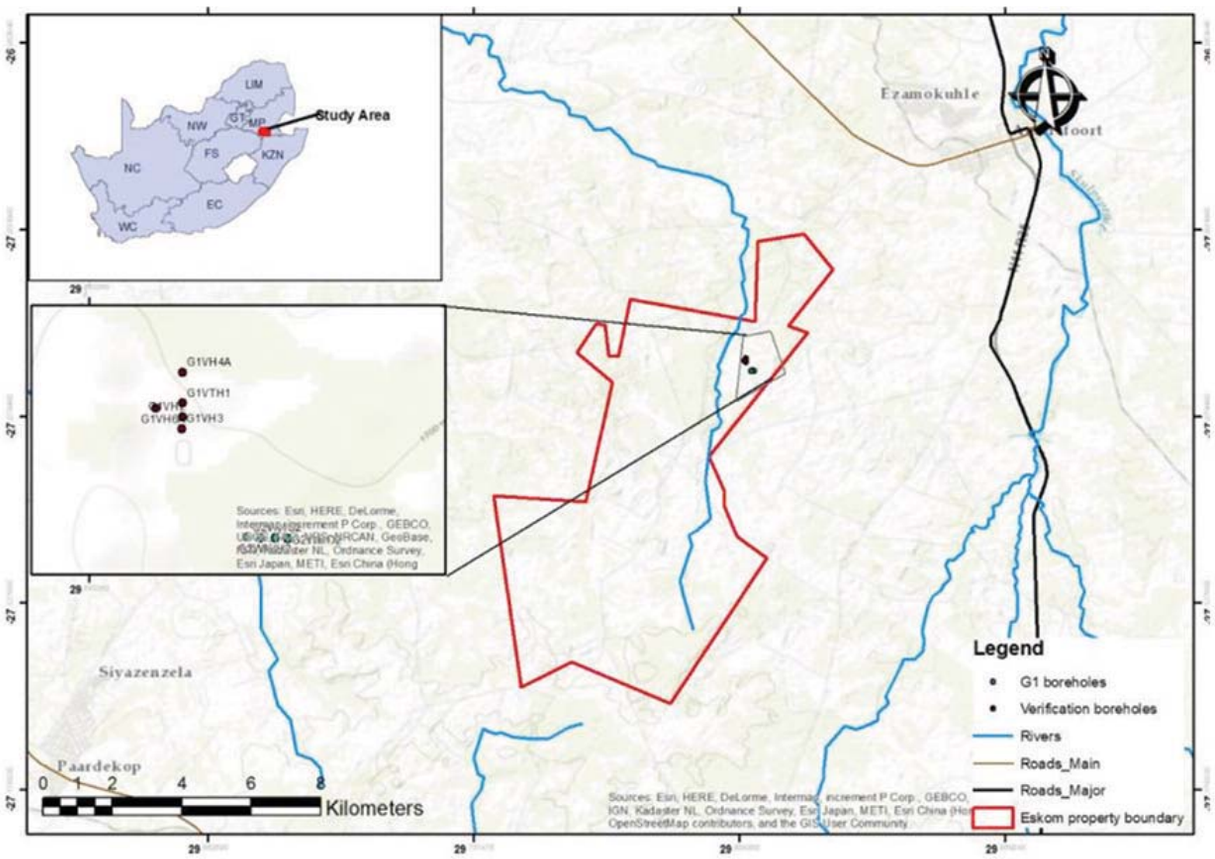

Figure 1—Majuba UCG pilot plant location

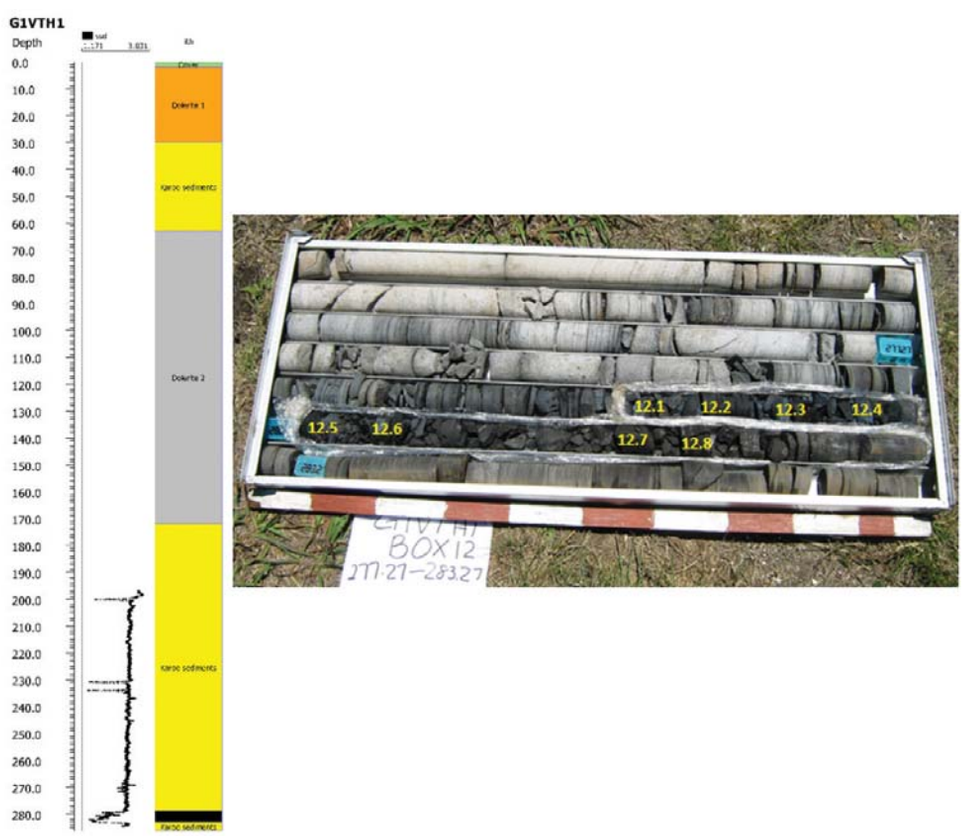

Figure 2—G1VTH1 core recovered by verification drilling

Negative *NNP* values indicate the potential for acid generation, while positive *NNP* values are associated with alkaline conditions. However, a *NNP* of more than 20 is generally required before non-acid conditions can be declared. There is, therefore, a region of uncertainty from –20 to +20 kg $CaCO_3$ *NNP*, which usually requires kinetic testing if the ABA results are inconclusive (Qureshi, Maurice, and Öhlander, 2016). The ratio of *NP* to AP, known as the neutralization potential ratio (NPR), can also be used to determine the potential for acidic conditions. Materials with a NPR of 2.5 are regarded as non-acid-producing, and those with NPR of 1 as acid-producing, while the uncertain region is between 1 and 2.5 (Qureshi, Maurice, and Öhlander, 2016).

Mineralogical compositions were determined using the QEMSCAN (Quantitative Evaluation of Minerals by Scanning Electron Microscopy) technique. The QEMSCAN is a scanning electron microscope-based system configured to automatically determine the mineralogical characteristics of particulate samples. Samples were also leached using water, acid, and hydrogen peroxide to determine the leaching dynamics in different environments. The water leach test is carried out over 24 hours using 50 ml of demineralized water to 5 g solid material. The peroxide leach test is carried out over 24 hours using hydrogen peroxide at 2 g solid material to 80 ml hydrogen peroxide. The acid leach test is carried out over 24 hours using 5 g solid material and 50 ml of approximately 0.1N sulphuric acid. All the leachates were analysed using inductively coupled plasma mass spectrometry (ICP-MS).

Table I

Analysis of unburned coal from the gasification zone (wt.%)

Sample	Moisture	Ash	Volatile matter	Fixed carbon	Total sulphur
12.1	5.3	46.9	3.7	44.1	0.41
12.2	6.4	63.6	5.6	24.4	0.35
12.3	5.7	47.9	4.4	42.0	0.46
12.4	5.4	50.3	4.4	39.9	0.47
12.5	4.5	69.4	5.5	20.6	0.21
12.6	4.7	40.1	3.7	51.5	0.53
12.7	4.3	39.7	1.7	54.3	1.4
12.8	4.4	10.4	2.7	82.5	0.57

Results and discussion

The proximate and sulphur analyses were carried out at the Eskom Research, Testing and Development (RT&D) laboratory in Johannesburg. The results for the char samples from the gasification zone are presented in Table I. The total sulphur values were used in the ABA analysis to determine the long-term risk of acid production.

The mineralogical results from QEMSCAN are presented in Table II. The samples were taken from both the Gus and the Alfred seams as they occurred close together in G1VTH1. The unburned coal recovered is shown in Figure 2, with the density log displayed. The down-the-well density log shows that low-density bright coal is situated towards the bottom of the seam while the dull coal is found predominantly in the upper parts of coal seam (Alfred and Upper Gus). A 3.16 m core loss was recorded from 280–286 m.

The mineralogical analyses are of the residual material after UCG, and due to absence of such detailed analyses prior to UCG they cannot be proportioned to the initial mineral composition. The mineralogical results show that all of the char samples from the Gus seam contain pyrite, which is the major contributor to ARD (Table II). Carbonate minerals, including calcite and siderite, were identified in the coal samples. Dissolution of carbonate minerals plays a role in the neutralization of acid, as seen in Equation [3]. Some of the silicate minerals found in the samples also contribute to neutralization reactions.

Table II

Mineralogical results from QEMSCAN (wt.%)

	Alfred seam				Gus seam			
	12.1	12.2	12.3	12.4	12.5	12.6	12.7	12.8
Pyrite	0	0	0	15.2	0.2	4	0.4	0.4
Oxidized pyrite	0	0	0	4.8	0	1.3	0.1	0.1
Siderite	0	0.2	0	32	2.4	0.4	0.3	0.1
Calcite	0	0	0	0.7	0.1	0.4	1	0.2
Dolomite	0	0	0	1.3	0	0	0	0
Gypsum	0	0	0	0.6	0	0	0	0
Apatite	0	0	0	0	0	0	0	0
Ca-Mg-(Al) silicate	1.1	4.3	0.6	12.8	4.7	5.1	6.3	0.1
Ca-Al silicate	11	11	3.6	2	9.4	3.3	5.9	0.9
Kaolinite	38.6	30.9	51.8	8.9	20.3	13	15.3	1.7
Quartz	11.5	17.2	18.5	5.5	8	5.8	4.5	0.2
Mica/illite	12.9	3.8	5.7	4.2	6.2	0.4	0.7	0
Microcline	2	0.8	1.4	1.5	1.1	0	0	0
Rutile	0.1	0.1	0	0.2	0.1	0.1	0	0
Alunite/gibbsite	0.1	0.5	0.1	0	0.6	0.3	0.2	0.1
Vitrinite	5.4	15.9	4.3	5.9	22.2	4	1.2	12.1
Semi-fusinite	8	5.7	6.8	2.1	11.6	17.2	17.4	15.1
Fusinite	9.4	9.6	7.2	2.1	13.1	44.8	46.6	68.9

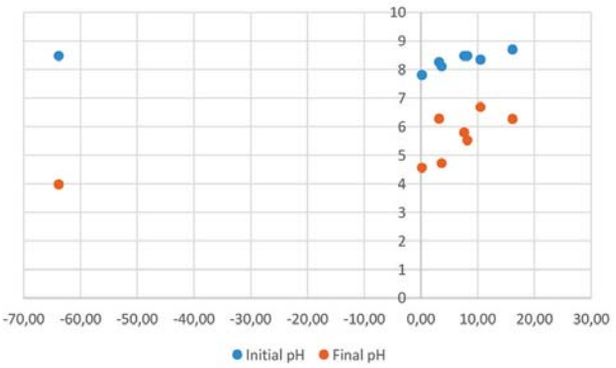

Figure 3—pH as a function of net neutralizing potential

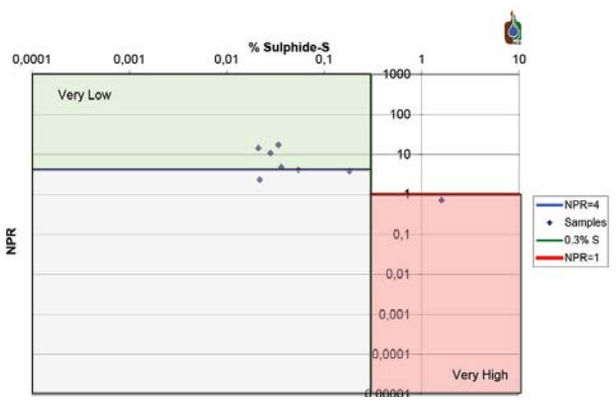

Figure 4—Neutralization potential ratio (NPR) as a function of sulphide content

The initial pH of the samples was above 7, as seen in Figure 3. The *NNP* was positive for all the samples except one. A positive *NNP* indicates non-acid-generating material whereas a negative *NNP* is associated with potentially acid-generating material. Sample 12.7 had a *NNP* of –63.78, which may be largely due to the higher levels of sulphur in this sample (1.4 wt.%) (Table I). This is more than twice the amount of sulphur in all the other samples. The final pH of this sample was also the lowest of all the samples which, together with the elevated pyrite content, indicates a high potential for acid generation.

The majority of the results in Figure 3 fall into the uncertainty region of –20 to +20 *NNP*. Although these samples have positive *NNPs* they cannot be conclusively regarded as non-acid-producing. The neutralization potential ratio (NPR) was used to determine the long-term acid production potential of the samples, as shown in Figure 4. The graph is divided into regions representing the likelihood for acid generation. The 'very low' region represents samples that are non-acid-producing while the 'very high' region represents acid-generating samples. The uncertain region is represented by the blue region under the 'very low' region. A NPR greater than 2.5 normally points to non-acid generation, while a NPR less than 1 indicates acid production if the sulphur content is also above 0.3 wt.%. The NPR results shown in Figure 4 indicate that only sample 12.7 has the potential for acid generation, as was indicated in Figure 3. The majority of the samples are non-acid-generating, with only one in the uncertain region. The general trend of the char samples taken from the gasification zone is that of non-acid-producing materials.

ARD is associated with iron being released into solution, as seen in Equations [1] and [2]. The leaching dynamics of the samples is shown in Figure 5. Very little Fe is released from the char samples when using demineralized water as a leaching medium. The same trend is seen when leaching is carried out under oxidizing conditions using hydrogen peroxide, with insignificant Fe being released. Under acidic conditions, Fe is released in greater quantities than under oxidizing conditions. Sample 12.7 released more Fe than any other char sample, which is consistent with the ABA and mineralogical analyses.

The leaching results show a similar trend as the ABA, where only one sample was considered as acid-producing. The general trend in Fe release also shows the same sample releasing higher amounts of Fe as compared to other samples. The highest levels of sulphur were also found in the same sample. This affirms that for acid generation to occur, an adequate quantity of sulphur has to be available to sustain the acidic conditions. The majority of samples did not show a tendency to leach high levels of Fe under different conditions.

The results show that even if the general conditions in the gasification zone become more oxidizing, the leaching dynamics for Fe may still be low. Groundwater will be the leaching medium for the unburned coal and much of the leaching behaviour will also depend on the chemistry of the local groundwater

Conclusions

The study gives key insights into the geochemistry of the gasification zone of the underground coal gasification project. The major conclusion is that the char does not pose an immediate of ARD formation, except for one sample. The geochemistry of the char samples shows the heterogeneous nature of coal in terms of mineralogical and chemical properties. More iron was leached under acidic conditions from samples with high levels of sulphur. Groundwater will be the leaching medium for the unburned coal and the leaching behaviour will depend on the chemistry of the local groundwater. It is possible that in a commercial UCG plant, most of the coal will be consumed and no unburnt coal will be left in the cavity. Most of the sulphur will be converted to

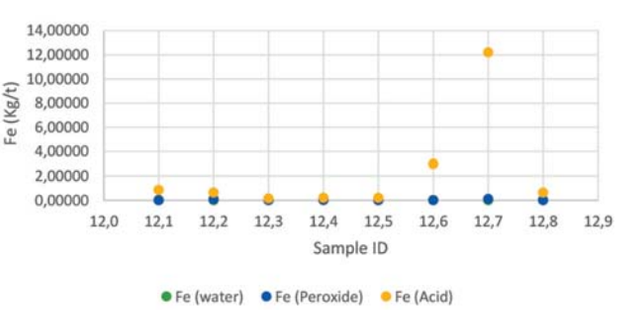

Figure 5—Leaching dynamics of Fe in water, hydrogen peroxide, and acid

H_2S during the gasification process and transported with the syngas to the surface, where it can be removed and captured as elemental sulphur. The coal seam at Majuba is at a depth of around 280 m below the ground level and the geohydrological conditions show no interaction between the coal seam aquifer and the shallow aquifer. Contamination of the shallow aquifer from any potential post-gasification acid rock drainage that may be generated in the UCG cavity is therefore unlikely.

References

Bhutto, A.W., Bazmi, A.A., and Zahedi, G. 2013. Underground coal gasification: From fundamentals to applications. *Progress in Energy and Combustion Science*, vol. 39, no. 1. pp. 189–214.

Bouzahzah, H., Benzaazoua, M., Plante, B., and Bussiere, B. 2015. A quantitative approach for the estimation of the 'fizz rating' parameter in the acid-base accounting tests: A new adaptations of the Sobek test. *Journal of Geochemical Exploration*, vol. 153. pp. 53–65.

De Oliveira, D.P.S. and Cawthorn, R.G. 1999. Dolerite intrusion morphology at Majuba Colliery, northeast Karoo Basin, Republic of South Africa. *International Journal of Coal Geology*, vol. 41, no. 4. pp. 333–349.

Kefeni, K.K., Msagati, T.A.M., and Mamba, B.B. 2017. Acid mine drainage: Prevention, treatment options, and resource recovery: A review. *Journal of Cleaner Production*, vol. 151. pp. 475–493.

Liu, S.-Q., Li, J.-G., Mei, M., and Dong, D.-L. 2007. Groundwater pollution from underground coal gasification. *Journal of China University of Mining and Technology*, vol. 17, no. 4, pp. 467–472.

Pershad, S., Pistorius, J., and van der Riet, M. 2018. Majuba underground coal gasification project. *Underground Coal Gasification and Combustion*. Blinderman, M.S. and Klimenko, A.Y. (eds.). Woodhead Publishing, Cambridge, UK. pp. 469–502.

Qureshi, A., Maurice, C., and Öhlander, B. 2016. Potential of coal mine waste rock for generating acid mine drainage. *Journal of Geochemical Exploration*, vol. 160. pp. 44–54.

Simate, G.S. and Ndlovu, S. 2014. Acid mine drainage: Challenges and opportunities. *Journal of Environmental Chemical Engineering*, vol. 2, no. 3. pp. 1785–1803. ◆

http://dx.doi.org/10.17159/2411-9717/2018/v118n10a5

Qualitative hydrogeological assessment of vertical connectivity in aquifers surrounding an underground coal gasification site

by L.S. Mokhahlane*, G. Mathoho†, M. Gomo*, and D. Vermeulen*

Synopsis

Underground coal gasification (UCG) is the conversion of coal *in situ* into a usable synthetic gas. One of the major environmental concerns with UCG is the possibility of groundwater from the coal seam aquifer contaminating the shallow aquifers via hydraulic connections. The coal seam aquifers are usually confined aquifers but can have hydraulic connections to the shallow aquifers due to faults/fractures or any man-made connections, including boreholes. The aim of this paper is to study groundwater hydraulic connections across various aquifers at the UCG site at Majuba, using hydrochemistry and stable isotope ($\delta^{18}O$ and $\delta^{2}H$) tools. Physical and chemical processes such as diffusion and condensation generate isotopic differentiation in natural waters that can be used to deduce the origins of different waters, and in groundwater the spatial isotopic distribution can be used to deduce hydraulic connections between different aquifers. The Majuba UCG site consists of shallow, intermediate, and saline deep aquifer systems at a depth of 70 m, 180 m, and 300 m respectively. Samples were taken from each aquifer system together with supplementary samples from an on-site water storage dam. The analyses of isotopic compositions led to the determination of the possible sources of each sample. The deep aquifer is represented by an isotopic signature that is depleted in heavy isotopes with average values of –41.7% and –7.02% for $\delta^{18}O$ and $\delta^{2}H$ respectively, while the shallow aquifer is enriched with corresponding average values of –19.9% and –3.3%. Hydrochemical data also showed different water types: a sodium chloride type in the deep aquifer and a sodium bicarbonate water in the shallow aquifer. The results indicate that the shallow aquifer and the deep aquifer are not hydraulically connected, and therefore it is unlikely that groundwater from the gasification zone would contaminate the shallow aquifer.

Keywords

underground coal gasification, hydraulic connectivity, stable isotopes, hydrochemistry, Majuba, aquifer.

Introduction

Underground coal gasification (UCG) is a mining method that exploits coal seams by *in situ* gasification that yields a usable synthetic gas. This process uses a panel of injection and production wells to achieve gasification and transport the synthetic gas to the surface without the need for people to go underground. Compared to conventional coal mining the appeal of UCG is multidimensional. The advantages include improved health and safety, reduction in process and waste handling, and less surface damage from mining activity (Imran *et al.*, 2014). The UCG process nonetheless raises some environmental concerns, some of which relate to the potential contamination of aquifers around the gasification zone (Kapusta and Stańczyk, 2015). This is due to the decomposition of coal in the gasification zone, which produces organic pollutants such as benzene, polycyclic aromatic hydrocarbons (PAHs), phenols, and inorganic compounds including ammonia and sulphides (Bhutto, Bazmi, and Zahedi, 2013; Kapusta and Stańczyk, 2011). These contaminants can migrate and penetrate the surrounding aquifers as a result of an outward pressure from the gasification zone if the gasifier is operated at a pressure higher than the hydrostatic pressure in the coal seam aquifer (Burton, Friedmann, and Upadhye, 2006). Once gasification is complete, the natural groundwater will begin to fill the cavity and cool the gasification zone. The flow of groundwater in the cavity will ultimately lead to leaching of residue products such as ash, unburned coal, and chars, which can lead to groundwater contamination (Liu *et al.*, 2007). The solubility of metals increases with increasing temperature and this can lead to long-term leaching of metals from the cavity.

Heat penetration can alter the overlying rocks and create fractures that result in the coal seam aquifer becoming hydraulically connected to the shallow aquifer, which can lead to the draining of the shallow aquifer into the gasification zone (Figure 1). The confined nature of the coal (deep) seam aquifer allows its water level (head) to stabilize at shallower levels above the coal seam depth (Dvornikova, 2018). The hydraulic connections can ultimately transmit water contaminated with inorganic and organic UCG products from the gasification zone to the shallow levels, where subsequent contamination of pristine shallow

* *Institute for Groundwater Studies, University of the Free State, South Africa.*

† *School of Chemical and Metallurgical Engineering, University of the Witwatersrand, South Africa.*

 ISSN 2225-6253. Paper received Apr. 2018; revised paper received Aug. 2018.

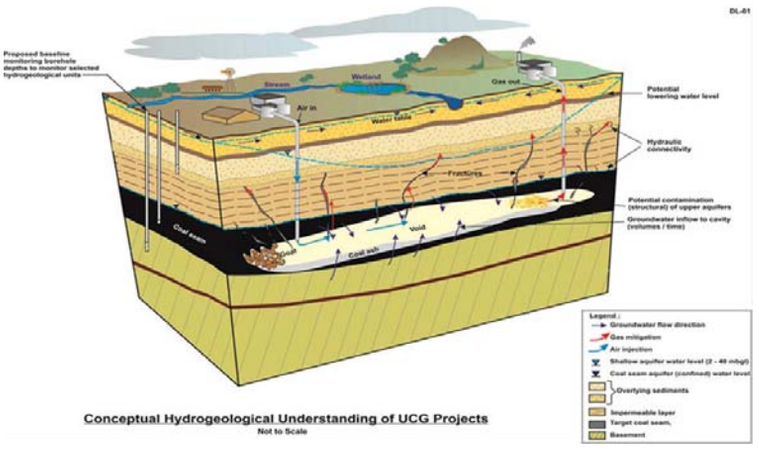

Figure 1—Conceptual hydrogeological model of a UCG plant (adapted from Love *et al.*, 2014)

aquifers can occur. UCG operators have to ensure that the site is well characterized and that the coal seam has limited connectivity with other water sources (Imran *et al.*, 2014)

Subsidence of the overburden above the UCG burn void can also result in serious groundwater contamination where aquifer cross-connection ensued during gasification operations, which can result in the transmission of pollutants generated in the burn zone via fractures triggered by subsiding overburden into overlying aquifers (Liu *et al.*, 2007). Overburden failure can create joints and fractures (Ghasemi *et al.*, 2012), similar to those seen in Figure 1, and these can act as pathways for contaminants to migrate from the UCG cavity to the shallower aquifers. The environmental risks of groundwater pollution from UCG activities are mostly site-specific. Appropriate site selection can mitigate most of the potential risks of groundwater contamination as factors such as depth of cover and competency of overlying rock play a role in roof collapse (Ghasemi *et al.*, 2012; Imran *et al.*, 2014). If there is no hydraulic connection between the shallow aquifers and the coal seam aquifer, where gasification is undertaken, there is little risk of groundwater contamination. Usually the water in the coal seam aquifer is of poor quality and is not used for any domestic or agricultural purposes. However, if faults and fractures exist within the strata, a hydraulic connection can be created between the coal seam aquifer and the shallow aquifer as seen in Figure 1.

Water is made up of oxygen and hydrogen atoms that exist as various stable isotopes. In natural waters the isotopic ratios of oxygen and hydrogen vary due to chemical, biological, and physical processes. For example in cooler regions the equilibrium water vapour would have an isotopic composition of $\delta^{18}O = -10.6\%$ and $\delta^{2}H = -93\%$, while over high-latitude seas the isotopic signature is as low as $\delta^{18}O = -11.6\%$ and $\delta^{2}H = -10\%$ (Clark and Fritz, 1997). These variations are a result of isotopic fractionation during phase transitions such as condensation and evaporation, and are also dependent on temperature changes. For example, during evaporation, the water in the vapour phase becomes is enriched in the lighter isotopic fractions $\delta^{16}O$ and $\delta^{1}H$, leaving behind water that is enriched in $\delta^{18}O$ and $\delta^{2}H$. The isotopic ratios can be used as a quantitative tool to identify the admixture between various surface water bodies and subsurface waters. This provides a means to determine the conditions during groundwater recharge by determining the $\delta^{18}O$ and $\delta^{2}H$ compositions in borehole samples (Clark and Fritz, 1997).

The aim of this paper is to study groundwater hydraulic connections across various aquifers at the UCG site at Majuba, using hydrochemistry and stable isotopes ($\delta^{18}O$ and $\delta^{2}H$), in order to assess the environmental risk to groundwater *post* the first gasification phase. A 3D geological model of the site will be developed and used to analyse the environmental risk.

Geological and hydrogeological setting

The Majuba UCG pilot plant is located in Mpumalanga Province of South Africa, about 35 km northwest of the town of Volkrust. Regular hills attributed to the erosion of the underlying dolerite sill typify the topography. The site covers an area of around 60 ha on the eastern bank of the Witbankspruit River and the surrounding area is mostly used for agricultural activities (Figure 2).

Four different dolerite intrusions (T1 to T4) that intersect the Karoo sediments at the Majuba Colliery have been identified (de Oliveira and Cawthorn, 1999). The intrusions have displaced the targeted Gus seam by over 70 m in some places. This has led to limitations in effective extraction of the coal seam by conventional mining. A 3D geological model of the Majuba UCG site is displayed in Figure 3. The model was developed from drill-hole core logs and generated using Leapfrog version 4.2. The geological model shows that the lateral extend of the two dolerite dykes is generally even across the study area. The dolerite intrusions have broken up the coal reserves into minor blocks, which is beneficial in containing the UCG process underground (Pershad, Pistorius, and van der Riet, 2018). The targeted coal seam (the Gus seam) is located at an average depth of over 250 m, and the second dolerite (T2) is over 100 m thick, which assists with the isolation of the gasification zone from the shallow aquifer.

The Gus seam forms part of the Vryheid Formation of the Ecca Group in the Karoo Supergroup (Snyman, 1998). The Gus seam varies from 1.8 to 4.5 m in thickness and at the

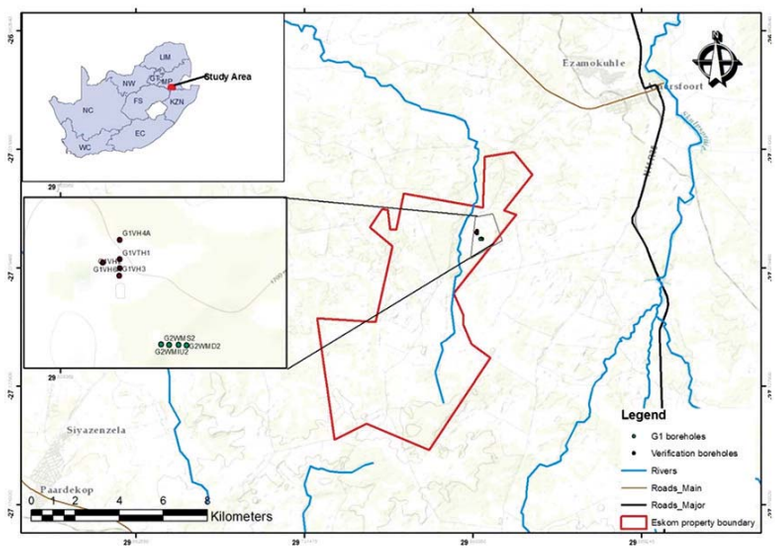

Figure 2—Location map of Majuba UCG pilot plant

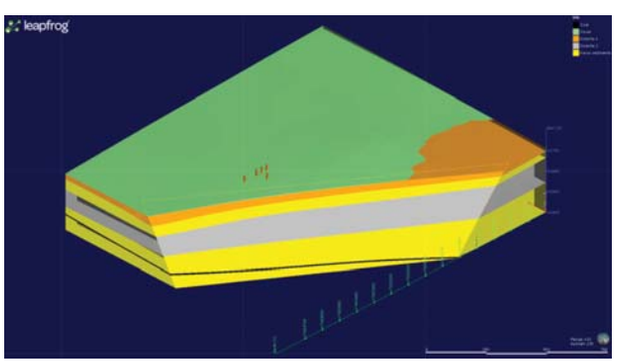

Figure 3—Geological model of the Majuba UCG site

Majuba UCG site it is encountered at a depth of around 280 m (Pershad, Pistorius, and van der Riet, 2018). The coal zone also bears several thin (5–20 cm) laterally impersistent bright coal layers below the Gus seam (de Oliveira and Cawthorn, 1999). There are three other coal seam above the Gus seam, namely the Eland, Fritz, and Alfred seams. These seams are generally thin and are not targets for gasification. Interbedded layers of sandstone, shale, and mudstone generally characterize the Karoo sediments (de Oliveira and Cawthorn, 1999).

Three distinct aquifers are present at the Majuba UCG site, as seen in Figure 4. The upper weathered (shallow) aquifer is usually low-yielding (range 1–10 m^3/d) owing to its trivial thickness, but contains good quality water due to years of groundwater flow through the weathered strata. The shallow aquifer is estimated to go as deep as 70 m and is underlain by the intermediate aquifer. Groundwater flow through the intermediate aquifer is mainly through fractures, cracks, and joints induced in the Karoo sediments by the intrusive dolerite sills. The aquifer can be divided into two zones: the intermediate upper (IU) aquifer and intermediate lower (IL) aquifer, as seen in Figure 4.

The coal seam aquifer forms part of the gasification zone and is located at a depth of around 280 m. The confined nature of the coal seam aquifer means the water is under

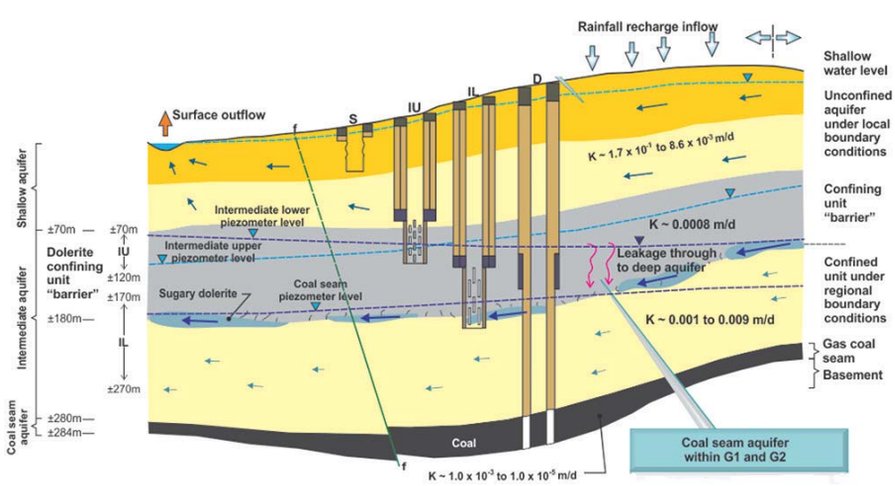

Figure 4—Conceptual hydrogeological model of Majuba UCG site (Love *et al.*, 2014)

pressure and hence the water level (head) stabilizes at shallow levels around 180 m below ground. Any fractures in the strata overlying the coal seam can act as a zone of groundwater transmission between the coal seam aquifer and the intermediate aquifer, leading to groundwater mixing. The groundwater in the coal seam aquifer is of poor quality and can generally be classified as saline, while the intermediate aquifer has better quality water. The groundwater monitoring network is placed in such a way that all aquifers are monitored, as depicted by the boreholes in Figure 4.

Methodology

Groundwater samples were taken from Majuba UCG site using plastic bailers and analysed for isotope fractions, D/H ($^2H/^1H$) and $^{18}O/^{16}O$, at iThemba Laboratories in Gauteng using a Thermo Delta V mass spectrometer. Equilibration time for the water sample with hydrogen was about 40 minutes and CO_2 was equilibrated with a water sample in about 20 hours. Laboratory standards, calibrated against international reference materials, were analysed with each batch of samples. The analytical precision is estimated at 0.2% for O and 0.8% for H. Analytical results are presented in the common delta-notation:

$$\delta^{18}O = \left[\left(^{18}O/^{16}O_{Sample}/^{18}O/^{16}Ov_{-SMOW}\right) - 1\right] \times 1000 \quad [1]$$

These delta values ($\delta^{18}O$ and δ^2H) are expressed as per mil deviation relative to a known standard, in this case standard mean ocean water (SMOW). The samples were taken from all the aquifers; shallow, intermediate lower, intermediate upper, and the coal seam aquifer. Hydrochemical data from the UCG site groundwater monitoring was also used to analyse hydraulic connections at the study site. Groundwater is sampled on a monthly basis from all aquifers using bailers and all samples were conserved and transported to the laboratory for chemical analysis. Major and minor elements were determined together with pH and electrical conductivity. The groundwater monitoring chemical data was plotted on diagnostic plots for geochemical analysis of the groundwater status.

Results and discussion

Isotopic analysis

The isotopic data for $\delta^{18}O$ and δ^2H is presented in Table I. The $\delta^{18}O$ values range from –7.08‰ to 4.15‰ while the δ^2H ranges from –42.2% to 14.91%. The stable isotope data is plotted on a $\delta^{18}O/\delta^2H$ diagram (Figure 5) with respect to the global meteoric water line (GMWL). The lack of historical rainfall data for $\delta^{18}O$ and δ^2H in the study area prompted the addition of the Pretoria meteoric water line (PMWL) from a Pretoria station which is situated approximately 267 km from the study area. This station collects and record isotopic rainfall data which is kept in the Global Network of Isotopes in Precipitation (GNIP) database managed by the International Atomic Energy Agency (IAEA). The recorded monthly precipitation data resulted in the following relationship isotopic trend: $2H = 6.5\ \delta^{18}O + 6.4\%$ (Mook, 2000).

The $\delta^{18}O$ and δ^2H values trended along the GMWL and are divided into two clusters, suggesting the possibility of two systems of groundwater at the Majuba UCG site. The samples that were enriched in $\delta^{18}O$ and δ^2H were from the shallower aquifers (shallow and intermediate upper), confirming that the water was subjected to the influence of evaporation. The samples showing depletion in $\delta^{18}O$ and δ^2H are from the deep aquifer, which confirms that they are not affected by evaporation and that recharge may have been by water from high altitudes, where heavy isotopes were removed from rainfall due to altitude/elevation effect. The variability in water isotopic composition between the shallow and the deep aquifer points to dissimilar recharge events, runoff conditions, sampling period salinity, and altitude effect (Ayadi *et al.*, 2018).

The less negative values were obtained from the upper and lower intermediate aquifers as well as the shallow aquifer. These waters may be more enriched in the stable isotopes since they have a shorter residence time in the ground than the deep aquifer waters.

The deep aquifer is represented by average values of –42 and –7.02 for $\delta^{18}O$ and δ^2H, respectively. These values are significantly different from the mean values observed in the other aquifers. The deep aquifer samples are clustered separately from the other aquifers. The positioning of the deep aquifer samples is consistent with the position of paleo-waters that have equilibrated with surrounding rocks, where little or no evaporation transpires. The deep aquifer is expected to receive little local recharge during precipitation events as compared to other aquifers. It is isolated from the rest of the aquifers with no evidence of mixing.

A clear distinction can be seen in the isotopic signatures of the different aquifer systems depicted in Figure 5. This is particularly portrayed in the deep and the shallow aquifer where the clustered points are closely packed for each system. One sample from the intermediate upper aquifer plots in the position dominated by the samples from the intermediate lower (encircled in Figure 5), which confirms mixing between the two aquifers through the T2 weathered dolerite but no mixing with the deep aquifer. The deep aquifer and the dam samples are the most distinctive and isolated compared to the other samples.

The evaporation line in Figure 5 has a slope of 4.6, which is in line with the global range of 4 to 8, for example GMWL

Table I

Isotopic data for groundwater in the study area

Borehole Identification and aquifer association	d^2D (‰)	$d^{18}O$ (‰)
WMD2 Deep aquifer	–42.2	–7.08
WMD3 Deep aquifer	–40.9	–6.98
WMD4 Deep aquifer	–42.0	–7.01
WMIL2 Intermediate lower	–23.5	–4.52
WMIL3 Intermediate lower	–27.1	–4.95
WMIL4 Intermediate lower	–29.1	–4.79
WMIU1 Intermediate upper	–16.3	–2.55
WMIU2 Intermediate upper	–25.7	–4.54
WMIU3 Intermediate upper	–5.4	–0.24
WMIU4 Intermediate upper	–13.6	–2.06
WMS2 Shallow	–19.1	–2.93
WMS3 Shallow	–19.7	–3.34
WMS4 Shallow	–20.5	–3.63
Dam	14.9	4.15

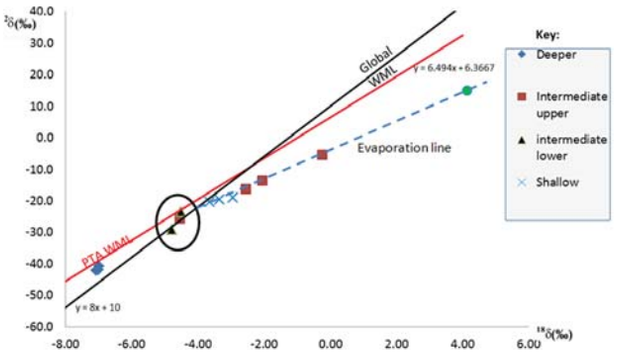

Figure 5—The Craig plot for Majuba UCG site, dam sample is plotted in green

has a slope close to 8 (Clark and Fritz, 1997). The slope depends on the relative humidity, temperature, and concentration in the atmospheric moisture (Yurtsever and Payne, 1978). Relative humidity is fairly constant at 80% in Mpumalanga Province during the summer season (Govere *et al.*, 2001). The Craig-Gordon (1965) model has established the relationship between the slope of the evaporation line and the relative humidity. The 4.6 slope value relates to a relative humidity value within the 50% to 75% range as described by Gordon *et al.* (1993). This deduced range corresponds with the 80% relative humidity in the Mpumalanga area. The isotopic signature for the shallow aquifer plots along the evaporation line, which suggests that the water from the surface sampling point (dam) and the shallow aquifer originated from similar precipitation. The shift in the isotopic signature of the dam to more positive $\delta^{18}O$ and $\delta^{2}H$ values is due to constant evaporation from the dam favouring the enrichment of water vapour in the lighter isotopes and the heavier isotopes remaining in the dam. The shallow aquifer plots along the evaporation line but with more negative $\delta^{18}O$ and $\delta^{2}H$ values compared to the dam. This is due to the isolation of groundwater from the atmosphere upon aquifer recharge, which leads to the isotopic signature being unaffected by fractionation due to evaporation.

The three points from the intermediate upper aquifer also plot along the evaporation line, which suggests that recharge was from the same water source as for the shallow aquifer. The more positive isotopic signature of these three points compared to the shallow aquifer suggest that fractures in the dolerite sill preferentially transmit groundwater, which drains some of the water from the shallow aquifer and transmits it quicker than the sandstones in the shallow aquifer. This means that groundwater that is recharged in the shallow aquifer, with a more positive isotopic signature, will travel slower (longer residence time) through the sandstone matrix. However, if the water encounters fractures at the contact zone of the dolerite sill with the sandstone (where the intermediate upper aquifer is located, see Figure 4) then water flows faster and undergoes less isotopic fractionation due to rock-water interactions. This leads to some of the intermediate upper aquifer points having a more positive isotopic signature than those of the shallow aquifer. This also shows that there is possible mixing between the shallow aquifer and the intermediate upper aquifer.

Hydrochemical analysis

Monthly groundwater monitoring data over a two-year period was used to characterize the water type of each aquifer system at the Majuba UCG site. The groundwater chemical data was also plotted in an expanded Durov plot as seen in Figure 6. The distinct appearance of the deep aquifer can be seen under the Chloride section, where water with high chloride concentration plots. This is expected, as deep aquifers contain higher levels of sodium chloride salinity due to remnant seawater (Clark and Fritz, 1997). Outliers (red dots) were experienced in only one month; this is likely a sampling or analytical error as this trend did not persist. All the other aquifers plot in the bicarbonate section. While the other aquifers may have similar chemistries it is clear that the deep aquifer maintains its discrete profile. All the samples were taken post-gasification, and from the chemical analyses no link can be established between the deep aquifer and its shallower counterparts. The hydrogeological conceptual model (Figure 4) shows that the three uppermost aquifers may be linked through fractures in the lithology. Fractures and the weathering of the intrusive dolerite rocks can also cause flow to be more rapid in these aquifers compared to the deep coal seam aquifer. This can lead to increased ion exchange in the aquifers which may lead to a sodium bicarbonate water type dominating.

The STIFF diagram in Figure 7 was used to analyse the chemistry of selected average groundwater data from boreholes from each aquifer system. The G2WMD2 (coal seam aquifer) has a distinct chemical profile that is high in Na, K, Cl, and SO_4. This is typical of deep minewater that has a low flow rate in the aquifer. The other boreholes from the shallower aquifers have high carbonate-bicarbonate levels synonymous with fresh aquifer water.

The general trends from the isotope and chemistry data indicate no link between the deep coal seam aquifer and the shallow aquifer. The deep aquifer is represented by an isotopic signature that is depleted in the heavy isotopes with average values of –41.7% and –7.02% for $\delta^{18}O$ and $\delta^{2}H$ respectively, while the shallow aquifer is enriched with average values of –19.9% and –3.3%. Hydrochemical data also indicated a sodium chloride water type for the deep aquifer and a sodium bicarbonate water for the shallow aquifer.

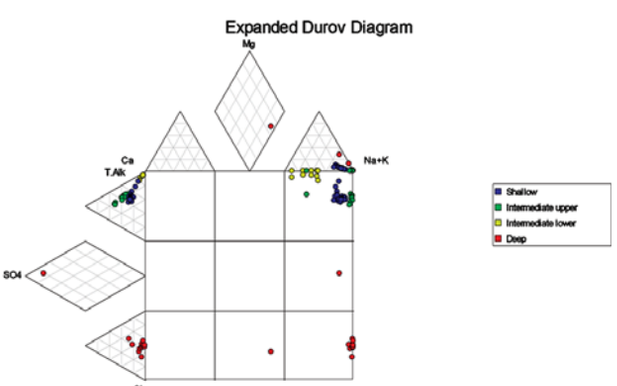

Figure 6—Expanded Durov plot of average groundwater data from different aquifers

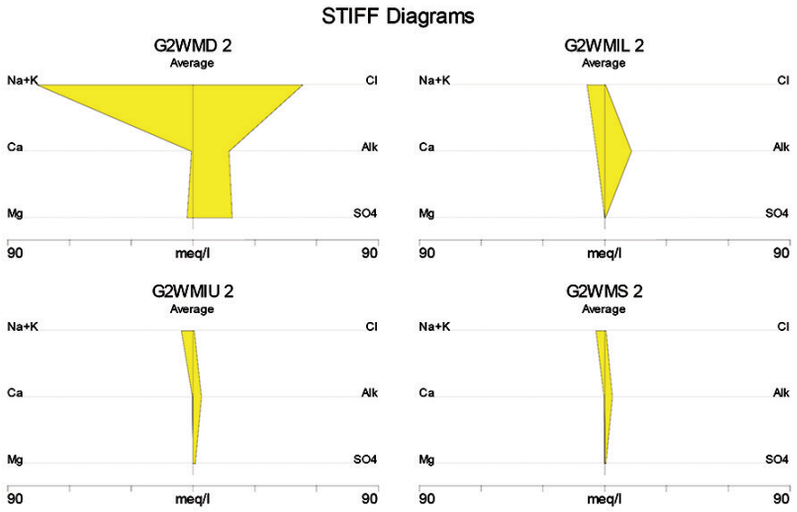

Figure 7—STIFF diagram of selected boreholes

Conclusions

The conceptual model of the site is supported by the stable isotope and hydrochemistry results. The water from the intermediate upper and intermediate lower aquifers had a mixture of signatures for the stable isotopes. This corresponds to the leakages depicted in the conceptual model that are associated with a weathered dolerite that is found in the intermediate upper and intermediate lower aquifers. The deep aquifer is characterized by an isotopic signature that is depleted in the heavy isotopes, with average values of –41.7% and –7.02% for $\delta^{18}O$ and $\delta^{2}H$ respectively, while the shallow aquifer is enriched with corresponding average values of –19.9% and –3.3%. The isotopic signature of the deep aquifer is distinct from those of the shallower aquifers, which confirms that there is no groundwater mixing between these aquifers. Hydrochemical data plotted in the diagnostic plots (expanded Durov and STIFF diagrams) also shows different types of waters: a sodium chloride water type for the deep aquifer and a sodium bicarbonate water for the shallow aquifer. The results show that the shallow aquifer and the deep aquifer are not hydraulically connected and therefore it is unlikely that groundwater from the gasification zone would contaminate the shallow aquifer.

References

Ayadi, Y., Mokadem, N., Besser, H., Khelifi, F., Harabi, S., Hamad, A., Boyce, A., Laouar, R., and Hamed, Y. 2018. Hydrochemistry and stable isotopes ($\delta^{18}O$ and $\delta^{2}H$) tools applied to the study of karst aquifers in southern Mediterranean basin (Teboursouk area, NW Tunisia). *Journal of African Earth Sciences*, vol. 137. pp. 208–217.

Bhutto, A.W., Bazmi, A.A., and Zahedi, G. 2013. Underground coal gasification: From fundamentals to applications. *Progress in Energy and Combustion Science*, vol. 39, no. 1. pp. 189–214.

Burton, E., Friedmann, J., and Upadhye, R. 2006. Best practices in underground coal gasification. Lawrence Livermore National Laboratory, USA.

Clark, I. and Fritz, P. 1997. Environmental Isotopes in Hydrology. Lewis, Boca Raton, FL.

Craig, H. and Gordon, L.I. 1965. Deuterium and oxygen 18 variations in the ocean and the marine atmosphere. *Proceedings of Stable Isotopes in Oceanographic Studies and Paleotemperatures*, Laboratorio di Geologia Nucleate, Spoleto, Italy. Tongiogi, E. (ed.). V. Lishi e F., Pisa. pp. 9–130. http://climate.colorado.edu/research/CG/

De Oliveira, D.P.S. and Cawthorn, R.G. 1999. Dolerite intrusion morphology at Majuba Colliery, northeast Karoo Basin, Republic of South Africa. *International Journal of Coal Geology*, vol. 41, no. 4. pp. 333–349.

Dvornikova, E.V. 2018. The role of groundwater as an important component in underground coal gasification. *Underground Coal Gasification and Combustion*. Blinderman, M.S. and Klimenko, A.Y. (eds.). Woodhead Publishing, Cambridge, UK. pp. 253–281.

Ghasemi, E., Ataei, M., Shahriar, K., Sereshki, F., Jalali, S.E., and Ramazanzadeh, A. 2012. Assessment of roof fall risk during retreat mining in room and pillar coal mines. *International Journal of Rock Mechanics and Mining Sciences*, vol. 54. pp. 80–89.

Gordon, J.J., Edward, T.W.D., Bursey, G.G., and Prowse, T.D. 1993. Estimating evaporation using stable isotopes: Quantitative results and sensitivity analysis for two catchments in northern Canada. *Nordic Hydrology*, vol. 24. pp. 79–94.

Govere, J.M., Durrheima, D.N., Coetzee, M., and Hunt, R.H. 2001. Malaria in Mpumalanga Province, South Africa, with special reference to the period 1987–1999. *South African Journal of Science*, vol. 97, no. 1–2. pp. 55–58.

Imran, M., Kumar, D., Kumar, N., Qayyum, A., Saeed, A., and Bhatti, M.S. 2014. Environmental concerns of underground coal gasification. *Renewable and Sustainable Energy Reviews*, vol. 31. pp. 600–610.

Kapusta, K. and Stańczyk, K. 2011. Pollution of water during underground coal gasification of hard coal and lignite. *Fuel*, vol. 90, no. 5. pp. 1927–1934.

Kapusta, K. and Stańczyk, K. 2015. Chemical and toxicological evaluation of underground coal gasification (UCG) effluents. The coal rank effect. *Ecotoxicology and Environmental Safety*, vol. 112. pp. 105–113.

Liu, S., Li, J., Mei, M., and Dong, D. 2007. Groundwater pollution from underground coal gasification. *Journal of China University of Mining and Technology*, vol. 17, no. 4. pp. 0467–0472.

Love, D., Beeslar, M.J., Blinderman, M., Pershad, S., van der Linde, G., and van der Riet, M. 2014. Ground water monitoring and management in underground coal gasification. *Proceedings of Unconventional Gas – Just the Facts*, Pretoria, South Africa, 18–19 August 2014. Groundwater Division of the Geological Society of South Africa and Mine Water Division of the Water Institute of South Africa.

Mook, W.G. 2000. Environmental Isotopes in the Hydrological Cycle, Volume 1: Introduction. IHP-V, UNESCO, Paris. 280 pp. http://www.iaea.org.at/programmes/ripc/ih/volumes/volumes.htm [accessed 28 August 2018].

Pershad, S., Pistorius, J., and van der Riet, M. 2018. Majuba underground coal gasification project. *Underground Coal Gasification and Combustion*. Blinderman, M.S. and Klimenko, A.Y. (eds.). Woodhead Publishing, Cambridge, UK. pp. 469–502.

Wilson, M.G.C. and Anhaeusser, C.R. (eds.). 1998. The Mineral Resources of South Africa. Handbook no. 16. Council for Geoscience, Pretoria.

Yurtsever, Y. and Payne, B.R. 1978. Application of environmental isotopes to groundwater investigation in Qatar. *Proceeding of the International Symposium on Isotope Hydrology*, Neuherberg, Germany, 19–23 June 1978, vol. 2. *International Atomic Energy Agency*, Vienna. pp. 465–490. ◆

http://dx.doi.org/10.17159/2411-9717/2018/v118n10a6

Temperature and electrical conductivity stratification in the underground coal gasification zone and surrounding aquifers at the Majuba pilot plant

by L.S. Mokhahlane, M. Gomo, and D. Vermeulen

Synopsis

Underground coal gasification (UCG) is a chemical process that converts coal *in situ* into a gaseous product at elevated pressures and temperatures. UGC creates an underground cavity that may be partially filled with gas, ash, unburned coal, and other hydrocarbons. A water stratification assessment can help assess the diffusion effects within the underground cavity. In this study we assessed the stratification by comparing the electrical conductivity (EC) profiles of background boreholes to the verification borehole that was drilled after gasification was complete. Stratification was seen in all boreholes, including the cavity borehole. The EC levels were lower in the cavity, which may be due to the dilution induced by injecting surface water during quenching of the gasifier. The thermal gradients showed a steady increase in temperature with depth, with higher temperatures measured in the verification borehole. This temperature increase suggests that heat is still being retained in the cavity, which would be expected. This study serves as the preliminary investigation of the stratification of temperature and EC, and will be followed by in-depth surveys that cover all the groundwater monitoring wells in the different aquifers at the site.

Keywords

stratification, underground coal gasification, Majuba pilot plant, electrical conductivity, temperature, aquifer.

Introduction

Underground coal gasification (UCG) is a technology that seeks to exploit coal reserves through gasification of *in situ* coal and extract a synthetic gas that can be used for electricity generation (Burton, Friedmann, and Upadhye, 2006). This is achieved by injecting oxidants through boreholes into the coal seams to induce gasification. The resultant synthetic gas (methane, hydrogen, and carbon monoxide) is piped to the surface via production wells, as seen in Figure 1. The UCG process offers some environmentally friendly outcomes such as no process tailings, reduced sulphur emissions, and low discharge of ash, mercury, and tar. The UCG cavity is, however, a source of gaseous and liquid pollutants (Liu *et al.*, 2007). Since the UCG process occurs in a natural environment, this raises concern about the impacts on the regional groundwater system.

The by-products of gasification can react with the surrounding strata or be dissolved in groundwater (Krzysztof and Krzysztof, 2014). However, this is unlikely to occur during gasification as the pressure in the cavity and the connected gas-filled voids must be kept below the hydrostatic pressure of the aquifer. This ensures that contaminants are always contained in the gasifier, as groundwater flows towards the cavity. A groundwater sink hence develops in the cavity as the gasifier consumes groundwater through evaporation, chemical reactions, and as part of the syngas in production wells.

Stratification is the vertical distribution of salinity, pH, and temperature of groundwater in a stepwise or layered manner (Ryuh *et al.*, 2017). Stratification within an underground cavity associated with coal mining is common in the Karoo coal-bearing formations (Johnstone, Dennis, and McGeorge, 2013). UGC creates an underground cavity as a result of coal being gasified *in situ*. Groundwater is an important input in the gasification process as water in the gaseous phase takes part in various chemical reactions to produce hydrogen gas, which forms part of the synthetic gas product. Upon completion of the gasification process, groundwater levels are expected to rebound in the gasification zone and the groundwater flow to resume. The geochemical evolution of the UCG cavity will proceed as a result of interactions between groundwater and the various residue products in the cavity, including ash, unburned coal, heat-affected surrounding strata, and hydrocarbons. Assessment of stratification in the UCG cavity is important as it may point to chemical processes such as diffusion, which may influence the evolution of contaminants. Johnstone, Dennis, and McGeorge (2013) reported stratification in cavities in coal mines at Ermelo, Mpumalanga Province, which

* *Institute for Groundwater Studies, University of the Free State.*

 ISSN 2225-6253. Paper received Apr. 2018; revised paper received Aug. 2018.

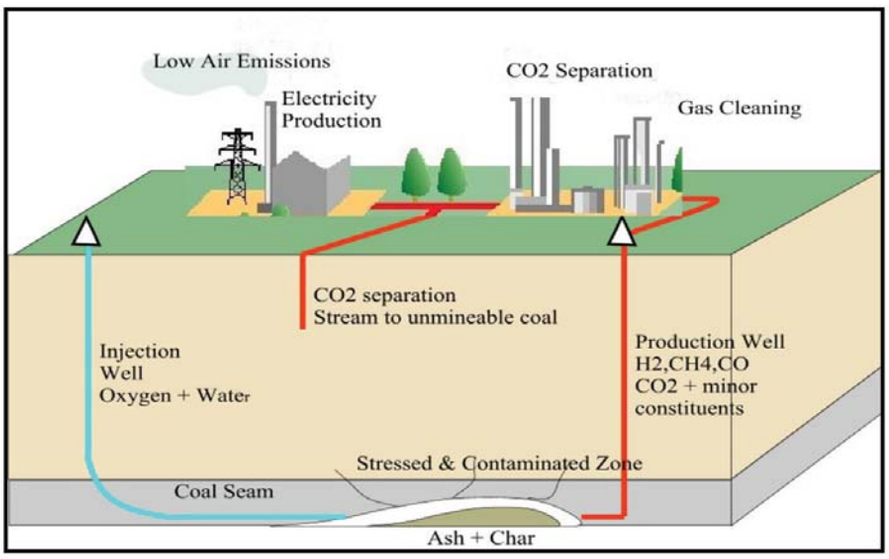

Figure 1—Diagram illustrating UCG process (Burton, Friedmann, and Upadhye, 2006)

showed groundwater quality evolves from sulphate-type water to sodium-type water due to the action of sulphate-reducing bacteria. The stratification led to the scrapping of the planned plant for treatment of decanting groundwater as the water quality at the top of the cavity was better than that at the bottom.

Groundwater contamination can be assessed using the source-pathway-receptor model in which the polluted groundwater travels through a flow path in order to impact a receptor or user of the resource. This study aims to assess the pathway section of the model using a borehole that intersects the gasification zone or cavity (source). This borehole is termed the verification borehole, and two other boreholes are used for comparison and as background boreholes. The water quality is assessed using electrical conductivity (EC). Temperature is assessed as an additional parameter but does not necessarily relate to the EC.

Study area

The initial groundwork on UCG at the Majuba coalfield began around 2005 and a pilot plant was successfully commissioned in January 2007, with product gas being co-fired into the nearby Majuba power station by October 2010.

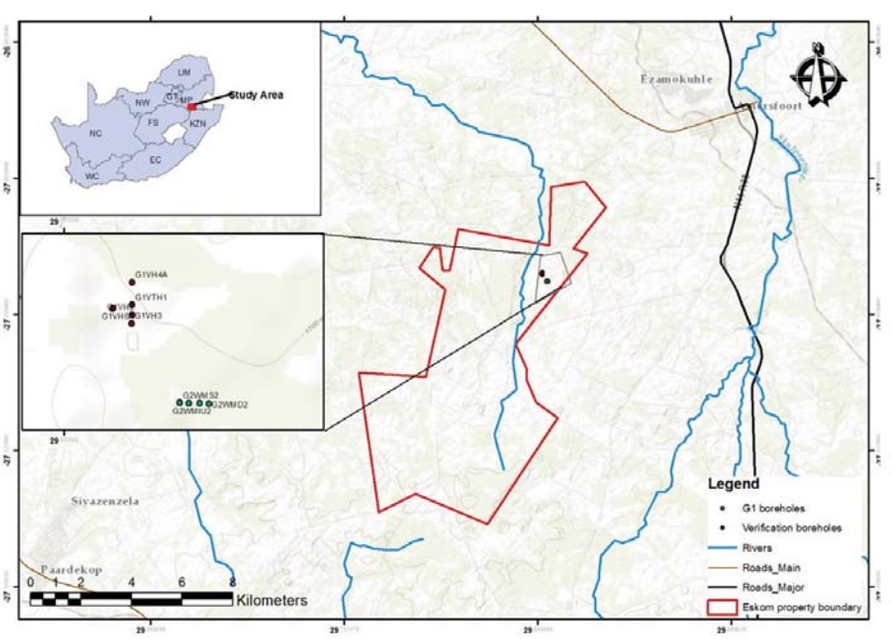

Figure 2—Location map for Majuba UCG

The Majuba pilot plant was successfully operated until September 2011, when decommissioning commenced with the shutdown of the gasifier (G1). Shutdown of G1 continued until May 2013 and involved complex activities included quenching using surface water and rebounding of the natural groundwater head. The successful performance and shutdown of the Majuba UCG pilot plant is a significant step towards full commercialization of UCG technology, as this was the first UCG plant in Africa. The shutdown of G1 presented an opportunity to investigate some of the key environmental questions regarding groundwater contamination.

The Majuba UCG pilot plant is located in South Africa's Mpumalanga Province, about 35 km north-west of the town of Volkrust. The site covers an area of around 60 ha on the eastern bank of the Witbankspruit (Figure 2). The topography is characterized by regular hills, attributed to erosion of the underlying dolerite sill.

Geology

The Majuba UCG site falls within the Vryheid Formation of the Lower Ecca Group, which is part of the Karoo Supergroup. The Karoo sequence is generally characterized by interbedded layers of sandstone, shale, and mudstone, with intrusive dolerite sills and dykes. At Majuba there are two dolerite sills. The shallower dolerite extends from roughly 70 m deep to around 170 m. The deep dolerite is located at around 50 m below the Gus coal seam, but in at other localities it transects the seam. A simplified geological profile of the Majuba UCG site is given in Table I.

Hydrogeology

Three distinct overlying groundwater systems are present at the Majuba UCG site, as seen in Figure 3. The upper weathered (shallow) aquifer is usually low-yielding (range 1–10 m³/d) owing to its trivial thickness, but the water quality is good due to years of groundwater flow through the weathered strata. It is estimated that the shallow aquifer can go as deep as 70 m. It is underlain by the intermediate aquifer. Groundwater flow through the intermediate aquifer is mainly through fractures, cracks, and joints as the Karoo sediments are excessively cemented, which prevents any substantial infiltration of water. The aquifer can be divided into three zones – the intermediate upper aquifer, intermediate lower aquifer, and the coal seam (deep) aquifer, as seen in Figure 3. The coal seam aquifer is at a depth of around 280 m and is underlain by the Dwyka sediments. The groundwater in the coal seam aquifer is of poor quality and can generally be classified as saline. The groundwater monitoring network had been placed in such a way that all the aquifers are monitored (Figure 3).

Table I

Simplified geology of the Majuba UCG site

Unit label	Lithology	Typical thickness range (m)	Typical thickness (m)
1	Overburden	0 to 4	4
2	Dolerite	4 to 35	31
3	Sandstone	35 to 64	29
4	Dolerite	64 to 185	121
5	Sandstone	185 to 287	102
6	Coal seam	287 to 291	4
7	Sandstone	291 to approx. 500	Unknown

Methodology

Three boreholes with depths of around 290 m were selected for this study. Two of the boreholes were groundwater monitoring boreholes for monitoring the coal seam aquifer within the production zone. The other was the verification borehole, which was drilled into the UCG cavity after the gasification process was concluded. The monitoring boreholes were used as background as they are outside the gasification zone and hence the geochemistry is not expected to be

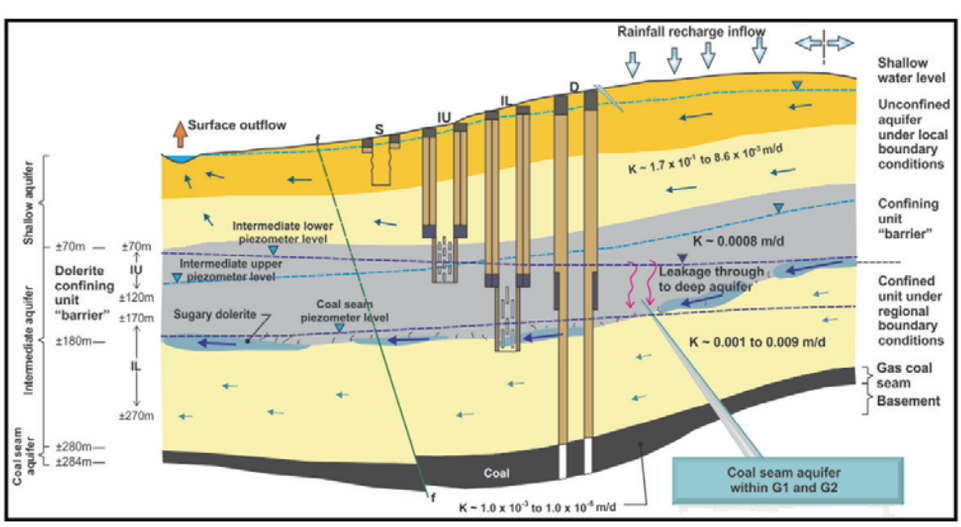

Figure 3—Conceptual model of the Majuba UCG site (Love *et al.*, 2014)

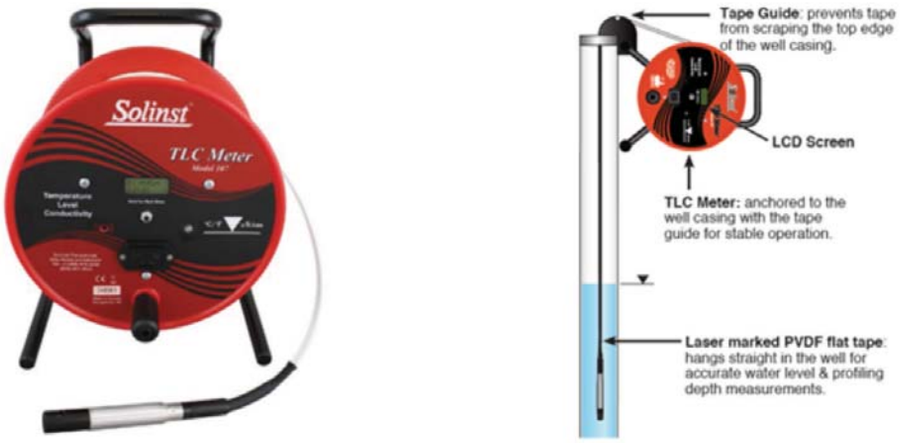

Figure 4—The Solinst TLC meter (left) and measurement arrangement (right)

influenced by the gasification process or its products. The verification borehole intersects the UCG cavity and hence provides useful information on the geochemical evolution of the gasification zone. Down-the-hole profiles of temperature and electrical conductivity (EC) were taken in order to investigate water stratification in the coal seam aquifer and UCG cavity. Stratification in old coal mine voids in the region has been reported by Johnstone, Dennis, and McGeorge (2013). This has resulted in dilution of polluted water, thereby eliminating the need for water treatment. A Solinst TLC (temperature, level, and conductivity) meter similar to the one depicted in Figure 4 was used to profile the EC down the borehole. Water level measurements can be read off the marked flat reeled tape made of polyvinylidene fluoride (PVDF) material. EC and temperature measurements are displayed on a convenient LCD display. The probe was lowered to the bottom of the borehole and depending on the measurement interval selected, measurements of temperature and EC were recorded simultaneously at each depth.

Results and discussion

The electrical conductivity and temperature profiles for the groundwater monitoring borehole G2WMD2 are shown in Figure 5. G2WMD2 is a monitoring borehole within the production zone that is used to monitor the coal seam aquifer (deep aquifer). The borehole is solid-cased from surface to 279 m, the depth of the coal seam.

The EC of the water increases with depth, with a maximum of 780 mS/m measured at a depth of 294 m below ground level (mbgl). The temperature also increases with depth until 244 mblg, where it levels off at 21.5°C. The EC profile shows erratic behaviour around 283 mbgl, which is approximately where the casing ends and is possibly a groundwater flow zone. This may be the best location to take groundwater samples as it might be where fresh water from the aquifer is flowing, as the borehole is cased above this point. Deeper than this a general trend of increasing EC is seen in the profile.

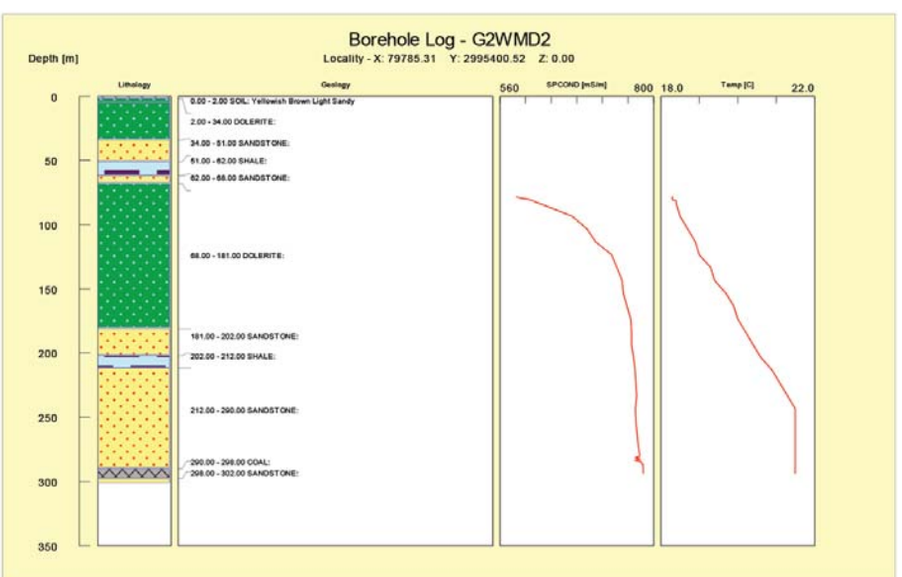

Figure 5—EC and temperature profiles of G2WMD2, which is solid-cased from the collar to 279 mbgl

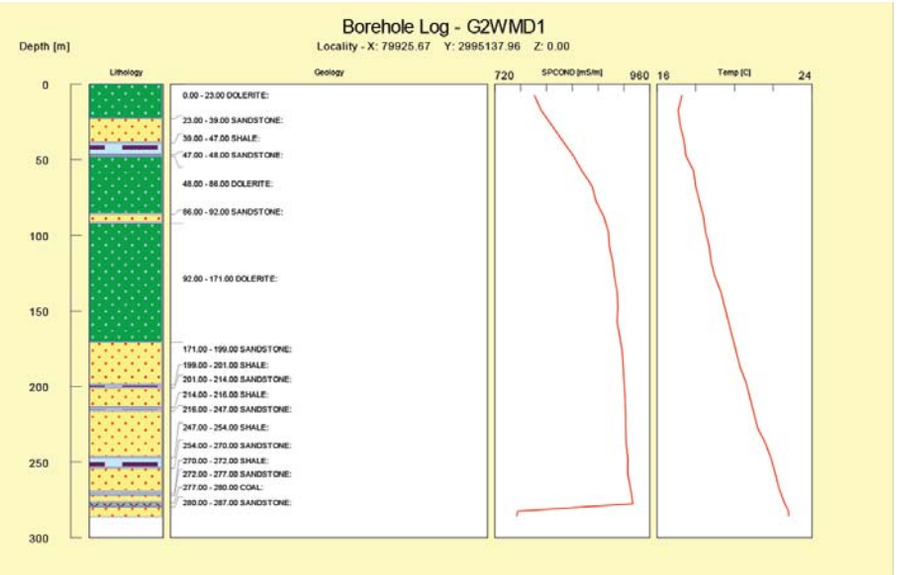

Figure 6—EC and temperature profiles of G2WMD1, which is solid-cased from the collar to 280 mbgl

The EC and temperature profiles for the groundwater monitoring borehole G2WMD1 are shown in Figure 6.

A similar trend of increasing EC and temperature to that observed in G2WMD1 was seen in G2WMD2. There is a drop in EC at depths greater than 283 mblg. This is also where the

casing ends and possibly represents an area where fresh aquifer water is flowing. The drop in EC suggests that fresh aquifer water is of a better quality than the stagnant water in the well. Purging of the borehole might lead to a better EC profile in terms of water quality. In contrast to G2WMD1, the temperature increases with depth without levelling off.

The EC and temperature profiles for the verification borehole G1VTH1 are shown in Figure 7.

G1VTH1 is the verification borehole drilled after gasification, and the EC and temperature profile are for the area in the borehole where water was encountered. The EC profile shows erratic behaviour, while the temperature increases with depth but levels off at a depth of 220 mbgl. The maximum temperature of 70°C was measured at a depth of around 250 m. The maximum temperature in G2WMD2 was 21.5°C, while in G2WMD1 it was 22.8°C. The erratic behaviour of the EC in G1VTH1 may be due to groundwater flow zones or fractures intersecting the well. This needs further investigation, but in general the EC is much lower in the verification borehole than in the monitoring boreholes. This could be due to dilution by surface water that was introduced into the cavity during quenching of the gasifier.

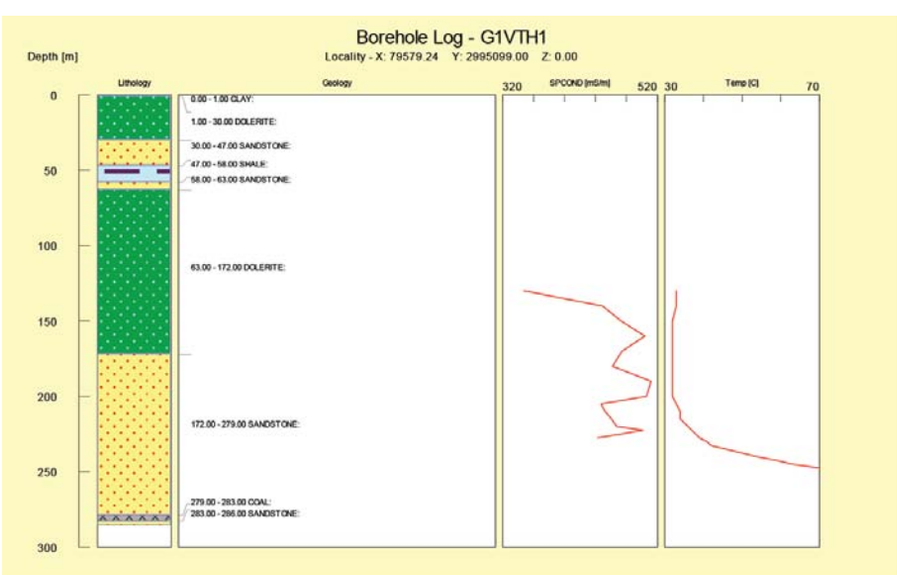

Figure 7—EC and temperature profiles of verification borehole G1VTH1, which is solid-cased from the collar to 200 mbgl. The borehole extends to around 286 mblg

Conclusions

The EC and temperature are stratified in all the boreholes (both monitoring and verification). The stratification in EC shows that the quality of water higher up in the well is better than that towards the bottom. The EC was erratic in the verification borehole but again the general trend indicated better quality water in the upper part of the well than in the gasification zone. This suggests that in the event of fractures forming due to roof collapses or any other event that could create a flow path between the cavity water and the shallower strata, the water quality will not be uniform throughout the hydraulic connection. Better quality water will tend to be located at the shallow levels, with poor quality water concentrated at the bottom. This may be due to chemical processes such as diffusion and needs further investigation. Johnstone, Dennis, and McGeorge (2013) found a similar trend in groundwater in an underground cavity induced by coal mining. There is a general increase in temperature in the verification borehole. This is expected at UCG sites, since it is a result of heat remaining in the UCG cavity even two years after the gasifier was shut down. The EC profile shows better quality water in the verification borehole than in the monitoring boreholes. This could be due to dilution by surface water introduced during quenching. The EC profile results were not related to groundwater transmission zones in the monitoring boreholes G2WMD1 and G2WMD2. This is due to the boreholes being cased for their entire length until the coal seam depth.

References

Burton, E., Friedmann, J., and Upadhye, R. 2006. Best practices in underground coal gasification. Lawrence Livermore National Laboratory, US Department of Energy.

Craig, H. and Gordon, L,I. 1965. Deuterium and oxygen 18 variations in the ocean and the marine atmosphere. *Proceedings of Stable Isotopes in Oceanographic Studies and Paleotemperatures*, Laboratorio di Geologia Nucleate, Spoleto, Italy. Tongiogi, E. (ed.). V. Lishi e F., Pisa. pp. 9–130. http://climate.colorado.edu/research/CG/ [accessed 5 July 2018].

Gordon, J.J., Edward, T.W.D., Bursey, G.G., and Prowse, T.D. 1993. Estimating evaporation using stable isotopes: Quantitative results and sensitivity analysis for two catchments in northern Canada. *Nordic Hydrology*, vol. 24, no. 79. pp. 79–94

Johnstone, A., Dennis, I., and McGeorge, N. 2013. Groundwater stratification and impact on coal mine closure. *Proceedings of the 13th Biennial Groundwater Division Conference*, Durban, South Africa. http://gwd.org.za/sites/gwd.org.za/files/03_A%20Johnstone%20et%20al_Groundwater%20Stratification%20and%20impact%20on%20coal%20mine%20closure%20final.pdf [accessed 5 July 2018].

Love, D., Beeslar, M.J., Blinderman, M., Pershad, S., van der Linde, G., and van der Riet, M. 2014. Ground water monitoring and management in underground coal gasification. *Proceedings of Unconventional Gas – Just the Facts*, Pretoria, South Africa, 18-19 August 2014. Groundwater Division of the Geological Society of South Africa and Mine Water Division of the Water Institute of South Africa.

Krzysztof, K. and Krzysztof, S. 2014. Chemical and toxicological evaluation of underground coal gasification (UCG) effluents: The coal rank effect. *Ecotoxicology and Environmental Safety*, vol. 112. pp. 105–113.

Mook, W.G. 2000. Environmental Isotopes in the Hydrological Cycle, Volume 1: Introduction. IHP-V, UNESCO, Paris. 280 pp. http://www.iaea.or.at/programmes/ripc/ih/volumes/volumes.htm [accessed 14 July 2015].

Liu, S., Li, J., Mei, M., and Dong, D. 2007. Groundwater pollution from underground coal gasification. *Journal of China University of Mining and Technology*, vol. 17, no. 4. pp. 0467–0472.

Govere, J.M., Durrheima, D.N., Coetzee, M., and Hunt, R.H. 2001. Malaria in Mpumalanga Province, South Africa, with special reference to the period 1987–1999. *South African Journal of Science*, vol. 97, no. 1–2. pp. 55–58

Ryuh, Y.-G., Do, H.-K., Kim, K.-H., and Yun, S.-T. 2017. Vertical hydrochemical stratification of groundwater in a monitoring well: Implications for groundwater monitoring on CO_2 leakage in geologic storage sites. *Energy Procedia*, vol. 114. pp. 3863–3869. ◆

http://dx.doi.org/10.17159/2411-9717/2018/v118n10a7

FACTSAGE™ thermo-equilibrium simulations of mineral transformations in coal combustion ash

by A.C. Collins*, C.A. Strydom*, J.C. van Dyk*†, and J.R. Bunt*‡

Synopsis

The aim of this investigation is to report on the influence of operating conditions, and of additives such as potassium carbonate, on the slagging behaviour of South African coal. This was done using a FACTSAGE™ model that was previously developed to simulate the chemistry and mineral transformations occurring during a fixed-bed countercurrent gasification process. The mineral transformations in K- and Al-containing inorganic compounds under certain thermal conditions were tracked to see whether these species remain in the minerals or are captured by the slag. The main contributors to slag formation and possible inorganic mineral transformations were identified. The addition of potassium carbonate to the coal before thermal processing decreases the melt formation temperature and the melt percentage. The mineral transformations and slagging behaviour depend on the percentage of potassium in the sample, as well as the basic components present in the coal.

Keywords

FACTSAGE™, coal combustion, potassium, aluminium, slagging behaviour.

Introduction

Coal is a heterogeneous material (sedimentary rock) composed of organic and inorganic components. The chemical and physical properties of coal vary depending on the source of the coal, *i.e.* the age and geological environment in which the coal was formed (Oboirien *et al.*, 2011; Yu, Lucas, and Wall, 2007). During gasification of coal, the organic matter partially decomposes (Kong *et al.*, 2011); while mineral transformations occur (Song *et al.*, 2009). Coal ash is thus a collection of mineral and non-mineral inorganic components that has undergone transformation as a result of thermal processing. The ash composition will depend on the organic and inorganic compounds present in the coal and/or any materials added to the coal prior to thermal processing (Kong *et al.*, 2014). This specific composition of the sample, the organic and inorganic components, determines the mineral matter transformation and thus the slag characteristics (van Dyk, 2006). Mineral behaviour during thermal processing depends on:

(i) The different types of minerals (modes of occurrence) and quantities present in the coal sample (Benson, Sondreal, and Hurley, 1995; Vassilev *et al.*, 1995)
(ii) The operating temperature
(iii) The oxygen partial pressure in the atmosphere (Jak *et al.*, 1998).

When the coal is subjected to high temperatures (> 1100°C), melting and reactions of the component mineral matter occur, forming slag (Song *et al.*, 2009). It is assumed that the slag composition depends on the minerals present in the coal, coupled with the operating conditions (Guo *et al.*, 2014). In addition, the slagging behaviour of coal ash depends on the ash composition, *i.e.* the inorganic species present in the ash, as these minerals determine the ash fusion temperature (AFT) (van Dyk and Waanders, 2008). Consequently, the ash fusibility is generally expressed as a function of the content of principal oxides: SiO_2, Al_2O_3, TiO_2, Fe_2O_3, CaO, MgO, Na_2O, and K_2O (Seggiani, 1999). The AFT is determined by the modes (vapour, solid mineral grains) in which these elements occur in the ash. Although AFT is still widely used as a parameter for determining ash fusibility and melting characteristics of minerals (Jak *et al.*, 1998), accurate results are difficult to obtain due to the complex composition of coal ash. Because of the complex nature of coal and the associated minerals, prediction of the mineral behaviour/transformation during thermal processing is a difficult task (Jak *et al.*, 1998) when applying tradition methods (Hanxu *et al.*, 2006).

FACTSAGE™ simulation of the slagging process provides a means by which mineral behaviour/transformation towards equilibrium conditions can be predicted. It is an important tool that can be used to describe equilibrium

* *Chemical Resource Beneficiation, North-West University, South Africa..*
† *African Carbon Energy, South Africa.*
‡ *School of Chemical and Minerals Engineering, North-West University, South Africa.*
 ISSN 2225-6253. Paper received Mar. 2018; revised paper received Aug. 2018.

ash properties, mineral transformation, behaviour of inorganic components, and the slagging tendency of coal ash at specific temperatures (van Dyk and Waanders, 2008), which can then be compared to experimental results. The modelling software was developed mainly for complex chemical equilibrium and process simulations, but can also be used to calculate and manipulate phase diagrams for minerals and mineral complexes (van Dyk *et al.*, 2009). One of the advantages of using the FACTSAGE™ databases is that carbon reactions can be studied in conjunction with minerals, while still being able to change atmospheric conditions (van Dyk *et al.*, 2006). The FACTSAGE™ software can also provide information on the phases that have reached equilibrium during thermal processing, the compositions of these phases and the proportions in which they are present (Hanxu *et al.*, 2006). A wide range of thermochemical calculations can also be performed with the FACTSAGE™ software (Hanxu *et al.*, 2006; Zhao *et al.*, 2013).

A FACTSAGE™ model was developed by van Dyk *et al.* (2006) in order to understand the chemistry and mineral transformation during a fixed-bed countercurrent gasification process. This model consisted of a three-zone simulation:

1. Drying and devolatilization zone
2. Gasification zone
3. Combustion and ash zone.

Van Dyk and Waanders (2008) subsequently developed a modified model that consisted of a two-zone simulation:

1. Drying, devolatilization, and gasification zone (reduction zone)
2. Combustion and ash zone (oxidation zone).

Both the original and improved thermodynamic equilibrium models were validated with high-temperature X-ray diffraction (HT-XRD) (van Dyk and Waanders, 2008; van Dyk *et al.*, 2008).

The recovery of inorganic compounds from coal ash produced during thermal processing may be economically viable. Potassium salts, for example, are used as gasification catalysts, *i.e.* they promote the production of methane during gasification (Nahas, 1983) and lower the operating temperatures of the gasification process (Green *et al.*, 1988). Coal ash represents a good potential source of potassium for re-utilization in industrial processes (Ge, Jin, and Guo., 2014).

The main aim of this investigation is to not only evaluate the influence of operating temperatures on slagging behaviour of South African coal ash, but also to determine if the addition of a potassium compound to the coal influenced the slagging behaviour. Various percentages of potassium (as potassium carbonate) were added to the system (modelling simulation) for each of the coal samples and the mineral transformations, especially Al- and K- containing minerals, tracked.

Materials and methods

Coal samples

Three South African coal samples (SA1, SA2, and SA3) and one from the USA (US1) were used. The South African samples originated from mines in the Mpumalanga region, and the USA coal from North Dakota. The samples were collected by the individual mines, and a representative sample of 50 kg was used during this study. The samples were selected so as to represent different ranks of coal, with ash fractions of various potassium contents and acidities. The coal rank was determined using the ASTM D388-12 standard. The acidity was determined from the XRF results (see Table III) using the following equation (van Dyk, Waanders, and van Heerden, 2008):

$$Acidity = (SiO_2 + Al_2O_3)/(Fe_2O_3 + CaO + MgO + Na_2O + K_2O) \quad [1]$$

The rank and acidity for the four coal samples are presented in Table I.

Sample preparation

The coal was prepared by air drying the entire sample as received from the mine, to reduce the excess moisture not associated with the coal structure. After drying, the samples were crushed to < 1 mm using a crusher and ball mill. The SA2 blend sample was prepared by the addition of potassium carbonate (5 wt%) to the coal during the milling step in order to ensure a heterogeneous mixture of additive and coal.

Predicting the influence of potassium content on the mineral transformation and slagging behaviour was investigated using FACTSAGE™ modelling. The percentage potassium added was calculated according to the ash yield of the coal, *i.e.* a specific percentage of potassium was loaded to the sample according to coal ash percentage.

Analytical methods

The coal samples were subjected to ultimate, proximate, and XRF analysis. Sample preparation was done according to ISO 13909-4: 2001. The ISO standard characterization methods used on the coal samples are summarized in Table II. The composition of the coal ash samples was determined by XRF analysis, and is presented as elemental oxides.

Table I

Rank and acidity values for the four coal samples

Sample	Rank	Acidity
SA1	Medium-volatile bituminous	18.4
US1	Lignite	2.95
SA2	High-volatile bituminous	2.91
SA3	Medium-volatile bituminous	6.31

Table II

Coal characterization methods

Analyses	Standard method
Proximate analysis	
Moisture content	ISO 11722: 1999
Ash content	ISO 1171: 2010
Volatile content	ISO 562: 2010
Fixed carbon	By calculation
Ultimate analysis	ISO 29541: 2010
Ash composition (XRF)	ASTM D4326

FACTSAGE™ Modelling

FACTSAGE™ 7.2 modelling software was used to investigate the mineral transformations and speciation of the four coal samples. The two-zone gasification simulation model (van Dyk *et al.*, 2008), described earlier, was used. In order to simulate a real gasification process, similar operating conditions (*i.e.* similar flows and conditions such as temperature, pressure, and mass flow) were used in the model, (van Dyk, Melzer, and Sobiecki, 2006). Although coal is a complex heterogeneous material that consists of different amounts of various organic and inorganic components, to accommodate the model used for the simulations it was assumed that coal consists of four basic components: moisture, fixed carbon, volatile matter, and minerals. The data was input to the FACTSAGE™ software in elemental form, *i.e.* carbon, hydrogen, nitrogen, sulphur, oxygen, and inorganic components. Input data can also be in mineral or compound form. For this investigation, the input data was derived from the results obtained from ultimate, proximate, and ash composition analyses. The mass flow data for the volatile matter and fixed carbon was normalized to an elemental composition, similar to that of ultimate analysis. Since the ash flow (melt) is composed of a variety of mineral species, it was normalized to a mass flow for the different mineral species (van Dyk, Melzer, and Sobiecki, 2006).

Simulation model

The model used in this investigation was developed on the principle that coal flows from the top into the gasifier as gas flows upwards into the zone that is being modelled. Thus, as the coal flows downwards into the drying, devolatilization, and gasification (reduction) zone, it comes into contact with and reacts with the gas that flows upwards from the combustion (oxidizing) zone. A similar approach was followed during the modelling of the combustion (oxidation) zone. As the organic and mineral components in coal enter the combustion (oxidation) zone, they react with the reagent gas that flows into the gasifier at 340°C (van Dyk *et al.*, 2009). The two modelling zones, as described in van Dyk *et al.* (2208), differ in two main respects: the input data used for the simulations and the temperature range at which the simulations are run. The temperature range used for the drying, devolatilization, and gasification (reduction) zone started at 25°C when the coal enters the gasifier and reacts with the gas that flows up from the combustion (oxidation) zone at a maximum temperature of 1400°C (van Dyk and Keyser, 2014; van Dyk *et al.*, 2009). The databases used for the FACTSAGE™ calculations were FactFS, FToxid, and FTmisc. The FactPS database was used for all pure and gaseous components during simulation, while the FTmisc database was used for the pure sulphur compound. The melt phase was imitated using the 'B-Slag-liq with SO_4' phase, which forms part of the FToxid database. During the simulations, only pure compounds from these databases were considered.

Results and discussion

Characterization

The ultimate and proximate analyses results are presented in Table III. The ash yield varied between 20% and 30% for the different samples. The South African coal samples had a high volatile content, similar to previous observations for South African coals (Hattingh *et al.*, 2011).

The ash compositions are presented in Table IV. These results indicate that the ash samples consist primarily of alumina (Al_2O_3) and silica (SiO_2), with the K_2O content between 0.43% and 2.06%. The SA2 blend sample with added potassium had a K_2O content of 16.1%. CaO, Fe_2O_3, Na_2O, and MgO, which were present in moderate percentages, are known for their fluxing potential during thermal processing of coal.

FACTSAGE™ modelling

Thermochemical calculations, using the EQUILIB uool which form part of the FACTSAGE™ modelling software, make it possible to predict the equilibrium behaviour of the inorganic compounds during thermal processing. Equilibrium mineral transformation and slag formation can therefore be predicted; under specific conditions. The influence of potassium additive was modelled using the following approach. Potassium addition was done according to the ash yield of the coal, *i.e.* a specific percentage (1, 5, or 10 mass%) of the ash yield is represented by the potassium oxide seen in Table IV. Figures 1–5 present the FACTSAGE™ simulation graphs for the feed

Table III

Ultimate and proximate analyses for the coal samples

	SA1	US1	SA2	SA2 blend	SA3
Proximate analysis (air-dried basis)					
Moisture (%)	3.3	18.0	3.7	4.6	4.0
Ash yield (%)	28.3	20.5	28.5	26.8	22.4
Volatiles (%)	18.2	30.5	21.2	21.5	21.9
Fixed (%)	50.2	31.0	46.5	47.1	51.7
Ultimate analysis (air-dried basis)					
Carbon (%)	56.4	43.3	53.7	54.6	59.1
Hydrogen (%)	3.0	3.2	2.58	3.4	3.1
Nitrogen (%)	1.2	0.7	1.26	1.3	1.4
Oxygen (%)	7.4	13.3	8.94	8.5	8.9
Sulphur (%)	0.5	1.0	1.26	0.8	1.1

Table IV

XRF analysis results for the coal ash samples (%)

	SA1	US1	SA2	SA2 blend	SA3
SiO_2	63.2	52.2	41.6	36.6	55.2
Al_2O_3	28.5	15.4	25.2	21.6	25.9
CaO	1.5	9.1	13.0	10.1	5.1
SO_3	1.5	8.1	7.6	5.1	4.3
Fe_2O_3	2.0	5.2	5.7	4.9	5.5
MgO	0.8	3.5	3.2	2.9	1.8
Na_2O	-	2.9	-	0.1	-
K_2O	0.7	2.1	1.1	16.1	0.4
TiO_2	1.5	0.8	1.8	1.6	1.3
BaO	-	0.6	0.2	0.5	0.1
SrO	-	0.3	0.3	0.3	0.1
MnO	-	0.1	0.1	0.1	0.1
P_2O5	0.1	0.1	0.3	0.3	0.1
Cr_2O_3	0.1	-	-	-	-

coal and coal blend samples in the reduction zone. Figure 6 indicates the AFT *versus* the percentage of basic compounds, and Figures 7–9 present the FACTSAGE™ simulation graphs for the feed coal and coal blend samples in the oxidizing zone.

As SA1 and SA3, which containeds the lowest percentages of K_2O and MgO, the highest percentages of SiO_2, and had the highest acidity, behave similarly according to the FACTSAGE™ simulation results, only the results obtained for SA1 are discussed. US1 and SA2 had similar acidity values as calculated from the XRF data, and both contained high percentages of K_2O and MgO; hence only the results from SA2 are discussed. The FACTSAGE™ results for both SA2 and the SA2 blend are discussed.

Drying, devolatilization, and gasification (reduction) zone

Mineral transformation

The mineral transformation simulation for SA1 is presented in Figure 1. From the graph it can be seen that the temperature at which melt stars to form was predicted to be 1175°C. The temperature at which the melt starts to form depends on the types of clays and fluxing minerals present in the coal, their concentrations in the sample, and their melting temperatures (Liu *et al.*, 2013). The transformation of quartz (SiO_2: S_2) to quartz (SiO_2: S_4) took place as the temperature increased above 800°C. Even though quartz is inactive during thermal processing, transformation of the mineral to a more stable polymorph will take place as the temperature increases. SiO_2 (S_x) refers to a stable phase for the mineral at a specific temperature (van Dyk, Waanders, and van Heerden, 2008). Stable phases of the different minerals present in the sample will influence the AFT. As the temperature increased above 1175°C, a decrease in the percentage quartz was observed during the simulation. This decrease may result from glass formation and partial melting of quartz (Zhou *et al.*, 2012). According to the simulation results, sillimanite (Al_2SiO_5), anorthite ($CaAl_2Si_2O_8$), cordierite ($Mg_2Al_4Si_5O_{18}$), and microcline ($KAlSi_3O_8$) contributed to the percentage melt as these minerals reached their melting temperatures. This same trend in mineral transformation was observed for SA3 during the simulation runs. However, the total percentage slag formed at 1400°C for SA3 (80%) was higher than that for SA1 (50%). This may be due to the higher anorthite and cordierite contents in SA3.

The mineral transformations for SA2 are presented in Figure 2. High percentages of anorthite are predicted. Other minerals such as microcline, quartz (S_2), quartz (S_4), and enstatite ($MgSiO_3$) are also present but at levels lower than 10%. The percentage melt increased with temperature as the minerals reach their melting temperatures. US1 exhibited similar mineral transformation trends to SA2 during the simulations, although the melt starting temperature was lower (1025°C) than that of SA2 (1125°C). The total percentage of slag formed from US1 (86%) at 1400°C was higher than for SA2 (55%). This may be due to the high contents of anorthite, diopside, and K- and Na-feldspars ($KAlSi_3O_8$ and $NaAlSi_3O_8$) in US1.

The mineral transformation simulation for SA2 blend, which is the coal sample with added potassium prior to thermal processing, is presented in Figure 3. From these results it can be seen that the temperature at which the melt starts to form was below 1000°C.

The influence of potassium addition to the coal prior to thermal processing can be seen by comparing the results for the SA2 blend (Figure 3) with those for SA2 in Figure 2. A decrease in the melt formation temperature (1125°C to 975°C) and percentage melt formation (55% to 43%) is observed.

Influence of added potassium salt on the slagging behaviour of coal

The modelled influence of added potassium (described in the previous section) on the slagging behaviour is presented in Figures 4–6. For SA1, increasing the potassium loading led to an increase in the percentage melt (Figure 4). The temperature at which melt formation started remains the same for the feed coal and blended coal samples. This has also been observed in other studies (van Dyk, 2006). The same trend was observed for SA3. The melt starting temperature was within 25°C for all the samples. The influence of potassium loading on the coal was observed only after the melt formation temperature was reached.

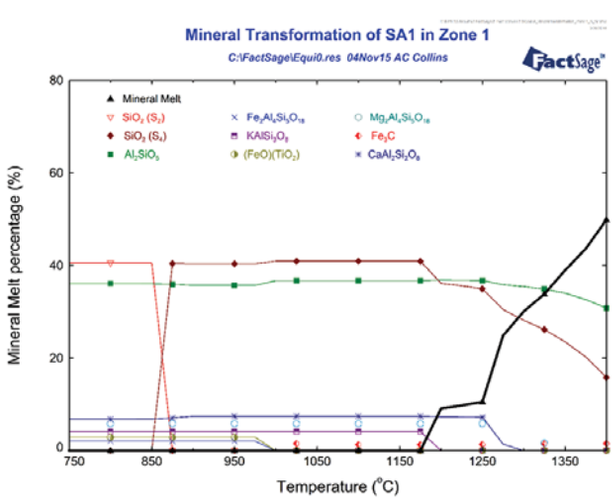

Figure 1—Calculated mineral transformations for SA1 in the reduction zone

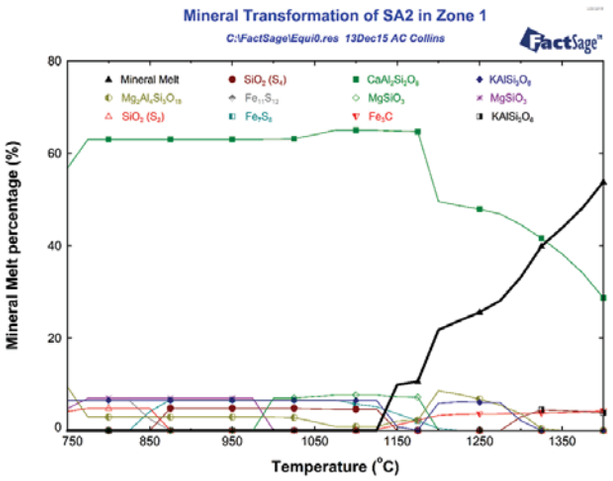

Figure 2—Calculated mineral transformations for SA2 in the reduction zone

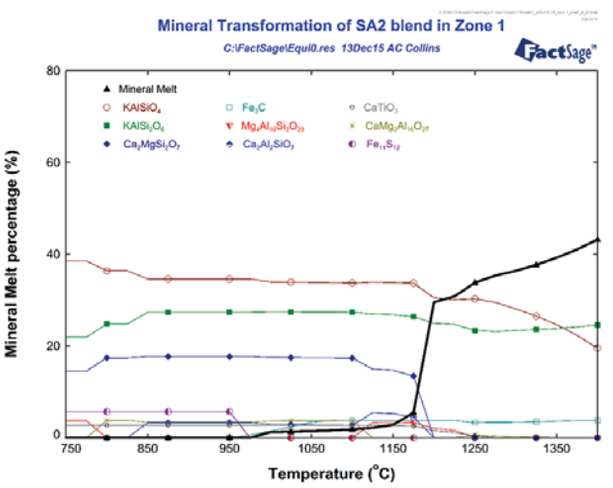

Figure 3—Calculated mineral transformations for SA2 blend in the reduction zone

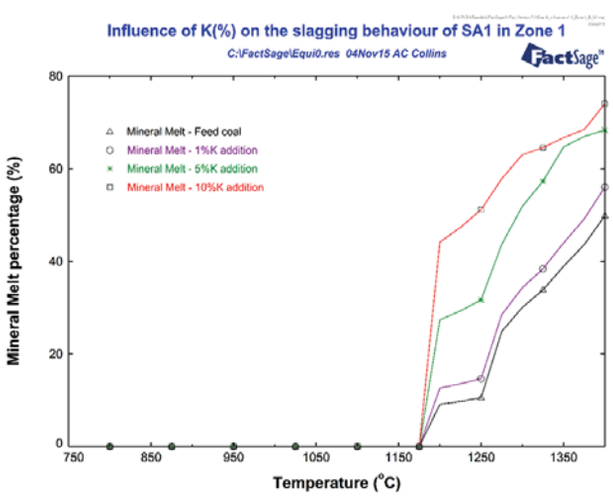

Figure 4—Calculated influence of K addition on slagging behaviour of SA1 in the reduction zone

Sample SA2 exhibited the opposite trend – a decrease in the melt percentage was observed with increasing potassium loading (Figure 5). The melt starting temperature increased with additions of 5 and 10 mass% potassium. The same trends for melt percentage and melt starting temperature were observed for US1.

A comparison of the melt formation results for the SA2 blend (Figure 3) and the theoretical results calculated for SA2 (Figure 5) shows that the predicted percentages of melt formation were similar (within 5%). The melt formation temperature for the SA2 blend (Figure 3) was lower (975°C) than the theoretical prediction results (1150°C) (Figure 5).

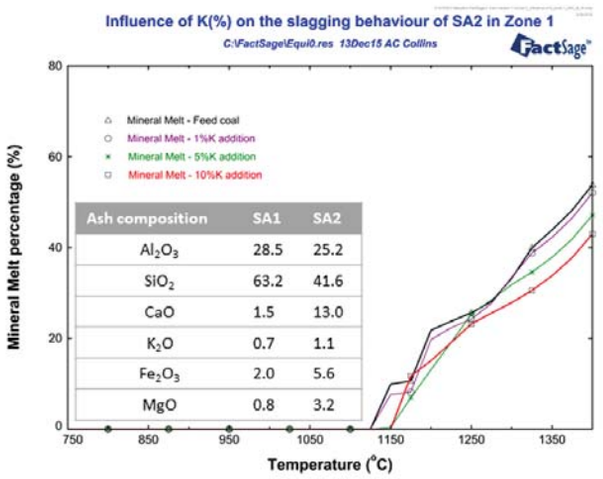

Figure 5—Calculated influence of K addition on slagging behaviour of SA2 in the reduction zone

From Figure 4 and Figure 5, it can be seen that addition of potassium carbonate to coal at different loadings had various influences on the slagging behaviour. The slagging behaviour of coal depends on the mineral matter present in the coal. From the XRF results presented in Table IV, it can be seen that SA2 contained high percentages of basic (K-, Ca-, Fe-, Na-, and Mg- containing) compounds. The basic compounds influence the AFT (increasing or decreasing it) (Hanxu *et al.*, 2006), and also act as fluxing agents when present in certain percentages in the coal (Jak *et al.*, 1998; van Dyk, Waanders, Hack, 2008). The concentration of these compounds, especially Ca-containing species, will determine their combined influence on the AFT. When high percentages of basic mineral compounds (Ca^{2+}, K^{+} Na^{+}, and Fe^{2+}) are present in a coal sample, an increase in the AFT will (possibly) be observed. This increase is due to the sub-liquidus transformation of the mineral phases (Song *et al.*, 2009). This implies that high percentages of basic mineral compounds lead to maximum mineral formation/transformation and the stabilization of these mineral phases, which in turn increases the AFT (van Dyk, Waanders, and Hack, 2008). A high AFT will also be observed with low percentages of basic mineral compounds present in the coal (Jak *et al.*, 1998). The influence of basic compounds, especially Ca, on the AFT is presented schematically in Figure 6. The results (source A and B) obtained by van Dyk, Waanders, and Hack (2008) are shown together with the coal samples used in this investigation (SA1, SA2, SA3, US1). The percentage of basic compounds in SA1 (4.9%) was lower than that of SA2 (22.9%). This indicates that SA2 would have a lower AFT than SA1. This influence of the basic compounds was also predicted by FACTSAGE™ modelling, and is presented in Figures 4 and 5.

Combustion and ash (oxidation) zone

Figures 7–9 presents the results obtained for the mineral transformation simulations for the different coal samples in the combustion and ash (oxidation) zone. The graphs should be read from right to left to better understand the flow of the material as it moves from the top to the bottom of the gasifier (cooling process). As the graph is read from right to left, formation of mineral phases is observed, which may indicate crystallization of mineral phases from the slag. Also seen in the figures is the decrease in melt percentage as the temperature of the operating process decreases.

Mineral transformation of coal samples

The mineral transformation simulation for SA1 is presented in Figure 7. As the cooling process starts, sillimanite (Al_2SiO_5) and SiO_2 (S_4 and S_2) minerals are formed. Small percentages of other minerals are also predicted to form during cooling. The same trend of mineral formation was again observed for SA3. Simulation of mineral transformation for SA2 is presented in Figure 8. Crystallization of minerals, such as calcium feldspar ($CaAlSi_3O_8$), cordierite ($Mg_2Al_4Si_5O_{18}$), calcium sulphate ($CaSO_4$), SiO_2 (S_4 and S_2), and potassium feldspar ($KAlSi_3O_8$) was predicted to occur as the temperature decreases. A similar trend was observed for US1. The simulation of mineral transformation for the SA2 blend is presented in Figure 9. During the cooling process, crystallization of minerals, such as leucite ($KAlSi_2O_6$) and kalisilite ($KAlSiO_4$) was predicted as the temperature decreased. The influence of the potassium loading on behaviour in the oxidizing zone will remain constant, since slag formation is determined at the highest temperature in the reducing zone.

Conclusions

The mineral transformation and slagging tendencies of different coal samples were investigated using the FACTSAGE™ modelling database. The extent of melt formation increased with increasing operating temperature as more of the minerals present in the coal undergo melting. Lower melting temperatures may be due to the fluxing influence of basic components such as Ca-, Mg-, K , and Fe-containing minerals. The slagging tendencies of the coal samples were dependent on the specific mineral composition of the coal and the transformation of these minerals during thermal processing. Increased potassium loadings according to the mineral content resulted in an increase in melt formation for samples SA1 and SA3, while for samples US1 and SA2 it decreased the amount of melt formation. The

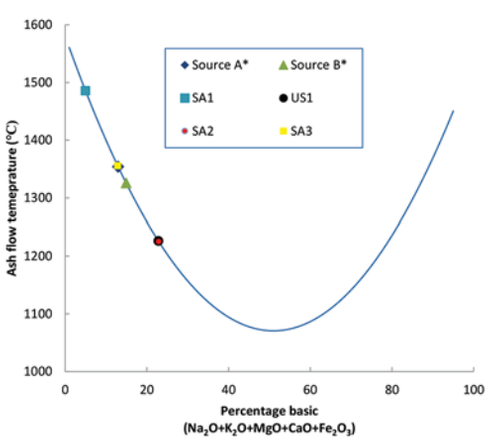

Figure 6—Ash fusion temperature *versus* the percentage of basic compounds (sources A and B: van Dyk, Waanders, and Hack, 2008)

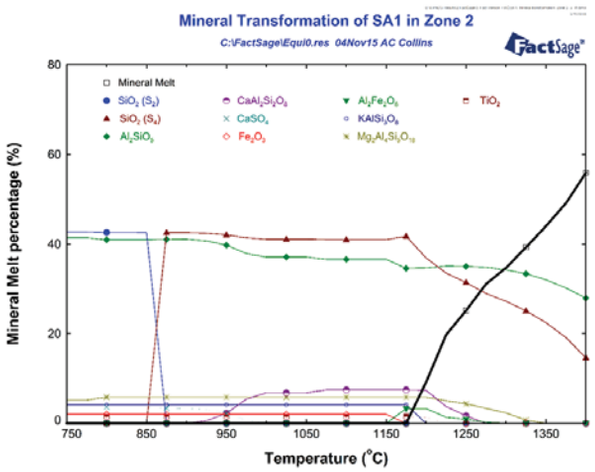

Figure 7—Calculated mineral transformations for SA1 in the oxidation zone

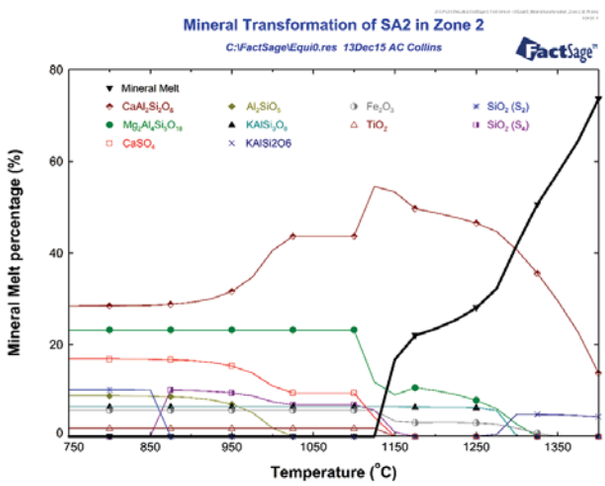

Figure 8—Calculated mineral transformations for SA2 in the oxidation zone

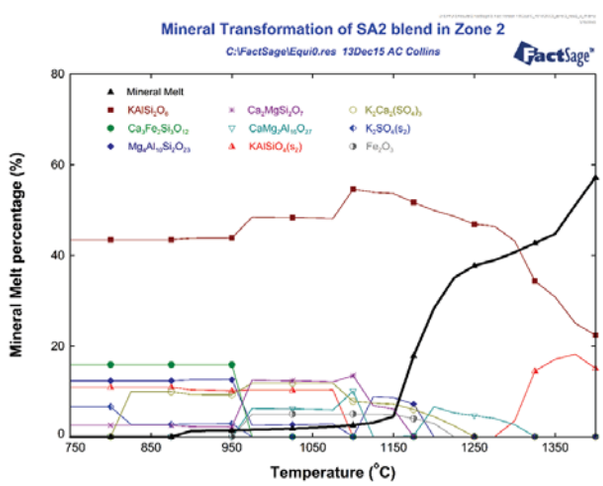

Figure 9—Calculated mineral transformations for SA2 blend in the oxidation zone

latter observation can be explained by the ratios of specific species and elemental composition, and may be attributed to the already high content of basic components in US1 and SA2.

The FACTSAGE™ simulations were modelled according to an equilibrium model for the gasifier, which predicts mineral transformations on the assumption that all minerals in the sample have reached equilibrium. Prediction studies were done on this basis, even though mineral transformations (reactions) do not reach equilibrium during thermal processing. Although melt (slag) predictions have been modelled and verified with the use of this software, not all mineral interactions between phases can be predicted due the limitations of the software database.

The following conclusions can be drawn.

- The temperature at which thermal processing occurs plays an important role in the extent of melt formation, mineral transformation, and also the recoverability of compounds from the ash.
- The addition of potassium to the coal prior to thermal processing influences not only the extent of melt formation, but also the AFT, depending on the coal mineral composition.
- Simulation predictions of the melt percentage from the theoretical (assumed) addition of potassium to the coal compared well to the simulation run on the blended sample (coal sample with potassium). The simulation runs indicated a ±200°C difference in the melt formation temperatures. This may due to complex reactions taking place between the potassium and mineral phases in the coal, which could not be predicted by the equilibrium model conditions.

It needs to be remembered that FACTSAGE™ simulations are only a prediction of what might occur during thermal processing, and that these predictions are based on thermodynamic equilibrium conditions. These simulations provide only an indication on what might actually occur during thermal processing. Despite this limitation, the FACTSAGE™ modelling software can be a powerful tool for predicting coal behaviour, which can be used to optimize conditions for the different coal burning technologies available.

Future work

- Prediction of the percentage potassium not captured in the melt or lost through gas formation. This may yield valuable insights when experimental work is conducted on the leachability of K-containing compounds.
- Simulation work on the influence of specific compounds, their percentages, and composition on the slagging behaviour of coal during thermal processing.
- Further investigations into the reactions of mineral phases with the potassium compound added to the coal.

Acknowledgements

The information presented in this paper is based on the research financially supported by the South African Research Chairs Initiative (SARChI) of the Department of Science and Technology and National Research Foundation of South Africa (Coal Research Chair Grant No. 86880).

Any opinion, finding, or conclusion or recommendation expressed in this material is that of the author(s) and the NRF does not accept any liability in this regard.

References

Benson, S.A., Sondreal, E.A., and Hurley, J.P. 1995. Status of coal ash behavior research. *Fuel Processing Technology*, vol. 44, no. 1-3. pp. 1–12.

Ge, Z., Jin, H., and Guo, L. 2014. Hydrogen production by catalytic gasification of coal in supercritical water with alkaline catalysts: Explore the way to complete gasification of coal. *Internation Journal of Hydrogen Energy*, vol. 39. pp. 19583–19592.

Green, P.D., Edwards, I.A.S., Marsh, H., Thomas, K.M., and Watson, R.F. 1988. Coal thermoplasticity and coke structure as related to gasification. *Fuel*, vol. 67. pp. 389–395.

Guo, Q., Zhou, Z., Wang, F., and Yu, G. 2014. Slag properties of blending coal in an industrial OMB coal water slurry entrained-flow gasifier. *Energy Conversion and Management*, vol. 86. pp. 683–688.

Hanxu, L.I., Ninomiya, Y., Zhongbing, D., and Mingxu, Z. 2006. Application of the FactSage to predict the ash melting behaviour in reducing conditions. *Chinese Journal of Chemical Engineering*, vol. 14. pp. 784–789.

Hattingh, B.B., Everson, R.C., Neomagus, H.W.J.P., and Bunt, J.R. 2011. Assessing the catalytic effect of coal ash constituents on the CO_2 gasification rate of high ash, South African coal. *Fuel Processing Technology*, vol. 92. pp. 2048–2054.

Jak, E., Degterov, S., Hayes, P.C., and Pelton, A.D. 1998. Thermodynamic modelling of the system Al_2O_3-SiO_2-CaO-FeO-Fe_2O_3 to predict the flux requirements for coal ash slags. *Fuel*, vol. 77. pp. 77–84.

Kong, L., Bai, J., Bai, Z., Guo, Q., and Li, W. 2014. Improvement of ash flow properties of low-rank coal for entrained glow gasifier. *Fuel*, vol. 120. pp. 122–129.

Kong, L., Bai, J., Li, W., Bai, Z., and Guo, Z. 2011. Effect of lime addition on slag fluidity of coal ash. *Journal of Fuel Chemistry and Technology*, vol. 39. pp. 407–411.

Liu, B., He, Q., Jiang, Z., Xu, R., and Hu, B. 2013. Relationship between coal ash composition and ash fusion tempretures. *Fuel*, vol. 105. pp. 293–300.

Nahas, N.C. 1983. Exxon catalytic coal gasification process. *Fuel*, vol. 62. pp. 239–241.

Oboirien, B.O., Engelbrecht, A.D., North, B.C., du Cann, V.M., Verryn, S., and Falcon, R. 2011. Study on the structure and gasification characteristics of selected South African bituminous coals in fluidised bed gasification. *Fuel Processing Technology*, vol. 92, no. 4. pp. 735–742.

Seggiani, M. 1999. Empirical correlations of the ash fusion temperatures and temperature of critical viscosity for coal and biomass ashes. *Fuel*, vol. 78, no. 9. pp. 1121–1125.

Song, W.J., Tang, L.H., Zhu, X.D., Wu, Y.Q., Rong, Y.Q., Zhu, Z.B., and Koyama, S. 2009. Fusibility and flow properties of coal ash and slag. *Fuel*, vol. 88, no. 2. pp. 297–304.

Van Dyk, J.C. 2006. Understanding the influence of acidic components (Si, Al, and Ti) on ash flow temperature of South African coal sources. *Minerals Engineering*, vol. 19. pp. 280–286.

Van Dyk, J.C. and Keyser, M.J. 2014. Influence of discard mineral matter on slag-liquid formation and ash melting properties of coal - A FACTSAGE simulation study. *Fuel*, vol. 116. pp. 834–840.

Van Dyk, J.C., Melzer, S., and Sobiecki, A. 2006. Mineral matter transformation during Sasol-Lurgi fixed bed dry bottom gasification - utilization of HT-XRD and FactSage modelling. *Minerals Engineering*, vol. 19. pp. 1126–1135.

Van Dyk, J.C. and Waanders, F.B. 2008. An improved thermodynamic FACTSAGE simulation to simulate mineral matter transformation during a fixed bed counter-current gasification process, validated with HT-XRD. *Proceedings of the XXIV International Mineral Processing Congress*. Beijing, China, 24–28 September 2008, vol. 2. Wang. D.Z. (ed.). Science Press, Beijing. pp. 2314–2321.

Van Dyk, J.C., Waanders, F.B., Benson, S.A., Laumb, M.L., and Hack, K. 2009. Viscosity predictions of the slag composition of gasified coal, utilizing FacSage equilibrium modelling. *Fuel*, vol. 88. pp. 67–74.

Van Dyk, J.C., Waanders, F.B., and Hack, K. 2008. Behaviour of calcium-containing minerals in the mechanism towards *in situ* CO_2 capture during gasification. *Fuel*, vol. 87. pp. 2388–2393.

Van Dyk, J.C., Waanders, F.B., Melzer, S., Baran, A., Hack, K., and Bunt, J.R. 2008. Validation of a thermodynamic equilibrium model developed on South-African coal sources in order to simulate mineral transformations of various coals during gasification. *Proceedings of the 25th International Annual Pittsburgh Coal Conference* Pittsburgh, PA.

Van Dyk, J.C., Waanders, F.B., and van Heerden, J.H.P. 2008. Quantification of oxygen capture in mineral matter during gasification. *Fuel*, vol. 87. pp. 2735–2744.

Vassilev, S.V., Kitano, K., Takeda, S., and Tsurue, T. 1995. Influence of mineral and chemical composition of coal ashes on their fusibility. *Fuel Processing Technology*, vol. 45. pp. 27–51.

Yu, J.L., Lucas, J.A., and Wall, T.F. 2007. Formation of the structure of chars during devolatilization of pulverized coal and its thermoproperties: A review. *Progress in Energy and Combustion Science*, vol. 33, no. 2. pp. 135–170.

Zhao, Y.L., Zhang, Y.M., Bao, S.X., Chen, T.J., and Han, J. 2013. Calculation of mineral phase and liquid phase formation temperature during roasting of vanadium-bearing stone coal using FactSage software. *International Journal of Mineral Processing*, vol. 124. pp. 150–153.

Zhou, C., Liu, G., Yan, H., Fang, T., and Wang, R. 2012. Transformation behaviour of mineral composition and trace elements during coal gangue combustion. *Fuel*, vol. 97. pp. 644–650. ◆

http://dx.doi.org/10.17159/2411-9717/2018/v118n10a8

Graphical analysis of underground coal gasification: Application of a carbon-hydrogen-oxygen (CHO) diagram

by S. Kauchali

Synopsis

Underground coal gasification (UCG) is recognized as an efficient mining technique capable of chemically converting the coal from deep coal seams into synthesis gas. Depending on the main constituents of the synthesis gas, chemicals, electricity, or heat can be produced at the surface. This paper provides a high-level graphical method to assist practitioners in developing preliminary gasification processes and experimental programmes prior to detailed designs or field trials. The graphical method identifies theoretical limits of operation for sensible gasification within a thermally balanced region, based primarily on the basic coal chemistry. The analyses of the theoretical outputs are compared to actual field trials from sites in the USA and Australia, with very favourable results. A South African coal is studied to determine the possible synthesis gas outputs achievable using various UCG techniques: controlled retractable injection point (CRIP) and linked vertical wells (LVW). For CRIP techniques, an important result suggests that pyrolysis, and subsequent char production, are important intermediate phenomena allowing for increased thermal efficiencies of UCG. The conclusion is that South African coals need to be studied for pyrolysis-char behaviour as part of any future UCG programme. The results also suggest that UCG with CRIP would be a preferred technology choice for Bosjesspruit coal where pyrolysis dynamics are important. Lastly, the use of CO_2 as oxidant in the gasification process is shown to produce syngas with significant higher heating value.

Keywords
Underground coal gasification, pyrolysis, char, thermal balance.

Introduction and literature survey

Coal is a commonly utilized fossil fuel, providing over 40% of global electricity demand and about 90% of South Africa's primary energy needs. However, less than 20% of the known world resources are suitable for possible extraction using conventional surface and underground mining techniques (Andrianopolous,, Korre, and Durucan, 2015). Underground coal gasification (UCG) has the potential to recover the energy stored in coal in an environmentally responsible manner by exploiting seams that are deemed unmineable by traditional methods. The UCG process, if successfully developed, can increase coal reserves substantially. For example, in the Limpopo region of South Africa alone, the estimated potential for UCG gas, based on existing geological records, is over 400 trillion cubic feet (TCF) natural gas equivalent – this is about a hundred times more gas than the existing 4-TCF Pande-Temane natural gas field reserve in Mozambique (de Pontes, Mocumbi, and Sangweni, 2014).

Sasol has been producing synthesis gas from surface gasifiers for over 60 years using South African bituminous coal that is mined using traditional methods (van Dyk, Keyser, and Coertzen, 2006). The authors acknowledge that South Africa will, for many years, rely on its abundant coal resources for energy, with gasification technology playing an enabling role.

The gasification propensity of low-grade South African coal was studied by Engelbrecht *et al.* (2010) in a surface fluidized bed reactor. The coal samples from New Vaal, Matla, Grootegeluk, and Duvha coal mines were high in ash (up to 45%), rich in inertinite (up to 80%), had a high volatile matter content (20%) and low porosity. The study established that these low-grade South African coals were able to gasify to produce syngas for downstream processes.

UCG is a thermo-chemical process which converts coal into a gas with significant heating value. The process requires the reaction of coal in air/oxygen (and possibly with the addition of steam and carbon dioxide) within the underground seam to produce synthesis gas (syngas). The primary components of syngas are the permanent gases hydrogen, carbon monoxide, carbon dioxide, and methane along with tars, hydrogen sulphide, and carbonyl sulphide. The ash is deliberately left below the ground within the cavity. A typical gasification cavity is carefully controlled to operate just below the hydrostatic pressure to ensure ingress of subsurface water into the cavity and the retention of products within the gasification system. The nature of UCG processes are such that a limited number of parameters can be

* *School of Chemical & Metallurgical Engineering, University of the Witwatersrand, South Africa.*

 ISSN 2225-6253. Paper received Apr. 2018; revised paper received Sep. 2018.

either controlled or measured. Furthermore, UCG processes require multidisciplinary integration of knowledge from geology, hydrogeology. and the fundamental understanding of the gasification process.

Recent review articles by Perkins (2018a, 2018b) provide an excellent basis for UCG practitioners. Perkins (2018a) covered the various methods of UCG as well as the performance of the methods at actual field sites worldwide. Of particular interest are the descriptions for drilling orientations, linking, and operational methods utilized for UCG: linked vertical wells (LVW), controlled retractable injection point (CRIP), and the associated variations. The factors affecting the performance of various UCG trials were studied as well as an assessment of economic and environmental issues around UCG projects. Guidelines are provided for site and oxidant selection based on field trials from the USA, Europe, Australia, and Canada.

Huang *et al.* (2012) studied the feasibility of UCG in China using field research, trial studies, and fundamental laboratory work comprising petrography, reactivity, and mechanical tests of roof material. In contrast, Hsu *et al.* (2014) performed a laboratory-scale gasification simulation of a coal lump and used X-ray tomography to assess the cavity formation. The cavity formation in the experiment was consistent with a teardrop pattern typical in UCG trials. The cavity shape and effect of operating parameters on the UCG cavity during gasification were studied by Jokwar, Sereshki, and Najafi (2018) using commercial COMSOL software.

Andrianopolous, Korre, and Durucan (2015) developed models to represent the chemical processes in UCG. In this study, models previously developed for surface gasifiers were adapted for UCG processes. The molar compositions and syngas production from the models were compared to reported results from a laboratory-scale experiment. A high correlation of the experimental and modelling results was achieved.

Zogala (2014a, 2014b) studied a simplistic coal gasification simulation method based on thermodynamic calculations for the reacting species as well as kinetic and computational fluid dynamics (CFD) models. Mavhengere *et al.* (2016) developed a modified distributed activation energy model (DAEM) for incorporation into advanced CFD calculations for gasification processes.

Yang *et al.* (2016) reviewed the practicalities of worldwide UCG projects and research activities over a five-year period. Their studies included developments in computational modelling as well as laboratory and field test results. The techno-economic prospects of combining UCG with carbon capture and storage (CCS) was also discussed.

Klebingat *et al.* (2018) developed a thermodynamic UCG model to maximize syngas heating values and minimize tar production from early UCG field trials at Centralia-PSC, Hanna-I, and Pricetown. The optimization suggested that tar production in the field trials could be eliminated, with significant improvements to the syngas heating values.

UCG development has been largely concerned with establishing methods to enhance well interconnectivity as well as techniques for drilling horizontal in-seam boreholes. In addition, methods are sought for the ignition of the coal as well as appropriate process control to ensure syngas quality. Site selection criteria have been considered crucial, while the contribution from laboratory work is considered to be limited. This undelines the need for site-specific piloting and testing.

In this study, the focus is restricted to the development of the UCG process based on the inherent chemical nature of coal and the specific reactions required to complete the conversion of solid coal into syngas. A graphical method is presented that allows an engineer with a basic competence in chemistry to develop high-level UCG processes without the need for detailed studies of kinetics, equilibrium, geology, and hydrogeology. The information obtained from such an exercise provides a target for the subsequent, and costly, field trials. The results obtained from the high-level graphical analyses are compared to UCG outputs from the Rocky Mountain (USA) and Chinchilla (Australia) trials. An interesting outcome is that the field trial outputs lie in a predictively narrow region, regardless of the UCG technique used. This is useful when new designs, with different coals, are being planned for UCG. Furthermore, the underground gasification of a South African coal from Bosjesspruit mine is studied to determine the possible regions of operation for producing syngas with the highest heating value suitable for power generation. A key result here shows that the preferred method for applying UCG to the coal from Bosjesspruit mine is the CRIP method, whereby the coal undergoes pyrolysis and char production prior to gasification.

Development of a graphical method for gasification reactions

The representation of gasification reactions on a bond equivalent phase diagram was advocated by Battaerd and Evans (1979). The bond equivalent phase diagram is a ternary representation of carbon, hydrogen, and oxygen (CHO) where species are represented by the bonding capacity of the constituent elements. To obtain the bond equivalent fraction for a species $C_xH_yO_z$, the contribution by carbon is 4(x), hydrogen is 1(y), and oxygen is 2(z), which is normalized for each species. Thus, CH_4 (methane) is represented by the midpoint between C and H. Similarly CO_2 (carbon dioxide) and H_2O (water) are midway between C-O and H-O respectively. CO (carbon monoxide) is one-third between C-O, as shown in Figure 1. According to Kauchali (2017), the important gasification reactions are obtained by considerations of the intersection of the feed (coal)-oxidant (steam, oxygen, or carbon dioxide) with the following lines: H_2-CO, H_2-CO_2, H_2-CO, CH_4-CO and CH_4-CO_2 (Figure 1). These intersections represent the stoichiometric region in which *sensible* gasification occurs – outside of these regions an excess amount of coal (carbon) or oxidants is evident, implying that they do not react within the gasification system. A further analysis of the intersections indicates the inherent thermal nature of the reactions, some of which are endothermic while others are exothermic. The endothermic and exothermic nature of the important reactions will be further explained in the examples that follow from the various field trials.

In an idealized underground gasification process the system must be overall thermally balanced so that there is no net heat released or added to the cavity. This requirement further limits the region of operation of thermally balanced gasification reactions.

In addition, the following criteria (Wei, 1979; Kauchali,

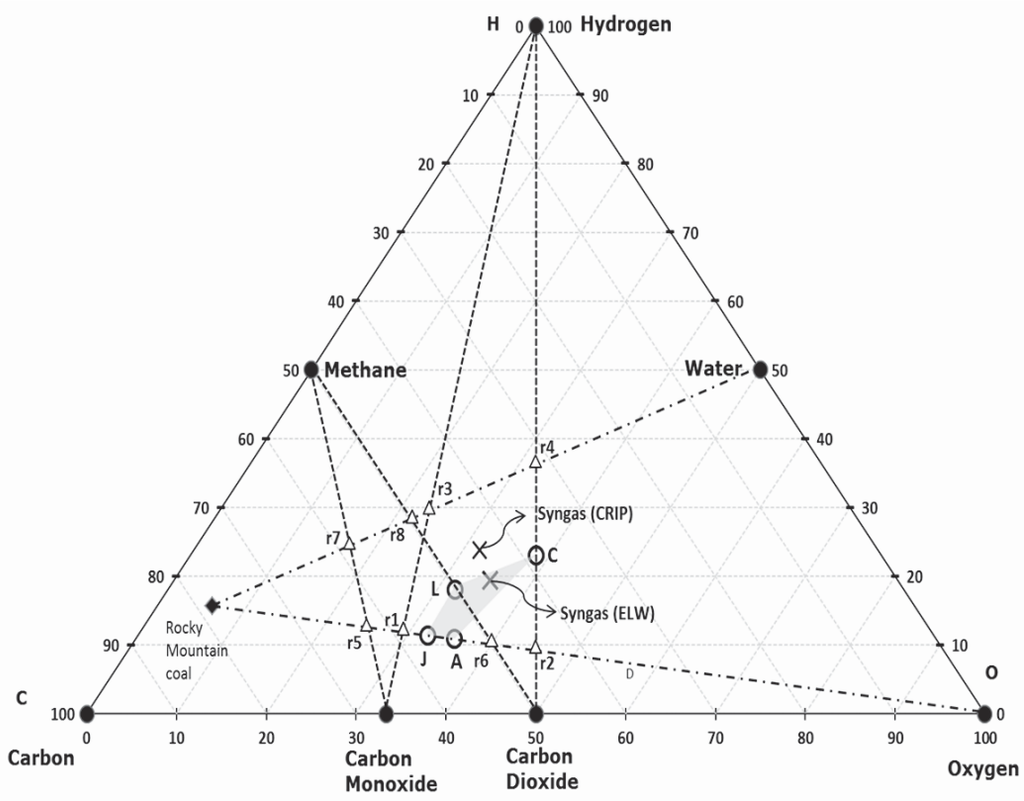

Figure 1—Graphical representation of Rocky Mountain underground coal gasification

2017) are used to decide on reactions that will form the overall mass and energy balances:

- Feed components may not appear in the product. For example, any gasification reaction that uses steam/oxygen as oxidant cannot have water as a product.
- The reactions on the CHO diagram represent the maximum region they enclose – mathematically, the intersection points represent the extreme points of a linearly independent reaction system.
- The extreme reactions points, representing overall stoichiometry, will lie on either of the lines H_2-CO, H_2-CO_2, H_2-CO, CH_4-CO and CH_4-CO_2.

Methodology and approach for graphical analysis of UCG processes

The graphical representation of the UCG processes is depicted on a ternary CHO diagram. The three different coals (USA, Australia, and South Africa) and the oxidants (steam, oxygen or carbon dioxide) are represented on the diagrams as feed points. From the representation of the feed points and the various intersections with the product lines (H_2-CO, H_2-CO_2, H_2-CO, CH_4-CO and CH_4-CO_2), a region of stoichiometrically acceptable gasification products is obtained. This stoichiometric region is a mass balance region indicating the possible combinations of elements (C, H, and O) resulting from the various reaction schemes during gasification. This stoichiometric region thus represents the maximum allowable area and possible products that can be obtained. Once the reactions governing the stoichiometry are obtained, the possible pairing of endothermic-exothermic reactions can be established. This requires the thermodynamic properties (heat of formation) of each species participating in the reaction. The combinations of the reaction pairs (exothermic and endothermic) lead to thermally balanced points where the reactions have a heat of reaction of zero (kJ/mol). This thermally balanced point represents a 'balanced' UCG process and is also plotted on the CHO diagram. Depending on the number of possible exothermic and endothermic stoichiometric reactions, a number of thermally balanced points exist. A study of the thermally balanced reaction points will result in identifying a smaller subset of reactions that will form the basic reactions, *i.e.* the extreme reactions that will form a boundary around all other thermally balanced reactions. These extreme reactions are referred to as 'linearly independent thermally balanced reactions' and are unique for every coal used. The linearly independent reactions are also plotted on the CHO diagram and the region enclosed by them is shaded to indicate the 'thermally balanced region' for the specific coal. These calculations can be repeated for chars resulting from the drying and pyrolysis of the parent coal, provided that the data is available.

The information thus obtained enables the determination of important gasification parameters such as the type of oxidants to use, the ratio of C:H or C:O going into the gasification process, the UCG technique required for maximum energy, and product recovery.

The following sections essentially provide the graphical development for a US and an Australian coal, and South African coal and char.

Table I

Ultimate and CV analysis of Rocky Mountain coal, dry (adapted from National Energy Technology Laboratory, 2012)

Rocky Mountain coal (Air-dry w/w%)	
Carbon	67.45
Hydrogen	4.56
Nitrogen	0.96
Sulphur	0.98
Chlorine	0.01
Ash	11.03
Oxygen	15.01
CV (MJ/kg)	19.8

Table II

Molar composition of Rocky Mountain syngas (adapted from Dennis, 2006)

Rocky Mountain syngas		
Component	ELW	CRIP
Hydrogen	32.7	39.6
Methane	10.1	10.3
Carbon monoxide	8.2	11.9
Carbon dioxide	45.7	35.3
Hydrogen sulphide	0.8	0.6
Nitrogen	0.5	0.5
Argon	0.2	0.1
Higher hydrocarbons	1.8	1.7

Analysis of Rocky Mountain (USA) field trials

Subbituminous coal from the Rocky Mountain site was gasified using UCG (Dennis, 2006). The coal had a chemical formula $CH_{0.811}O_{0.167}$ and a calculated heat of formation (from coal CV) of –203.1 kJ/mol. Table I represents the ultimate analysis. In Table II, the syngas output from the two UCG operations employed is shown, namely extended linking well (ELW) / linked vertical well (LVW) and controlled retractable injection point (CRIP) (Dennis, 2006). The ELW technique used two vertical wells about 40 m apart but linked to a horizontally drilled gas production well. The CRIP method used two directionally drilled horizontal wells into the coal seam: one for steam and oxygen injection and the second for syngas recovery. The ELW and CRIP methods produced syngas with different compositions.

In the final technical report on the site, Dennis (2006) discussed two technologies, both using a combination of steam and oxygen as oxidants. The report details the dry gas composition for ELW and CRIP operations. The ELW site used a steam to oxygen ratio of approximately 1.88 and the CRIP site a ratio of approximately 2.04. Tables III and IV represent the stoichiometric reaction scheme adapted for the Rocky Mountain coal and the thermally balanced reactions respectively. Table V lists the standard heat of formation per compound required to determine the heat of reaction for the respective systems for all samples considered in this study. In Table V, the standard heat of formation for coal was calculated from the coal CV, assuming total combustion to liquid water and carbon dioxide only. For the char, an estimate of the CV of char from South African coals was used as derived by Theron and le Roux (2015).

Table III is obtained by consideration of the intersection of the line joining Rocky Mountain coal with oxygen/steam and the lines H_2-CO, H_2-CO_2, H_2-CO, CH_4-CO and CH_4-CO_2 (Figure 1). It is noted that eight reactions (r_1 to r_8) form the basis of the stoichiometric region within which gasification occurs. Moreover, two of these reactions are exothermic: r_2 and r_6. Table IV is thus obtained by taking linear combinations of exothermic-endothermic pairs such that the overall heat of reaction is zero, leading to a further 16 reactions. At these conditions the gasification reactions are considered to be thermally balanced and are considered the 'desirable' operation from a mass and energy perspective. For UCG, this implies that the cavity is 'self-sustaining' from an energy perspective and assuming that there are no heat or mass losses from the system.

A matrix analysis of the thermally balanced reactions in Table IV indicates that there are in fact only four linearly independent thermally balanced reactions (zero heat of reaction). Also included are the calculated standard state higher heating values (HHV), in MJ/m³, of the syngas produced (with air as the source of oxygen), as given by Li *et al.* (2004).

Table III

Balanced stoichiometric reactions for Rocky Mountain coal

No.	Reaction	Heat of reaction (kJ/mol)
r_1	$CH_{0.811}O_{0.167} + 0.4165O_2 \rightarrow CO + 0.4056H_2$	91.9 (endothermic)
r_2	$CH_{0.811}O_{0.167} + 0.9165O_2 \rightarrow CO_2 + 0.4056H_2$	–191.3 **(exothermic)**
r_3	$CH_{0.811}O_{0.167} + 0.8331H_2O \rightarrow CO + 1.2387H_2$	293.3 (endothermic)
r_4	$CH_{0.811}O_{0.167} + 1.8331H_2O \rightarrow CO_2 + 2.2387H_2$	251.92 (endothermic)
r_5	$CH_{0.811}O_{0.167} + 0.3151O_2 \rightarrow 0.2028CH_4 + 0.7972CO$	99.1 (endothermic)
r_6	$CH_{0.811}O_{0.167} + 0.7137O_2 \rightarrow 0.2028CH_4 + 0.7972CO_2$	–126.7 **(exothermic)**
r_7	$CH_{0.811}O_{0.167} + 0.4202H_2O \rightarrow 0.4129CH_4 + 0.5871CO$	208.1 (endothermic)
r_8	$CH_{0.811}O_{0.167} + 0.7137H_2O \rightarrow 0.5597CH_4 + 0.4403CO_2$	159.62 (endothermic)

Table IV

Thermally balanced reactions for Rocky Mountain coal

No.	Reaction	Combination
A	$CH_{0.811}O_{0.167} + 0.5788O_2 \rightarrow 0.6756CO + 0.32446CO_2 + 0.4056H2$	$r_2 + r_1$
B	$CH_{0.811}O_{0.167} + 0.3289H_2O + 0.5547O_2 \rightarrow 0.3948CO + 0.6052CO_2 + 0.7345H_2$	$r_2 + r_3$
C	$CH_{0.811}O_{0.167} + 0.7912H_2O + 0.5209O_2 \rightarrow CO_2 + 1.1969H_2$	$r_2 + r4$
D	$CH_{0.811}O_{0.167} + 0.5203O_2 \rightarrow 0.1336CH_4 + 0.3412CO_2 + 0.5252CO + 0.1384H_2$	$r_2 + r_5$
E	$CH_{0.811}O_{0.167} + 0.2013H_2O + 0.4776O_2 \rightarrow 0.1978CH_4 + 0.521CO_2 + 0.2812CO + 0.2114H_2$	$r_2 + r_7$
F	$CH_{0.811}O_{0.167} + 0.3891H_2O + 0.4169O_2 \rightarrow 0.3051CH_4 + 0.6949CO_2 + 0.1845H_2$	$r_2 + r_8$
G	$CH_{0.811}O_{0.167} + 0.5415O_2 \rightarrow 0.0853CH_4 + 0.3351CO_2 + 0.5796CO + 0.2351H_2$	$r_6 + r_1$
H	$CH_{0.811}O_{0.167} + 0.2513H_2O + 0.4984O_2 \rightarrow 0.1416CH_4 + 0.5567CO_2 + 0.3016CO + 0.3736H_2$	$r_6 + r_3$
I	$CH_{0.811}O_{0.167} + 0.6134H_2O + 0.4749O_2 \rightarrow 0.135CH_4 + 0.865CO_2 + 0.7491H_2$	$r_6 + r_4$
J	$CH_{0.811}O_{0.167} + 0.4901O_2 \rightarrow 0.2028CH_4 + 0.3498CO_2 + 0.4473CO$	$r_6 + r_5$
K	$CH_{0.811}O_{0.167} + 0.159H_2O + 0.4437O_2 \rightarrow 0.2823CH_4 + 0.4956CO_2 + 0.2221CO$	$r_6 + r_7$
L	$CH_{0.811}O_{0.167} + 0.3158H_2O + 0.3979O_2 \rightarrow 0.3607CH_4 + 0.6393CO_2$	$r_6 + r_8$

Table V

Heats of formation for standard compounds, coals, and char

Component	Heat of formation (kJ/mol)
Water (g)	–241.80
Water (l)	–285.80
Carbon monoxide	–111.25
Carbon dioxide	–394.45
Methane	–75.75
Rocky Mountain coal	–203.13
Chinchilla coal	–112.27
Bosjesspruit Coal	–212.67
Bosjesspruit char	–14.11

Figure 1 illustrates the thermally balanced region (shaded grey area) based on the four basic reactions A, C, L, and J. It is of interest to note the position of the syngas (X) from the ELW and CRIP UCG field trials, which the proximity of the field trial results relative to the theoretical developments (grey shaded region) based only on the coal thermodynamic properties. Furthermore, it is noted that the theoretical HHV ranges from 6.95–14.34 MJ/m^3 (for pure oxygen blown) with an average of 10.64 MJ/m^3 and confirms the actual values of about 9.5 MJ/m^3 reported by Perkins (2018a). The highest HHV reported at L is not achievable due to equilibrium considerations, as the high temperatures required for gasification favour the destruction of methane and the production of CO_2, leading to lower HHV values.

Table VI

Linear independent thermally balanced reactions with higher heating values (MJ/m$_3$) for Rocky Mountain coal

No.	Reaction	HHV (MJ/m^3) Air-blown UCG
A	$CH_{0.811}O_{0.167} + 0.5788O_2 \rightarrow 0.6756CO + 0.32446CO2 + 0.4056H_2$	3.84
C	$CH_{0.811}O_{0.167} + 0.7912H_2O + 0.5209O_2 \rightarrow CO2 + 1.1969H_2$	3.68
J	$CH_{0.811}O_{0.167} + 0.4901O_2 \rightarrow 0.2028CH_4$+0.3498CO2+ 0.4473CO	4.84
L	$CH_{0.811}O_{0.167} + 0.3158H_2O + 0.3979O_2 \rightarrow 0.3607CH_4$+0.6393$CO_2$	5.77

Table VII

Ultimate analysis of Macalister coal seam, dry, ash-free basis (adapted from Queensland Department of Mines and Energy, 1999)

	Macalister coal
Carbon	80.2
Hydrogen	6
Nitrogen	1.5
Sulphur	0.7
Oxygen	11.6
CV (MJ/kg)	28

Table VIII

Molar composition of syngas from the Macalister coal Seam

Components (mol %)	UCG Sites			
	Chinchilla (LVW) Kacur *et al*. (2014)	Chinchilla (L-CRIPa) Perkins (2018a)	Chinchilla (L-CRIPo) Perkins (2018a)	Bloodwood Creek (P-CRIP) Perkins (2018a)
Nitrogen	43	45	-	44.7
Hydrogen	22	20	44.5	20.9
Carbon monoxide	7	10	10.1	2.6
Carbon dioxide	19	15	31.9	21.6
Methane	8	10	10.6	8.6
Heating value (MJ/m3)	6.6	5	9.9	5.7

Table IX

Balanced stoichiometric reactions for the Macalister coal seam

No.	Reaction	Heat of reaction (kJ/mol)
r_1	$CH_{0.898}O_{0.108} + 0.4458O_2 \rightarrow CO + 0.4489H_2$	1.02 (endothermic)
r_2	$CH_{0.898}O_{0.108} + 0.9458O_2 \rightarrow CO2 + 0.4489H_2$	–282.2 (exothermic)
r_3	$CH_{0.898}O_{0.108} + 0.8915H_2O \rightarrow CO + 1.3404H_2$	216.6 **(endothermic)**
r_4	$CH_{0.898}O_{0.108} + 1.8915H_2O \rightarrow CO2 + 2.3404H_2$	175.2 (endothermic)
r_5	$CH_{0.898}O_{0.108} + 0.3335O_2 \rightarrow 0.2244CH_4 + 0.7756CO$	8.9 (endothermic)
r_6	$CH_{0.898}O_{0.108} + 0.7213O_2 \rightarrow 0.2244CH_4 + 0.7756CO_2$	–210.6 **(exothermic)**
r_7	$CH_{0.898}O_{0.108} + 0.4447H_2O \rightarrow 0.4468CH_4 + 0.5532CO$	124.4 (endothermic)
r_8	$CH_{0.898}O_{0.108} + 0.7213H_2O \rightarrow 0.5851CH_4 + 0.4149CO_2$	78.7 (endothermic)

Table X

Thermally balanced reactions for the Macalister coal seam

No.	Reaction	Combination
A	$CH_{0.898}O_{0.108} + 0.4476O_2 \rightarrow 0.9964CO + 0.0036CO_2 + 0.4489H_2$	$r_2 + r_1$
B	$CH_{0.898}O_{0.108} + 0.5044H_2O + 0.4107O_2 \rightarrow 0.5657CO + 0.4343CO_2 + 0.4489H_2$	$r_2 + r_3$
C	$CH_{0.898}O_{0.108} + 1.167H_22O + 0.3623O_2 \rightarrow CO_2 + 1.6159H_2$	$r_2 + r4$
D	$CH_{0.898}O_{0.108} + 0.3524O_2 \rightarrow 0.2175CH_4 + 0.0309CO2 + 0.7516CO + 0.0139H2$	$r_2 + r_5$
E	$CH_{0.898}O_{0.108} + 0.3086H_2O + 0.2894O_2 \rightarrow 0.3101CH_4 + 0.306CO_2 + 0.3839CO + 0.1374H_2$	$r_2 + r_7$
F	$CH_{0.898}O_{0.108} + 0.564H_2O + 0.2063O_2 \rightarrow 0.4575CH_4 + 0.5425CO_2 + 0.0979H2$	$r_2 + r_8$
G	$CH_{0.898}O_{0.108} + 0.4471O_2 \rightarrow 0.0011CH_4 + 0.0037CO_2 + 0.9952CO + 0.4467H2$	$r_6 + r_1$
H	$CH_{0.898}O_{0.108} + 0.4396H_2O + 0.3657O_2 \rightarrow 0.1138CH_4 + 0.3932CO_2 + 0.493CO + 0.6609H_2$	$r_6 + r_3$
I	$CH_{0.898}O_{0.108} + 1.033H_2O + 0.3275O_2 \rightarrow 0.1019CH_4 + 0.8981CO_2 + 1.278H_2$	$r_6 + r_4$
J	$CH_{0.898}O_{0.108} + 0.3494O_2 \rightarrow 0.2244CH_4 + 0.0317CO_2 + 0.7438CO$	$r_6 + r5$
K	$CH_{0.898}O_{0.108} + 0.2796H_2O + 0.2678O_2 \rightarrow 0.3642CH_4 + 0.288CO_2 + 0.3478CO$	$r_6 + r_7$
L	$CH_{0.898}O_{0.108} + 0.5251H_2O + 0.1962O_2 \rightarrow 0.487CH_4 + 0.513CO_2$	$r_6 + r_8$

Analysis of Chinchilla and Bloodwood Creek (Australia) field trials

The Australian UCG projects were performed on the Macalister coal seam of the Walloon Coal Measures. At the Bloodwood Creek location the coal seam was about 200 m deep and 13 m thick, while at the Chinchilla, the depth was 130 m and the seam thickness 4 m. Coal quality data was obtained from the Queensland Department of Mines and Energy (1999) with respect to the use of Walloon coals (sub-bituminous) for power generation. Though analysis of the coal was reported on both the as-received and dry ash-free basis, the product gas was reported (in Kačur *et al*., 2014) only on a moisture-free basis. For this reason, the Macalister coal points are plotted as dry only, as seen in Table VII. Table VIII provides the syngas compositions obtained from various UCG methods and trials (Queensland Department of Mines and Energy, 1999).

The chemical formula for the Macalister coal seam is $CH_{0.898}O_{0.108}$, with the heat of formation being –112.27 kJ/mol. Table IX considers the eight balanced stoichiometric reactions for gasification of Macalister coal with steam and oxygen. Table X provides the thermally balanced reactions

Table XI

Linear independent thermally balanced reactions for the Macalister coal seam with higher heating values (MJ/m³)

No.	Reaction	HHV (MJ/m³) Air-blown UCG
A	$CH_{0.898}O_{0.108} + 0.4476O_2 \rightarrow 0.9964CO + 0.0036CO_2 + 0.4489H_2$	5.86
C	$CH_{0.898}O_{0.108} + 1.167H_2O + 0.3623O_2 \rightarrow CO_2 + 1.6159H_2$	5.19
J	$CH_{0.898}O_{0.108} + 0.3494O_2 \rightarrow 0.2244CH_4 + 0.0317CO_2 + 0.7438CO$	7.95
L	$CH_{0.898}O_{0.108} + 0.5251H_2O + 0.1962O_2 \rightarrow 0.487CH_4 + 0.513CO_2$	11.18

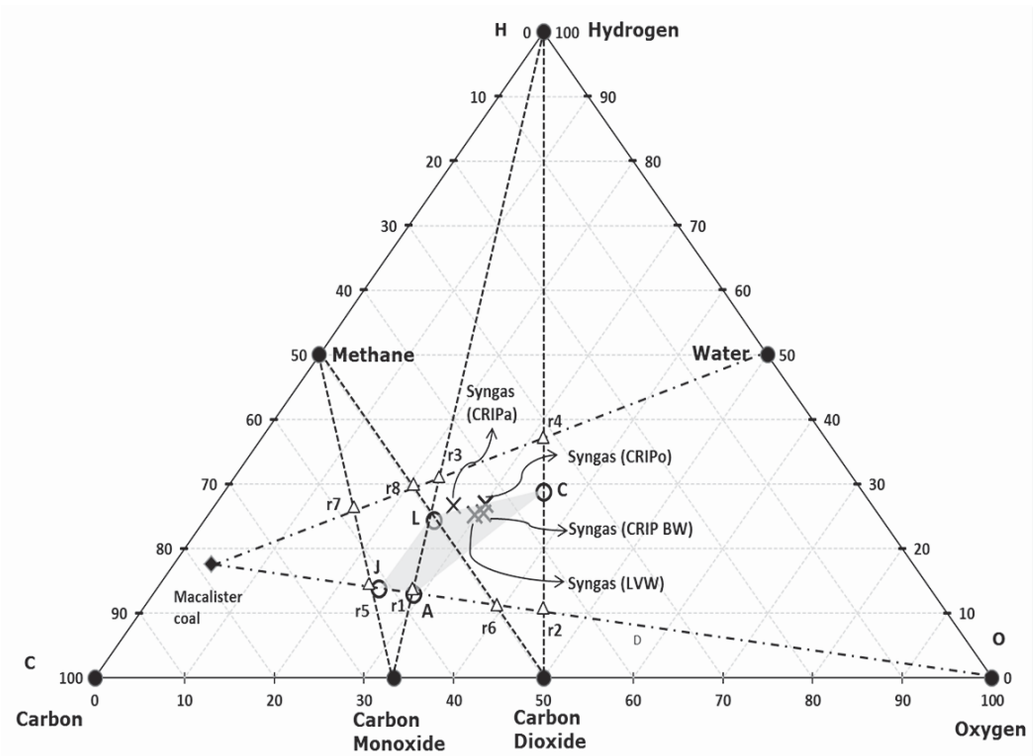

Figure 2—Graphical representation of Macalister underground coal gasification

associated with pairing the two exothermic reaction (r_2 and r_6) with the other endothermic reactions. Table XI lists the four independent linear equations for the Macalister coals.

Figure 2 represents the gasification propensity of the Macalister coal. The thermally balanced region, represented by the shaded grey area, outlines the possible region where favourable UCG conditions may occur. The field test results (X) of the syngas composition from Chinchilla and Bloodwood Creek fall within the thermally balanced region. This confirms the method of UCG operation practised by the operators. Of particular interest is that all UCG methods (CRIP or LVW *etc.*) appear to operate within or near the thermally balanced region. The range of HHV for the UCG syngas is predicted to be within 5.19–11.18 MJ/m³ (Table XI). The Macalister coal seam data exhibits another interesting feature in that a portion of the thermally balanced region crosses the H_2-CO line toward the CH_4-CO line, indicating that methane formation at equilibrium (high temperature) may be feasible. This could also be a possible reason for the presence of coal seam methane in Australian coals, not seen in USA coals (Figure 1). Lastly, the operation of a UCG cavity for power generation at L (where the HHV appears to be the highest) may not be feasible due to the equilibrium being favoured to H_2-CO. However, the equilibrium may be favourable at J, allowing for the production of methane and hence a higher heating value syngas (7.95 MJ/m³) may be obtained from air-blown gasification only without the need to use steam. The natural ingress of water into the cavity may not allow for air-blown UCG only and in this case, to obtain the highest HHV, the UCG would be operated along line J-L and not L-C as trialled by the different sites. It is noted that points along L-C for the field trials were to produce syngas for downstream liquid fuels production.

Gasification analysis of South African Bosjesspruit coal for UCG

Based on the findings from the CHO diagrams for US and Australian coals developed here, this study attempts to predict syngas production by UCG of a South African coal from Sasol's Bosjesspruit Colliery. The colliery is based in the

Table XII

Characteristics of Bosjesspruit coal and volatile matter for sub-bituminous coal

Parameter	Value
Proximate analysis (air-dry w/w%) (Pinheiro, 1999)	
Moisture	3.9
Ash	32.8
Volatile matter	21.6
Fixed carbon	52.2
Calorific value as-received (MJ/kg)	18.88
Ultimate analysis (air-dry w/w%)	
Carbon	50.48
Hydrogen	2.74
Oxygen	7.24
Molecular formula (as received	$CH_{0.75}O_{0.16}$)
Heat of formation (calculated) (KJ/mol)	-212.6
Volatile matter analysis (w/w%) for sub-bituminous coal (van Dyk, 2014)	
H_2O	2.9
H_2	0.15
CH_4	4.01
CO	0.98
CO_2	7.2
N_2	2.1
Tar and oils	5.6
Char analysis (calculated)	
Calorific value (MJ/kg)	34
Molecular formula	$CH_{0.477}O_{0.042}$
Heat of formation (KJ/mol)	-14.1

Highveld Coalfield, South Africa. The bituminous coal is high in ash and typically inertinite-rich. The CHO diagram is used to demonstrate the stoichiometric region in which sensible gasification (*i.e.* conversion of solid coal to syngas) occurs. From the analysis of the thermally balanced reactions, a region for UCG is determined from which various syngas compositions are analysed for downstream processes: syngas for the Fischer Tropsch (FT) process requiring $2H_2$:1CO ratios and syngas for power production. An analysis of the ELW and CRIP methods for UCG of Bosjesspruit coal will be studied. Lastly, the feasibility of using CO_2 as oxidant for UCG is considered.

Characteristics of Bosjesspruit coal

The characteristics of the Bosjesspruit coal are provided in Table XII, from which the molecular formula is determined to be $CH_{0.75}O_{0.16}$ (for coal as received), with the heat of formation being –212.6 KJ/mol (Pinheiro, 1999). It must be noted that the volatile matter and char analyses used here were not determined experimentally but are derived from another South African sub-bituminous coal (van Dyk, 2014). The molecular formulae and heats of formation of Bosjesspruit coal and the Rocky Mountain coal are similar.

Analysis of UCG for Bosjesspruit coal and char

An analysis of the Bosjesspruit coal, similar to the US and Australian coals, is considered based on the details in Table XII. The oxidants are assumed to be air and steam, from

Table XIII

Balanced stoichiometric reactions for Bosjesspruit coal

No.	Reaction	Heat of reaction (kJ/mol)
r_1	$CH_{0.75}O_{0.16} + 0.42O_2 \rightarrow CO + 0.375H_2$	101.3 (endothermic)
r_2	$CH_{0.75}O_{0.16} + 0.92O_2 \rightarrow CO2 + 0.375H_2$	–181.9 **(exothermic)**
r_3	$CH_{0.75}O_{0.16} + 0.84H_2O \rightarrow CO + 1.215H_2$	304.4 (endothermic)
r_4	$CH_{0.75}O_{0.16} + 1.84H_2O \rightarrow CO2 + 2.215H_2$	263.0 (endothermic)
r_5	$CH_{0.75}O_{0.16} + 0.326O_2 \rightarrow 0.187CH_4 + 0.812CO$	107.9 (endothermic)
r_6	$CH_{0.75}O_{0.16} + 0.73O_2 \rightarrow 0.187CH_4 + 0.812CO_2$	–122.1 **(exothermic)**
r_7	$CH_{0.75}O_{0.16} + 0.435H_2O \rightarrow 0.405CH_4 + 0.595CO$	220.9 (endothermic)
r_8	$CH_{0.75}O_{0.16} + 0.732H_2O \rightarrow 0.554CH_4 + 0.446CO_2$	171.7(endothermic)

Table XIV

Linear independent thermally balanced reactions for Bosjesspruit coal with higher heating values (MJ/m3)

No.	Reaction	HHV (MJ/m^3) Air-blown UCG
A	$CH_{0.75}O0.16 + 0.599O_2 \rightarrow 0.642CO + 0.358CO_2 + 0.375H_2$	3.6
C	$CH_{0.75}O0.16 + 0.752H_2O + 0.544O_2 \rightarrow CO_2 + 1.127H_2$	3.5
J	$CH_{0.75}O0.16 + 0.517O_2 \rightarrow 0.187CH_4 + 0.381CO_2 + 0.431CO$	4.4
L	$CH_{0.75}O0.16 + 0.304H_2O + 0.428O_2 \rightarrow 0.34CH4 + 0.66CO_2$	5.2

Table XV

Balanced stoichiometric reactions for Bosjesspruit char

No.	Reaction	Heat of reaction (kJ/mol)
r_1	$CH_{0.477}O_{0.0428} + 0.4786O_2 \rightarrow CO + 0.2385H_2$	–97.1 **(exothermic)**
r_2	$CH_{0.477}O_{0.0428} + 0.9786O_2 \rightarrow CO_2 + 0.2385H_2$	–380.3 **(exothermic)**
r_3	$CH_{0.477}O_{0.0428} + 0.9572H_2O \rightarrow CO + 1.1957H_2$	134.3 (endothermic)
r_4	$CH_{0.477}O_{0.0428} + 1.9572H_2O \rightarrow CO_2 + 2.19575H_2$	92.9 (endothermic)
r_5	$CH_{0.477}O_{0.0428} + 0.4189O_2 \rightarrow 0.1193CH_4 + 0.8807CO$	–92.9 **(exothermic)**
r_6	$CH_{0.477}O_{0.0428} + 0.8593O_2 \rightarrow 0.1193CH_4 + 0.8807CO_2$	–342.3 **(exothermic)**
r_7	$CH_{0.477}O_{0.0428} + 0.5586H_2O \rightarrow 0.3986CH_4 + 0.6014CO$	52.1 (endothermic)
r_8	$CH_{0.477}O_{0.0428} + 0.8594H_2O \rightarrow 0.5489CH_4 + 0.4511CO_2$	2.4 (endothermic)

Table XVI

Linear independent thermally balanced reactions for Bosjesspruit char with higher heating values (MJ/m³)

No.	Reaction	HHV (MJ/m³) Air-blown UCG
Ac	$CH_{0.477}O_{0.0428} + 0.4017H_2O + 0.2777O_2 \rightarrow CO + 0.6403H_2$	7.7
Cc	$CH_{0.477}O_{0.0428} + 1.573H_2O + 0.1921O_2 \rightarrow CO2 + 1.8115H_2$	6.5
Jc	$CH_{0.477}O_{0.0428} + 0.1505O_2 + 0.358H_2O \rightarrow 0.2983CH_4 + 0.7017CO$	13.3
Lc	$CH_{0.477}O_{0.0428} + 0.8534H_2O + 0.006O_2 \rightarrow 0.5459CH_4 + 0.4541CO_2$	21.2

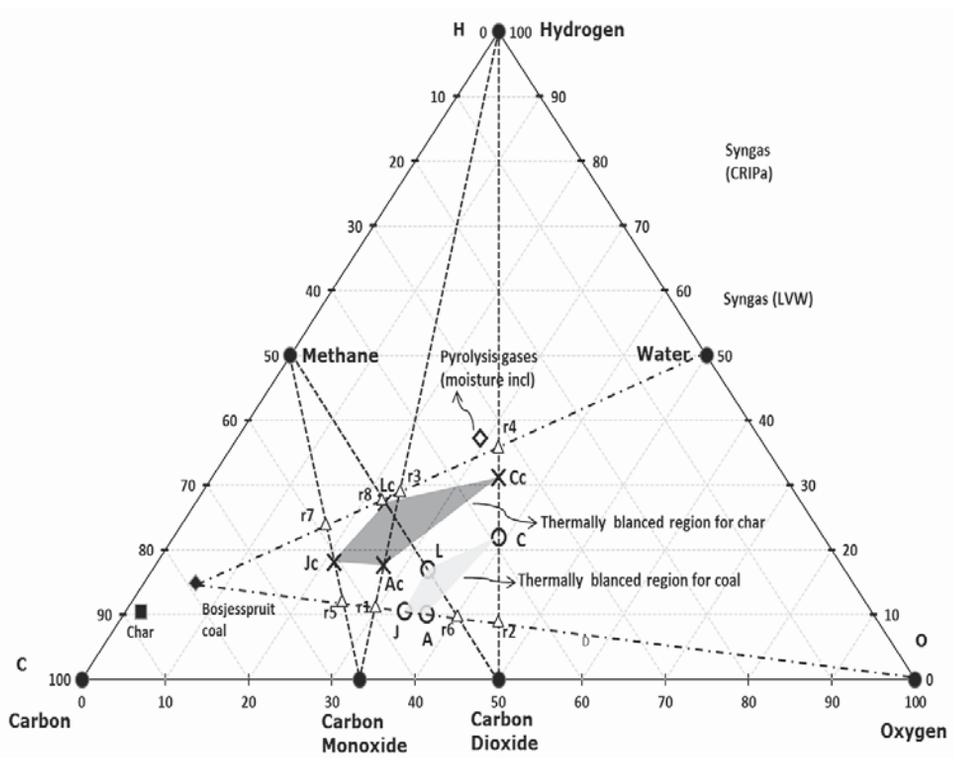

Figure 3—Graphical representation of Bosjesspruit coal and char underground coal gasification

which Tables XIII and XIV are derived for the stoichiometric basis reactions and the four thermally balanced independent reactions respectively. Table XV and Table XVI are for the char resulting from the drying and pyrolysis of the Bosjesspruit coal. The char analyses for the US and Australian coals have not been considered due to lack of information on the pyrolysis and char products of those coals.

Figure 3 represents the gasification reactions for the Bosjesspruit coal and char. The thermally balanced region for

coal is represented by the light grey area bounded by points A,C,L, and J, and for the char by Ac, Cc, Lc, and Jc (dark grey). There is a resemblance to Rocky Mountain coal (Figure 1) as both the molecular formulae and heat of formation values are similar, and hence the thermally balanced regions appear very similar. The syngas resulting from the CRIP method for Rocky Mountain coal appears to be an outlier from the thermally balanced region in Figure 1. However, if the similarity of the Bosjesspruit coal is applied to the Rocky Mountain coal, then the Bosjesspruit char thermally balanced region will be sufficient to predict the Rocky Mountain char gasification behaviour. In this case, the CRIP result for Rocky Mountain coal would fall within the char gasification thermally balanced region. This is an important result, suggesting that UCG using CRIP leads to pyrolysis and subsequent char gasification, which is not prominent in LVW methods.

The effect of coal drying and pyrolysis is evident from Figure 3, where the char thermally balanced region has significantly enlarged with a higher achievable HHV (6.5–21.2 MJ/m^3) than for coal (3.5–5.2 MJ/m^3). This thermally balanced region is more efficient and shows the importance of allowing the coal to dry and pyrolysis to occur prior to gasification. Also, the equilibrium at Jc is favourable, thus allowing the production of methane and carbon monoxide with higher HHV (13.3 MJ/m^3) with air as oxidant.

LVW vs. CRIP for Bosjesspruit coal

The models for UCG methodologies are complex (Perkins, 2018a). Andrianopolous, Korre, and Durucan (2015) attempted to model LVW and CRIP. Their description of the mechanisms for CRIP suggests that there are roof-top and floor-bottom (spalled roof material that falls to the bottom) gasification steps resulting in different gas compositions that ultimately mix and exit the reactor cavity. This suggests that there is a greater degree of drying and pyrolysis products mixing with the syngas from char gasification. In comparison to the LVW method, the high-temperature gasification zone is localized near the reactor injection point, implying that any pyrolysis product from freshly exposed coal surfaces will eventually react to form the final exit gases. The implication of this analysis is that LVW follows the UCG thermally balanced results obtained for coal (Figure 3 – light grey area), while CRIP follows the char reactions (Figure 3 – dark grey area). These results for LVW (or ELW) are confirmed by the USA (Figure 1) and Australian (Figure 2) trials, where both ELW/LVW lie within the thermally balanced region for the coals (not char). This leads to the conclusion that South African coals need to be studied further to determine the pyrolysis-char behaviour prior to deciding on the UCG method. The results also suggest CRIP would be the preferred technology choice for Bosjesspruit coal, where the pyrolysis dynamics are important.

Predictions of syngas output for LVW and CRIP for Bosjesspruit coal

Based on the analysis above, Figure 4 depicts the possible outputs for CRIP and LVW (dotted semicircles) with the optimal steam-oxygen ratios (solid semicircles) for liquid fuel production. The outputs are based on the assumption that field trials will obtain gasification outputs similar to surface gasifiers, which are typically designed for $2H_2$:1CO – this ratio is satisfied along line PQ in Figure 4. The estimated HHV for CRIP would be around 8 (max. 13.3) MJ/m^3 and 3.5 (max. 4.4) MJ/m^3 for LVW. However, for power generation the UCG CRIP would operate close to Jc, where the maximum equilibrium HHV is 13.3 MJ/m^3 for an air-blown system.

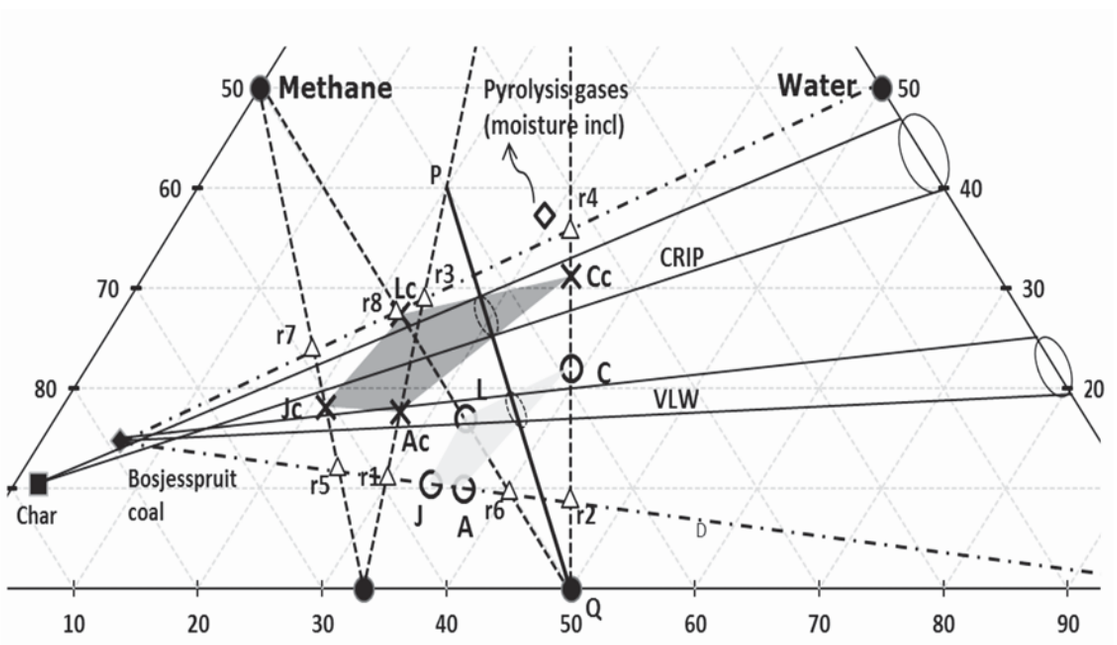

Figure 4—UCG syngas outputs for LVW and CRIP for Bosjesspruit coal and char

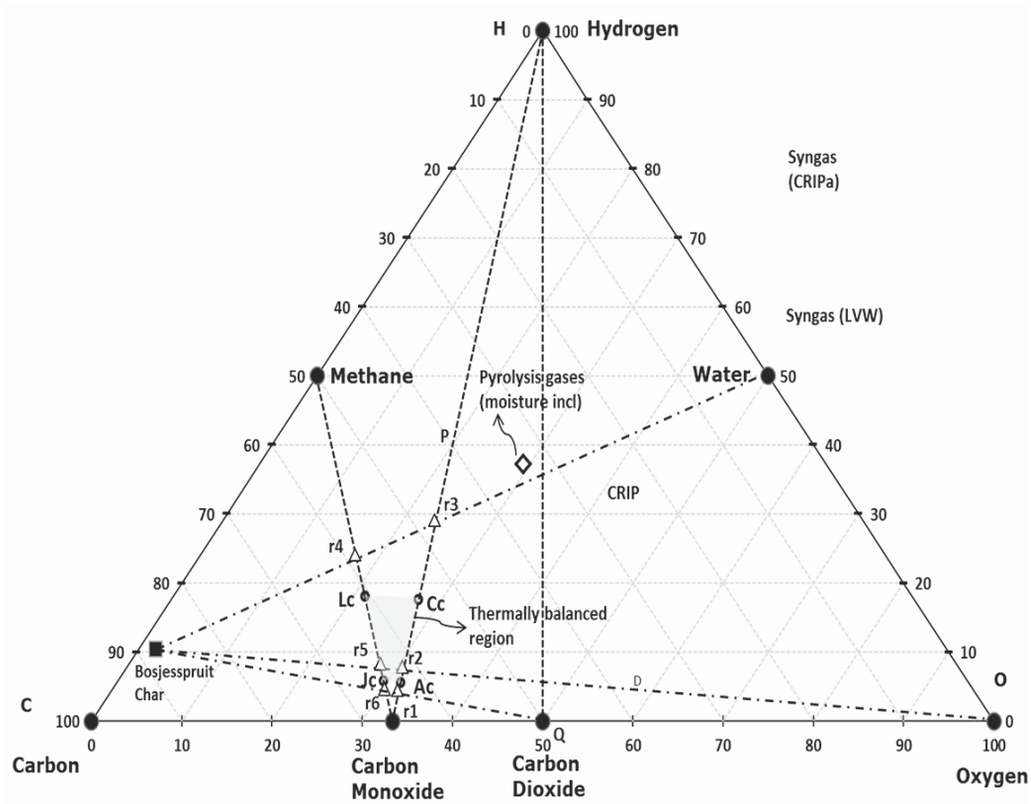

Figure 5—Graphical representation of Bosjesspruit char UCG with CO_2/H_2O/air

Table XVII

Thermally balanced reactions for Bosjesspruit char CO_2 with higher heating values (MJ/m³)

No.	Reaction	HHV (MJ/m³) Air-blown UCG
Ac	$CH_{0.477}O_{0.0428} + 0.343CO_2 + 0.3071O_2 \rightarrow 1.343CO + 0.2385H_2$	7.3
Cc	$CH_{0.477}O_{0.0428} + 0.4017H_2O + 0.2777O_2 \rightarrow CO + 0.6403H_2$	7.7
Jc	$CH_{0.477}O_{0.0428} + 0.1505O_2 + 0.358H_2O \rightarrow 0.2983CH_4 + 0.7017CO$	13.3
Lc	$CH_{0.477}O_{0.0428} + 0.3281CO_2 + 0.2549O_2 \rightarrow 1.2088CO + 0.1193CH_4$	8.8

Analysis of UCG for Bosjesspruit char and CO_2/steam/air oxidants

A CO_2-fed UCG process is possible where a source of pure CO_2 is available, as would be the case at Sasol's facility in Secunda where near-pure CO_2 is vented to the atmosphere. Perkins and Vairakannu (2017) considered oxidant and gasifying medium selection in UCG processes and discussed the use of CO_2/O_2. Figure 5 and Table XVII indicate the theoretical feasibility of operating a UCG process with CO_2/steam/air injection with Bosjesspruit charred coal. Of particular interest is that the syngas output from such a process will comprise predominately CO, H_2, and CH_4, with significantly high HHV values ranging from 7.3 to 13.3 MJ/m³. A sensible strategy for operating a UCG site with CO_2 injection would be to operate near the thermally balanced line joining Jc and Lc (Figure 5), and preferably slightly to the right-hand side so that the cavity is operating 'hot'. The advantage of operating on the 'hot' side is that the excess heat can be used to create the char required for better thermodynamic efficiency of the system.

Conclusions

The CHO phase diagram proved to be a useful tool for analysing gasification systems, and in particular for UCG where a limited number of control parameters exist. The development of a thermally balanced system for the coals allowed the prediction of the syngas output within a narrow region – these regions were tested for US and Australian field trials and were found to correlate with reasonably accuracy. This method was able to predict, without prior knowledge of the UCG technique employed, the flow rates of oxidants, reaction kinetics, heat and mass transfer kinetics, and hydrogeology. It was shown that only four reactions govern the output of any thermally balanced UCG system.

A South African coal was assessed and the effects of pyrolysis were shown to enhance the thermodynamic efficiency of the system, leading to a key conclusion that the determination of pyrolysis propensity and char characteristics should form part of any future UCG programme. It was suggested that the CRIP method be used for the Bosjesspruit coal, where a theoretical maximum syngas HHV can be obtained (13.3 MJ/m^3) when air is used as oxidant. The use of CO_2 in addition to steam and air indicates that a UCG process for the Bosjesspruit char would be possible and capable of producing syngas with a HHV value as high as 8.8 MJ/m^3.

Acknowledgements

A part of this work was presented at the workshop held in 2016 by the South African Underground Coal Gasification Association (SAUCGA). Also, my thanks to Keeshan Moodley for the presentation, development of the ternary CHO diagram, and some of the literature field data collation.

References

Andrianopoulos, E., Korre, A., and Durucan S. 2015. Chemical process modelling of underground coal gasification and evaluation of produced gas quality for end use. *Energy Procedia*, vol. 76. pp. 444–453.

Battaerd, H.A.J. and Evans, D.G. 1979. An alternative representation of coal composition data. *Fuel*, vol. 58, no. 2. pp.105–108.

De Pontes, M., Mocumbi, P., and Sangweni, C.J. 2014. Gas resources and reserves in Southern and East Africa. *Proceedings of the FFF Gas Conference*, Johannesburg, 21 May. Fossil Fuel Foundation.

Dennis, S. 2006. Rocky Mountain underground coal gasification test project (Hanna, Wyoming): Final technical report for the period 1986 to 2006. National Energy Technology Laboratory, US Department of Energy. pp. 1–51.

Engelbrecht, A.D., Everson,R.C., Neomagus, H.W.P.J., and North B.C. 2010. Fluidized bed gasification of selected South African coals. *Journal of the Southern African Institute of Mining and Metallurgy*, vol. 110. pp. 225–230.

Hsu, C., Davies, P.T., Wagner N.J., and Kauchali S. 2014. Investigation of cavity formation in lump coal in the context of underground coal gasification. *Journal of the Southern African Institute of Mining and Metallurgy*, vol. 114. pp. 305–309.

Huang, W.G., Wang, Z.T., Xin L., Duan T.H., and Kang G.J. 2012. Feasibility study on underground coal gasification of No. 15 seam in Fenghuangshan Mine. *Journal of the Southern African Institute of Mining and Metallurgy*, vol. 112. pp. 879–903.

Jowkar, A., Sereshki, F., and Najafi, M. 2018. A new model for evaluation of cavity shape and volume during underground coal gasification process. *Energy*, vol. 148. pp. 756–765.

Kačur, J., Durdan, M., Laciak, M., and Flegner, P. 2014. Impact analysis of the oxidant in the process of underground coal gasification. *Measurement*, vol. 51. pp. 147–155.

Kauchali, S. 2017. Development of sustainable coal to liquid processes: Minimising process CO_2 emissions. *South African Journal of Chemical Engineering*, vol. 24. pp.176–182.

Klebingat, S., Kempka, T., Schulten, M., and Azzam, R. 2018. Optimization of synthesis gas heating values and tar by-product yield in underground coal gasification. *Fuel*, vol. 229. pp. 248–261.

Li, X.T., Grace, J.R., Lim, C.J., Watkinson, A.P., Chen, H.P., and Kim, J.R. 2004. Biomass gasification in a circulating fluidizing bed. *Biomass and Bioenergy*, vol. 26. pp.171–193.

Mavhengere, P., Vittee, T., Wagner, N.J., and Kauchali, S. 2016. An algorithm for determining kinetic parameters for the dissociation of complex solid fuels. *Journal of the Southern African Institute of Mining and Metallurgy*, vol. 116. pp. 55–63.

Perkins, G. 2018a. Underground coal gasification – Part I: Field demonstrations and process performance. *Progress in Energy and Combustion Science*, vol. 67. pp. 158–187.

Perkins, G. 2018b. Underground coal gasification – Part II: Fundamental phenomena and modeling. *Progress in Energy and Combustion Science*, vol. 67. pp. 234–274.

Perkins, G. and Vairakannu, P. 2017. Considerations for oxidant and gasifying medium selection in underground coal gasification. *Fuel Processing Technology*, vol. 165. pp. 145–154.

Pinheiro, H.J. (ed.) 1999. A techno-economic and historical review of the South African coal industry in the 19th and 20th centuries, and analyses of coal product samples of South African collieries 1998 - 1999. *SABS Bulletin* 113. pp. 68–74.

Queensland Department of Mines and Energy 1999. Utilisation of Walloon coals of Southern Queensland for power generation, Department of Mines and Energy, Queensland, Australia. pp. 1–38.

Theron, J.A. and le Roux, E. 2015. Representation of coal and coal derivatives in process modelling. *Journal of the Southern African Institute of Mining and Metallurgy*, vol. 116. pp. 339–348.

Van Dyk, J.C., Keyser, M., and Coertzen, M. 2006. Syngas production from South African coal sources using Sasol–Lurgi gasifiers. *International Journal of Coal Geology*, vol. 65. pp. 243–253.

Van Dyk, J.C., Waanders, F. and Brand, J. 2014. Applying Thermo 350M underground: A Factsage™ equilibrium study for undergound coal gasification. *Proceedings of the GTT Workshop*, Aachen, Germany, July 2014.

Wei, J. 1979. A stoichiometric analysis of coal gasification. *Industrial & Engineering Chemistry Process Design and Development*, vol. 18, no. 3. pp. 554–558. doi: 10.1021/i260071a034

Yang, D., Koukouzas, N., Green, M., and Sheng, Y. 2016. Recent development on underground coal gasification and subsequent CO_2 storage. *Journal of the Energy Institute*, vol. 89. pp 469–484.

Zogala, A. 2014a. Critical analysis of underground coal gasification models. Part I: equilibrium models – literary studies. *Journal of Sustainable Mining*, vol. 13, no. 1. pp. 22–28.

Zogala, A. 2014b. Critical analysis of underground coal gasification models. Part II: kinetic and computational fluid dynamics models. *Journal of Sustainable Mining*, vol. 13, no. 1. pp. 29–37. ◆

http://dx.doi.org/10.17159/2411-9717/2018/v118n10a9

Fully mechanized longwall mining with two shearers: A case study

by Y. Yuan*, H. Liu*, S. Tu*, H. Wei*, Z. Chen*, and M. Jia†

Synopsis

To reduce production costs and increase efficiency in ageing coal mines, a system that utilizes two shearers in a fully mechanized longwall working face is proposed. Using theoretical and engineering experience, three issues pertaining to the system were determined: (a) the two-shearer mining technique; (b) matching and modifying the equipment; (c) and coal-cutting task allocation for each shearer. Two mining processes are proposed, with the two shearers travelling in either the same or opposing directions. To avoid breakage of chains and pan extrusion of the armoured face conveyor (AFC), the length of the AFC 'snake' was controlled. To ensure continuous cutting and transporting of coal, the cross-sectional dimensions of the AFC were checked and the shearer closer to the head drive was modified. Based on the assumption of equal cutting times for each shearer, the meeting position of the two shearers was obtained by using a theoretical model of mining task allocation. Application of this technique at No. 2 Jining Mine, China, has shown remarkable benefits: daily production capacity was increased by 54% and personnel efficiency was improved by 33 t/d per person.

Keywords

super-long working face, two shearers, AFC.'snake' length, shearer modification, coal-cutting task allocation.

Introduction

All coal mines aim to increase the unit output of the working face to reduce mining costs and improve the economic efficiency of the operation. To achieve this goal, a production model known as *one mining face of the mining area* has been adopted by most Chinese coal mines (Hu, Meng, and Zhu, 2008; Zhang, Zhang, and Wang, 2000). Under these conditions, the main technical approaches to maximize the output are increasing the width of the working face (Qu, Xu, and Xue, 2009) and accelerating the advancing speed (Robbins, 2000). In coalfields with shallow seams, the width of a fully mechanized face exceeds 300 m (Ju and Zhu, 2015; Fu, Song, and Xing, 2010); in coalfields with deep seams, the width of the face is usually greater than 240 m (Liu *et al.*, 2016; Li *et al.*, 2013). The term 'super-long working face' was proposed to describe working faces with a width of over 240 m (Zhao and Song, 2016; Xu *et al*, 2007) in China. To support these long working faces with rapid advancing speeds, high-powered mining equipment is required (Kulshreshtha and Parikh, 2001, 2002; Tu *et al.*, 2009; Mishra, Sugla,and Singha, 2013). This is easily achieved in newly built mines, but is not a good choice for ageing mines because of the low return on a high investment on account of the limited remaining resources. It is therefore difficult for ageing mines to significantly increase their unit output with the existing mining equipment. This study focused on this problem: two shearers were applied to a longwall fully mechanized working face (LFMWF) to achieve increased unit output.

It is easy to understand that longwall fully mechanized mining with two shearers (LFMMTS) can increase the unit output by accelerating the advancing speed; however, this also exacerbates the difficulty of matching mining equipment and the risks of production accidents. Jurecka (1987) proposed that it was reasonable to use two shearers in cases with tectonic faulting and for cutting roadways. Bolilasi (1985), using numerical simulation, proposed that the advancing speed can be increased by 55 m/d by adding mining equipment. Niu (2009) theoretically determined that the efficiency can be increased by 600 t/h by using two shearers in a 400 m wide longwall face. Zhang *et al.* (2009) proposed and proved the feasibility of a concept named '*longwall coal mining face with a multi coal shearers combined mining technology*'. Wu and Zhang (2012) and Ceng *et al.* (2016) showed that using LFMMTS increased the output and advancing speed of the LFMWF 11502 at Yushujing Mine, China.

* *Key Laboratory of Deep Coal Resource Mining, Ministry of Education of China, School of Mines, State Key Laboratory of Coal Resources and Safe Mining, China University of Mining and Technology, China.*

† *Yancon Group Company Limited, China.*

 ISSN 2225-6253. Paper received Dec. 2017; revised paper received Jun. 2018.

All previous studies showed that the application of two shearers can increase the output and efficiency of a working face; however, use of LFMMTS also exacerbates the difficulty of matching mining equipment, for example if the capacity of the AFC does not match the total capacity of the two shearers. There are also risks of production accidents, such as the rupture of chains and compression of the AFC when workers push the AFC to the coal wall and head-on collisions of two shearers travelling in opposite directions, as there will be one more AFC 'snake'.

Based on the current mining equipment in LFMWF 9303 in No. 2 Jining Mine, China, the mining process, equipment matching and modification, and coal-cutting task allocations for each shearer were studied. It was shown that LFMMTS can achieve safe and high-efficiency production. This case study can provide a reference for a new technical scheme for safe and efficient mining in coal seams with similar conditions.

Geological condition of LFMWF 9303, Jining Mine

LFMWF 9303 is 1624.6 m long and 330 m wide across the gateroad centre. The coal seam dip ranges from 0° to 12° and is 5° on average. The seam thickness is 2.68 m. The main roof is interbedded medium- and fine-grained sandstone with an average thickness of 37.1 m; the friable immediate roof is siltstone with an average thickness of 0.43 m; the immediate floor is siltstone with an average thickness of 1.91 m; the main floor is medium-grained sandstone with an average thickness of 16.2 m. The geological parameters of the surrounding rock of LFMWF9303 are shown in Table I.

Equipment selection for an LFMWF should take into account geological and mining conditions, capacity and size matching of equipment, and coal yield of the face (Álvarez *et al.*, 2003; Toraño *et al.*, 2008). Based on the coal face parameters and these principles, the technical parameters of the major equipment in LFMWF 9303 are summarized in Table II. The equipment layout of two-shearer fully mechanized working face (TSFMWF) is shown in Figure 1.

Techniques using TSFMWF mining

The TSFMWF technique can be classified according to whether the two shearers travel in the same direction or in the opposite directions, as shown in Figure 2.

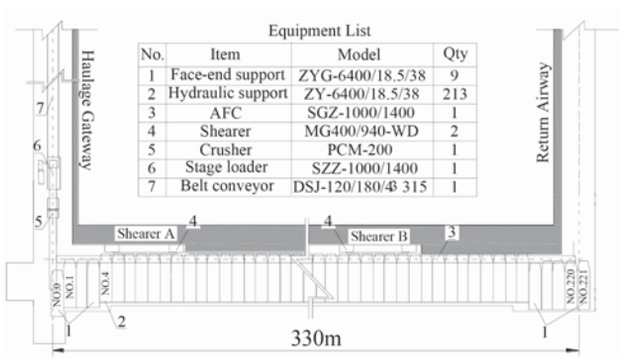

Figure 1—Equipment layout in LFMWF 9303

Table I

Geological parameters of surrounding rock of LFMWF9303

Item	Lithology	Average thickness (m)	Pry's coefficient[a]
Main roof	Interbedded medium- and fine-grained sandstone	37.1	6.0–12.0
Friable immediate roof	Siltstone	0.43	2.0–4.0
Coal seam	Bright coal	2.68	1.91
Immediate floor	Siltstone	1.91	2.0–4.0
Main floor	Medium-grained sandstone	16.2	4.0–8.0

[a]Pry's coefficient = protodyakonov coefficient, whose value is equal to one-tenth of the uniaxial compression strength

Table II

Technical parameters of major equipment in LFMWF 9303

Item	Model	Manufacturer	Main technical parameters	
Shearer	MG400/940-WD	Jixi Coal Mining Machinery Co. Ltd., China	Cutting height (m)	2.2-3.5
			Web (m)	0.8
			Drum diameter (m)	1.8
Hydraulic support	ZY-6400/18.5/38	Zhengzhou Coal Mining Machinery Group Co. Ltd., China	Working height (m)	1.85-3.8
			Width (m)	1.43
			Working resistance (kN)	5753-6540
			Setting load (kN)	4557-5180
			Supporting intensity (MPa)	0.91
AFC	SGZ-1000/1400	ChinaCoal Zhangjiakou Coal Mining Machinery Co. Ltd., China	Length (m)	330
			Carrying capacity (t/h)	2500

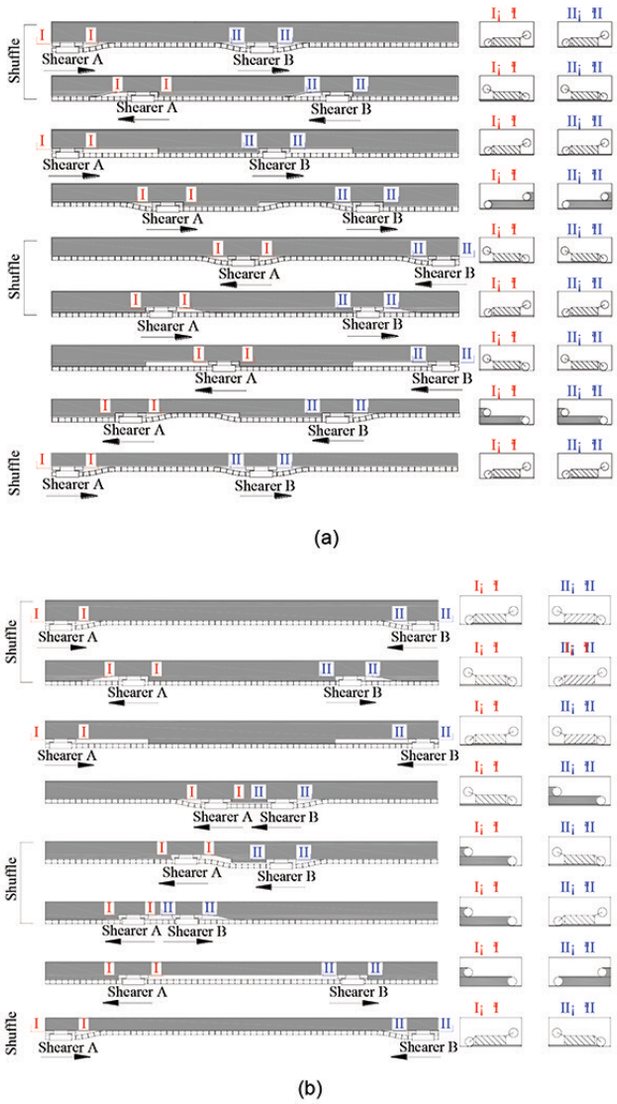

Figure 2—Process forTSFMWF mining showing (a) same travelling direction mining (STDM) and (b) opposite travelling direction mining (OTDM) techniques

In the same travelling direction mining (STDM) technique, shown in Figure 2a, shearer A travels from the head drive to the middle of the working face and shearer B travels from the middle of the working face to the tail drive. The two shearers cut into the coal wall with an inclined shuffle and a certain distance is required for completing the shuffle. After the inclined shuffle, the AFC is pushed straight. The two shearers then return to their initial positions along the AFC to cut the triangular area by exchanging the positions of the leading and trailing drums. Shearers A and B then start to cut coal regularly towards the tail drive, until they complete the cutting cycle. After one cutting cycle, each shearer returns to its initial position via the same process, but towards the head drive.

In the opposite travelling direction mining (OTDM) technique, shown in Figure 2b, shearers A and B travel from the head drive and tail drive, respectively, to the middle of working face. They first cut into the coal wall with an inclined shuffle, after which the AFC is pushed. A certain distance is required to complete the inclined shuffle. Shearers A and B then return to cut the remaining triangular area. After that process, the two shearers start to cut coal regularly towards each other, until they reach the shared coal-cutting area. In this technique, the two shearers meet in the middle of the face, after which shearer A will have an inclined shuffle and then return to the head drive with regular cutting, while shearer B will cut the coal wall between the two shearers and the triangular area left by shearer A, and then return to the tail drive with regular cutting.

AFC constraints and modification of shearer A

The requirements for the AFC and shearers in LFMMTS differ from those in LFMWF with a single shearer. The AFC should be checked to avoid rupture of its chains or compression of its pans. Shearer A should be modified to meet the demands of coal transportation.

Requirements for AFC

Control of 'snake' length: When using the OTDM technique, the chains may be broken and pans squeezed when workers push the AFC to the coal wall during mid-face operations. It is therefore necessary to determine the reasonable 'snake' length of the AFC.

Checking of cross-sectional dimensions: In productive practice, the carrying capacity of the AFC must exceed the total cutting capacity of two shearers. It is necessary to check that the cross-sectional dimensions of coal piled on the AFC are adequate to accommodate the coal cut by the two shearers.

Requirements for shearer A

- *Slipper height*—Massive coal is transported by an AFC in LFMMTS, which needs a higher clearance between shearer A and the AFC. The slippers of shearer A must be heightened to enlarge this clearance.
- *Drum diameter*—Once the slippers are heightened, the drum diameter of shearer A should be increased appropriately to cut the coal at the bottom of coal wall.

Procedure to check constraints of AFC

Determination of the minimum 'snake' length

The minimum 'snake' length (MSL) of the AFC is a very important parameter for safe and high-efficiency mining. Two problems can occur if the actual snake length is less than the MSL: difficulty in pushing the AFC can increase because the pans are prone to be abraded, and there is an increased risk of the chains breaking if the tensions between two chains of the AFC are unbalanced.

Considering the symmetry of the bending section, a theoretical model (Edwards, 1981; Edwards and Yazdi, 1983) for a half-bending section was established, as shown in Figure 3, where N is the number of pans in the half-bending section, β is the included angle between two pans, b_w is the chord length corresponding to β, L is the length of a pan and a is the width, W is the length of 'snake; S is the width. B is the distance that the AFC is moved at each turn, and ΔS is the infinitesimal flexion of a bending section for chain number N.

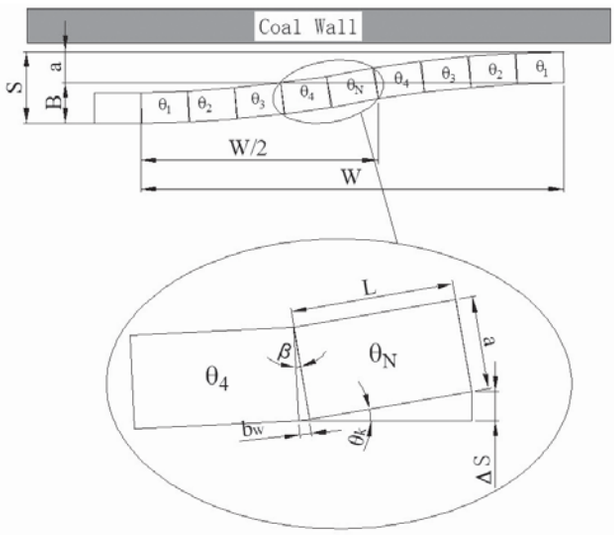

Figure 3—Theoretical model for the half length of the 'snake' of the AFC

Considering the geometrical relationship of those parameters shown in Figure 3, an expression for ΔS can be given as:

$$\Delta S = (L + b_w)\sin\theta_k \quad [1]$$

By integration:

$$S/2 = \sum_{k=1}^{N}\Delta S = \sum_{k=1}^{N}(L+b_w)\sin\theta_k = (L+b_w)\sin\theta_1 + (L+b_w)\sin\theta_2 + \mathrm{L} + (L+b_w)\sin\theta_N = (L+b_w)(\sin\theta_1 + \sin\theta_2 + \mathrm{L} + \sin\theta_N) \quad [2]$$

where θN is the included angle between pan N and the longitudinal line of the AFC ($\theta_1 = 1\beta$, $\theta_2 = 2\beta$, $\theta N = \mathrm{N}\beta$) and b_w is the chord length that corresponds to β ($b_w = a\beta/360$). Equation [2] can be rewritten as follows:

$$S/2 = \frac{1}{2}\csc\frac{\beta}{2}(l+b_w)[\cos\frac{\beta}{2} - \cos\frac{(2N+1)\beta}{2}] \quad [3]$$

In production practice, $B = S - a$, so this equation becomes:

$$B + a = S = \csc\frac{\beta}{2}(l+b_w)[\cos\frac{\beta}{2} - \cos\frac{(2N+1)\beta}{2}] \quad [4]$$

Equation [4] can be simplified to an expression for N:

$$N = \frac{1}{\beta}arc\cos\left(\cos\frac{\beta}{2} - \frac{\sin\frac{\beta}{2}(B+\mathrm{a})}{l+b_w}\right) - \frac{1}{2} \quad [5]$$

The AFC used in LFMWF 9303 is a SGZ1000/1400 model (ChinaCoal Zhangjiakou Coal Mining Machinery Co. Ltd., China) whose pan is 1500 mm long and 1000 mm wide. Their angle of rotation is 1°. The distance that the AFC is pushed at each turn is 800 mm. N is related to B, β, and a. The values of N for different values of B, β, and a are shown in Figure 4.

In Figure 4, the values of N are 7.79, 7.80, and 7.80 when the values of a, β, and B are 1000 mm, 1°, and 800 mm, respectively. Therefore, the maximum value of N is equal to 7.80 and $W = 2NL = 23.4$ m. When using the OTDM technique, a safe distance between two shearers is required to avoid accidents: this should be greater than the MSL. In production practice, a safe distance of 30 m is adopted, known as the *shared coal-cutting area*. As shown in Figure 2b, the two shearers will be conducting different mining processes when they reach the shared coal-cutting area.

Cross-sectional dimension checking for coal piled on the AFC

According to the number and type of spill plates installed on the AFC, the method for calculating the cross-sectional dimensions of coal conveyed by the AFC differs (Walker, 1987). The cross-sectional dimensions are shown as Figure 5.

In Figure 5a, the maximum cross-sectional dimension (A_d) of the coal conveyed can be described by:

$$N = \frac{1}{\beta}arc\cos\left(\cos\frac{\beta}{2} - \frac{\sin\frac{\beta}{2}(B+\mathrm{a})}{l+b_w}\right) - \frac{1}{2} \quad [6]$$

where A_1, A_2, and A_3 are the cross-sectional dimensions of coal piled in the pan, coal blocked by the spill plate, and coal in the guiding tube, respectively; h_0, b_0, and b_1 are the internal height, width, and thickness of the pan, respectively; h_{1a} is the clear height of coal blocked by the spill plate; b_2 is the distance from the spill plate to the outer edge of the pan; D is the diameter of the guiding tube; and C_e is the loading coefficient, the value of which is usually 0.9 (Nie *et al.*, 2015).

In Figure 5b, the maximum cross-sectional dimension (A_w) of the coal piled on the AFC can be described as follows:

$$A_w = A_1 + A_4 = b_0h_0 + \frac{1}{2}(b_0 \times h_{1b}) = b_0(h_0 + \frac{1}{2}h_{1b}) \quad [7]$$

where A_4 is the cross-sectional dimension of coal piled in a pan without a spill plate and h_{1b} is the clear height of coal blocked by the spill plate.

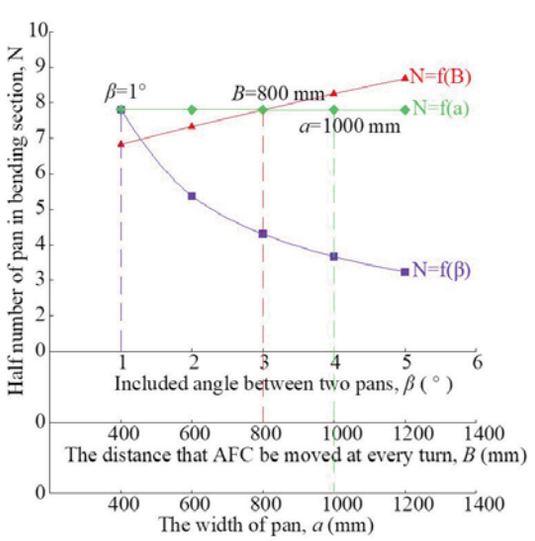

Figure 4—Function curve of *N* for different values of *B*, *β*, and *a*

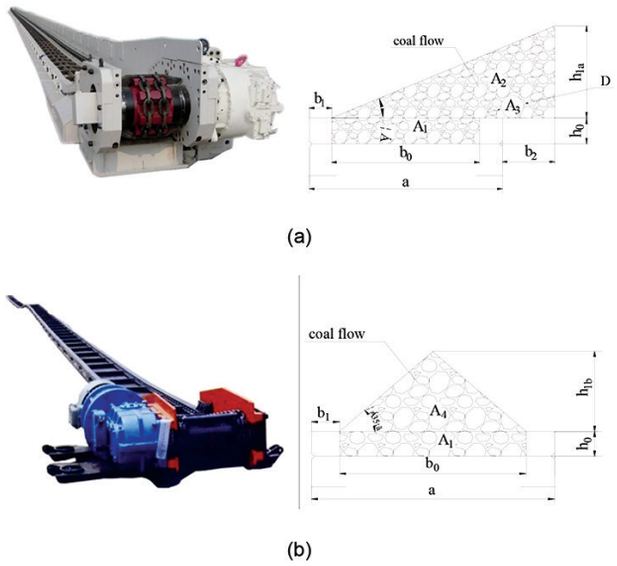

Figure 5—Cross-sectional dimensions of coal piled on an AFC (a) with and (b) without a spill plate

The relationship between Q (the maximum coal-transporting capacity of the AFC) and A (the cross-sectional dimension of coal piled on the AFC) can be described as follows (Nie *et al.*, 2015):

$$Q = 3600Av\lambda\gamma \quad [8]$$

where v is the speed of the chain, λ is the bulk density of coal piled on the AFC (taken as 0.9 (Nie *et al.*, 2015)), and γ is the density of the coal.

Combining Equations [6] and [8]:

$$h_{1a} = \frac{20\left(\frac{Q}{3600v\gamma} + \frac{\pi D^2}{4} - b_0 h_0\right)}{9\left(a + b_2 - b_1\right)} \quad [9]$$

Combining Equations [7] and [8]:

$$h_{1b} = 2\left(\frac{Q}{3240v\gamma b_0} - h_0\right). \quad [10]$$

Supposing α is the angle of repose of coal piled on the AFC, then the maximum heights of coal piled on the AFC with and without a spill plate can be described, respectively, as follows:

$$h_{1a\max} = \left(a + b_2 - b_1\right)\tan a \quad [11]$$

$$h_{1b\max} = \frac{b_0}{2}\tan a \quad [12]$$

For LFMWF 9303, $\alpha = 35°$, $v = 1.2$ m/s, $\gamma = 1.35$ t/m^3, $Q_{\max} = 1800$ t/h, $b_0 = 1$ m, $h_0 = 0.352$ m, and the AFC used has no spill plate, as shown in Figure 5b; therefore, the maximum height is given by:

$$h_{1b\max} = 0.35 \text{ m} > h_{1b} = 0.009 \quad [13]$$

This means that the cross-sectional dimensions of the coal piled on the AFC can satisfy the yield requirement for LFMMTS.

Structural modification of shearer A

Heightening of slippers of shearer A

In LFMMTS, more coal gets through the clearance between shearer A and the AFC, which may cause deposition of coal and gangue plugging. To enlarge the clearance, the slipper height of shearer A needed to be increased by adding one idle wheel that can transmit the same power as the original. The method of increasing the slipper height is shown in Figure 6.

With continuous coal cutting and loading, the maximum coal-transporting capacity of the AFC (Q) can be described by Equation [8]. In production practice at LFMWF 9303, $\overline{Q_m}$ = 937.5 t/h, $v = 1.2$ m/s, $\gamma = 1350$ kg/m^3. The value of A can then be obtained: $A = 0.16$ m^2.

The underneath clearance should satisfy the following equation:

$$\bar{h} \geq h = \frac{A}{d} \quad [14]$$

where $\bar{h}$ is the clearance actually needed; h is the theoretical clearance; and d is the centre distance of the chain and has a value of 0.26 m.

Substituting the values of A and d into Equation [14] gives $\bar{h} \geq 0.61$ m. Suppose that the initial height of the slippers is l, then the height increase from this modification should be equal to $\bar{h} - l$. In production practice, the slipper height of shearer A was increased by 0.219 m.

Increasing drum diameter of shearer A

Owing to the increase in the height of the shearer slippers, the drums of shearer A cannot reach and cut the coal at the bottom of the coal wall. To avoid this problem, the drum diameter has to be increased. The necessary increment of the drum diameter can be described as:

$$\Delta D = 2\left(\bar{h} - l\right) \quad [15]$$

For the slipper increment of 0.219 m, the drum diameter should theoretically be increased by 0.438 m. In LFMWF 9303, the actual increment of the drum diameter is 0.428 m, which was essentially coincident with the theoretical value.

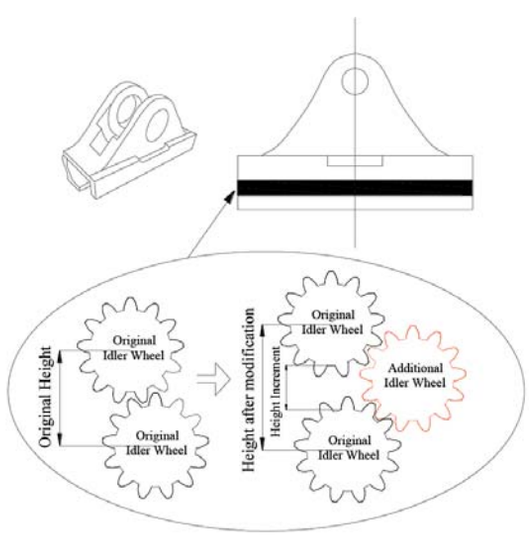

Figure 6—Schematic of method for increasing slipper height

Coal-cutting task allocation for two shearers

Same travelling direction mining

Mathematical model for travelling distance of shearer A

The task allocation model for two shearers when using the STDM technique is shown in Figure 7. The key to this technique is to determine the correct placement of shearer B. To ensure that all the coal in a working face can be cut, shearer B should be placed within the range that can be reached by shearer A.

To save time in a cutting cycle, the mining times of the two shearers should be equal. An equation for mining time can then be obtained:

$$\begin{aligned}&\frac{L_a+L_g}{V_{xa}}+\frac{L_a+L_g}{V_{xb}}+\frac{L_a+L_g}{V_k}+\frac{L_h-(L_a+L_g)}{V_a}=\\&\frac{L_b+L_g}{V_{xa}}+\frac{L_b+L_g}{V_{xb}}+\frac{L_b+L_g}{V_k}+\frac{L-L_h-(L_b+L_g)}{V_b}\end{aligned} \quad [16]$$

where L is the width of the working face; L_h is the longest distance of shearer A from the head drive; L_g is the length of the AFC bending section; L_a is the length of shearer A; L_b is the length of shearer B; V_{xa}, V_{xb}, and V_k are the haulage speeds for inclined shuffle, cutting the triangular area, and of the shearer when not cutting coal, respectively; and V_a and V_b are the haulage speeds of shearers A and B for regular cutting, respectively.

Because shearers A and B are the same dimensions, L_a is equal to L_b. From Figure 7, the following equation can be obtained:

$$L_a+L_g=L_b+L_g \quad [17]$$

Because V_{xa}, V_{xb}, and V_k are slow and easily controlled, we assumed that these parameters are also equal for the two shearers. The following equation can then be obtained:

$$\begin{aligned}&\frac{L_a+L_g}{V_{xa}}+\frac{L_a+L_g}{V_{xb}}+\frac{L_a+L_g}{V_k}=\\&\frac{L_b+L_g}{V_{xa}}+\frac{L_b+L_g}{V_{xb}}+\frac{L_b+L_g}{V_k}\end{aligned} \quad [18]$$

Equation [17] can be simplified by substituting Equation [19]:

$$\frac{L_h-L_x}{V_a}=\frac{L-L_h-L_x}{V_b} \quad [19]$$

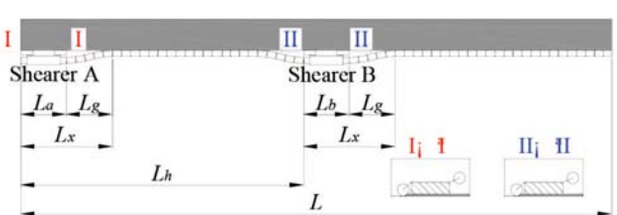

Figure 7—Theoretical model for cutting task allocation in the STDM technique

An equation for L_h can then be described as follows:

$$L_h=\frac{(L-2L_x)V_a}{V_a+V_b}+L_x \quad [20]$$

Determination of placement of shearer B

In actual production, the cutting capacity of a shearer depends on the carrying capacity of transport equipment. In LFMWF 9303, the equipment with the least transport capacity is the belt conveyer, which has a carrying capacity of 1600 t/h. To ensure that the belt conveyer is not overloaded, the total cutting capacity of the two shearers must be less than its carrying capacity. Therefore, the combined mining speed of the two shearers should be less than 9.6 m/min. Furthermore, owing to the speed limit for pulling supports, the range of haulage speeds for the shearers is 3.6 to 6 m/min. Equation [21] can therefore be simplified as follows:

$$L_h=26.58V_a+37.4 \quad [21]$$

Using the limit equilibrium method, the range that can be reached by shearer A can then be obtained as follows: (i) when V_a is equal to 6.0 m/min, the maximum value of L_h is 196.9 m, which means that the furthest travelling range of shearer A will be 196.9 m away from the head drive; (ii) when V_a is equal to 3.6 m/min, the minimum value of L_h is 133.1 m, which means that the nearest travelling range of shearer A is 133.1 m from the head drive.

According to engineering data, the haulage speed of a shearer satisfies a normal distribution, $V_a \approx N(4.8,0.28)$, and satisfies $P\{|X-\mu|<3\delta\}=0.9974$, so the probability of V_a satisfying $P\{3.21<V_a<6.39\}$ is 0.9974. The haulage speed range of shearer A (3.6 to 6.0 m/min) is an event with large probability, which is consistent with the actual speed requirement.

In the STDM technique, suppose that L_p is the advance distance of shearer A at the end of one working cycle, then a historical curve of L_h corresponding to L_p can be drawn. The historical curve of L_h is in production practice is shown in Figure 8.

When LFMWF 9303 uses the STDM technique, the distance between shearer A and the drive head is in the range of 154 m to 177 m after a working cycle, as obtained from Figure 8. Therefore, the initial arranged placement for shearer B should be in the same range to ensure that the sum of two shearers' movement ranges is equal to the width of the working face.

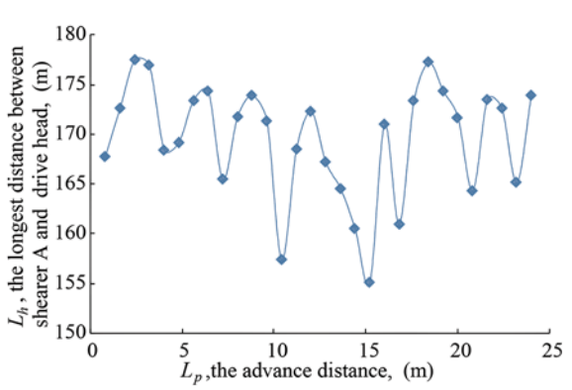

Figure 8—Historical curve of L_h in the STDM technique

Opposite travelling direction mining

Mathematical model for meeting

The meeting of the two shearers is a crucial problem that needs to be resolved when employing the OTDM technique. As too small an interval between the two shearers may cause the shearers' drums to crash into each other, a safe distance is needed to avoid their meeting. A theoretical meeting model for two shearers is shown in Figure 9.

Suppose that the mining time of the two shearers is equal, then the following equation can be obtained:

$$\frac{L_g+L_a}{V_{xa}}+\frac{L_a+L_g}{V_{xb}}+\frac{L_a+L_g}{V_k}+\frac{L_1-(L_a+L_g)}{V_a}=\frac{L_g+L_a}{V_{xa}}+\frac{L_a+L_g}{V_{xb}}+\frac{L_a+L_g}{V_k}+\frac{L-30-L_1-(L_a+L_g)}{V_b} \quad [22]$$

where L_1 is the distance from shearer A to the head drive when the distance between two shearers is equal to 30 m. The other parameters are as defined for Equation [16].

The same shearers and AFC are used in both the STDM and OTDM techniques, so Equations [17] and [18] can also be used for the OTDM technique. Equation [22] can then be simplified as follows:

$$\frac{L_1-L_x}{V_a}=\frac{L-30-L_1-L_x}{V_b} \quad [23]$$

An expression for L_1 can be given as follows:

$$L_1=\frac{(L-2L_x-30)V_a}{V_a+V_b}+L_x \quad [24]$$

Determination of the meeting position of two shearers

The haulage speed of each shearer ranges from 3.6 m/s to 6.0 m/s and since the values of the other parameters are fixed, then Equation [24] can be simplified as follows:

$$L_1=23.45V_a+37.4 \quad [25]$$

The value of L_1 ranges from 121.82 m to 178.64 m away from the head drive. Shearer A is in the range of hydraulic supports no. 80 to 118. According to the value of V_a, there are two cases for describing the equation for the meeting position. (i) If V_a is less than 4.8 m/min, the two shearers will meet closer to the head drive. In this case, shearer A should continue mining towards the tail drive until the shared coal-cutting area is completely cut, while shearer B should have an inclined shuffle towards the tail drive. The equation for the meeting position can be described as follows: $L_m = L_1 + 30$ (where L_m is the distance between shearer A and the head drive when two shearers meet). (ii) If V_a is greater than 4.8 m/min, then the two shearers will meet closer to the tail drive. In this case, shearer B should continue mining towards the head drive until the shared coal-cutting area is completely cut, while shearer A should have an inclined sump towards the head drive, and now, $L_m = L_1$.

The historical curve of L_m corresponding to L_p when using the OTDM technique in production practice is shown in Figure 10.

As shown in Figure 10, when two shearers meet in the middle of the working face, the distance between the shearers and head drive ranges from 140 to 180 m. Because the meeting position is in the middle of the face, the rock pressure is higher, which makes it more difficult to support (Liu *et al.* 2016). More attention should therefore be paid to rock pressure and workers' safety at the meeting position.

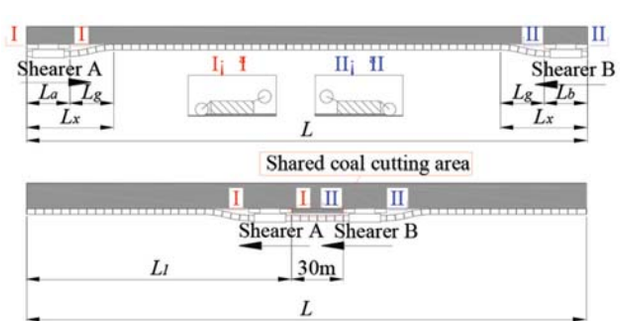

Figure 9—Theoretical model for cutting task allocation in the OTDM technique

Application of the two-shearer concept

Comparison with a single-shearer working face

LFMWF 9302 is a single-shearer fully mechanized working face located adjacent to and east of LFMWF 9303, and the geological conditions of two working face are similar. The width of LFMWF 9302 is 330 m, and the model of shearer, hydraulic support, and AFC are the same as those of LFMWF 9303. The main difference between two working faces is the number of shearers used. The work efficiencies of LFMWF 9303 and 9302 are shown in Table III. Compared with LFMWF 9302, the time of a single cutting cycle in LFMWF 9303 was reduced by 84 minutes, the workers' efficiency increased by 33 t per person, and the daily output increased by 4537 t (54%). Furthermore, the distance that the workers need to walk is less because the travelling distance of each shearer is shorter in a double-shearer face.

Direct economic benefits of two-shearer working face

The super-long two-shearer face is merged from two ordinary faces. With this design, one 3.5 m wide pillar and two 1900 m long gateways are not required, which gives a saving of $6.05 million on each working face layout. In addition, the number of workers on a two-shearer face is just 1.3 times that of a one-shearer face, in other words, just 62.5% of that of two single-shearer faces, which saves about $0.476 million annually on labour costs. So with LFMMTS, the

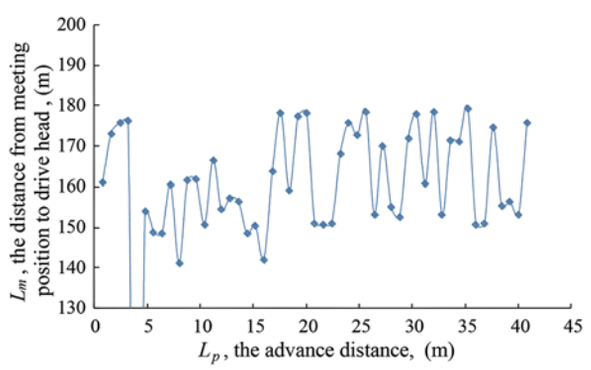

Figure 10—Historical curve of Lm in the OTDM technique

Table III

Comparison of work efficiencies of single- and two-shearer working faces

LFMWF	One cutting cycle (min)	Equipment			Efficiency	
		Hydraulic support	Shearer	AFC	Daily output (t)	Individual efficiency (t)
9303	138	213	2	1	12 894	179
9302	222	213	1	1	8 357	146

production cost was decreased by $6.526 million in total. In addition, the net profit from per ton coal was $5.05. As the daily output of LFMWF 9303 was increased to 12 894 t, the daily net profit that No. 2 Jining Mine obtained from LFMWF 9303 was more than $65 000.

Conclusion

To enable high production and high efficiency in ageing coal mines, while still using existing mining equipment, a new technical scheme, named LFMMTS, is proposed. This involves mining using shearers travelling in either the same direction or in opposite directions. The mining processes for the two techniques are described. This scheme has been successfully applied in LFMWF 9303 of Jining Mine and yielded a 54% increase in output.

Theoretical models to determine the MSL and check the cross-sectional dimensions of the AFC were built. A 30 m safe distance, named the *shared coal-cutting area*, in LFMWF 9303 was employed to avoid AFC accidents involving chain rupture or compression of the pans. The structure of the shearer closer to the head drive was modified to satisfy the transportation demands of an LFMMTS face, including increasing the slipper height and drum diameter by 0.219 m and 0.428 m respectively.

Theoretical models for coal-cutting task allocation for the two mining techniques were constructed, based on equal mining times for each shearer in a single cutting cycle. For the case of LFMWF 9303, when using the STDM technique, shearer B should be arranged in the working face at a distance of 154 m to 177 m from the head drive, which is where shearer A can reach; when using the OTDM technique, the meeting positions range from 140 m to 180 m away from the head drive.

Acknowledgements

Financial support for this work was provided by the National Key R&D Program of China (No. 2018YFC0604701), the Natural Science Foundation of Jiangsu Province (No. BK20181358),a scholarship from the China Scholarship Council and the Priority Academic Program Development of Jiangsu Higher Education Institutions. We thank Kathryn Sole, PhD, from Liwen Bianji, Edanz Group China (www.liwenbianji.cn/ac), for editing the English text of a draft of this manuscript.

References

Álvarez, J.T., Rodríguez, R., Rivas, J.M., and Casal, M.D. 2003. GEWINNUNG-Economic and technical results mining a 4 m thick coal seam in Spanish Carbonar colliery. *Gluckauf*, vol. 139, no. 6. pp. 323–328.

Bolilasi, L.J. and Zhao, C.J. 1985. Mining with two continuous miners. *Coal Technology*, vol. 4, no. 4. pp. 2–46.

Ceng, X.W., Wang, F.J., and Guo, Z.C. 2016. Feasibility analysis and application of bidirectional coal mining technology of double coal machine. *Inner Mongolia Coal Economy*, vol. 14. pp. 113–114.

Edwards, J.B. 1981. The modelling of semiflexible conveyor structures for coal-face steering investigations. *ARCHIVE Proceedings of the Institution of Mechanical Engineers 1847-1982*, vol. 1–196, no. 196. pp. 387–400.

Edwards, J.B., and Yazdi, A.M.S.R. 1983. Modelling the steering characteristics of coal face conveyors by random signal testing. *IFAC Proceedings*, vol. 16, no. 15. pp. 561–570.

Fu, Y.P., Song, X.M., and Xing, P.W. 2010. Study of the mining height of caving zone in large mining height and super-long face of shallow seam. *Journal of Mining & Safety Engineering*, vol. 27, no. 2. pp.190–194.

Hu, X.J., Meng, X.R., and Zhu, J.M. 2008. Geological condition evaluation system of high yield and high efficiency mines. *Coal Mining Technology*, vol. 26. pp. 947–953.

Ju, J., Xu, J., and Zhu, W. 2015. Longwall chock sudden closure incident below coal pillar of adjacent upper mined coal seam under shallow cover in the Shendong Coalfield. *International Journal of Rock Mechanics & Mining Sciences*, vol. 77. pp. 192–201.

Jurecka, H. 1987. Experience with the Edw 450l shearer in a thick seam at Ensdorf colliery. *Gluckauf*, vol. 123. pp. 282–289.

Kulshreshtha, M. and Parikh, J.K. 2001. A study of productivity in the Indian coal sector. *Energy Policy*, vol. 29, no. 9. pp. 701–713.

Kulshreshtha, M. and Parikh, J.K. 2002. Study of efficiency and productivity growth in opencast and underground coal mining in India: a DEA analysis. *Energy Economics*, vol. 24, no. 5. pp. 439–453.

Li, Z.H., Hua, X.Z., Zhu, R.J., and Zhou, D.S. 2013. Numerical simulation of strata behavior in super-long and large mining height working face. *Advanced Materials Research*, vol. 634–638, no. 1. pp. 3428–3432.

Liu, Y., Zhou, F., Geng, X., Chang, L., Kang, J., Cui, G., and Zhang, S. 2016. A prediction model and numerical simulation of the location of the longwall face during the highest possible failure period of gob gas ventholes. *Journal of Natural Gas Science & Engineering*, vol. 37. pp.178–192.

Mishra, D.P., Sugla, M., and Singha, P. 2013. Productivity improvement in underground coal mines - a case study. *Journal of Sustainable Mining*, vol. 12, no. 3. pp. 48–53.

Nie, R., He, B.Y., Yuan, P.F., Zhang, L.H., and Li, G.P. 2015. Novel approach to and implementation of design and analysis of armored face conveyor power train. *Science China Technological Sciences*, vol. 58, no. 12. pp. 2153–2168.

Niu, X.Y. 2009. Feasibility analysis of coal mining with double shearers in extended working face. *Shaanxi Coal*, vol. 28, no. 1. pp. 29–30.

Qu, Q.D., Xu, J.L., and Xue, S. 2009. Improving methane extraction ratio in highly gassy coal seam group by increasing longwall panel width. *Procedia Earth & Planetary Science*, vol. 1, no. 1. pp. 390–395.

Robbins, R.J. 2000. Mechanization of underground mining: a quick look backward and forward. *International Journal of Rock Mechanics & Mining Sciences*, vol. 37, no. 1. pp. 413–421.

Toraño, J., Diego, I., Menéndez, M., and Gent, M. 2008. A finite element method (FEM) – fuzzy logic (soft computing) – virtual reality model approach in a coalface longwall mining simulation. *Automation in Construction*, vol. 17, no. 4. pp. 413–424.

Tu, S.H., Yuan, Y., Zhen, Y., Ma, X.T., and Qi, W. 2009. Research situation and prospect of fully mechanized mining technology in thick coal seams in china. *Procedia Earth & Planetary Science*, vol. 1, no. 1. pp. 35–40.

Walker, A.J. 1987. The development and use of very heavy duty face conveyors. *Advances in Mining Science & Technology*, vol. 1. pp. 199–211.

Wu, S.H. and Zhang, H.L. 2012. Practical application of double-shearer in fully mechanized face with soft rock condition. *Shandong Coal Science and Technology*, vol. 4. pp. 23–23.

Xu, J.L., Yu, B.J., Lou, J.F., and Wang, D. P. 2007. Characteristics of gas emission at super-length fully-mechanized top coal caving face. *Journal of China University of Mining and Technology*, vol. 17, no. 4. pp. 447–452.

Zhang, D., Zhang, M., and Wang, B. 2000. Analysis and selection of mining patterns for high-output-and-high-efficiency mines. *Journal of China University of Mining and Technology*, vol. 29, no. 4. pp. 363–367.

Zhang, Y., Wan, Z.J., Li, G.W., and Wang, C. 2009. Idea on combined coal mining technology with multi coal shearers for longwall coal mining face. *Coal Engineering*, vol. 10. pp. 8–11.

Zhao, Y.H., and Song, X.M. 2016. Stability analysis and numerical simulation of hinged arch structure for fractured beam in super-long mining workface under shallow seam. *Rock & Soil Mechanics*, vol. 37, no. 1. pp. 203–209. ◆

http://dx.doi.org/10.17159/2411-9717/2018/v118n10a10

Market implications for technology acquisition modes in the South African ferrochrome context

by E. van der Lingen and A. Paton

Synopsis

The South African ferrochrome industry has been faced with various challenges during the past few years, such as influences from the market, manpower strikes, China's control over the demand for both ferrochrome and chrome ore from South Africa, and electricity supply constraints, placing increased pressure on the local industry to improve output in order to remain globally competitive. The year 2016 brought a dramatic change in the local ferrochrome industry, being marked by higher chrome ore prices and the takeover of some idle smelters.

This study investigates the methods of technology acquisition used in various parts of the ferrochrome smelter value chain throughout a business cycle, and whether there is a preference for a specific acquisition in an explicit part of the value chain. The study also considers whether companies prefer to partner with local or global institutions for collaborative development, and the methods used by companies to protect their technologies.

Keywords
Technology acquisition modes, ferrochrome, value chain, business cycle.

Introduction

South Africa holds the world's largest chrome ore reserves and was the world's largest producer of ferrochrome until 2012, when China became the leading ferrochrome-producing country. South Africa's chrome ore (chromite) supply into the Chinese market has risen significantly from 36% of China's total chrome ore imports in 2010 to more than 70% in 2016 (Fowkes, 2014; Creamer, 2017). China controls the demand for both ferrochrome and chrome ore from South Africa (Fowkes, 2014). China's high import rate of chrome ore has resulted in ferrochrome prices being driven down and a depressed ferrochrome market. The South African industry meets the chrome ore demands but loses out on ferrochrome beneficiation.

Furthermore, the local ferrochrome industry has been threatened with the overall poor competitiveness over the past few years, resulting in four of the eight producers ceasing operations at the beginning of 2016. Challenges experienced by the producers, some of which are directly linked to production costs, include influences from the market, productivity that was affected by wildcat strikes, China's control over the demand for both ferrochrome and chrome ore, and electricity supply issues (Fowkes, 2014, 2013; Biermann, Cromarty, and Dawson, 2012). Ferrochrome production is energy-intensive and South African producers have faced higher electricity costs, electricity supply complications, and a weaker currency exchange rate since 2009.

Ferrochrome is an iron-chromium alloy that contains between 50% and 70% chromium by weight. Chromium is one of the fundamental metals used in modern steelmaking and superalloys due to its excellent corrosion resistance, and it is regarded as a commodity of critical and strategic importance (Murthy, Tripathy, and Kumar, 2011). China is currently the world's top producer of ferrochrome, despite its lack of significant chrome resources, as well as the world's leading stainless steel producer (US Geological Survey, 2017). Global stainless steel production rose by more than 8% in 2016, resulting in an increase in chrome ore and ferrochrome demand (see Figure 1). The year 2016 brought a dramatic change in the local ferrochrome industry. It was marked by idle smelters in the beginning of that year, take-overs in the industry, and chrome ore prices reaching the highest levels since the global economic downturn in the third quarter of 2016.

The purpose of this study is to link the value chain and business cycle to the choice of technology acquisition mode (TAM) in the South African ferrochrome industry. Although this area has been studied extensively in the electronics industry, there is a gap in the body of knowledge in the mining industry. Previous research has been fragmented, with only a few parameters being studied at a specific time for

* *Department of Engineering and Technology Management, University of Pretoria, South Africa.*

 ISSN 2225-6253. Paper received Aug. 2017; revised paper received Jun. 2018.

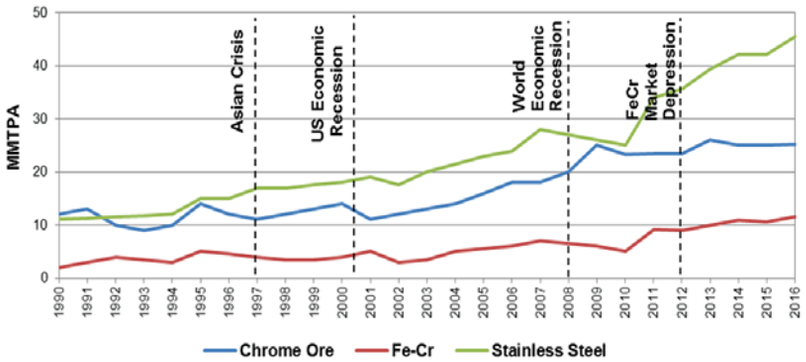

Figure 1—Global production of stainless steel, chrome ore, and ferrochrome (FeCr) for the period 1990–2016 (Kleynhans, 2011; Richard, 2015; International Ferro Metals (IFM), 2013; CRU Group, 2017)

appropriate modes. The theory does not link these aspects together, but it is important to understand the mining context because of the increasing pressures to improve management outputs to attain global competitiveness.

Literature study

Technology acquisition modes

Technology acquisition strategy is seen as the process of selecting acquisition modes using technical and non-technical capabilities and integration of the selected technology into the value chain (Burgelman, Christensen, and Wheelwright, 2004; Cho and Pyung-Il, 2000). According to Lundquist (1999), the technology developed must be a value creator that meets the organization's needs. There are various types of technology acquisition mode (TAMs), but in-house development and technology purchasing are the umbrella terms used to describe a whole range. A third mode that is considered in this study, collaborative development, requires the involvement of internal and external capabilities.

In-house development is defined as the execution of development as a task in the organization's existing structures, namely its research and development (R&D) department (Cho and Pyung-Il, 2000). The advantages of in-house development are as follows (Schlorke, 2011):

- Tacit knowledge is gained
- The technology that is developed becomes the property of the developer
- Competitive advantage becomes exclusive to the developer
- There is an opportunity to increase revenue by the sale or licensing of the developed technology.

The disadvantages of in-house development are as follows:

- Long development times
- Increased development costs
- Potential disruption of production
- The possible lack of internal resources to complete the development.

Technology purchasing is broadly defined as acquiring technologies by contracts, licensing, or simply purchasing from a provider. This mode neither utilizes internal capabilities nor requires any technical collaboration (Cho and Pyung-Il, 2000). The advantages of technology purchasing are potential cost reduction, lower risks, and shorter implementation times (Schlorke, 2011). However, purchasing of technology does not guarantee a competitive advantage and there is usually no valuable exchange of tacit knowledge in the process. Sourcing technologies externally may reduce the need to sustain internal technical capabilities and may also speed up the implementation of products and processes (Tsai and Wang, 2008).

Collaborative development can be defined as the complementing of internal resources in the innovation process, enhancing both the innovation input and output measured by the realization of innovations (Becker and Dietz, 2004).

Cho and Pyung-Il (2000) used the integrated framework set out in Figure 2 to investigate how companies acquire the necessary technology using an integrated approach on the basis of previous studies.

Cho and Pyung-Il (2000) stated that a company's historical pattern of choice was the most significant factor in discriminating between the modes. Based on an evolutionary economics perspective, routines are more likely to affect how firms perceive changes in the environment, their possible responses, and the choices they make. The environment and framework represent the dynamic influences that any management system must be able to accommodate to determine the best acquisition modes.

Kurokawa (1997) investigated variables that affect technology acquisition decisions. The variables included the influence of the time-to-revenue and time-versus-cost relationships, as well as intervening variables. The most relevant variables to manufacturing operations are the following:

Variables that influence the time-to-revenue relationship

- *The degree of competition*—An increase in competitors stimulates external acquisitions because the increased competitive pressures further diminish the potential revenue of technology laggards.
- *The degree of protection*—If new products require a high degree of protection of technical know-how through patents, copyrights, or trade secrets, in-house R&D is preferred over technology purchasing.

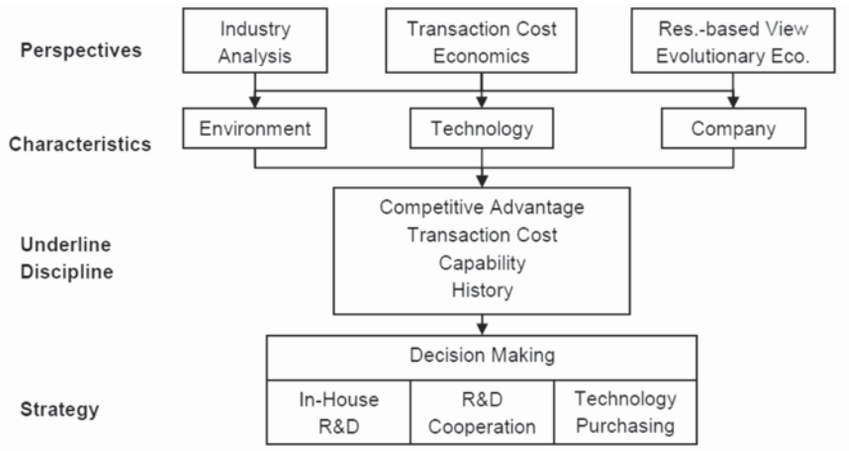

Figure 2—The adapted integrated framework for technology acquisition modes (Cho and Pyung-Il, 2000)

Variables that affect the time-versus-cost relationship

- *Relatedness of the technology*—If the company's development focus is related to its core technology, its own personnel and resources are utilized. In-house development becomes cheaper and less time-consuming than purchasing. The opposite is true if the development focus is on non-core technologies if in-house development is used.

Intervening variables

- *History*—A firm is more likely to select the same TAM that has been used in the past.
- *R&D capability*—The more advanced the in-house development capability of a company, the more it will utilize the capabilities available for R&D, and the more likely it is to purchase technology to advance its in-house R&D capabilities.

Simatupang (2006) found that few studies have been conducted into the practices and characteristics of the technology acquisition process for companies in developing countries. Most of the current studies were conducted in the developed nations, such as the USA, UK, and Japan, where competitiveness is driven by technology development. Schlorke (2011) provides the most recent study linking technology acquisition and product development processes in the South African electronics industry. The studies conducted in the different countries all evaluated the electronics industry and focused on product development and programme management, unlike the ferrochrome industry, which focuses on production capacity and process efficiency.

Business cycle

Industry-specific business cycles are characterized by four phases: boom, recession, depression, and recovery. Figure 3 depicts the key activities and events during the four different phases of the business cycle in the mining industry as related specifically to smelting operations. Business cycles are consequences of either a large sole cause or smaller events in the market, such as the sub-prime crisis (2009 recession) or capital projects (Roberts, 2009). The end consumption of the mining industry's products depends on the level of activity in industries such as construction and automotive manufacturing. Inventories tend to grow during recessions and shrink during booms, a fluctuation based on demand which affects market price (Vinell, 1997). There has been a consistent growth in consumer demand, but the mining industry's capacity has often exceeded that demand in the past, leading to cyclicality (Sheridan, 1997).

During the boom periods, investment for increased capacity in anticipation of future growth based on current assumptions tends to be delayed (Alajoutsijärvi *et al.*, 2012). In 2006, the mining industry faced a boom period driven by the high rate of infrastructure construction in China. China's huge demand for metals created a market situation that encouraged the exploitation of any reserve (Alajoutsijärvi *et al.*, 2012).

The sub-prime crisis put a strain on many mining companies. When prices are lower, outputs are limited and capital projects postponed. Expansions and new projects in the mining industry depend strongly on commodity prices, as they influence the volatility of the project cash flows. One of the main purposes of predictive models for commodities is to aid the appraisal process and justify risk in relation to returns. Mine or smelter expansions require a sound knowledge of the mine life, cost of production (affected by the selected technology), a view on the commodity price for the life of the project, and an understanding of the specific commodity demand projection (Shafiee and Topal, 2010; Crowson, 2001).

Inventory shortages result in inflated markets and can indicate an imminent economic recession. The potential recovery from this recession is marked by the introduction of new buyers that gradually grow demand (Alajoutsijärvi *et al.*, 2012). Individual investors, pension fund portfolio managers, and hedge funds are examples of buyers who create a demand for mining products. Resource-rich countries that generate large tax revenues and royalties tend to have governments with a strong influence over the demand for their own mining products (Jerrett and Cuddington, 2008).

This section provides background to the different phases within a business cycle. Within this study the business cycle phases will be linked to the selection of TAM in the South African ferrochrome industry.

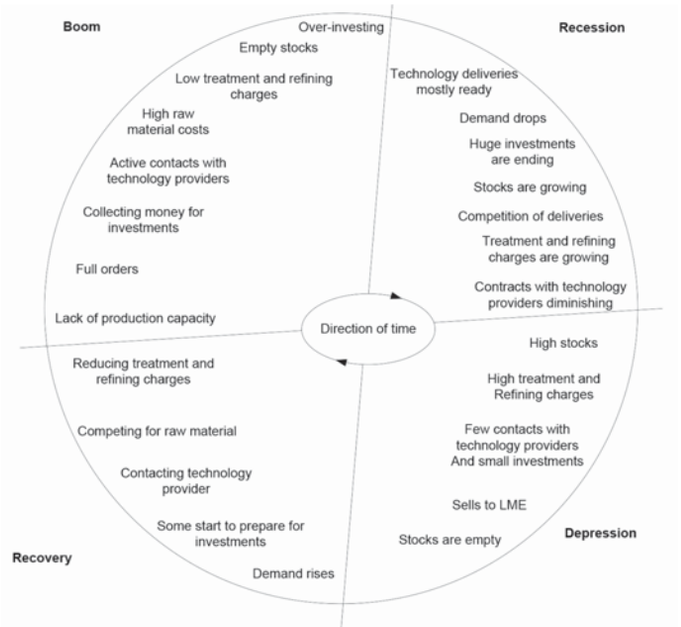

Figure 3—The key activities and events during different phases of the business cycle in the mining industry pertaining to smelters (Alajoutsijärvi *et al.*, 2012)

Conceptual framework and research objectives

Ford (1988) states that it is important to evaluate the company's level of knowledge concerning its own and emerging technologies. This evaluation must be understood across the value chain, from upstream development to downstream activities of marketing and aftermarket services. The conceptual framework in which to investigate relationships in the ferrochrome smelting industry includes the variables, TAMs, and the smelter product value chain areas (VCAs). A longitudinal study was conducted in order to assess the changes of these modes throughout a business cycle. The linking of TAMs to the VCAs and the business cycle is depicted in the framework in Figure 4.

The main objective of the current study is to determine whether the methods of technology acquisition used in various parts of the ferrochrome smelter value chain have an impact on the company throughout the business cycle. Other objectives include determining whether there is a preference for a specific acquisition in an explicit part of the value chain, whether companies prefer to partner with local or global institutions for collaborative development, and methods used by companies to protect their technologies.

The following research questions were investigated:

1. Do TAMs used by the ferrochrome industry change during different phases of the business cycle?
2. Will a greater focus on specific key and support process areas result in an increased preference for in-house development?
3. Will the departments responsible for technological innovation and selecting the TAMs in the ferrochrome industry differ between private and public entities?
4. Does the South African ferrochrome industry approach local institutions, such as the science councils, universities, and consultants, rather than global institutions when conducting collaborative development?
5. Does the ferrochrome industry use protection methods to safeguard its distinctive technologies?

Research methodology

To address the research objectives, the research design combines qualitative and quantitative analysis methods of non-experimental research (no variables are controlled). The qualitative methods consisted of electronic surveys and follow-up telephonic interviews with the management of the ferrochrome producers. The research questions asked in the survey are related to the described conceptual framework and are designed to answer the research problem by avoiding bias. The quantitative methods included the assessment of

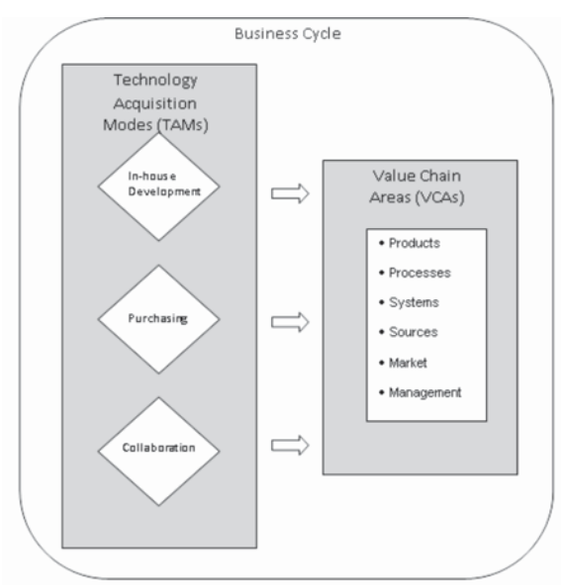

Figure 4—Integrated conceptual framework

open-source data, such as production figures and high-level market share values published in the annual reports of the various ferrochrome producers, as well as government reports.

There are 14 ferrochrome smelters in South Africa. They were operated by eight different companies at the beginning of 2016 (see Table I). Some three-quarters of the companies were publicly listed. Although quantitative data was not available for the privately owned companies, the correlations observed in the study provide a good indication of the impacts of the market conditions in the industry itself.

Responses to the surveys were received from managers from all eight companies (26 respondents) in the population. The respective companies' responses are summarized by assigning weights to the position and experience of the respondent. The population is stratified into publicly listed and privately owned companies because of the limited quantitative data available for the private companies.

Results and discussion

Do TAMs used by the ferrochrome industry change during different phases of the business cycle?

Table II and Figure 5 show the influence of different phases of the business cycle on TAMs. Technology purchasing was the predominant acquisition mode during the boom phase. The overall trend of diminishing technology purchasing as the business cycle changes from boom to recession and then depression is confirmed. As soon as the recession hits, investment shrinks, which leads to a focus on internal capabilities driving technology development. The preference for in-house development appears to be independent of in-house capabilities, but depends rather on the business cycle phase. Collaborative development is preferred over purchasing only during a depression. This means that consultants and institutions should have more opportunities during this time in the context of ferrochrome smelters.

There are gaps in the body of knowledge regarding the actual impact of the phases in a business cycle on the preferred TAM. Many theories describe various factors that affect the mode selection (Cho and Pyung-Il, 2000; Kurokawa, 1997; Schlorke, 2011), but none have highlighted the business cycle, which is important to a commodity producer, such as the ferrochrome industry, as this is what drives demand for the product. The ferrochrome industry is vulnerable to many factors and requires consistent adaptation to changes. Difficulties in sustaining technology management strategies are particularly experienced in developed countries.

The study also investigated whether there is a difference between the TAMs that private and public companies select during the depression phase (see Figure 6). Public companies use mainly in-house development and private companies use collaboration and purchasing.

Table I

Ferrochrome producers in South Africa at the beginning of 2016

Company	Company structure
Glencore Chrome	Public
Samancor Chrome	Private
Hernic	Private
Sinosteel ASA Metals	Private/state-owned
Assmang	Public
IFM	Public
Tata Steel KZN	Public
Mogale	Public

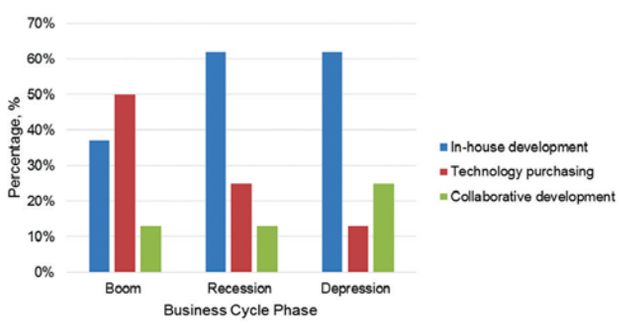

Figure 5—TAM preferences in different phases of the business cycle

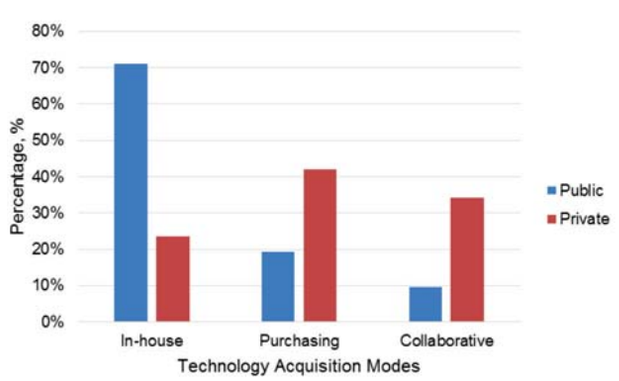

Figure 6—Preferred TAMs for public and private ferrochrome companies during the depression phase

Table II

Phases of the business cycle and modes of technology acquisition

Phases of business cycle	Acquisition mode			
	In-house development	Technology purchasing	Collaborative development	Total
Boom (2004–2007)	37%	50%	13%	100%
Recession (2008–2009)	62%	25%	13%	100%
Depression (2010–2016)	62%	13%	25%	100%

- Technology purchasing was the predominant acquisition mode during the boom period, with in-house development dominating during the recession and depression phases. Collaborative development is preferred over purchasing only during a depression phase.

Will greater focus on specific key and support areas result in an increased preference for in-house development?

Table III shows that technologies are developed mostly for key area processes and support area systems, followed by management innovation. Furthermore, for key area processes and support area systems, the preferred TAM is technology purchasing. Similar results were obtained for the TAMs in-house development and collaborative development for the key and support focus areas. On the other hand, the preferred TAMs for management innovations are in-house development and collaborative development, with the lowest score being that of technology purchasing.

Lastly, the value chain is well understood in the industry and each area of the value chain is managed accordingly. It is clear that these relationships have not been investigated in an integrated way in the past because it is not clear who manages technology development in a company. It is unlikely that a software engineer manages technological innovation in the key process area or that production departments manage innovation in the finance department. For these reasons, and because the body of knowledge is still very vague, it is not deemed pragmatic to address the relationship between TAMs and the value chain in an integrated framework.

- The focus areas of the investigated value chain showed that technology purchasing was the preferred TAM for both the key and support focus areas, and was preferred above in-house development, as anticipated. In-house development is one of the most important TAMs for management innovation, but cannot be singled out.

Will the responsible departments for technological innovation and selecting the TAMs in the ferrochrome industry differ between private and public entities?

The management of each ferrochrome producer functions in a different organogram, which means that technology management and thus TAM selection is performed by specific functional groups in the business. Table IV shows the distribution among departments that are responsible for technological innovation in the South African ferrochrome industry during a depression period. The distribution of innovation responsibility is relatively evenly spread among the departments in the industry as a whole, except for lower values for the technology and capital projects departments. In the private sector, a slightly higher assignment resulted in the business integration systems (BIS) department being assigned responsibility for developing technologies, whereas a slightly lower assignment was found for the technology department (Figure 7). For public companies, the distribution was relatively equal among the different departments with technology, maintenance, and production departments scoring slightly higher.

The primary focus of the responsible departments is not restricted to a single dimension, as shown in the results in Figure 8. The focus of private and public companies is mainly on increased productivity, profit, and improved quality. However, public companies also reported some focus on the job satisfaction of staff members and increased market share.

- The departments chiefly responsible for technological innovation differ between the public and private sectors, with the BIS departments being mainly responsible in the private sector and the maintenance and production departments being responsible in the public sector.

Table IV

The departments responsible for technology management and TAMs in both public and private companies

Responsible department	Average distribution
Technology department	13%
Capital projects	13%
Maintenance	20%
Controls and instrumentation	17%
Production	20%
BIS	17%

Table III

Focus areas of the value chain and modes of technology acquisition

Focus area			Acquisition mode		
			In-house development	Technology purchasing	Collaborative development
Key	Products	18%	21%	12%	22%
	Processes	32%	33%	41%	30%
	Sources	-	-	-	4%
Support	Systems	27%	29%	41%	30%
Management	Market	-	4%	-	-
	Management	23%	13%	6%	13%
Total		100%	100%	100%	100%

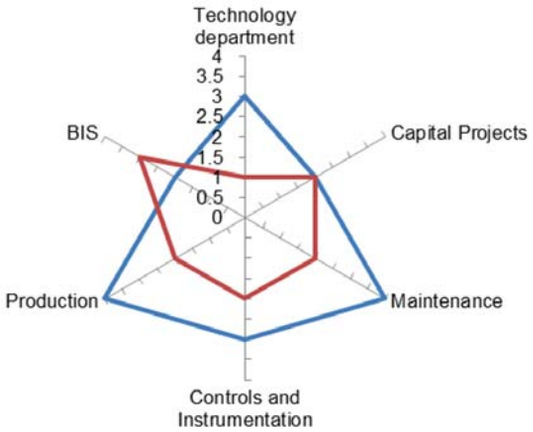

Figure 7—The departments responsible for technological innovation in a company

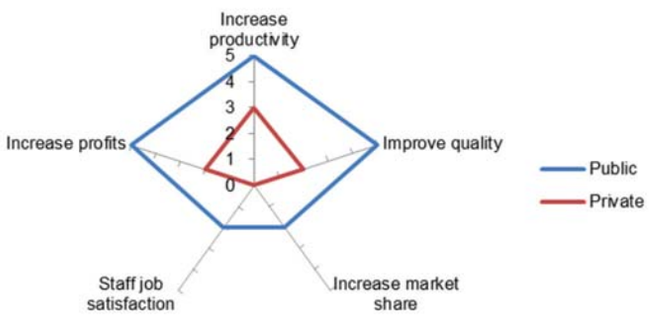

Figure 8—The focus of the department responsible for technological innovation in the organization

Does the South African ferrochrome industry approach local institutions, such as science councils, universities, and consultants, rather than global institutions when conducting collaborative development?

The South African ferrochrome industry is inclined to collaborate with local institutions (see Figure 9). The majority of the collaborative work is conducted with the South African science councils, followed by consultants, and then universities. As South Africa is a major producer of FeCr, the local organizations have significant know-how in the field and the country is a leading user of the best available smelting technology. Global institutions constitute less than 20% of the partnerships in collaborative development.

- The South African ferrochrome industry prefers local institutions for collaborative development.

Does the ferrochrome industry use protection methods to safeguard its distinctive technologies?

The South African ferrochrome industry is in general very protective of its technologies and uses various methods to protect them, as shown in Figure 10. Confidentiality agreements, followed by retaining know-how in-house, appeared to be the foremost means of protecting technologies. Legal protection methods, such as patenting and licensing, are also often employed in this sector. None of the companies use trademarks as a protection mode.

- The South African ferrochrome industry often uses protection methods, such as confidentiality agreements, retaining know-how in-house, patents, and licences.

Conclusions

The study found that the TAM used by the ferrochrome industry changes during the different periods in a business cycle. Technology purchasing was the predominant acquisition mode during the boom period. As the cycle moved from a boom to a recession and then to a depression,

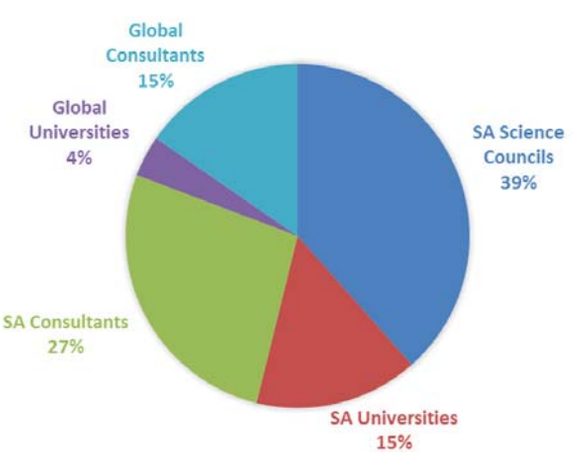

Figure 9—Preferred partners for collaborative development

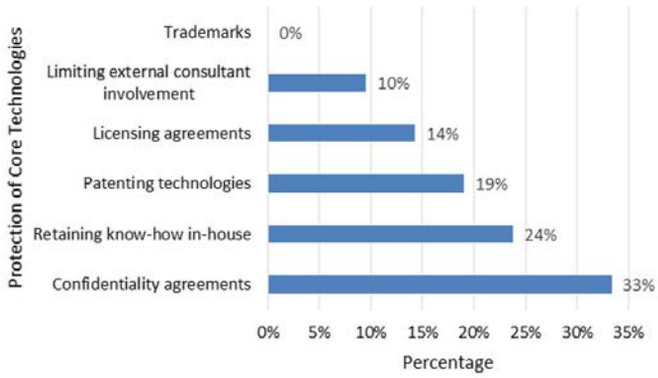

Figure 10—The protection methods used by the ferrochrome industry

technology purchasing became less dominant and in-house development became the preferred TAM. Collaborative development is preferred over purchasing only during a depression.

Technology purchasing was the preferred TAM for both the key and support focus areas. The departments that are mainly responsible for technological innovation differ between the public and private sectors, with the BIS departments being mainly responsible in the private sector, and the maintenance and production departments in the public sector.

The majority of collaborative development projects are conducted with South Africa science councils, followed by consultants, and then universities. Furthermore, the South African ferrochrome industry often uses protection methods, such as confidentiality agreements, retaining know-how in-house, patents, and licences.

Since the original investigation, there has been a significant reconsolidation of the local ferrochrome industry. This occurred mainly due to increased production costs that were no longer sustainable (based on follow-up interviews with personnel).

References

Alajoutsijärvi, K., Mainela, T., Ulkuniemi, P., and Montell, E. 2012. Dynamic effects of business cycles on business relationships. *Management Decision*, vol. 50. pp. 291–304.

Becker, W. and Dietz, J. 2004. R&D cooperation and innovation activities of firms: evidence for the German manufacturing industry. *Research Policy*, vol. 33, no. 2. pp. 209–223.

Burgelman, R.A., Christensen, C., and Wheelwright, S. 2004. Strategic Management of Technology and Innovation. 4th edn. McGraw-Hill/Irwin, New York.

Beukes, J.P., Dawson, N.F., and van ZyL, P.G. 2010. Theoretical and practical aspects of Cr(VI) in the South African ferrochrome industry. *Journal of the Southern African Institute of Mining and Metallurgy*, vol. 110. pp. 743–750.

Biermann, W., Cromarty, R.D., and Dawson, N.F. 2012. Economic modelling of a ferrochrome furnace. *Journal of the Southern African Institute of Mining and Metallurgy*, vol. 112. pp. 301–308.

Cho, D. and Pyung-Il, Y. 2000. Influential factors in the choice of technology acquisition mode: an empirical analysis of small and medium size firms in the Korean telecommunication industry. *Technovation*, vol. 20. pp. 691–704.

Creamer, M. 2017. Strong outlook for recovering ferrochrome industry – Merafe. *Polity*. http://www.polity.org.za/article/strong-outlook-for-recovering-ferrochrome-industry-merafe-2017-03-08.

Crowson, P. 2001. Mining industry profitability? *Resources Policy*, vol. 27, no. 1. pp. 33–42.

Ford, D. 1988. Develop your technology strategy. *Long Range Planning*, vol. 21. pp. 85–95.

Fowkes, K. 2013. Developments in production costs and competitiveness in ferrochrome. *Proceedings of the Metal Bulletin International Ferroalloys Conference*. Barcelona, Spain, 10–12 November 2013.. http://www.alloyconsult.com/files/MB_conf_presentation_-_SA_Sep_2013.pdf

Fowkes, K. 2014. Is there a limit to the market share of South African chrome units? *Proceedings of the 7th South African Ferroalloys Conference*, Johannesburg, South Africa, 4 September 2014. http://www.alloyconsult.com/files/MB_conf_presentation_-_SA_Sep_2014.pdf

International Ferro Metals (IFM) 2013. Integrated Annual Report 2013. International Ferro Metals, Sydney.

Jaipuria, S. and Mahapatra, S.S. 2014. An improved demand forecasting method to reduce bullwhip effect in supply chains. *Expert Systems with Applications*, vol. 41. pp. 2395–2408.

Jerrett, D. and Cuddington, J.T. 2008. Broadening the statistical search for metal price super cycles to steel and related metals. *Resources Policy*, vol. 33, no. 4. pp. 188–195.

Kleynhans, E. 2011. Unique challenges of clay binders in a pelletised chromite pre-reduction process – a case study. MSc dissertation, North-West University. http://repository.nwu.ac.za/handle/10394/7370

Kurokawa, S. 1997. Make-or-buy decisions in R&D: small technology-based firms in the United States and Japan. *Engineering Management, IEEE Transactions*, vol. 44. pp. 124–134.

Lundquist, G. 1999. Technology and the Agents of Change. Parker, C.O. (ed.). The Market Engineering Press, Parker, co.

Murthy, Y.R., Tripathy, S.K., and Kumar, C.R. 2011. Chrome ore beneficiation challenges and opportunities – a review. *Minerals Engineering*, vol. 24. pp. 375–380.

Richard, P. 2015. Overview of global chrome market. *Proceedings of the 1st INDINOX Stainless Steel Conference*, Ahmedabad, India, 25 January 2015. International Chromium Development Association. pp. 1–21.

Roberts, M.C. 2009. Duration and characteristics of metal price cycles. *Resources Policy*, vol. 34, no. 3. pp. 87–102.

Shafiee, S. and Topal, E. 2010. An overview of global gold market and gold price forecasting. *Resources Policy*, vol. 35, no. 3. pp. 178–189.

Schlorke, K.H. 2011. Technology acquisition modes and product development performance in the electronics industry in South Africa. MEng dissertation, University of Pretoria.

Sheridan, J.H. 1997. Managing peaks and valleys. *Industry Week*, 3 November, pp. 13–20.

Simatupang, T. 2006. Study of technology acquisition modes: the choice between making and buying technology. PhD thesis, RMIT Universityy, Melbourne.

Tsai, K. and Wang, J. 2008. External technology acquisition and firm performance: a longitudinal study. *Journal of Business Venturing*, vol. 23, no. 1. pp. 91–112.

US Geological Survey 2017. Mineral commodity summaries 2017. p. 202. https://doi.org/10.3133/70180197

Vinell, L. 1997. Business cycles and steel markets. Beckmans Bokforlag AB, Stockholm. ◆

http://dx.doi.org/10.17159/2411-9717/2018/v118n10a11

The effect of nC_{12}-trithiocarbonate on pyrrhotite hydrophobicity and PGE flotation

by C.F. Vos*, J.C. Davidtz†, and J.D. Miller‡

Synopsis

This work presents the potential for improving the flotation recovery of slow-floating sulphide minerals with the use of starvation dosages of a normal dodecyl (n-C_{12}) trithiocarbonate (TTC) co-collector, together with a sodium isobutyl xanthate (SiBX) and dithiophosphate (DTP) collector mixture.

At potentials below –150 mV (SHE), addition of nC_{12}-TTC with SiBX improves the hydrophobicity of pyrrhotite, yielding captive bubble contact angles greater than those measured for SiBX or nC_{12}-TTC alone, suggesting a low potential synergistic effect. This synergistic effect is further studied using Fourier transform infrared (FTIR) spectroscopy, the results indicating an increase in the surface concentration of the collector species when in a mixture. Thus, nC_{12}-TTC with SiBX may act as an immobile surface anchor to which SiBX/$SiBX_2$ molecules bond, increasing the localized concentration of collector species.

Bench-scale flotation tests using mixtures of SiBX/DTP/nC_{12}-TTC on a platinum group element (PGE)-bearing ore from the Bushveld Complex in South Africa confirm an improved metallurgical performance at very low substitutions (approx. 5 molar per cent) of SiBX. The improved recoveries for PGE, Cu, and Ni are correlated with improvements in the flotation kinetics of their slow-floating components.

Keywords
sulphide flotation, hydrophobicity, collector, nC_{12}-trithiocarbonate, synergistic effect.

Introduction

Short-chain (less than C_6) xanthates are very effective for the bulk flotation of sulphides (Fuerstenau, 1982), and early work (Leja, 1968; Gaudin, 1957; Plaksin and Bessonov, 1957; Taggart, Giudice, and Ziehl, 1934) indicated that the presence of oxygen in flotation slurries is necessary for the oxidation of the xanthate collector at the sulphide mineral surface to induce hydrophobicity. Fundamental research into the chemistry and adsorption mechanisms of xanthates over the years (Finkelstein and Poling, 1977; Woods, 1976; Winter and Woods, 1973) has revealed that for iron-bearing sulphide minerals, adsorption occurs predominantly through a charge transfer process. Oxidation of the adsorbed collector to the corresponding dimer takes place if the mixed potential of the system is greater than the reversible potential for dimer formation. In oxygenated slurries the rate of adsorption and oxidation of the collector depends greatly on the substrate surfaces. For chalcopyrite (Guler *et al.*, 2005; Leppinen, 1990; Roos, Celis, and Sudrassono, 1990) and pentlandite (Hodgson and Agar, 1989) a two-step interaction with xanthate is proposed in which the chemisorbed xanthate is further oxidized to the dimer. The initial interaction of xanthate with pyrrhotite is through physisorption where xanthate physisorbs onto positive surface sites followed by oxidation to dixanthogen (Khan and Kellebek, 2004; Bozkurt, Xu, and Finch., 1998). This process is, however, slow and increased reaction time is needed to improve flotation recovery (Buswell and Nicol, 2002).

Research into short-chain (less than C_6) trithiocarbonate (TTC) molecules as sulphide collectors has been undertaken since the 1980s, and has shown that the short-chain molecules are superior compared to xanthates, dithiophosphates, or their mixtures (Steyn, 1996; Coetzer and Davidtz, 1989; Slabbert, 1985). This is brought about by the third sulphur atom replacing the oxygen atom in the xanthate molecule. It has been suggested that this reduces the interaction between the adsorbed TTC and the surrounding bulk water (Davidtz, 1999), improving sulphide flotation metallurgy (Davidtz, 1999; Steyn, 1996; Coetzer and Davidtz, 1989; Slabbert, 1985).

The flotation chemistry of short-chain TTC collectors was studied (du Plessis, Miller, and Davidtz, 2003, 2000) to understand the underlying flotation mechanisms brought

* *Impala Platinum Limited, Concentrator Technical Department, South Africa.*
† *Department of Materials Science and Metallurgical Engineering, University of Pretoria, South Africa.*
‡ *Department of Metallurgical Engineering, University of Utah, USA.*

 ISSN 2225-6253. Paper received Mar. 2018; revised paper received Jun. 2018.

about by the third sulphur atom and it was shown that, in the presence of oxygen, a hydrophobic sulphide mineral surface can be established well below the reversible potential for TTC dimer formation. This was the first evidence that a hydrophobic surface in the presence of TTC molecules is less sensitive to the formation of the corresponding dimer. It was postulated that one or more of the TTC decomposition or hydrolysis products, potentially the mercaptan, may be adsorbing under reduced conditions, rendering the mineral hydrophobic (du Plessis, 2003). Research on the interaction of the TTC with copper and pyrite electrodes (Venter and Vermaak, 2008a; Venter, 2007) confirmed the difference between the adsorption mechanisms of xanthate and the TTC and found that the TTC interacts with the sulphide surface independently of the surface potential, confirming du Plessis' unexpected findings. Two adsorption mechanisms were proposed, one under cathodic potentials during which the mineral acts as catalyst for TCC decomposition into its corresponding thiol or thiolate, and a second that takes place under anodic potentials during which TTC chemisorbs via a charge transfer process. Under anodic potentials, as with xanthate, the chemisorbed TTC is oxidized to the dimer (Venter and Vermaak, 2008a; du Plessis, 2003).

Although the mechanisms of short-chain TTCs are understood, the longer chain molecules (nC_{12}) have also shown significant benefits when used in low-dosage applications (Breytenbach, Vermaak, and Davidtz, 2003, Vos Davidtz, and Miller, 2007) in combination with xanthate and dithiophosphate. The synergistic effects of this new mixed collector system have not been studied extensively to date. This paper reports on findings involving mixed SiBX/nC_{12}-TTC contact angle measurements and adsorption studies on pyrrhotite, a major sulphide mineral component of the Merensky Reef ores, followed by bench-scale flotation tests on Merensky Reef ores to evaluate the nC_{12}-TTC as a co-collector with a traditional SiBX/DTP mixture.

Experimental

The processing of the Merensky PGE-bearing ore used in this study takes place at the buffering pH of the ore, which is alkaline at approximately pH 9.0–9.5. In other studies (Vos, 2006) it was demonstrated that pyrrhotite hydrophobicity improved at more acid conditions. However, the overall purpose here was to determine if its surface hydrophobicity could be improved at the natural or buffer pH of the Merensky ore used in the study, therefore for the batch tests and small-scale tests that follow, no pH modifications were done or reported for this paper.

Contact angle measurements and FTIR spectroscopy

Captive bubble contact angle measurements were performed on a polished pyrrhotite crystal (> 95 mass% purity) sourced from the Geology Curator at the University of Utah, USA. Prior to every measurement the mineral electrode was polished using a 1 m corundum suspension. The surface oxidation was minimized by transferring the polished mineral directly into the test solution. The electrode was then conditioned at the desired potential for one minute prior to collector addition (SiBX, nC_{12}-TTC, or a mixture). The electrode was then conditioned in the collector solution for ten minutes at the desired potential. Whenever a mixture was used the electrode was conditioned for five minutes with nC_{12}-TTC prior to SiBX addition, followed by a further five minutes of conditioning. An initial xanthate concentration of 10^{-3} mol/L was employed and the nC_{12}-TTC additions were made according to Figure 2 and Figure 3. The solution pH was buffered at 9.2 using a 0.05 mol/L sodium borate solution.

The C-H stretching spectra were collected using a Biorad-Digilab FTS-6000 FTIR spectrometer with a liquid-nitrogen-cooled detector having a wide-band MCT. The FTIR chamber was flushed with dry air before any spectra were taken. All absorbance spectra are the result of 512 co-added scans ratioed against 512 co-added background scans, all at a resolution of 4 cm^{-1}. Before placing the pyrrhotite crystal into the spectrometer the mineral was contacted with SiBX, nC_{12}-TTC, or a mixture of the two. The same contact times given above were applied and care was taken not to contaminate the surface during handling.

Bench-scale flotation tests

A bulk sample (about 600 kg of 25 mm top size) of a PGE-bearing ore from a South African producer was used in this investigation. The bulk sample was crushed to –2.36 mm (moving from point A to B in Figure 1), homogenized, and split into smaller 3.3 kg sub-samples (moving from point B to

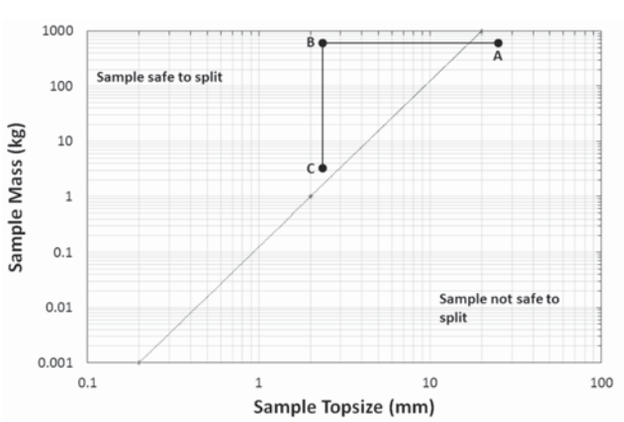

Figure 1—Application of Gy's Safety Line (adapted from Lotter, Whiteman, and Bradshaw, 2014) to demonstrate preservation of sub-sample integrity after splitting

C in Figure 1) which were used for the milling and flotation experiments. Because the bulk sample and sub-samples are located to the left of Gy's Safety Line their integrity has not been compromised during processing.

From a milling curve the required time to achieve a grind of 60% passing 75 μm was established and used throughout the flotation experiments. The samples were milled at approximately 45% solids (w/w) in a stainless steel rod mill with rods of various sizes.

After milling, the slurry was transferred into an 8 L Denver float cell and topped up with potable water from the mine site in Rustenburg, South Africa to produce a slurry of approximately 32% solids (w/w). Reagent dosages and conditioning times are noted in Table I.

Collector ratio (1) and the remainder of the chemicals (activator, collector spike, depressant, and frother dosages) were selected so as to represent the applied dosages on the Impala Platinum Merensky flotation circuit at that time. The dosages in collector ratio (2) were selected to align with those tested during the fundamental contact-angle measurements and FTIR spectroscopy studies.

After conditioning, the air flow to the cell was initiated and concentrates were collected at 1, 6, 16, and 30 minutes by scraping the froth every 15 seconds. A constant froth depth of approximately 2 cm was employed throughout each test. The concentrates and tailings samples were dried, weighed, and assayed for 4E-PGE (sum of Pt, Pd, Rh, and Au grades), copper, and nickel content.

Results and discussion

Contact angle measurements

The use of copper and lead activating ions had failed to improve the measured contact angle on the surface of this pyrrhotite crystal at pH 9.2 (Vos, 2006). Higher xanthate concentrations (10^{-3} M *vs.* 10^{-4} M) also failed to increase the measured angle beyond approximately 25–30° for open circuit potentials.

In alkaline systems the activation of pyrrhotite with copper ions is not fully understood, leading to many controversial conclusions. Some researchers (Nicol, 1984) have reported that at pH > 8 pyrrhotite activation is not possible due to the formation of insoluble copper hydroxide species. Others (Kelebek, Wells, and Fekete, 1996; Senior, Trahar, and Guy, 1995; Leppinen, 1990) reported improved pyrrhotite flotation after copper ion addition.

This contradiction was explained (Finkelstein, 1997) as being in part due to the presence of iron (from grinding media, mill liners) in contact with the sulphide minerals. This contact reduces the rest potential of the mineral and increases copper uptake significantly. As copper xanthate species are orders of magnitude less soluble than those of nickel or iron (Rao, 2004a; Chander, 1999) they form preferentially and subsequently stabilize the pyrrhotite surface (Buswell and Nicol, 2002).

The purpose of nC_{12}-TTC addition with SiBX is to establish whether the surface hydrophobicity, as measured by captive bubble contact angles, can be improved in alkaline systems and to what extent this is affected by the electrode potential.

The results of the contact angle measurements, as a function of applied electrode potential and degree of xanthate substitution, are shown in Figure 2.

In Figure 2, TTC refers to solutions containing TTC only but at the indicated SiBX substitution concentrations. A 2.5% SiBX substitution refers to a solution containing SiBX at 97.5% of the initial molar concentration and the rest substituted with TTC. The 5% SiBX substitution tests are the same in that 5% of the initial SiBX is substituted with TTC.

The addition of pure nC_{12}-TTC at 5×10^{-5} M (at 5 molar per cent of the initial xanthate concentration) produces a contact angle very similar to that with 10^{-3} M SiBX at potentials above 200 mV (*vs.* SHE). This result can be expected since the longer chain molecule is much more

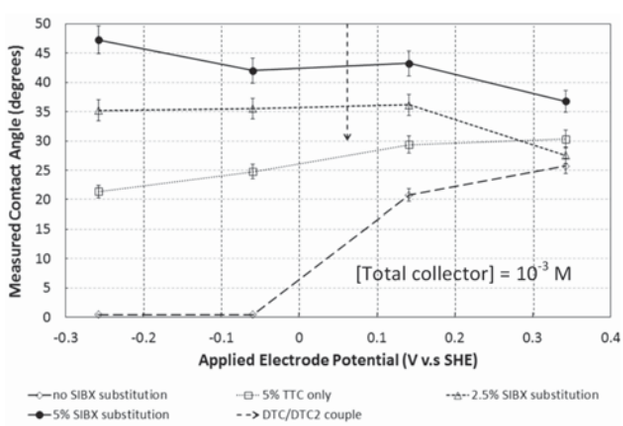

Figure 2—Captive bubble contact angle measurements for a pyrrhotite electrode

Table I

Reagent addition and conditioning time for bench flotation experiments

Reagent	Addition point	Dosage (g/t)	Conditioning time
Collector: (1) SiBX/DTP only (2) SiBX/DTP/TTC mixture	To mill	(1) 90 g/t with a 70:30 split of SiBX:DTP (2) TTC at 5,10 and 100 % of initial SiBX molar dosage while DTP was constant	-
Activator	Float cell	80 g/t copper sulphate	5 minutes
Collector spike	Float cell	10 g/t of a 70:30 mix of SiBX and DTP	3 minutes
Depressant	Float cell	90 g/t carboxyl methyl cellulose (CMC)	1 minute
Frother	Float cell	60 g/t cresylic acid frother	1 minute

hydrophobic than the shorter chain SiBX. Furthermore, the size of the TTC molecule, compared to SiBX, results in it covering a larger substrate area upon adsorption, which results in a similar surface hydrophobicity but at much lower concentrations.

At lower potentials, a contact angle is measured with the nC_{12}-TTC but none for SiBX only. This is because at lower potentials the TTC is more effective due to its much lower standard redox potential (du Plessis, 2003), implying that it forms the dithiolate much more readily at the mineral surface.

The formation of a hydrophobic pyrrhotite surface below the reversible potential for the DTC/DTC_2 couple (indicated in Figure 2) is not possible with only SiBX, which is in agreement with the literature in that dixanthogen is a prerequisite for pyrrhotite hydrophobicity (Hodgson and Agar, 1989).

As the electrode potential is lowered even further (below –150 mV) for nC_{12}-TTC-containing solutions, it is observed that a finite contact angle is maintained. This indicates that the formation of a hydrophobic pyrrhotite surface in the presence of nC_{12}-TTC is much less sensitive to the substrate surface potential. This is in line with previous observations reported for a pyrite (Venter, 2007; du Plessis, 2003) and a pure copper (Venter, 2007) electrode respectively. These earlier works suggested that under reduced potentials the decomposition product (possibly a thiolate) is responsible for the observed hydrophobicity. As the thiolate is a poor collector on its own (Venter and Vermaak, 2008b; Venter, 2007) its adsorption is believed to be catalysed through the TTC ions as an intermediate (Venter and Vermaak, 2008a).

When the same amount of nC_{12}-TTC (5 molar per cent) is used with SiBX, a clear improvement in the surface hydrophobicity is measured for all electrode potentials tested. Although not that significant above 200 mV, the effect is clear at more reducing potentials. This is a significant observation as it provides early evidence of a low-potential synergistic effect between the nC_{12}-TTC and SiBX. The result is an improved surface hydrophobicity for pyrrhotite. Even in the absence of the dimer at the mineral surface the nC_{12}-TTC, when attached to the pyrrhotite surface, seems to act as an immobile anchor for SiBX and the SiBX dimer at the surface. This can be seen as equivalent to the role of dithiophosphates in collector mixtures (Bradshaw, 1997) but at reduced potentials.

When related to flotation, the contact angle measurements indicate that there is a potential to improve the recovery of slow-floating, possibly rapidly oxidizing minerals (which are associated with difficulty in the formation of hydrophobic surface states).

FTIR spectroscopy

To further study the synergistic mechanism between nC_{12}-TTC and SiBX, FTIR spectroscopy was completed on a pyrrhotite crystal conditioned in solutions containing various concentrations of SiBX and nC_{12}-TTC. This was done to evaluate the effect of nC_{12}-TTC on the concentration of collector at the pyrrhotite surface, as can be inferred from the intensity of the absorbance peaks at 2925 cm^{-1} and 2850 cm^{-1}. The effect of nC_{12}-TCC substitutions is shown by the C-H absorbance peaks in Figure 3.

The absorbance peaks located at approximately 2925 cm^{-1} indicate that more collector is present at the pyrrhotite surface when contacted with 5% and 10% nC_{12}-TTC solutions compared to SiBX only. This is mainly because the nC_{12}-TTC molecule contains significantly more CH_2-functional groups in its hydrophobic tails compared to SiBX. The SiBX peak is hardly visible.

When the two collectors are combined (spectra 4 and 5) an increase in the absorbance of the CH_2- peaks is observed. The changes in the peak heights for spectra 4 and 5 are greater than the sum of the peak heights for spectra (1 + 2) and (1 + 3) respectively (see Table II). This observation further alludes to the presence of a synergistic effect, resulting in a localized increase in the collector concentration. A similar observation is made for the peaks at approximately 2850–2860 cm^{-1}, which are the C-H symptotic stretching vibrations. For all the measurements, the total collector conditioning time was kept constant.

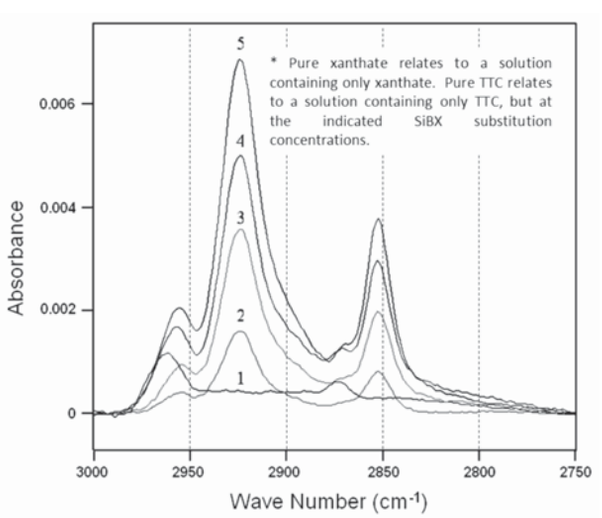

Figure 3—ERS-FTIR spectra of the C-H stretching region on a pyrrhotite surface at pH 9.2 and open circuit potentials treated with (1) SiBX, 10^{-3} M; (2) nC_{12}-TTC, 5 × 10^{-3} M; (3) nC_{12}-TTC, 10^{-4} M; (4) 5% nC_{12}-TTC + 95% SiBX, 10^{-3} M; (5) 10% nC_{12}-TTC + 90% SiBX, 10^{-3} M

Table II

FTIR absorbance peak heights at 2925 cm-1

Spectrum no.	Collector combination	Peak height (× 1000)	Ratio (to no. 1)
1	Pure xanthate (SiBX)	0.41	1.0
2	nC_{12}-TTC only at 5 molar % of SiBX dosage in (1)	1.59	3.9
3	nC_{12}-TTC only at 10 molar % of SiBX dosage in (1)	3.56	8.7
4	SiBX + nC_{12}-TTC (95:5% molar ratio)	5.00	12.2
5	SiBX + nC_{12}-TTC (90:10% molar ratio)	6.85	16.7

Bench-scale flotation tests

Based on the fundamental studies with pyrrhotite it seems that a collector mixture of SiBX with nC_{12}-TTC may offer an improved flotation recovery of sulphide minerals from the PGE ore, which in turn may translate to improved PGE recovery. The purpose of the bench-scale flotation tests was to establish the effect of mixed collector composition on the flotation performance of a PGE-bearing Merensky Reef ore, and to determine the best collector composition for optimum metallurgical performance.

For the bench-scale flotation tests, two levels of SiBX substitution with nC_{12}-TTC were tested, namely 5% and 10% molar substitutions. The concentration of DTP remained constant.

Grade and recovery profiles

For the batch flotation tests, only the collector mixture was varied and as such all other dosages (refer to Table II) remained constant throughout. The standard collector suite consisted of a SiBX/DTP mixture (condition 1 in line 1 of Table I), with the SiBX replacement tests as potential alternatives.

For each condition, triplicate flotation experiments were conducted to determine reproducibility. Timed concentrates were collected after 1, 6, 16, and 30 minutes of flotation. These concentrate samples and final tailings samples were assayed and the results used in calculating the cumulative grade and recovery of the minerals/metals of interest at each time interval. This was done as follows.

- Cumulative elemental recovery after $t = i$ minutes ($R_{m,t=i}$):

$$R_{m,t=i} = \frac{\sum_{n=1}^{n=i}(Grade_{concentrate} \cdot Mass_{concentrate})_n}{Grade_{feed} \cdot Mass_{feed}} \times 100 \quad [1]$$

- Cumulative elemental grade after $t = i$ minutes ($G_{m,t=i}$):

$$G_{m,t=i} = \frac{\sum_{n=1}^{n=i}(Grade_{concentrate} \cdot Mass_{concentrate})_n}{\sum_{n=i}^{n=i}(Mass_{concentrate})_n} \quad [2]$$

In the above equations the following are defined:

$Grade_{concentrate}$: the elemental grade of the concentrate at time i
$Grade_{feed}$: the elemental grade of the feed
$Mass_{concentrate}$: the incremental concentrate dry mass at time i
$Mass_{feed}$: the initial dry mass of the feed
$R_{m,t=i}$: cumulative component recovery at time = i minutes
$G_{m,t=i}$: cumulative component grade at time = i minutes

Figure 4 shows the effect of SiBX substitutions on the PGE grade-recovery relationship. It is evident that with a very small substitution of SiBX (as low as 5 molar per cent) an improvement in the PGE grade and recovery profile is observed. At a very similar final concentrate grade of 40–41 g/t PGE a recovery improvement of approximately 4.4% is measured. With very small variability between triplicate tests for both conditions, this difference is statistically significant.

When 10% of the SiBX is replaced with the nC_{12}-TTC no marked difference is observed in the final metallurgical performance. What is observed is a downwards shift in the grade-recovery relationship. The lower initial concentrate grade is attributed to an increase in the rate of recovery of gangue, and may imply overdosing conditions.

Figure 5 shows the grade-recovery relationship for copper (Cu) and nickel (Ni). An improvement in the recovery of Cu- and Ni-bearing sulphide minerals is also observed at 5% replacement. This improvement appears to be true for 10% replacement of SiBX with nC_{12}-TTC as well, and is more evident for Cu than for Ni. Again, improved sulphide flotation with the preferred mix of collectors is evident.

Flotation kinetics

The grade and recovery data from the various flotation tests can be modelled using the two-parameter Kelsall equation.

$$r_t = 1 - \theta_f \cdot e^{-K_f \cdot t} - \theta_s \cdot e^{-K_s \cdot t} \quad [3]$$

where

r_t = cumulative recovery after t minutes
θ_f, θ_s = fast and slow floating mass fractions respectively

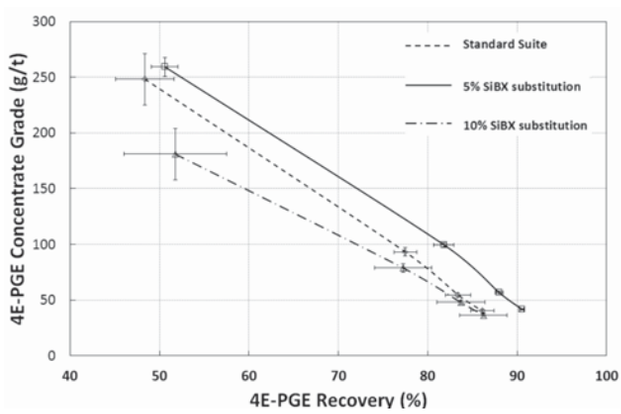

Figure 4—Grade-recovery relationship for 4E PGE as a function of SiBX substitution

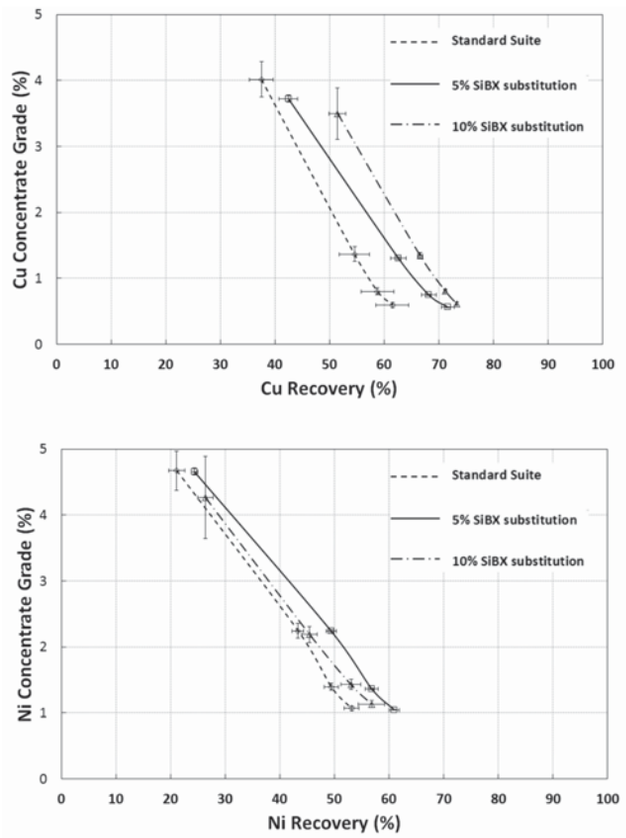

Figure 5—Grade-recovery relationships for Cu and Ni as a function of SiBX substitution

Table III

Feed composition and recovery of slow-floating components at different nC_{12}-TTC dosages

Components	Distribution of slow-floating component in feed (%)	Recovery of slow-floating component from feed		
		Standard suite (%)	5% SiBX substitution (%)	10% SiBX substitution (%)
PGE	23.6	42.4	66.5	42.9
Cu	40.9	2.4	32.8	40.6
Ni	55.6	15.3	32.6	23.0

K_f and K_s = fast and slow floating first-order flotation rate constants respectively

To evaluate the flotation kinetics under the different chemical conditions it is assumed that the ore in each test has the same mass fractions of fast-, slow-, and non-floating material, *i.e.* θ_f and θ_s are the same for all tests. Only the flotation rate constants are varied to fit the experimental data (grades and recoveries) by minimizing the sum of errors. This is a reasonable assumption since the various sub-samples are taken from a homogenized bulk sample.

By only examining the rate constants it is not possible to rapidly assess the impact of the new collector mixture on the flotation kinetics. As the fast-floating fractions for PGE, Cu, and Ni achieve 100% recovery within the first two concentrates, it is reasonable to argue that an increase in their flotation rates will not influence the overall recoveries after half an hour. The only effect it may have is on the initial concentrate grade, if the fast-floating valuable minerals are recovered preferentially to the fast-floating gangue.

A summary of the recovery of the slow-floating fraction after 30 minutes of flotation for all valuable elements is presented in Table III. The predominant influence of the nC_{12}-TTC as a co-collector is evaluated in more detail by considering the response of the slow-floating fractions of each of the elements considered. Figure 6 presents the flotation-time profile for the slow-floating PGEs as modelled using the parameters determined from Equation [3].

A very significant increase in the recovery of the slow-floating PGE fraction is observed at 5 molar per cent replacement of SiBX. As the feed consists of approximately 23.6% slow-floating PGEs (refer to Table III), an increase of this magnitude results in an overall PGE recovery improvement of approximately 4%.

As with PGEs, both Cu and Ni show a significant improvement in the recovery of the slow-floating component with the addition of nC_{12}-TTC. As the dosage is increased to 10% of the initial SiBX dosage, the recovery of slow-floating Cu continues to increase and does not show the same

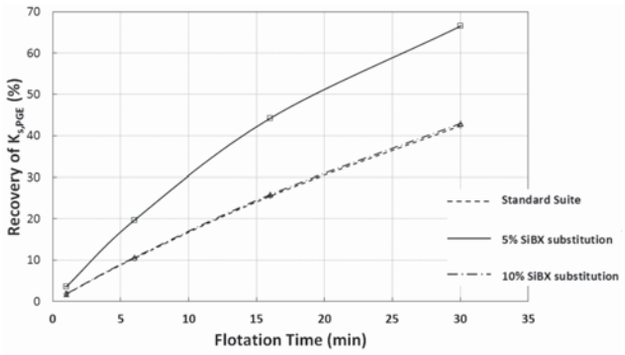

Figure 6—Modelled recovery profile of slow-floating PGEs using parameters from Equation [3]

maximum at a 5% SiBX replacement as found for the PGEs and Ni. This can possibly be explained in terms of the affinity of the collector molecule for the mineral of interest. Cu-xanthate complexes are known to be orders of magnitude less soluble than Ni and Fe complexes (Chander, 1999), and as the hydrocarbon chain length increases the solubility decreases further. In the same way it is expected that the nC_{12}-TTC will have a much higher affinity for the Cu mineral and the recovery will improve as the dosage increases.

The Ni recoveries from the slow-floating fraction show maximum improvement at 5 molar per cent replacement of SiBX, in line with the observations for 4E-PGE. This is not surprising as pentlandite is known as a primary host for all of the PGEs present except for platinum (Godel, Barnes, and Maier, 2007).

Similar outcomes have been reported for Cu, S, Ni, and Fe elsewhere (Breytenbach, Vermaak, and Davidtz, 2003). In that work the optimum nC_{12}-TTC dosage was found to be in the order of 7.5 molar per cent replacement of SiBX, which is in close agreement with our findings of 5 molar per cent. At complete substitution, however (Vos, 2006), selectivity is lost and the recovery of the valuable minerals decreases substantially.

Long-chain xanthates of seven or more carbon atoms in the hydrophobic tail are known to have surfactant properties similar to those of long-chain carboxylic acids. Beyond their critical micelle concentrations (CMC), the long-chain xanthates form micelles (Hamilton and Woods, 1986). At high dosages these molecules can absorb onto non-sulphide minerals such as oxides (silicates), in which case adsorption is through a physical mechanism (Rao, 2004b) and one deals with insoluble collector colloids or emulsions. A similar mechanism for adsorption of nC_{12}-TTC molecules onto non-sulphide gangue at high dosages may be a possibility, and more work in this area is required to clarify this phenomenon.

Summary and conclusions

- Small replacements of SiBX with nC_{12}-TTC improve the surface hydrophobicity of pyrrhotite in alkaline (pH 9.2) conditions, and the effect is more pronounced at reduced potentials (lower oxygen activity). This can have significant implications when viewed in conjunction with PGE and base metal grinding and flotation in a mild steel media environment, or where a valuable mineral is subjected to rapid oxidation.
- The synergistic effect at low concentration is believed to be in part due to a crowding of the collectors at the surface, which increases the localized surface concentration and improves hydrophobicity even at low substitutions of SiBX.
- At the bench scale, low substitutions of SiBX noticeably improve the recovery of PGE, Cu, and Ni. Overall recovery improvements are achieved at similar concentrate grades. Improved grades at the beginning of the flotation tests indicate that slow-floating, liberated minerals are being recovered.

Recommendations for future work

Further mineralogical data would add valuable information to this study. For this Merensky ore, copper is primarily associated with chalcopyrite and nickel with pentlandite, which are the two minerals expected to show recovery improvements in this regard. Overall, PGE recovery improvements as demonstrated may be due to the association of PGEs with these sulphide minerals, or to improvements in the recovery of PGMs. Detailed spare-phase mineralogical studies will be required to answer this question and it is important to include such studies in future work addressing this new chemical. Furthermore, since pyrrhotite flotation is pH-dependent, it will be useful for future experimenters to study the effect of pH using the methodologies in this paper and to determine if the correlations identified here are transferrable.

The application of nC_{12}-TTC with mild steel grinding media to improve the flotation activity of xanthate and DTP is a subject that has not been explored in great detail. From preliminary captive bubble contact angle measurements under controlled potentials, there appears to be a benefit in using this new co-collector along with SiBX and potentially DTP. This is a novel application of the nC_{12}-TTC due to its low sensitivity to oxygen activity and surface oxidation products (du Plessis, 2003).

It is well known that the choice of surfactants (especially collectors and frothers) has a significant effect on flotation metallurgy as the joint actions between them are widely acknowledged (Rao, 2004a, 2004b; Laskowski, 1993; Leja, 1989). The interaction of the nC_{12}-TTC with various frother types, and how it affects bubble capture and flotation kinetics, also needs to be investigated.

It will be of value to further test this novel co-collector on problematic ore types as well, where rapid surface oxidation and poor collector adsorption are causes of substandard metallurgical performance.

Acknowledgements

The authors acknowledge and extend their appreciation to Impala Platinum Ltd, and in particular Johan Theron and Dave Marshall, for their generous involvement in the R&D as well as their academic support for this research. The NSF, Grant Int. – 0352807, for facilitating collaborative flotation research between South Africa and the USA is also acknowledged. Dr Ronel Kappes from Newmont is also acknowledged for very helpful discussions and a review of the initial manuscript.

References

Bozkurt, V., Xu, Z., and Finch, J.A. 1998. Pentlandite/pyrrhotite interaction and xanthate adsorption. *International Journal of Mineral Processing*, vol. 52. pp. 203-214.

Bradshaw, D.J. 1997. Synergistic effects between thiol collectors used in the flotation of pyrite. PhD thesis, Faculty of Engineering and Built Environment, University of Cape Town.

Breytenbach, W., Vermaak, M.K.G., and Davidtz, J.C. 2003. Synergistic effects among dithiocarbonate (DTC), dithiophosphate (DTP) and trithiocarbonate (TTC) in the flotation of Merensky ores. *Journal of the South African Institute of Mining and Metallurgy*, vol. 103, no. 10. pp. 667–670.

Buswell, A.M. and Nicol, M.J. 2002. Some aspects of the electrochemistry of the flotation of pyrrhotite. *Journal of Applied Electrochemistry*, vol. 32. pp. 1321–1329.

Chander, S. 1999. Fundamentals of sulphide mineral flotation. *Advances in Flotation Technology*. Parekh, B.K. and Miller, J.D. (eds.). Society for Mining, Metallurgy & Exploration, Littleton, CO.

Coetzer, G. and Davidtz, J.C. 1989. Sulphydryl collectors in bulk and selective flotation. Part 1. Covalent trithiocarbonate derivatives. *Journal of the South African Institute of MIning and Metallurgy*, vol. 89, no. 10. pp. 307–311.

Davidtz, J.C. 1999. Quantification of the flotation activity by means of excess Gibbs free energies. *Minerals Engineering*, vol.12, no. 10. pp. 11471–11161.

Dippernaar, A. 1982. The destabilisation of froth by solids. I. The mechanism of film rupture. *International Journal of Mineral Processing*, vol.9. pp. 1–14.

Du Plessis, R. 2003. The thiocarbonate flotation chemistry of auriferous pyrite. PhD thesis. Department of Metallurgical Engineering, University of Utah, Salt Lake City, UT.

Du Plessis, R., Miller, J.D., and Davidtz, J.C. 2000. Preliminary examination of the electrochemical and spectroscopic features of trithiocarbonate collectors for sulfide mineral flotation. *Transactions of Nonferrous Metals Society of China*, vol. 10. pp. 12–18.

Du Plessis, R., Miller, J.D., and Davidtz, J.C. 2003. Thiocarbonate collectors in pyrite flotation - fundamentals and applications. *Proceedings of the XXII International Mineral Processing Congress*, Cape Town, South Africa, 29 September - 3 October 2003. Lorenzen, L. and Bradshaw, D.J. (eds.). Southern African Institute of Mining and Metallurgy, Johannesburg. pp. 892–901.

Finkelstein, N.P. 1997. The activation of sulphide mineral for flotation: a review. *International Journal of Mineral Processing*, vol. 52, no. 2–3. pp. 81–120.

Finkelstein, N.P. and Poling, G.W. 1977. The role of dithiolates in the flotation of sulphide minerals. *Mineral Science and Engineering*, vol.9, no. 4. pp. 177–197.

Fuerstenau, M.C. 1982. Sulfide mineral flotation. *Principles of Flotation.* King, R.P. (ed.). Southern African Institute of Mining and Metallurgy, Johannesburg. pp. 159–182.

Gaudin, A.M. 1957. *Flotation*. McGraw-Hill, New York. Chapter 9.

Godel, B., Barnes, S.J., and Maier, W.D. 2007. Platinum-group elements in sulfide minerals, platinum-group minerals, and whole-rock of the Merenksy Reef (Bushveld Complex, South Africa): Implications for the formation of the reef. *Journal of Petrology*, vol.48, no. 8. pp. 1569–1604.

Guler, T., Hicyilmaz, C., Gokagac, G., and Z.E. 2005. Electrochemical behaviour of chalcopyrite in the absence and presence of dithiophosphate. *International Journal of Mineral Processing*, vol. 75. pp. 217–228.

Hamilton, I.C. and Woods, R. 1986. Surfactant properties of alkyl xanthates. *International Journal of Mineral Processing*, vol. 17. pp. 113–120.

Hodgson, M. and Agar, G.E. 1989. Electrochemical investigations into the flotation chemistry of pentlandite and pyrrhotite. *Canadian Metallurgy Quarterly*, vol. 28. pp. 189–198.

Kelebek, S., Wells, P.F., and Fekete, S.O. 1996. Differential flotation of chalcopyrite, pentlandite and pyrrhotite in Ni-Cu sulphide ores. *Canadian Metallurgy Quarterly*, vol. 35, no. 4. pp. 329–336.

Khan, A. and Kellebek, S. 2004. Electrochemical aspects of pyrrhotite and pentlandite in relation to their flotation with xanthate. Part I: Cyclic voltammetry and rest potential measurements. *Journal of Applied Electrochemistry*, vol. 34. pp. 849–856.

Laskowski, J.S. 1993. Frothers and flotation froth. *Mineral Processing and Extractive Metallurgy Review*, vol. 12. pp. 61–89.

Leja, J. 1968. On the mechanisms of surfactant adsorption. *Proceedings of the VIII International Mineral Processing Congress*, Leningrad. vol. S-1. pp. 1–7.

Leja, J. 1989. Interactions among surfactants. *Minerals Processing and Extractive Metallurgy Review*, vol. 5. pp. 1–24.

Leppinen, J.O. 1990. FTIR and flotation investigation of the adsorption of ethyl xanthate on activated and non-activated minerals. *International Journal of Mineral Processing*, vol. 30. pp. 245–263.

Lotter, N.O., Whiteman, E., and Bradshaw, D.J. 2014. Modern practice of laboratory flotation testing for flowsheet development – A review. *Minerals Engineering*, vol. 66–68. pp. 2–12

Nicol, M.J. 1984. An electrochemical study of the interaction of copper (II) ions with sulfide minerals. *Proceedings of the International Symposium on Electrochemistry in Mineral and Metal Processing*. Richardson, P.E., Srinivasan, S., and Woods, R. (eds.). The Electrochemical Society, Pennington, NJ. pp. 152–168.

Plaksin, I.N. and Bessonov, S.V. 1957. The role of gases in flotation reactions. *Proceedings of the 2nd International Congress on Surface Activity*, vol. 3. Butterworths, London. pp. 361–367.

Rao, S.R. 2004a. Flotation surfactants. *Surface Chemistry of Froth Flotation*. 2nd edn. Kluwer Academic/Plenum Publishers, New York. pp. 385–478.

Rao, S.R. 2004b. Physical chemistry of interfaces. *Surface Chemistry of Froth Flotation*. 2nd edn. Kluwer Academic/Plenum Publishers, New York. pp. 143–207.

Robertson, C., Bradshaw, D., and Harris, P. 2003. Decoupling the effect of depression and dispersion in the batch flotation of a platinum bearing ore, *Proceedings of the XXII International Mineral Processing Congress*, Cape Town, South Africa, 29 September - 3 October 2003. Lorenzen, L. and Bradshaw, D.J. (eds). Southern African Institute of Mining and Metallurgy, Johannesburg. pp. 920–928.

Roos, J.R., Celis, J.P., and Sudrassono, A.S. 1990. Electrochemical control of metallic copper and chalcopyrite-xanthate flotation. *International Journal of Mineral Processing*, vol. 28. pp. 231–245.

Senior, G.D., Trahar, W.J., and Guy, P.J. 1995. The selective flotation of pentlandite from a nickel ore. *International Journal of Mineral Processing*, vol. 43, no. 3-4. pp. 209–234.

Slabbert, W. 1985. The role of trithiocarbonate and thiols on the flotation of some selected South African sulfide ores. MSc thesis. Department of Chemical Engineering, Potchefstroom University for Christian Higher Education, Potchefstroom.

Steyn, J.J. 1996. The role of collector functional groups in the flotation activity of Merenky Reef samples. MSc thesis. Department of Chemical Engineering, Potchefstroom University for Christian Higher Education, Potchefstroom.

Taggart, A.F., Giudice, G.R.M., and Ziehl, O.A. 1934. The case of chemical theory of flotation. *Transactions of the American Institute of Mining and Metallurgical Engineers*, vol. 112. pp. 348–381.

Venter, J.A. 2007. Dithiocarbonate and trithiocarbonate interactions with pyrite and copper. MSc thesis. Faculty of Engineering, Built Environment and Information Technology, University of Pretoria, Pretoria.

Venter, J.A. and Vermaak, M.K.G. 2008a. EIS measurements of dithiocarbonate and trithiocarbonate interactions with pyrite and copper. *Minerals Engineering*, vol. 21, no. 5. pp. 440–448.

Venter, J.A. and Vermaak, M.K.G. 2008b. Mechanisms of trithiocarbonate adsorption: A flotation perspective. *Minerals Engineering*, vol. 21. pp. 1044–1049.

Vos, C.F. 2006. The role of long-chain trithiocarbonates in the optimisation of Impala Platinum's flotation circuit. MSc thesis, Department Material Science and Metallurgical Engineering, University of Pretoria, Pretoria.

Vos, C.F., Davidtz, J.C., and Miller, J.D. 2007. Trithiocarbonates for PGM flotation. *Journal of the Southern African Institute of Mining and Metallurgy*, vol. 107. pp. 23–28.

Winter, G. and Woods, R. 1973. The relation of collector redox potential to flotation efficiency: monothiocarbonates. *Separation Science*, vol. 8, no. 2. pp. 261–267.

Woods, R. 1976. Electrochemistry of sulfide flotation. *Flotation*. Fuerstenau, M.C. (ed.). AIME, New York. pp. 298–333. ◆

http://dx.doi.org/10.17159/2411-9717/2018/v118n10a12

Informal settlements and mine development: Reflections from South Africa's periphery

by L. Marais*, J. Cloete*, and S. Denoon-Stevens†

Synopsis

Historically, mining companies worldwide provided housing and developed towns to accommodate their employees. At the end of the 1980s this approach became less prevalent and attempts were made to mitigate the effects of mine development and mine closure on communities living near the mines. Permanent settlement in mining towns urgently needed to be minimized. Since the advent of democracy, South African policy has moved in the opposite direction, shifting the emphasis to creating integrated communities and encouraging home ownership. Despite this policy shift, however, mines continue to influence local housing conditions. One direct outcome has been the development of informal settlements. We surveyed 260 informal settlement households in Postmasburg, a small and remotely located town in the Northern Cape Province of South Africa. We found that because they employ contract workers and thus arouse expectations of employment, the mines here contribute extensively to the development of informal settlements. But local factors also contribute, and the functional role of informal settlements as a form of housing that supports mobility should not be underestimated. We also found that both municipal and mining company policies for informal settlements were inadequate. Finally, we found that low-income informal settlers not associated with mine employment suffered the highest levels of social disruption.

Keywords
mining, mining towns, informal settlements, housing policy.

Introduction

A mine generates demand for labour, which in turn generates demand for housing. When settlements spring up near a mine this often means poor housing conditions. In South Africa in the 1960s and 1970s mining companies invested heavily in company towns or mining settlements, but they have become increasingly hesitant to do so, for three reasons. First, declining resource prices in the mid-1980s and the 1990s compelled them to focus on core business interests and reduce the costs of peripheral activities such as housing (Bryceson and MacKinnon, 2013); second, at the turn of the 20th century they were often accused of taking over the role of local government (IIED, 2002) and consequently became hesitant to invest in developing mining towns; and third, changing labour regimes also curbed their investment in such towns (Haslam McKenzie, 2010). Increasingly, the companies began to endorse block-roster shifts, and outsourcing also became more common in the early 1990s. Block-roster shifts in Australia (together with improved technology) have meant that miners do not need to settle near the mines but can fly in and fly out and have their urban houses as their stable homes. This has had serious negative implications for housing in remote towns in Australia, particularly worker camps, large-scale renting out of available accommodation, and 'hot-bedding'.

In South Africa, the history of mining is closely related to apartheid planning (Mabin, 1991). Housing for black miners was constrained by influx control and institutionalized migrant labour and mostly took the form of compound living (Crush, 1994). By the mid-1980s mining companies had started to consider ownership models for their workers. By the end of the 1990s they were under pressure to upgrade their compounds to single living quarters, and living-out allowances became the norm in the industry (Crush, 1989, 1992; Rubin and Harrison, 2016). The upgrading of compounds meant that they had fewer people to accommodate and the living-out allowances made miners responsible for finding their own housing. These measures did not, however, necessarily improve the miners' living conditions and it has been argued that they contributed directly to the development of informal settlements around the mines (Marais and Venter, 2006; Rubin and Harrison, 2016). While block-roster shifts have largely failed to make inroads into the South African mining labour regime, mining has not escaped the consequences of outsourcing, which has meant

* *Centre for Development Support, University of the Free State, South Africa.*
† *Department of Urban and Regional Planning, University of the Free State, South Africa.*
 ISSN 2225-6253. Paper received Sep. 2017; revised paper received Jun. 2018.

that large numbers of people have flocked to mining areas in the hope of being employed as contract workers. The result has been the development of large-scale informal settlements in mining towns (Cronje, 2014). As these contract workers are not directly employed by the companies, they fall outside the ambit of the companies' social responsibility and housing support programmes.

Postmasburg, in the semi-arid and sparsely populated Northern Cape Province of South Africa, was until 2010 a sleepy little town. Two events in the local mining scene were a shake-up. In 2010 Assmang, the company that owns the Beeshoek iron-ore mine about 15 km from Postmasburg, announced that it was relocating the people from its company town at the mine to Postmasburg itself, to make room for expansion at the mine. And then in 2011, Kumba (a company in which Anglo American has a majority share) announced that, because of the increased demand for iron ore, it was opening a new mine, Kolomela, about 23 km from Postmasburg. The result was an increase in Postmasburg's population from about 19 000 in 1996 to the current 35 000 (Statistics South Africa, 2016). In the process, large informal settlements developed in and around Postmasburg. By 2015, approximately 2500 informal housing structures had been erected, constituting about 25% of Postmasburg's housing.

Yet we do not know many details about these informal settlers, such as their place of origin, the composition of their households, their employment status, the number of household members who work on the mines, their current levels of wealth, and their place attachment to Postmasburg. The study on which this paper is based investigated these matters against the background of the international literature on mine housing and the history of mine housing in South Africa. We argue that both the local municipality and the mines (through employment, contract work, and the prospects of obtaining a job) have contributed to informal settlement development. Furthermore, the original inhabitants of the informal settlements, mostly low-income earners or unemployed, have found the influx of people a serious concern. For the many contract workers and job seekers flocking to Postmasburg, an informal housing structure represents some form of temporary accommodation that does not require a large investment and is easy to dismantle should a decision be taken to leave the town. Although informal settlement in South Africa is a much-researched topic (Cirolia *et al.*, 2016), far less work has been done on informal settlements in the context of mining (*c.f.* Rubin and Harrison, 2016, as an exception).

Methods

In 2015–2016, as part of a larger household survey in Postmasburg, we carried out a survey of 260 households in the town's informal settlements. We split the informal settlements into eight areas and conducted between 30 and 40 interviews at informal dwellings in each area, including some backyard shacks. We used a convenience sampling method to select households in the eight areas. The interviews included questions on migration, household wealth, income and expenditure, and a further range of questions on housing and social cohesion in the community. Our paper also refers to census data on the growth of informal settlements in Postmasburg.

Housing problems in mining settlements: the international experience

Up to the early 1980s mining companies globally were eager to develop company towns (Crawford, 1995). This meant that the houses belonged to the company and the miners had relatively cheap housing near the mines (Littlewood, 2014). Company towns provided good living conditions for the miners and ensured that the mines had access to labour. But the resource price slump in the mid-1980s saw the first changes being made to this policy (Marais *et al.*, 2017). Declining commodity prices made mining companies rethink their commitment to non-core activities such as housing and the maintenance of mining towns. This trend had two consequences for the towns. In many cases their governance was transferred to democratically elected local councils, giving these councils a larger degree of local political responsibility but also burdening them with the long-term maintenance risks. In other cases the mining companies privatized the houses on their books, thus transferring the risk of homeownership to the households.

Despite the trend towards minimizing the role of mining companies in housing, the companies in many cases continued to dominate settlement development. In a global rethink of practice, the International Institute for Environment and Development (IIED, 2002) noted that, in too many cases, mining companies performed the functions of local authorities. The IIED recommended that this dominant role be reduced and a greater emphasis placed on partnerships and collaborative planning initiatives. However, the companies also wanted to guarantee a good quality of life in order to recruit skilled employees and a younger workforce.

Besides encouraging companies to investigate alternatives to mining towns, the changing labour regime has caused them to invest less in the concept of mining or company towns (Haslam McKenzie, 2010). Block-roster shifts have ensured higher salaries for miners and also substantially improved their mobility. Coupled with the introduction of fly-in fly-out arrangements in Australia, this meant that miners could fly in for three weeks of work and go home to one of the main urban areas for a week (or various permutations of this arrangement). The outcome was that formal family housing was no longer needed at mining sites. The IIED (2002, p. 221) sums up the situation thus: 'Under this system, remote mineral deposits are mined without developing traditional mining towns, and workers are brought in from outside.' The original communities are, moreover, protected from the negative implications of mining, such as a huge influx of people to the town.

Despite these changes, unintended effects of mining on settlements near mines continue to be described in the international literature. Housing and planning problems associated with mining have been recorded in North America (Halseth, 1999), Europe (Feagin, 1990), and Australia (Haslam McKenzie *et al.*, 2009). Mining developments result in rapid population growth, and consequently pressure to release land for new houses and services (Haslam McKenzie, 2013), and also rapid increases in house prices and rental fees (Rolfe *et al.*, 2007; Carrington, Hogg, and McIntosh, 2011; Grieve and Haslam McKenzie, 2011; Lawrie, Tonts,

and Plummer, 2011; Akbar, Rolfe, and Kabir, 2011; Chapman, Tonts, and Plummer, 2015). The IIED (2002, p. 65) says miners 'still live in isolation in many parts of the world, or in overcrowded "boom towns" with few social and cultural opportunities'. The increased housing demand generated by mining raises the price of houses, making them too expensive for existing residents. Often, housing expenditure exceeds the norm of 30% of a household's total expenditure (Haslam McKenzie *et al.*, 2009). The high prices of housing and African countries' inability to provide infrastructure have led to widespread informality around mines (Littlewood, 2014; Negi, 2014). These negative effects of an influx of people can disturb the local community's place attachment and cause social disruption (England and Albrecht, 1984).

In Australia, informality seems to have taken a somewhat different form and includes tents, temporary housing, caravans, overcrowding, 'hot-bedding', and the illegal subdivision of urban stands (Haslam McKenzie *et al.*, 2009). The setting up of worker camps and the block booking of motels are common practices that tend to complicate long-term planning. High house prices also have negative consequences for existing mine communities, low-income families, and indigenous societies. According to Ennis, Tofa, and Finlayson (2014, p. 338), '[for] residents living in the economic shadow of major projects, the resultant housing shortages and high living costs generate economic insecurity, especially among already vulnerable populations and those on low or fixed incomes'. Obeng-Odoom (2014, p. 8) describes these negative consequences of mining as the 'local implications of the resource curse'.

Mine housing in South Africa:

Historically, mine housing was split along racial lines, with white miners enjoying the benefit of company towns or extensive housing allowances while black miners were mainly housed in high-density compounds and subject to institutionalized migrant labour control and influx control. Compounds originated in the diamond mining industry in Kimberley, owing to concerns about security and controlling the black miners (Crush, 1992). In this way, mobility was controlled by the state and the private sector.

By the mid-1980s the notion of home ownership for black miners had become prominent (Crush, 1989). It became possible when government lifted influx control and started granting homeownership to black middle-class residents, and when banks followed suit by offering mortgage finance. By the early 1990s, however, this new wisdom was under threat as high interest rates, mortgage boycotts, and the rapid drop in the gold price made home ownership less attractive (Tomlinson, 2007), especially in mining areas. Although various agreements between government and the private sector helped to address the situation, they did not solve the problem in areas that had to bear the consequences of mining decline (Marais, 2013). During the later 1980s and the early 1990s, many mining companies privatized their housing stock to their middle-income white employees.

With the advent of democracy in 1994, the search was on for an appropriate policy response to the years of underinvestment in housing under the apartheid government. Despite some reference to mine housing in the original White Paper, it was only in 2002 that mine housing again rose to prominence with the Minerals and Petroleum Development Act (2002). While the Act does not refer to housing in mining areas, it requires mining companies to develop social and labour plans that are aimed at supporting local strategic plans (called integrated development plans). These social and labour plans could include housing-related matters. More specifically, government has included housing issues in the various versions of the Mining Charter (Department of Minerals and Energy, 2002; Department of Mineral Resources, 2010, 2016). By requiring that compounds be transformed into single living quarters, the various versions have rightfully got rid of the compound system. A living allowance was introduced from the mid-1990s so that miners could find their own housing, an unintended consequence of which has been the informal settlements that have developed near mining towns (Rubin and Harrison, 2016). The Mining Charter also refers to the development of integrated settlements rather than mining towns. Our review of the international literature made it clear that this approach stands in contrast to what is being done in Australia, where only limited settlement occurs near the mines. The most direct government response to housing miners in South Africa came when government introduced the Strategy for the Revitalisation of Mining Towns (Tshangana, 2015). This strategy largely focused on improving the housing conditions of miners following the Marikana massacre in 2012. This improvement has to be achieved mainly by means of the existing housing subsidy that largely (though not exclusively) provides ownership housing. To date, both municipal and mining company policies on informal settlements have been inadequate.

What started as a system controlled by both government and business has now become more flexible. The lifting of influx control, the provision of home ownership, the dismantling of the compound, and living-out allowances have shifted the onus onto the mineworkers. Mineworkers are now able make decisions and a large number have opted for housing systems that ensure mobility between places and jobs. The need to be mobile is, moreover, reinforced by the fact that mine work, especially contract work, is by definition of limited duration.

Research findings

Postmasburg offers an example of how the logic of creating integrated settlements by integrating mine and non-mine households was put into practice. The expansion of Beeshoek made both Assmang and government keen to integrate the company-town mining population with that of Postmasburg. For the company it was a way to discard activities peripheral to its core business, and the associated long-term liabilities; for government it was a way to integrate the miners with other communities. Together Assmang and Kolomela have been instrumental in constructing more than 1 000 dwellings to house their staff in Postmasburg (Cloete and Denoon-Stevens, 2018). This has involved considerable investment by the mines. Whereas in the case of Assmang ownership was provided, Kolomela provided rental housing. The Assmang approach to home ownership is especially innovative in that a capital subsidy offered by the mine is linked to a housing allowance and an instalment-based sale

(as opposed to a mortgage) (Stewart and Drewes, 2018). We have mentioned the large influx of people this brought to the town, and the mushrooming of informal settlements. We have also noted that, to date, policy responses in respect of informal settlements are inadequate.

In the following sections we present our study findings about Postmasburg's informal settlers, and we compare them with the residents in formal housing.

The growth of informal settlements

According to data from Statistics South Africa (2016), Postmasburg has experienced large-scale growth in terms of the number of informal settlements. In 1996, only 750 households resided either in informal backyard dwellings or in informal houses on separate stands. By 2011, this figure had risen to nearly 2 300 (current estimates are that there are now more than 3 000). While the 2011 figure indicates that 28% of the households in Postmasburg were at the time living in informal settlements, the figure for South Africa, by comparison, stood at just below 14% (Statistics South Africa, 2016).

In Figure 1 we provide an overview of the location of the current informal settlements in Postmasburg. The most prominent space invaded by informal settlers happens to be the space between Newton and Postmasburg, this being largely due to its favourable location.

Relationship with the mines

The development of informal settlements near mining sites is often attributed to mining. Figure 2 shows the profile of informal households and their relation to mining in Postmasburg. In our survey, 75 of the 260 households (29%) in informal houses were linked to employment by a mining company or by a contractor to the mine. Approximately 8% of these informal dwellers were employed directly by a mining company and the rest (21%) by a contractor to one of the two big mines. The remaining 71% of households did not have anybody in the household employed by a mining company. But 35% settled in Postmasburg in the last ten years – most likely looking for employment. The remaining 46% largely originated from formal Postmasburg. These figures suggest that mining has been either directly or indirectly responsible for informal settlement development. In other evidence, looking at miners only, we found that 73% of the miners in informal housing were contract workers but in formal housing the portion was only 19%. These figures show that contract workers in a changing labour regime do indeed contribute to informal settlement development, as is often claimed in the media and in the academic literature.

The question then arose as to how many of the households in the informal settlements had moved to Postmasburg in search of employment, settled in informal settlements, but could not find employment. We asked non-mining households if they had been living in Postmasburg ten years earlier, and found that approximately 35% of them had moved to Postmasburg from elsewhere during the past ten years. We can thus categorize informal settler households living in Postmasburg at the time of the survey as follows:

- 46% were local households who had moved there in search of land
- 29% were employed in mine-related work (8% directly by the mine and 21% by subcontractors to the mine)
- The other 35% of households associated with mining were not employed by the mines at the time of the survey but, according to our data, had moved to Postmasburg in the intervening 10 years, in search of employment.

Our data shows that it is incorrect to assume that mining alone drives informal settlement development, though the pressure exerted by mining could well have been

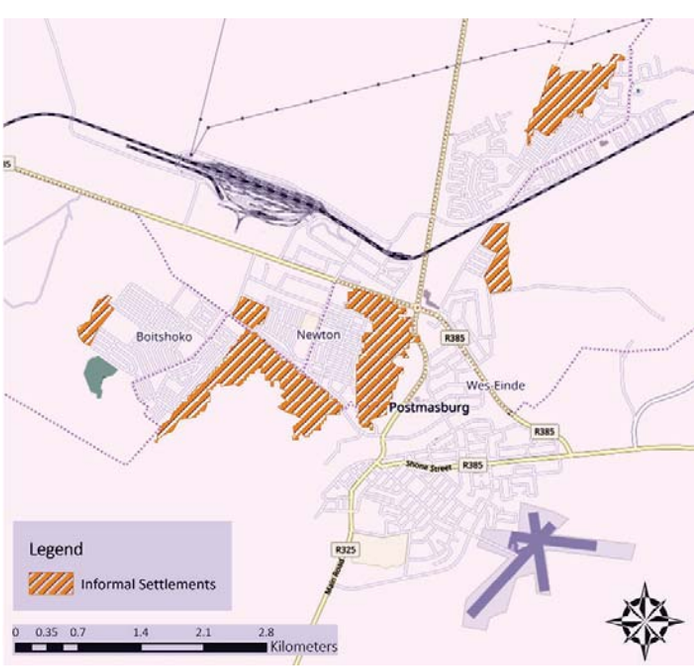

Figure 1—Location of informal settlements in Postmasburg in 2011

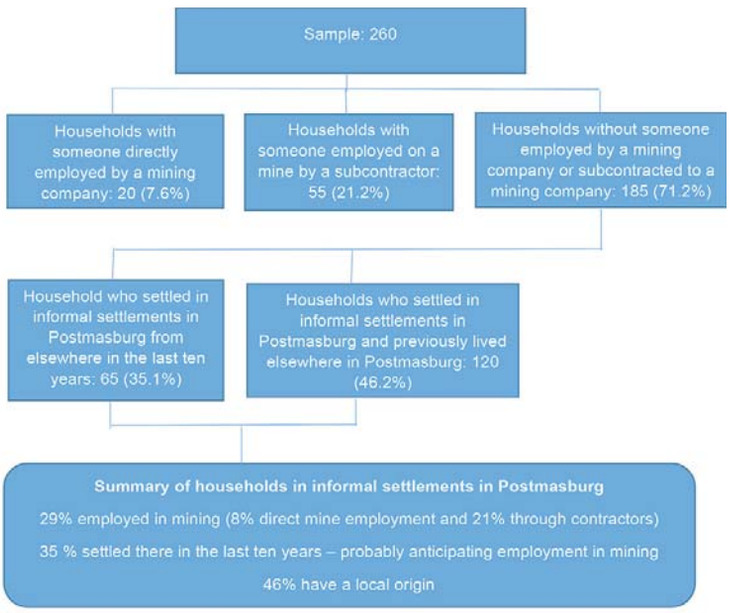

Figure 2—Overview of origin and employment of informal settlement dwellers in Postmasburg

instrumental in forming informal settlements in mining areas. Our data also shows that where mining does play a role in informal settlement formation, it is more likely to do so indirectly through contract workers or through people who have migrated to find employment than through those directly employed by the mines. Although the mines have largely provided their own employees with adequate housing, a small percentage of those directly employed by the companies still live in informal housing.

Migration trends

Given that mines historically employed migrant labour, we wanted to determine the migration trends of households living in informal houses. The overall patterns did not differ much from those of households living in formal houses, just over 28% of whom had previously lived in another town. The corresponding percentage for informal housing was 35%. Consequently, some migration was ascribable to expectations of employment.

When asked whether they had lived in Postmasburg 10 years earlier, 77% of the formal and 67% of the informal dwellers said they had indeed lived in Postmasburg at that time. These figures show that a higher degree of mobility was associated with the informal settlements (a relationship that is also statistically significant): thirty-three per cent of the household members living in informal houses at the time of the survey had lived elsewhere 10 years earlier.

Housing and demographic characteristics

The household demographics show that males constituted a slight majority in informal settlement households (61.8%). Conversely, 49.5% of members of formal households were male. Although this difference is not statistically significant, it does tend to show a predominance of male-dominated households in the informal settlements. Language differences did, however, exhibit statistically significant relationships: Afrikaans- and Setswana-speaking households (the two dominant local languages) were less likely to be living in an informal settlement than were Sesotho- and Xhosa-speaking households. As for education levels, the households in informal settlements had substantially fewer Grade 12 or post-Grade 12 qualifications. For example, while 32% of the residents in formal houses had a Grade 12 or a post-Grade 12 certificate, this was true of only 16% of those who lived in informal houses.

We found a substantial difference between the formal and informal housing profiles. The average number of rooms in informal houses was 2.15, compared with 5.5 in formal houses. Household size was slightly smaller in the informal houses (three persons per household) in comparison with 3.3 persons in formal houses. This means that there were 0.72 rooms per household member in the informal houses compared with 1.7 rooms per person in the formal houses. The non-mining households in the informal settlements had larger houses (on average 2.32 rooms per house) than did mining households (1.85). Overall, 78% of households in the informal settlements said they owned their houses. In this regard, there was not much difference between mining and non-mining households, with approximately 78% of both groups saying they owned the informal house. The current market value of these informal houses (at the time of the survey) was just over R16 000. But households linked to mining employment (either directly employed or as contract workers) had paid substantially more for their informal houses (R9216) than those not engaged in mining (R5800). This confirms that mining salaries do indeed create some demand for informal houses. Furthermore, 13.1% of the respondents living in informal houses said that they were paying rent. It is noteworthy that the average monthly rentals of non-miner households were higher (R713) than those of miner households (R550). Mine employment and informal housing seem to provide contract workers with a means of reducing expenditure and saving on living costs.

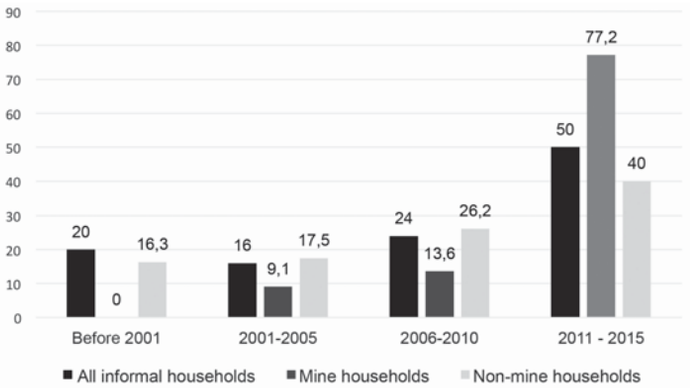

Figure 3—The percentage of households buying their informal houses in Postmasburg

As is to be expected, respondents from informal houses were much less satisfied than those in formal houses with the condition of their housing. Only 30% claimed to be happy, and 57% said that they were unhappy (the scale made provision for 'happy', 'satisfied', and 'unhappy'). The corresponding figures for those in formal houses were 51% 'happy' and 18% 'unhappy'. When we compared mining households with non-mining households, we found that 35% of the households employed in mining were happy, in comparison with only 27% of the non-mining households.

Possession of second homes was less common among households living in informal houses. Only seven (2.7%) of these respondents said they had a second home, compared with 9.5% of the households in formal houses. Three of the seven respondents living in informal houses were letting the second house and the remaining four said friends and family used the second home.

A substantial percentage of respondents in the informal settlement said they had bought their houses. Figure 3 shows that 50% of the informal houses were bought between 2011 and 2015. This coincides with the resettlement of employees from Beeshoek to Postmasburg and the construction and opening of the Kolomela mine. The fact that non-mine households constituted about 45% of households in informal settlements shows that local factors not connected with the mining industry also contributed to informal settlement development.

Access to infrastructure and services

As expected, informal households had substantially lower access to basic infrastructure than did formal households. Only 40% of informal houses had access to water on the stand and the remaining 60% had to use a public tap. However, only 9% of the respondents in informal houses said that they were paying the municipality for water – largely because the municipality has been unable to extend services to these areas. Respondents living in informal houses and who had mining employment were more likely to have to use a public tap (68%) than those who did not have mining employment (55%). Only 14% of the households in informal housing had water access further than 200 m away – the national benchmark in this regard. Once again, this percentage was slightly higher for mine-employed respondents. An interesting finding is that the informal housing respondents were less likely to say they had had water disruptions during the previous six months. Only 50% of the respondents living in informal houses said that they had had water disruptions, as against 70% of those living in formal houses.

Similar disparities featured in respect of sanitation. Just under 60% of the respondents in informal housing had either a bucket system or no system at all. Because recent research has shown that sharing a toilet facility has negative health implications (Marais and Cloete, 2014), we investigated the situation in Postmasburg. Having to share such a facility was slightly more common for respondents in informal (26%) than formal housing (23%). However, having to share a toilet facility was more common for miner households in formal (27%) than in informal housing (26%).

Only 31% of those living in informal houses had electricity. Power cuts because of non-payment were virtually absent in both informal and formal houses because most of them had prepaid electricity meters.

Only 10% of respondents living in informal houses said that waste removal took place, compared with 86% of respondents who lived in formal houses.

Economic status

As regards employment, there was not much difference between households in the informal and formal settlements. In the informal settlements, 41% of the adult residents were employed, compared with 43% in the formal settlements. More specific findings in respect of employment were that 73% of formal households and 63% of informal households had income from employment. Self-employment income in informal settlements (5.8%) was also lower than in the formal settlements (7.9%). Although households receiving an old-age grant were substantially fewer in informal houses (7%) than in formal houses (18%), substantially more households in informal houses reported receiving a child support grant (40%) than was the case in formal houses (25%). Interestingly enough, the informal households were less likely to receive donations or remittances from elsewhere (6%) than were formal households (10%).

There was a marked difference between formal and informal households' average monthly incomes: on average

Table I

Distribution of assets in Postmasburg

Number of assets	Formal housing		Informal housing		Informal: mine employed	
	n	%	n	%	n	%
0–3	39	5.2	169	64.5	63	68.5
4–7	177	23.8	63	24.0	22	23.9
9–11	430	57.8	28	10.7	7	7.6
12–15	98	13.2	2	0.8	0	0.
Total	744	100.0	262	100.0	92	100.0
Average	8.4	3.2	3.3			

just over R8200 for the former but below R4000 for the latter. The difference in average monthly household expenditure was similar: R6230 for formal households and R3320 for informal households. Similar disparities were found in income and expenditure for informal households both linked and not linked to the mining industry: income of R7501 and expenditure of R5248 for the former, and income of R2730 and expenditure of R2270 for the latter.

We also assessed informal and formal households' assets (Table I). In the absence of reliable income and expenditure data in surveys such as this, access to household assets usually provides a good indication of households' economic status. Of a list of 15 household assets, households in informal settlements owned an average of 3.2 compared with 8.4 in formal settlements. The housing assets of informal mining households were marginally more (3.3), which points to miners earning better salaries, though it also shows that the circumstances of informal housing do not support the accumulation of household assets.

Having asked about household income and assets, we next asked respondents two questions about how they ranked themselves in comparison to other households. First they had to rate their own income relative to other households on a five-point Likert scale, with 1 representing 'much above average income' and 5 'much below average income'. As could be expected, the informal respondents' average ranking of their own income at 3.9 was lower than the 3.2 ranking returned by formal dwellers. Also, the rankings by respondents from mining households were higher than those of non-mining households (3.6 compared with 4.1), which supports the income and expenditure disparities we have already mentioned.

The respondents were then asked to rank themselves on a six-rung ladder, with the first rung representing the poorest and the sixth the richest, at age 15, 10 years ago, and at the time of the survey, 2015 (Table II). The 2015 rating should be interpreted against the fact that the survey followed the slump in iron ore prices in June of that year. The overall economic climate in the town was grim, and the 2015 ratings are consequently all much lower than those of 2005. The fact that contract workers are generally the first to suffer the effects of mine downscaling is the main reason why residents in the informal houses, where more contract workers live, returned lower rankings than those living in formal houses.

Place attachment

Broadly, 'place attachment' refers to a positive relationship between people and places (Hummon, 1992). To measure place attachment, we asked respondents whether they wanted to stay on at their current location; whether they thought it was likely that a lost wallet containing R200 and contact details would be returned to them by someone from the community; and how they perceived the crime situation in the area. Given the prevailing insecurity of tenure in informal settlements, place attachment in these settlements is usually much stronger than in formal settlements – mainly because of the fear of being evicted. We found that 76% of respondents in the informal settlements had a very strong preference for staying on at their current location, compared to 57% of respondents from the formal settlements. As regards the likelihood of getting the wallet back if it was picked up by someone from the community, many more respondents in the informal (34%) than formal settlements (7%) considered it very likely. Strangely, however, more respondents from mining (46%) than non-mining households (27%) considered it very likely. This might be an indication that the non-mining households perceive the mining households as intruding into 'their' space and not part of their community.

To measure differences in perceptions of crime we again used a five-point Likert scale, with 5 representing a specific crime being a very common occurrence and 1 as never happening. Table III shows that in the 'burglaries, muggings or theft' category and the 'drug or alcohol abuse' category there were virtually no differences between the perceptions of respondents in formal and informal houses. However, for the four other categories we found that the informal dwellers considered themselves exposed to higher levels of those crimes. And further, informal dwellers not involved in mining employment considered themselves exposed to higher levels of crime than did informal dwellers engaged in mine-related employment. These findings strongly suggest that the highest level of social disruption is experienced by the informal dwellers who have been living in Postmasburg for a longer time and who are not employed in mining.

Table II

Postmasburg respondents' wealth ranking

Time of ranking	Formal housing	Informal housing
Aged 15	3.06	2.92
Ten years ago (2005)	2.92	2.54
At the time of the survey (2015)	2.76	2.39

Table III

Postmasburg respondents' perceptions of crime (Likert-scale ratings)

Crime	Formal housing	Informal housing	Informal non-mine households	Informal mine households
Burglaries, muggings, or thefts	3.61	3.68	3.87	3.44
Violence between members of the same household	2.77	3.20	3.37	2.90
Violence between members of different households	2.68	3.19	3.37	2.88
Gangsterism	3.43	3.78	4.05	3.30
Murder, shootings, or stabbings	2.86	3.32	3.52	2.98
Drug or alcohol abuse	4.22	4.22	4.42	3.87

Conclusion

Globally, mining activities exert pressure on existing settlements near mines. Since the early 1990s, mining companies have been withdrawing from the peripheral responsibilities involved in company towns and company-provided housing. Although changing labour regimes have, in some locations, reduced the industry's dependence on mining towns, in other cases they have led to the deterioration of local housing conditions. Since the 1990s, a larger degree of outsourcing has created a situation in which mining companies are no longer responsible for housing everyone working on the mine.

This paper has outlined the poor housing conditions in Postmasburg. The mushrooming of 2300 informal houses has been closely (though not exclusively) associated with mining development. We compared the residents in the informal houses with those in formal houses. We conclude with four observations, taking into account the international literature and the policy environment.

Firstly, our evidence shows that mining is directly and indirectly responsible for the massive growth in informal houses experienced in Postmasburg. In its direct manifestation, it is apparent from the evidence in this paper that mine-employed households have been buying informal housing structures since 2011. Indirectly, then, there is also evidence that most households with mine employment (nearly two-thirds) are employed on a contract basis at the mines. Outsourcing and mine contract work have thus definitely contributed to increased informal housing development in Postmasburg. There is also more indirect evidence in that people in informal settlements have migrated to Postmasburg in the hope of finding employment. In essence, the influx of people living in informal settlements is the result of a combination of mine employment, contract work, and the expectation of finding work at one of the two mines.

Secondly, we question whether the informal settlement development associated with mine contract work is necessarily a negative phenomenon. The limited duration of contract work means that mobility is an important factor for such households, and living in an informal house provides the necessary mobility. Further evidence that these contract workers themselves do not have long-term prospects of remaining in Postmasburg is demonstrated in that miners living in the informal settlements tend to have smaller households and invest less in their houses or the associated infrastructure – despite their receiving larger salaries and spending more money than do households in informal settlements who do not have mine employment. These factors all show that living in an informal house represents an attempt to manage specific housing needs without having to invest too heavily. Postmasburg's remote location means that finding non-mining employment there is unlikely, so the mobility that informal settlement allows is an asset to job seekers.

Thirdly, mining is not the only driving force in the formation of informal settlements. More than 50% of the households in Postmasburg's informal houses are not linked to mine development. The high levels of child support grants and the low levels of old age pensions paid to informal dwellers indicate that local household formation also contributes to informal settlement development. However, it is not clear whether the growth in informal settlements associated with mine development has sparked further informal settlement development among local people. What is clearer is that informal settlement development started long before the post-2011 mining boom.

Fourthly, the question arises as to what the most appropriate policy responses from mining companies and the municipality would be. Government policy emphasises the integration of mining communities and home ownership. But since our evidence shows that these informal settlements are dependent on mining, perhaps government emphasis on ownership should be challenged? The current policy on informal settlement upgrading provides for interim service delivery even though the land has not been proclaimed. This policy acknowledges that the mobility concerns of households do not necessarily end with the provision of ownership. Perhaps the important point here is that the mines have taken pains to provide both ownership and rental housing to their employees. However, neither the mines nor the municipality have attempted (within the existing policy framework) to address the plight of informal dwellers. The mines could well justify their active involvement from a health point of view. This could mean fewer households having to share toilet facilities and more households having good access to water and electricity, which should indeed contribute to better health and enhance productivity. In the final analysis, an approach that accommodates some form of informality would be a sensible response. It is, however, up to the municipality and the mining companies to make the mind-shift. One should also acknowledge the presence of serious capacity constraints at the municipal level, such as those related to technical ability and the ability of the governance structures to deal with the mines on an equal footing. Thus, even though the presence of mining ought to be an asset to local government in remote locations, this seldom occurs in practice.

Finally, we found that the informal dwellers not employed by the mines have experienced the highest degrees of social disruption in Postmasburg. Increases in the numbers of informal dwellers have been viewed most negatively by the original community and by those informal dwellers not directly associated with mine employment. This supports one of the most important findings of many social disruption studies, namely that disruption of place attachment usually has the most damaging effects on the poorest households.

References

Akbar, D., Rolfe, J., and Kabir, Z. 2011. Predicting impacts of major projects on housing prices in resource based towns with a case study application to Gladstone, Australia. *Resources Policy*, vol. 38. pp. 481–489.

Bryceson, D. and Mackinnon, D. 2013. Eureka and beyond: mining's impact on African urbanisation. *Journal of Contemporary African Studies*, vol. 30, no. 4. pp. 513–517.

Carrington, K., Hogg, R., and McIntosh, A. 2011. The resource boom's underbelly: criminological impacts of mining development. *Australian and New Zealand Journal of Criminology*, vol. 44, no. 3. pp. 335–354.

Chapman, R., Tonts, M., and Plummer, P. 2015. Resource development, local adjustment, and regional policy: resolving the problem of rapid growth in Pilbara, Western Australia. *Journal of Rural and Community Development*, vol. 9, no. 1. pp. 72–86.

Cirolia, L Görgens, T., Van Donk, M., Smit, W., and Drimie, S. 2016. Upgrading Informal Settlements in South Africa: A Partnership-based Approach. University of Cape Town Press, Cape Town.

Cloete, J. and Denoon-Stevens, S. 2018. Mineworker housing. *Mining and Community in South Africa: From Small Town to Iron Town*. Marais, L., Burger, P., and Van Rooyen, D. (eds.). Routledge, London. pp. 141–157.

Crawford, M. 1995. Building the Workingman's Paradise: The Design of American Company Towns. Verso, London.

Cronje, F. 2014. Digging for Development: The Mining Industry in South Africa and Its Role in Socio-economic Development. South African Institute for Race Relations, Johannesburg.

Crush, J. 1989. Accommodating black miners: home-ownership on the mines. *South African Review 5*. Ravan Press, Johannesburg. pp. 335–347.

Crush, J. 1992. The compound in post-apartheid South Africa. *Geographical Review*, vol. 82, no. 4. pp. 388–400.

Crush, J. 1994. Scripting the compound: power and space in the South African mining industry. *Environment and Planning D: Society and Space*, vol. 12, no. 3. pp. 301–324.

Department of Mineral Resources. 2010. Publication of the Amendment of the Broad-based Socio-economic Empowerment Charter for the South African Mining and Minerals Industry. Pretoria.

Department of Mineral Resources. 2016. Review of the Broad-based Black Economic-Empowerment Charter for the South African Mining and Minerals Industry. Government Printer, Pretoria.

Department of Minerals and Energy. 2002. Broad-based Socio-economic Empowerment Charter for South Africa's Mining Industry. Department of Minerals and Energy and Chamber of Mines, Johannesburg.

England, J. and Albrecht, S. 1984. Boomtowns and social disruption. *Rural Sociology*, vol. 49, no. 2. pp. 230–246.

Ennis, G., Tofa, M., and Finlayson, M. 2014. Open for business but at what cost? Housing issues in boomtown Darwin. *Australian Geographer*, vol. 45, no. 4. pp. 447–464.

Feagin, J. 1990. Extractive regions in developed countries: a comparative analysis of the oil capitals, Houston and Aberdeen. *Urban Affairs Quarterly*, vol. 25. pp. 591–619.

Grieve, S. and Haslam McKenzie, F. 2011. Local housing strategies: responding to the affordability crisis. *Planning Perspective in Western Australia: A Reader in Theory and Practice*. Alexander, G. S., and Hedgcock, D. (eds.). Freemantle Press, Freemantle. pp. 66–85.

Halseth, G. 1999. We came for the work': Situating employment migration in B.C.'s small, resource-based communities. *The Canadian Geographer*, vol. 43, no. 4. pp. 363–381.

Haslam McKenzie, F. 2010. Fly-in fly-out: the challenges of transient populations in rural landscapes. *Demographic Change in Australia's Rural Landscapes. Landscape Series,* vol. 12. pp. 353–374.

Haslam McKenzie, F. 2013. Delivering enduring benefits from a gas development: governance and planning challenges in remote Western *Australia. Australian Geographer*, vol. 44, no. 3. pp. 341–358.

Haslam McKenzie, F., Phillips, R., Rowley, S., Brereton, D., and Birdsall-Jones, C. 2009. Housing market dynamics in resource boom towns. *AHURI final report* no. 135, Australian Housing and Urban Research Institute Limited, Melbourne. http://www.ahuri.edu.au/publications/p80370/

Hummon, D. 1992. Community attachment: local sentiment and sense of place. *Place Attachment*. Altman, I. and Low, S. (eds.). Springer, New York. pp. 253–276.

IIED (International Institute for Environment and Development). 2002. Breaking New Ground: Mining, Minerals, and Sustainable Development. Earthscan, London.

Lawrie, M., Tonts, M., and Plummer, P. 2011. Boomtowns, resource dependence and socio-economic well-being. *Australian Geographer*, vol. 42, no. 2. pp. 139–164.

Littlewood, D. 2014. 'Cursed' communities? Corporate social responsibility (CSR), company towns and the mining industry in Namibia. *Journal of Business Ethics*, vol. 120. pp. 39–63.

Mabin, A. 1991. The dynamics of urbanisation since 1960. *Apartheid City in Transition*. Swilling, M., Humphries, R., and Shubane, K. (eds.). Oxford University Press, Cape Town. pp. 33–47.

Marais, L. 2013. The impact of mine downscaling on the Free State Goldfields. *Urban Forum*, vol. 24. pp. 503–521.

Marais, L. and Cloete, J. 2014. "Dying to get a house?" The health outcomes of the South African low-income housing programme. *Habitat International*, vol 43, no 1. pp. 48–60.

Marais, L. and Venter, A. 2006. Hating the compound, but … Mineworker housing needs in post-apartheid South Africa. *Africa Insight*, vol. 36, no. 1. pp 53–62.

Marais, L., van Rooyen, D., Burger, P., Lenka, M., Cloete, J., Denoon-Stevens, S., Mocwagae, K., Jacobs, M., and Riet, J. 2017. The background to the Postmasburg study. *Mining and Community in South Africa: From Small Town to Iron Town*. Marais, L., Burger, P., and Van Rooyen, D. (eds.). Routledge, London. pp. 5–22.

Negi, R. 2014. 'Solwezi mabanga': ambivalent developments on Zambia's new mining frontier. *Journal of Southern African Studies*, vol. 40, no. 5. pp. 999–1013.

Obeng-Odoom, F. 2014. Oiling the Urban Economy: Land, Labour Capital and the State in Sekondi-Takoradi, Ghana. Routledge, London.

Rolfe, J., Miles, B., Lockie, S., and Ivanova, G. 2007. Lessons from the social and economic impacts of the mining boom in the Bowen Basin, 2004–2006. *Australasian Journal of Regional Studies*, vol. 13, no. 2. pp. 134–153.

Rubin, M. and Harrison, P. 2016. An uneasy symbiosis: mining and informal settlement in South Africa, with particular reference to the Platinum Belt in North West Province. *Upgrading Informal Settlements in South Africa: A Partnership-based Approach*. Cirolia, L., Görgens, T., van Donk, M., Smit, W., and Drimie, S. (eds.). University of Cape Town Press, Cape Town. pp. 145–173.

Statistics South Africa. 2016. Census data. Statistics South Africa, Pretoria.

Stewart, T. and Drewes, E. 2018. The Khumani approach to homeownership in Postmasburg. *Mining and Community in South Africa: From Small Town to Iron Town*. Marais, L., Burger, P., and Van Rooyen, D. (eds). Routledge, London. pp. 141–157.

Tomlinson, M. 2007. The development of a low-income housing finance sector in South Africa: Have we finally found a way forward? *Habitat International*, vol. 31, no. 1. pp. 77–86.

Tshangana, M. 2015. Selected Committee Presentation on the Revitalisation of Distressed Mining Towns Programme. National Department of Human Settlements, Pretoria. ◆

TAILING STORAGE CONFERENCE 2019

Investing in a Sustainable Future

17–18 October 2019
Johannesburg

BACKGROUND

Engineers designing tailing storage facilities are faced with a number of new challenges resulting from the encroachment of both formal and informal housing projects, legislation pertaining to water usage and pollution control, shortages of water for processing, and the requirements for tailing dam closure.

This has resulted in the introduction of new designs for construction of more stable dams, alternative deposition methods, the introduction of non-permeable linings, and the capping of dams to encourage rehabilitation and minimize dust pollution. The shortage of water in Southern Africa has necessitated changes in dam design to minimize water usage by either reducing the amount of water to the dam or increasing the amount of water recovered.

Understandably, new legislation has been passed to regulate the construction and operation of tailing storage facilities. This knowledge resides with few specialists in the industry, and the operators on the mines are sometimes unaware of the consequences of these changes for their operations. In many cases the operations engineer has been misinformed and the need has arisen to get the parties together to discuss the implications of the changes.

Reprocessing of existing tailings adds to the complexity of operating a tailing storage facility, and many new operators have little or no reference material to assist them when planning a retreatment project.

Ultimately, the design must be focused on the future closure of the facility, and this has been further complicated by changes in the minimum environmental requirements.

Industry has requested a tailing seminar for interested and affected parties to share ideas and solutions with their peers. We invite all operations, designers, technology providers, and legislators to get together for what could be a very informative and successful event.

SAIMM
THE SOUTHERN AFRICAN INSTITUTE OF MINING AND METALLURGY

OBJECTIVE

This will cover a broad range of topics including:

- Latest trends in tailing disposal
- Environmental considerations and latest trends in tailing facility closure
- Minimizing of dust pollution
- Maximizing water recovery
- Legal considerations in operating a tailing storage facility
- Designing a tailings storage facility
- Permitting and application for licences
- Current legislation
- Re-mining of tailing dams – design and operation
- Rehabilitation of land following remining

WHO SHOULD ATTEND

- Senior and operational management of mines
- Engineers responsible for tailing facility management
- Regional and national officials from DoE, DMR, DWA, and DEA
- Companies and individuals offering tailings processing solutions
- Researchers
- Environmentalists and NGO's
- Legal representatives from mining companies

Key Dates:

Submission of Abstracts:	1 May 2019
Submission of Papers:	19 June 2019
Conference:	17–18 October 2019

Conference Announcement

For further information contact: Camielah Jardine
Head of Conferencing • Saimm • P O Box 61127, Marshalltown 2107
Tel: (011) 834-1273/7 • Fax: (011) 833-8156 or (011) 838-5923
E-mail: camielah@saimm.co.za • Website: http://www.saimm.co.za

http://dx.doi.org/10.17159/2411-9717/2018/v118n10a13

A modified Wipfrag program for determining muckpile fragmentation

by A. Tosun

Synopsis

The size distribution of the muckpile formed as a result of open pit blasting operations has a considerable effect on the efficiency of loading, hauling, and crushing. Various researchers have developed specialized computer software that uses image analysis methods for determining the size distribution of the muckpile. However, these methods have some limitations. One of the most important of these limitations is that the very fine fragments in the muckpile cannot be used in the size distribution calculation. In this study, 18 test blasts in total were carried out in two limestone quarries belonging to Batıçim Corp. in Izmir, Turkey. A new model was developed in order to ensure that very fine fragments are used in the size distribution calculation. The size distributions of the test blasts were calculated by both the Wipfrag computer program and the new model. Correlations were established between the muckpile size distributions determined by both methods and the parameters determining the efficiency of the loader.

Keywords
Muckpile size distribution, blast efficiency, Wipfrag program.

Introduction

The size distribution of the muckpile formed as a result of open pit blasting operations has a considerable effect on the efficiency of loading, hauling, and crushing. Various researchers have established certain correlations for predicting the efficiency of the operations according to the muckpile size distribution so that production can be carried out economically (Tunstall and Bearman, 1997; Nielsen and Kristiansen, 1996; Workman and Eloranta, 2004; Michaud and Blanchet, 1996; Frimpong, Kabongo, and Davies, 1996; Osanloo and Hekmat, 2005; Molotilov *et al.*, 2010). In these studies, the 50% passing size (X_{50}) is generally used. These methods rely on the correct measurement of the size distribution of the muckpile formed by the blast. The most reliable measurement method would be to subject the entire muckpile to a sieve analysis, but this is obviously impracticable. Therefore, computational method based on image analysis have been developed. These include IPACS (Dahlhielm, 1996), Tucips (Havermann and Vogt, 1996), Fragscan (Schleifer and Tessier, 1996), Cias (Downs and Kettunen, 1996), GoldSize (Kleine annd Cameron, 1996), Wipfrag (Maerz, Palangio, and Franklin, 1996), Split Desktop (Kemeny, 1994), PowerSieve (Chung and Noy, 1996), and Fragalyst (Raina *et al.*, 2002). In these methods, the size limits of the fragments forming the material are determined by image analysis on photographs of the muckpile. However, the computer software has some limitations. It does not take into account the third dimension of the muckpile, nor the size distribution of very fine fragments. In particular, the fragment size ranges below 2.5 to 3 cm cannot be determined, and therefore these cannot be included in the muckpile size distribution. However, the muckpile formed by a bench blast contains a wide range of particle sizes (Tosun *et al.*, 2015).

In this study, a new model was developed in order to ensure that the very fine fragments in the muckpile are included in the size distribution calculation. Eighteen test blasts in total; eight at the Arkavadi limestone quarry and ten at the Upper Aravadi limestone quarry, both belonging to Batıçim Corp. in Izmir,Turkey, were carried out. Initially, the muckpile size distributions from the test blasts (X_{50}) were determined by the Wipfrag computer program. The size distributions were then calculated for each blast using a new model, which incorporates the very fine fragments. In order to determine which method gives better results, the parameters determining the loading efficiency were used. Many researchers have emphasised that the loading efficiency of the loader depends directly on the muckpile size distribution (Michaud and Blanchet, 1996; Frimpong, Kabongo, and Davies, 1996; Osanloo and Hekmat, 2005; Molotilov *et al.*, 2010). Total pressure values measured in the hydraulic

* *Dokuz Eylul University, Department of Mining Engineering and Bergama vocational school Bergama-Izmir/Turkey.*

 ISSN 2225-6253. Paper received Aug. 2017; revised paper received Jun. 2018.

pistons of the loader and the average fuel consumption of the loader were used as the parameters determining the loading efficiency. Correlations were examined between the muckpile size distribution determined both by the Wipfrag computer program and according to the new model with these loader parameters.

Determination of the muckpile size distribution by the Wipfrag program

The muckpile was divided into sections and photographs were taken of the separated sections. The size ranges of the fragments forming the material were determined by image analysis of the photographs using the Wipfrag program. The size distribution representing the entire muckpile was determined by combining the size distributions obtained from each photograph. For example, nine images in total were obtained by dividing the muckpile of the second test blast in the Arkavadi limestone quarry into sections and each of them was subjected to fragment size analysis using Wipfrag (Figure 1).

A total of 3496 fragments were included in the examination by processing nine images taken from the muckpile, their size distribution graphs were determined, and the average fragment size distribution of the muckpile was obtained by combining the nine graphs into a single graph. The X_{50} value from this graph was calculated as 23.40 cm. The results obtained from the size distribution analyses of this muckpile are given in Tables I and II and Figure 2.

Table III presents the fragment size values (X_{50}) of the blast tests. The size value of the eighth test blast carried out in the Upper Aravadi limestone quarry could not be determined due to a data storage problem.

Determination of the muckpile size distribution by the new model

The Wipfrag software calculates the muckpile size distribution according to the number of fragments whose limits can be determined. However, it is not possible to calculate the distribution for fragments in the very fine size range, that is, under 2–3 cm. Even if this were possible, the image would contain millions of fragments. This limitation will result in a biased calculation of the size distribution of the entire muckpile.

A new model was developed in order to ensure that very fine fragments are included in the determination of the size distribution too. Very fine fragments below 2.5–3.0 cm in each photographic image taken over the muckpile in this model are blacked out, as seen in Figure 3, since their limits cannot be determined. The percentile area of these blacked-

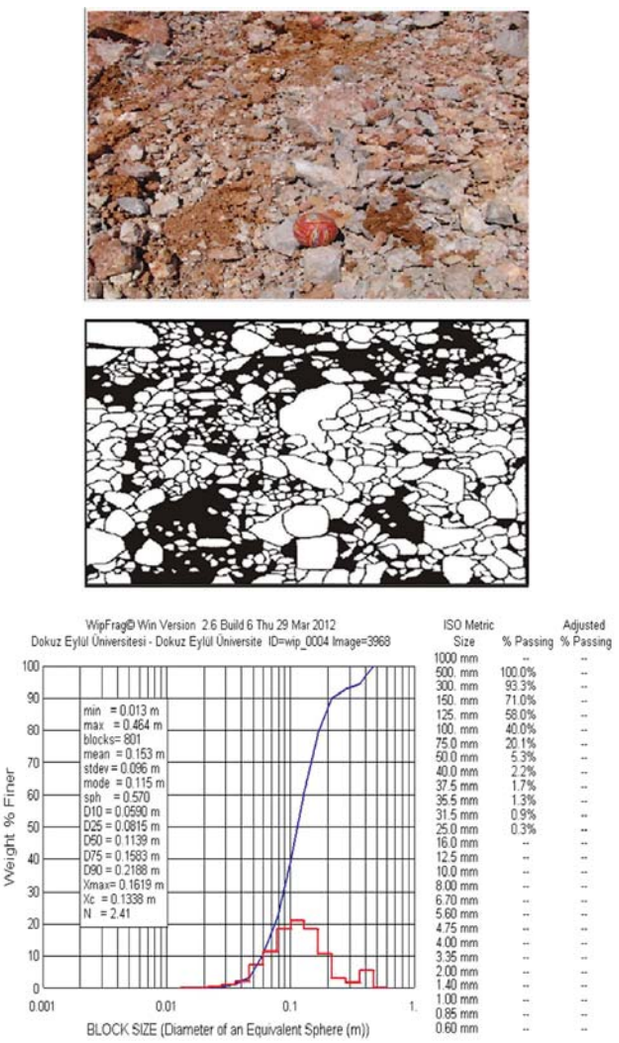

Figure 1—Image analysis phases of a photograph of a portion of the second muckpile blast carried out at the Arkavadi limestone quarry

Table I

The fragment size values derived from a photograph of the second test blast carried out at the Arkavadi limestone quarry

Photo no.	The analysis results provided by the Wipfrag software			
	Minimum fragment size (mm.)	Maximum fragment size (mm.)	X_{50} (mm)	Number of fragment
1	13	1668	417.7	379
2	13	774	192.5	609
3	13	774	297.1	343
4	13	774	140.6	670
5	13	464	113.9	801
6	13	774	299.4	300
7	10	599	373.2	156
8	17	1668	526.2	165
9	17	2154	905.2	73

Table II

The average percentage distribution of nine muckpile images according to fragment size from the second test blast carried out at the Arkavadi limestone quarry

Fragment size (mm)	Weighted (%)
1000	95.43
500	80.85
300	66.35
150	41.16
125	32.98
100	21.80
75	11.07
50	2.72
40	1.09
37.5	0.81
35.5	0.57
31.5	0.38
25	0.11

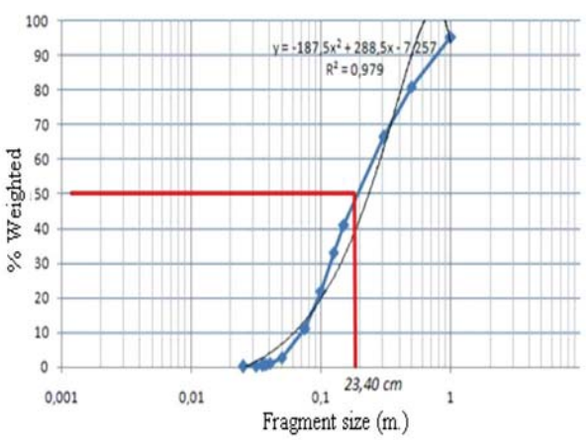

Figure 2—The average fragment size distribution chart from the second test blast carried out at the Arkavadi limestone quarry

out fine fragments was calculated for each image taken over the muckpile. Subtracting the percentile area of blacked-out fine fragments from 100 gives the percentile area of the fragments whose limits can be determined. The weighted average and new size distribution values are then found using the values of average percentile area in the images and the size distribution of the fragments and the fine fragments whose limits can be determined and therefore are used in the calculation of the size distribution (Equation [1]). The size below maximum of very fine fragments that are not used in the size distribution calculation can be seen from the size analysis results determined by Wipfrag. Very fine fragments in the muckpile are not handled according to the number of fragments, but according to the area of the image that they cover.

$$MW_{50} = \frac{(X_{50} * p) + (f * s)}{100} \quad [1]$$

MW_{50} = Average fragment size calculated according to the new model (cm)

X_{50} = 50% passing size of the material calculated by the Wipfrag method (cm)

f = Fragment size of upper limit of fines (cm)

p = Average area of the fragments whose limits can be determined (%)

s = Average area of the fragments whose limits cannot be determined (%)

Table III

Muckpile fragmentation values calculated according to the Wipfrag software (X_{50})

Test no.	X_{50}, cm
Arkavadi limestone quarry	
1	21.01
2	23.40
3	24.62
4	22.82
5	23.52
6	24.78
7	21.20
8	19.90
Upper Aravadi limestone quarry	
1	27.53
2	23.58
3	27.28
4	23.03
5	22.93
6	24.74
7	28.26
8	-
9	25.02
10	31.34

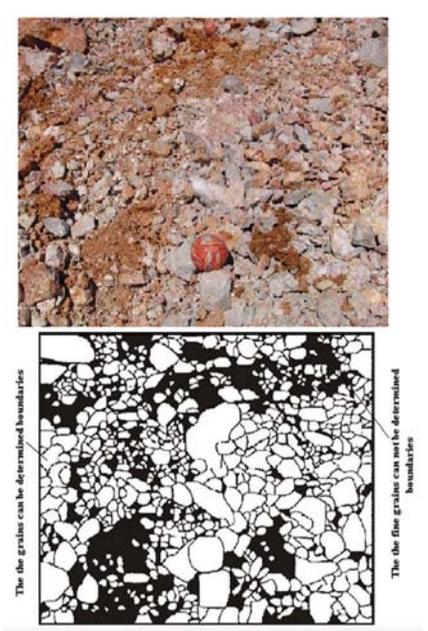

Figure 3—The fine fragments and the fragments whose size can be determined, from a photograph of the second test blast carried out at the Arkavadi limestone quarry

The Wipfrag size analysis program does not use fragments larger than 1 m in its calculation of size distribution. Therefore, the real values were found on the

basis of the fragments used in the size analysis calculation with the Wipfrag size analysis program by extracting the fragments larger than 1 m in each photograph taken over the muckpile. It was accepted that the > 1 m fragments were formed as a result of drilling of hard rocks.

For example, nine images were taken over the muckpile in a manner representing the entire muckpile in order to determine the average size distribution of the muckpile formed as a result of the second test blast at the Arkavadi limestone quarry. The percentile areas of fine fragments whose limits cannot be determined and fragments whose limits can be determined in each image were calculated for each image (Table IV).

It was understood from the Wipfrag dimensional analysis program that the fine fragments in this test blast are those smaller than 2 cm. Afterwards, the fragment size value (MW_{50}) from which 50% of the new material is smaller was calculated by means of Equation [1].

$$MW_{50} = \frac{(23{,}4*75{,}83)+2*24{,}17}{100} = 18.23 \text{ cm found}$$

Table V presents the fragment size values (MW_{50}) of the test blasts according to new model. The MW_{50} of the eighth test blast carried out in the Upper Aravadi limestone quarry could not be determined due to a data storage problem.

Determination of loader efficiency

Loading at the Arkavadi limestone quarry is carried out by a PC 450 LC 45 t backhoe hydraulic loader with a bucket capacity of 3 m³, and at the Upper Aravadi limestone quarry by a PC 550 LC 55 t backhoe hydraulic loader with a bucket capacity of 3.6 m³.

To determine the loader efficiency, the oil pressure in the hydraulic pistons of the loader and the average fuel consumption during loading were used. Hydraulic pressure was measured in the front pump, back pump, arm closure, and bucket closure pistons of the loader. The pressures can be monitored instantaneously as numerical values from the monitor in the cabin of the loader. Image processing was used for recording the instantaneous image data on the loader monitor.

Table V

Muckpile fragmentation values calculated according to the new model (MW_{50})

Test no.	MW_{50}, cm
Arkavadi limestone quarry	
1	16.73
2	18.23
3	18.19
4	18.80
5	16.34
6	15.15
7	15.73
8	16.40
Upper Aravadi limestone quarry	
1	18.60
2	19.70
3	19.20
4	17.35
5	16.70
6	17.10
7	19.10
8	-
9	18.90
10	17.80

Electronic (digital) image data can be transformed into numeric data that represents the pressures in the front pump, back pump, arm closure, and bucket closure pistons of the loader by using special software (Tosun *et al.*, 2012). Except for the first test blast at the Arkavadi limestone quarry, the pressures were recorded in a computer environment during completion of the loading of blasted material (Table VI). Hydraulic pressure values during loading of the first test blast at Arkavadi could not be recorded due to certain problems experienced on-site.

The average amount of fuel consumed by the loader while loading the muckpile will vary depending on the size distribution. Fuel consumption values can be monitored from the data tracking monitor on the loader. Before beginning to load the material, the fuel consumption value was reset from

Table IV

The calculating muckpile fragmentation values according to both the Wipfrag software (X_{50}) and the new model (MW_{50}) for the second test blast carried out at the Arkavadi limestone quarry

Photo no.	Area of fragments that can be determined (%)	Area of fragments that cannot be determined (%)	Muckpile fragmentation value calculated by Wipfrag (X_{50}, cm)	Muckpile fragmentation value calculated according to the new model (MW_{50}, cm)
1	76.05	23.95	23.40	18.23
2	73.67	26.33		
3	79.07	20.93		
4	63.96	36.04		
5	57.93	42.07		
6	82.21	17.79		
7	83.31	16.69		
8	83.16	16.84		
9	83.14	16.86		
Average	75.83	24.17		

the loader data tracking monitor. After the completion of loading, the fuel consumption values were measured as an average for each blast (Table VI). The pressures in the hydraulic pistons of the loader and the amounts of material loaded for each blast are also shown in Table VI.

Evaluation

The correlations between the muckpile size distribution calculated both by the Wipfrag program and according to the new model with total hydraulic pressure in the loader pistons of the loader and the average fuel consumption during loading were examined (Table VII, Figures 4–11). Since different loaders are used at Arkavadi and Upper Aravadi, the correlations were determined separately for each site.

The muckpile size distribution (X_{50}) calculated by the Wipfrag program shows poor correlation with the parameters determining loader efficiency, while very meaningful corrrelations are found between the parameters and the size

Table VI

The data used for determining loader efficiency

Test no.	Loader hydraulic pressures (kg/cm²)				Total	Total number of data	Amount of loaded material (t)	Loader fuel consumption (l/h)
	Front pump	Back pump	Arm closure	Bucket closure				
Arkavadi limestone quarry								
1	-	-	-	-	-	-	5512.33	27.10
2	192.46	185.83	12.09	14.67	405.04	138712	4156.98	37.70
3	181.20	183.83	5.56	23.42	394.02	13812	3721.76	33.80
4	189.24	193.02	9.74	8.09	400.10	12060	2447.66	34.90
5	172.72	177.19	7.80	10.83	368.54	91048	3167.98	27.80
6	161.10	160.85	4.83	9.42	336.21	146380	3814.88	23.90
7	165.56	169.85	7.31	10.69	353.41	85828	5987.43	25.30
8	169.82	176.69	5.53	8.10	360.14	59060	2272.54	30.70
Upper Aravadi limestone quarry								
1	149.39	152.43	7.21	6.44	315.47	162804	2343.94	36.20
2	152.27	156.58	10.00	14.90	333.70	240232	2350.10	39.30
3	149.11	161.90	8.13	6.72	325.90	241640	7816.74	38.70
4	128.13	140.73	6.69	6.53	282.09	447308	4965.16	34.70
5	116.60	119.19	5.08	4.26	245.12	188868	995.80	29.90
6	137.76	139.52	7.86	5.35	290.49	149328	2084.94	35.10
7	147.60	151.61	7.53	15.23	321.97	85172	5861.80	37.10
8	146.34	150.66	8.62	6.58	312.20	146652	1673.46	35.80
9	147.99	160.10	7.39	8.65	324.10	197844	2653.40	38.30
10	140.05	148.13	6.79	5.91	300.88	234232	2305.12	35.00

Table VII

The data determining loader efficiency and muckpile fragmentation values calculated according to both the Wipfrag software (X_{50}) and the new model (MW_{50})

Test no.	Loader hydraulic pressures (kg/cm²)				Total	Loader fuel consumption (l/h)	Muckpile fragmentation calculated according to the Wipfrag (X_{50},cm)	Muckpile fragmentation calculated according to the new model (MW_{50},cm)
	Front pump	Back pump	Arm closure	Bucket closure				
Arkavadi limestone quarry								
1	-	-	-	-	-	27.10	21.01	16.73
2	192.46	185.83	12.09	14.67	405.04	37.70	23.40	18.23
3	181.20	183.83	5.56	23.42	394.02	33.80	24.62	18.19
4	189.24	193.02	9.74	8.09	400.10	34.90	22.82	18.80
5	172.72	177.19	7.80	10.83	368.54	27.80	23.52	16.34
6	161.10	160.85	4.83	9.42	336.21	23.90	24.78	15.15
7	165.56	169.85	7.31	10.69	353.41	25.30	21.20	15.73
8	169.82	176.69	5.53	8.10	360.14	30.70	19.90	16.40
Upper Aravadi limestone quarry								
1	149.39	152.43	7.21	6.44	315.47	36.20	27.53	18.60
2	152.27	156.58	10.00	14.90	333.70	39.30	23.58	19.70
3	149.11	161.90	8.13	6.72	325.90	38.70	27.28	19.20
4	128.13	140.73	6.69	6.53	282.09	34.70	23.03	17.35
5	116.60	119.19	5.08	4.26	245.12	29.90	22.93	16.70
6	137.76	139.52	7.86	5.35	290.49	35.10	24.74	17.10
7	147.60	151.61	7.53	15.23	321.97	37.10	28.26	19.10
8	146.34	150.66	8.62	6.58	312.20	35.80	-	-
9	147.99	160.10	7.39	8.65	324.10	38.30	25.02	18.90
10	140.05	148.13	6.79	5.91	300.88	35.00	31.34	17.80

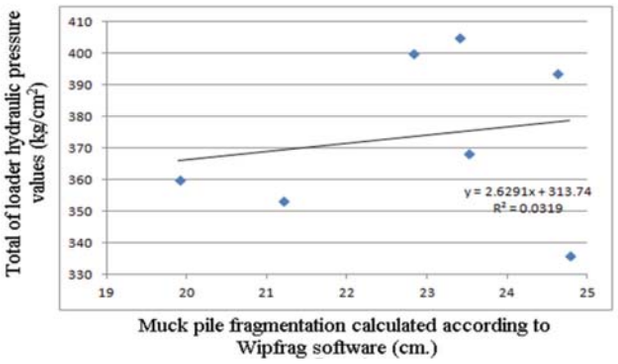

Figure 4—Relationship between total loader hydraulic pressure values and muckpile fragmentation calculated according to Wipfrag (X_{50}) for the Arkavadi limestone quarry

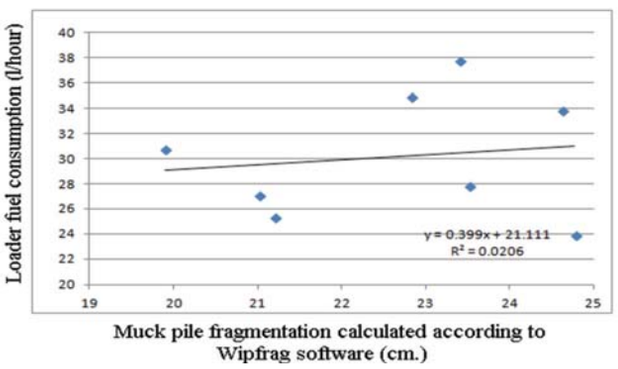

Figure 5—Relationship between loader fuel consumption and muckpile fragmentation calculated according to the Wipfrag software (X_{50}) for the Arkavadi limestone quarry

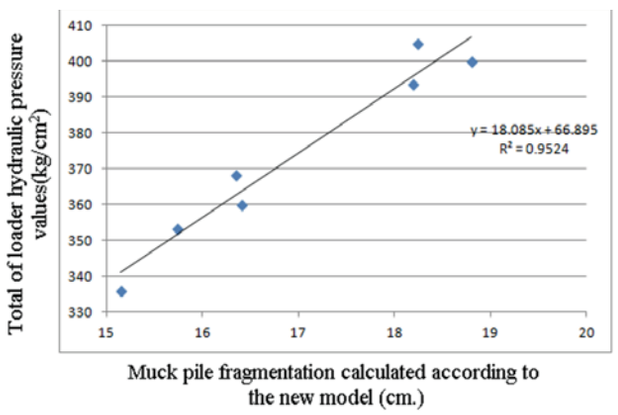

Figure 6—Relationship between total loader hydraulic pressure values and muckpile fragmentation calculated according to the new model (MW_{50}) for the Arkavadi limestone quarry

distribution (MW_{50}) determined according to the new model, in which the very fine fragments are also evaluated.

Total hydraulic pressure in the pistons of the loader and the average fuel consumption by the loader used in the determination of the loader efficiency according to the muckpile size distribution are the net data where no error occurred. Therefore, it is understood that the new model circumvents certain deficiencies of the Wipfrag computer program used in the determination of the muckpile size distribution.

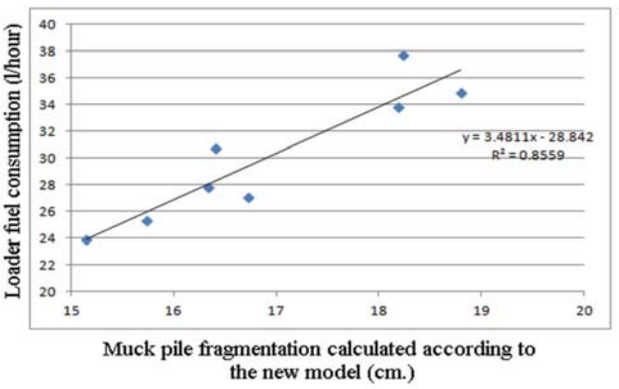

Figure 7—Relationship between loader fuel consumption and muckpile fragmentation calculated according to the new model (MW_{50}) for the Arkavadi limestone quarry

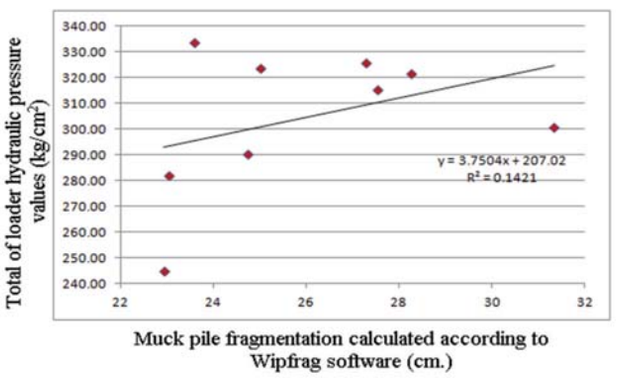

Figure 8—Relationship between total loader hydraulic pressure values and muckpile fragmentation calculated according to the Wipfrag software (X_{50}) for the Upper Aravadi limestone quarry

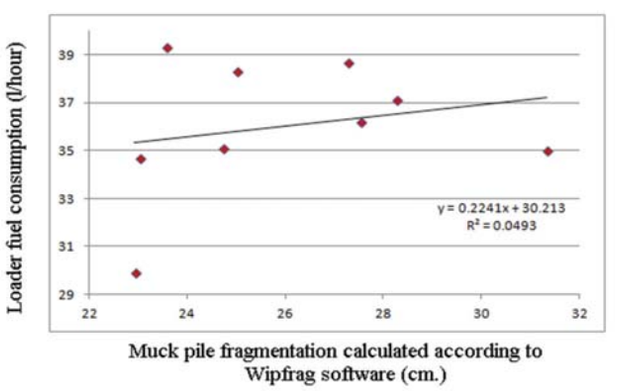

Figure 9—Relationship between loader fuel consumption and muck pile fragmentation calculated according to the Wipfrag software (X_{50}) for the Upper Aravadi limestone quarry

Conclusion

In this study, 18 test blasts in total; eight at the Arkavadi limestone quarry and ten at the Upper Aravadi limestone quarry belonging to Batıçim Corp. in Izmir, Turkey, were carried out. Muckpile size distribution values were calculated for each blast using the Wipfrag computer program (X_{50}) and a new model which also evaluated very fine fragments in the

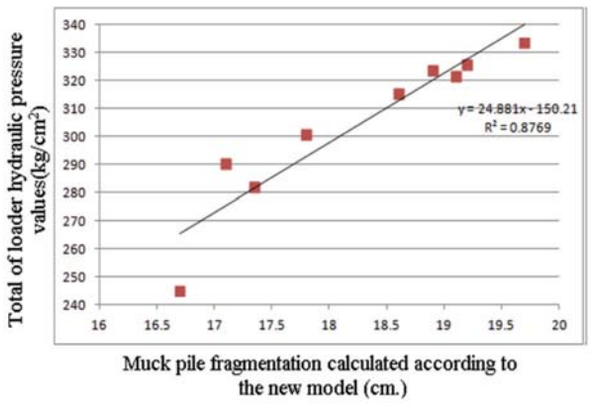

Figure 10—Relationship between total loader hydraulic pressure values and muckpile fragmentation calculated according to the new model (MW_{50}) for the Upper Aravadi limestone quarry

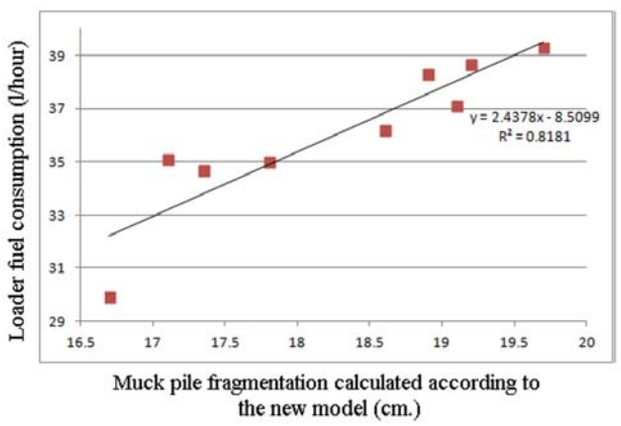

Figure 11—Relationship between loader fuel consumption and muckpile fragmentation calculated according to the new model (MW_{50}) for the Upper Aravadi limestone quarry

muckpile. The relationships between the muckpile size distributions calculated by both methods were compared with the total hydraulic pressure values in the hydraulic pistons of the loader and the average fuel consumptions by the loader, which are the parameters determining the loader efficiency, were examined. No relationship whatsoever was determined between the loader efficiency and the muckpile size distribution (X_{50}) by the Wipfrag computer program, but very meaningful relationships were seen between the parameters and the size distribution according to the new model.

Acknowledgments

I wish to thank the Scientific and Technological Research Council of Turkey (TUBITAK) for providing funding for this research project, and Western Anatolia Cement Factory for their help during field studies.

References

Chung, S.H. and Noy, M.J. 1996. Experience in fragmentation control. *Measurement of Blast Fragmentation: Proceedings of the Fragblast-5 Workshop on Measurement of Blast Fragmentation*, Montreal, Quebec, Canada, 23-24 August 1996. Franklin, J.A. and Katsabanis, P.D. (eds.). Balkema, Rotterdam. pp. 247–252.

Dahlhielm, S. 1996. Industrial applications of image analysis – The IPACS System. *Measurement of Blast Fragmentation: Proceedings of the Fragblast-5 Workshop on Measurement of Blast Fragmentation*, Montreal, Quebec, Canada, 23-24 August 1996. Franklin, J.A. and and Katsabanis, P.D. (eds.). Balkema, Rotterdam. pp. 67–71.

Downs, D.C. 1996. Kettunen B E. On-line fragmentation measurement utilizing the CIAS system. *Measurement of Blast Fragmentation: Proceedings of the Fragblast-5 Workshop on Measurement of Blast Fragmentation*, Montreal, Quebec, Canada, 23-24 August 1996. Franklin, J.A. and Katsabanis, P.D. (eds). Balkema, Rotterdam. pp. 79–82.

Frimpong, M., Kabongo, K., and Davies, C. 1996. Diggability in a measure of dragline effectiveness and productivity. *Proceedings of the 22nd Annual Conference on Explosives and Blast Techniques*. International Society of Explosives Engineers. pp. 95–104.

Havermann, T. and Vogt, W. 1996. Tucips – A System for the estimation of fragmentation after production blasts. *Measurement of Blast Fragmentation: Proceedings of the Fragblast-5 Workshop on Measurement of Blast Fragmentation, Montreal*, Quebec, Canada, 23–24 August 1996. Franklin, J.A. and Katsabanis, P.D. (eds). Balkema, Rotterdam. pp. 59–65.

Kemeny, J.M. 1994. Practical technique for determining the size distribution of blasted benches waste dump and heap leach sites. *Mining Engineering*, vol. 46, no. 11. pp. 1281–1284.

Kleine, T.H. 1996. Cameron A R. blast fragmentation measurement using Goldsize. *Measurement of Blast Fragmentation: Proceedings of the Fragblast-5 Workshop on Measurement of Blast Fragmentation*, Montreal, Quebec, Canada, 23–24 August 1996. Franklin, J.A. and Katsabanis, P.D. (eds). Balkema, Rotterdam. pp. 83–89.

Maerz, N.H., Palangio, T.C., and Franklin, J.A. 1996. The Wipfrag image based granulometry system. *Measurement of Blast Fragmentation: Proceedings of the Fragblast-5 Workshop on Measurement of Blast Fragmentation*, Montreal, Quebec, Canada, 23–24 August 1996. Franklin, J.A. and Katsabanis P.D. (eds). Balkema, Rotterdam. pp. 91–98.

Michaud, P.R. and Blanchet, J.Y. 1996. Establishing a quantitative relation between post blast fragmentation and mine productivity: a case study. *Measurement of Blast Fragmentation: Proceedings of the 5th International Symposium on Rock Fragmentation by Blast*, Montreal, Quebec, Canada, 23–24 August 1996. Franklin, J.A. and Katsabanis, P.D. (eds.). Balkema, Rotterdam. pp. 386–396.

Molotilov, S.G., Cheskidov, V.I., Norri, V.K., Botvinnik, A.A., and. Il'bul'din, D. 2010. Methodical principles for planning the mining and loading equipment capacity for open cast mining with the use of dumpers, Part III: Service capacity determination. *Journal of Mining Science*, vol. 46, no. 1. pp 38–49.

Nielsen, K. and Kristiansen, J. 1996. Blast-crushing-grinding optimization of an integrated comminution system. *Proceedings of the 5th International Symposium on Rock Fragmentation by Blast*. Mohanty, B. (ed.). Balkema, Rotterdam. pp. 269–278

Osanloo, M. and Hekmat, A. 2005. Prediction of shovel productivity in the Gol-E-Gohar mine. *Journal of Mining Science*, vol. 41, no 2. pp. 177–184.

Raina, A.K., Choudhury, P.B., Ramulu, M., Chrakraborty, A.K., and Dudhankar, A.S. 2002. Fragalyst – An indigenous digital image analysis system for fragment size measurement in mines. *Journal of the Geological Society of India*, vol. 59. pp. 561–569.

Schleifer, J. and Tessier, B. 1996. Fragscan, a. tool to measure fragmentation of blasted rock. *Measurement of Blast Fragmentation: Proceedings of the Fragblast-5 Workshop on Measurement of Blast Fragmentation*, Montreal, Quebec, Canada, 23-24 August 1996. Franklin, J.A. and Katsabanis, P.D. (eds.). pp. 73–78.

Tunstall, A.M. and Bearman, R.A. 1997. Influence of fragmentation on crushing performance. *Mining Engineering*, vol. 49. pp. 65–70.

Tosun, A., Konak, G., Karakus, D., and Onur, A.H. 2012. Determination of loader efficiency with hydraulic pressure values. *Proceedings of the International Multidisciplinary Scientific Geoconference*. Curran Associates. pp. 531–538.

Tosun, A., Konak, G., Öngen, T., and Onur, A.H. 2015. Patlatma sonucu olusan yıgının boyut dagılımının belirlenmesinin arastırılması, 7. Ulusal Kırmatas Sempozyumu (National Kırmatas Symposium).

Workman, L. and Eloranta, J. 2004. The effects of blast on crushing and grinding efficiency and energy consumption. *Proceedings of the ISEE 29th Annual Conference on Explosives and Blasting Technique*, vol. I. International Society of Explosives Engineers, Cleveland, OH. pp. 131–140. ◆

Advertisement Bookings
Barbara Spence · Avenue Advertising
PO Box 71308, Bryanston, 2021
Tel: 011 463 7940 · Cell: 082 881 3454
E-mail: barbara@avenue.co.za

SAIMM
THE SOUTHERN AFRICAN INSTITUTE OF MINING AND METALLURGY

SAIMM ADVERTISING MARKETING OPPORTUNITIES

- SAIMM Journal
- SAIMM Website and Newsletter
- YPC (Young Professionals Council) Handbook
- YIMM (Youth in Mining and Metallurgy) Magazine

The SAIMM offers businesses wanting to reach decision-makers, thought-leaders and key opinion-formers in the mining environment different opportunities and essential platforms to do so.

Include the SAIMM in your marketing plan if you want to get noticed, grow your market share and assure your existing client base that they are dealing with the right service provider.

The SAIMM's monthly, highly regarded Journal, website and various specialist magazines are distinctly differentiated from other available commercial mining publications, and online digital avenues.

The SAIMM offerings are essential for the mining industry, representing cutting-edge research and thinking that is a must for professionals in the minerals industry who are serious about their work portfolios. Our platforms are not diluted by advertorials or press-releases and our content is peer-reviewed and accredited by acknowledged authorities, specialists and industry experts.

'Content is king' and our content is 'must read'.

Attractive package deals across all platforms can be negotiated.

Fifth Floor, Minerals Council South Africa Building, 5 Hollard Street, Marshalltown 2107, South Africa
P O Box 61127, Marshalltown, 2107, South Africa
Tel: 27-11-834-1273/7, Fax 27-11-838-5923 or 833-8156
E-mail: journal@saimm.co.za, Website: http://www.saimm.co.za

NATIONAL & INTERNATIONAL ACTIVITIES

2018

14–17 October 2018 — **Furnace Tapping 2018 Conference**
Nombolo Mdhluli Conference Centre, Kruger National Park,
South Africa
Contact: Camielah Jardine
Tel: +27 11 834-1273/7
Fax: +27 11 838-5923/833-8156
E-mail: camielah@saimm.co.za
Website: http://www.saimm.co.za

24 October 2018 — **15th Annual Student Colloquium**
'*Mining and Metallurgy in a sustainable world*'
Johannesburg
Contact: Yolanda Ndimande
Tel: +27 11 834-1273/7
Fax: +27 11 838-5923/833-8156
E-mail: yolanda@saimm.co.za
Website: http://www.saimm.co.za

30 October 2018— **Cobalt Processing Short Course Hydrometallurgical Processing of Cobalt**
WorleyParsons, Melrose Arch, Johannesburg
Contact: Camielah Jardine
Tel: +27 11 834-1273/7
Fax: +27 11 838-5923/833-8156
E-mail: camielah@saimm.co.za
Website: http://www.saimm.co.za

28–30 November 2018 — **The SAIMM Zimbabwe Branch is proud to host Mining in Zimbabwe**
'*Expections and Opportunities*'
Sango Conference Centre, Cresta Hotel, Msasa, Harare
Contact: Yolanda Ndimande
Tel: +27 11 834-1273/7
Fax: +27 11 838-5923/833-8156
E-mail: yolanda@saimm.co.za
Website: http://www.saimm.co.za

11–13 December 2018 – **Mauritanides 2018 5th Mauritanian Mining, Oil & Gas Conference and Exhibition**
Nouakchott, Mauritania
Tel: +65 6717 6016
Fax: +65 6717 6015
Enquiry@spire-events.com

2019

11–13 March 2019— **7th Sulphur and Sulphuric Acid 2019 Conference**
Swakopmund Hotel, Swakopmund, Namibia
Contact: Camielah Jardine
Tel: +27 11 834-1273/7
Fax: +27 11 838-5923/833-8156
E-mail: camielah@saimm.co.za
Website: http://www.saimm.co.za

24–27 June 2019— **Ninth International Conference on Deep and High Stress Mining 2019 Conference**
Misty Hills Conference Centre, Muldersdrift, Johannesburg
Contact: Camielah Jardine
Tel: +27 11 834-1273/7
Fax: +27 11 838-5923/833-8156
E-mail: camielah@saimm.co.za
Website: http://www.saimm.co.za

5–7 August 2019 — **The Southern African Institute of Mining and Metallurgy in collaboration with the Zululand Branch is organising The Eleventh International Heavy Minerals Conference**
'*Renewed focus on Process and Optimization*'
The Vineyard, Cape Town, South Africa
Contact: Yolanda Ndimande
Tel: +27 11 834-1273/7
Fax: +27 11 838-5923/833-8156
E-mail: yolanda@saimm.co.za
Website: http://www.saimm.co.za

17–18 October 2019— **Tailing Storage Conference 2019**
'*Investing in a Sustainable Future*'
Johannesburg
Contact: Camielah Jardine
Tel: +27 11 834-1273/7
Fax: +27 11 838-5923/833-8156
E-mail: camielah@saimm.co.za
Website: http://www.saimm.co.za

13–15 November 2019 — **XIX International Coal Preparation Congress & Expo 2019**
New Delhi, India
Contact: Coal Preparation Society of India
Tel/Fax: +91-11-26136416, 4166 1820
E-mail: cpsidelhi. india@gmail.com, president@cpsi.org.
inrksachdevO1@gmail.com,
hi.sapru@monnetgroup.com

Company Affiliates

The following organizations have been admitted to the Institute as Company Affiliates

3M South Africa (Pty) Limited
AECOM SA (Pty) Ltd
AEL Mining Services Limited
Air Liquide (Pty) Ltd
Alexander Proudfoot Africa (Pty) Ltd
AMEC Foster Wheeler
AMIRA International Africa (Pty) Ltd
ANDRITZ Delkor(Pty) Ltd
Anglo Operations Proprietary Limited
Anglogold Ashanti Ltd
Arcus Gibb (Pty) Ltd
Atlas Copco Holdings South Africa (Pty) Limited
Aurecon South Africa (Pty) Ltd
Aveng Engineering
Aveng Mining Shafts and Underground
Axis House Pty Ltd
Bafokeng Rasimone Platinum Mine
Barloworld Equipment -Mining
BASF Holdings SA (Pty) Ltd
BCL Limited
Becker Mining (Pty) Ltd
BedRock Mining Support Pty Ltd
BHP Billiton Energy Coal SA Ltd
Blue Cube Systems (Pty) Ltd
Bluhm Burton Engineering Pty Ltd
Bouygues Travaux Publics
CDM Group
CGG Services SA
Coalmin Process Technologies CC
Concor Opencast Mining
Concor Technicrete
Council for Geoscience Library
CRONIMET Mining Processing SA Pty Ltd
CSIR Natural Resources and the Environment (NRE)
Data Mine SA
Department of Water Affairs and Forestry
Digby Wells and Associates
DMS Powders
DRA Mineral Projects (Pty) Ltd
DTP Mining - Bouygues Construction
Duraset
Elbroc Mining Products (Pty) Ltd
eThekwini Municipality
Expectra 2004 (Pty) Ltd
Exxaro Coal (Pty) Ltd
Exxaro Resources Limited
Filtaquip (Pty) Ltd
FLSmidth Minerals (Pty) Ltd
Fluor Daniel SA (Pty) Ltd
Franki Africa (Pty) Ltd-JHB
Fraser Alexander (Pty) Ltd
G H H Mining Machines (Pty) Ltd
Geobrugg Southern Africa (Pty) Ltd
Glencore
Hall Core Drilling (Pty) Ltd
Hatch (Pty) Ltd
Herrenknecht AG
HPE Hydro Power Equipment (Pty) Ltd
Immersive Technologies
IMS Engineering (Pty) Ltd
Ivanhoe Mines SA
Joy Global Inc.(Africa)
Kudumane Manganese Resources
Leco Africa (Pty) Limited
Longyear South Africa (Pty) Ltd
Lonmin Plc
Lull Storm Trading (Pty) Ltd
Maccaferri SA (Pty) Ltd
Magnetech (Pty) Ltd
MAGOTTEAUX (Pty) LTD
Maptek (Pty) Ltd
MBE Minerals SA Pty Ltd
MCC Contracts (Pty) Ltd
MD Mineral Technologies SA (Pty) Ltd
MDM Technical Africa (Pty) Ltd
Metalock Engineering RSA (Pty)Ltd
Metorex Limited
Metso Minerals (South Africa) Pty Ltd
Minerals Council of South Africa
Minerals Operations Executive (Pty) Ltd
MineRP Holding (Pty) Ltd
Mintek
MIP Process Technologies (Pty) Limited
Modular Mining Systems Africa (Pty) Ltd
MSA Group (Pty) Ltd
Multotec (Pty) Ltd
Murray and Roberts Cementation
Nalco Africa (Pty) Ltd
Namakwa Sands(Pty) Ltd
Ncamiso Trading (Pty) Ltd
New Concept Mining (Pty) Limited
Northam Platinum Ltd - Zondereinde
OPTRON (Pty) Ltd
PANalytical (Pty) Ltd
Paterson & Cooke Consulting Engineers (Pty) Ltd
Perkinelmer
Polysius A Division Of Thyssenkrupp Industrial Sol
Precious Metals Refiners
Rand Refinery Limited
Redpath Mining (South Africa) (Pty) Ltd
Rocbolt Technologies
Rosond (Pty) Ltd
Royal Bafokeng Platinum
Roytec Global (Pty) Ltd
RungePincockMinarco Limited
Rustenburg Platinum Mines Limited
Salene Mining (Pty) Ltd
Sandvik Mining and Construction Delmas (Pty) Ltd
Sandvik Mining and Construction RSA(Pty) Ltd
SANIRE
Schauenburg (Pty) Ltd
Sebilo Resources (Pty) Ltd
SENET (Pty) Ltd
Senmin International (Pty) Ltd
Smec South Africa
Sound Mining Solution (Pty) Ltd
SRK Consulting SA (Pty) Ltd
Technology Innovation Agency
Time Mining and Processing (Pty) Ltd
Timrite Pty Ltd
Tomra (Pty) Ltd
Ukwazi Mining Solutions (Pty) Ltd
Umgeni Water
Webber Wentzel
Weir Minerals Africa
Worley Parsons RSA (Pty) Ltd

DEEP MINING 2019 CONFERENCE

NINTH INTERNATIONAL CONFERENCE ON DEEP AND HIGH STRESS MINING 2019

24–25 JUNE 2019 - CONFERENCE

26 JUNE 2019 - SANIRE SYMPOSIUM

27 JUNE 2019 - TECHNICAL VISIT

MISTY HILLS CONFERENCE CENTRE, MULDERSDRIFT, JOHANNESBURG, SOUTH AFRICA

BACKGROUND

The Ninth International Conference on Deep and High Stress Mining (Deep Mining 2019) will be held at the Misty Hills Conference Centre, Muldersdrift, Johannesburg on 24 and 25 June 2019. Conferences in this series have previously been hosted in Australia, South Africa, Canada, and Chile. Around the world, mines are getting deeper and the challenges of stress damage, squeezing ground, and rockbursts are ever-present and increasing. Mining methods and support systems have evolved slowly to improve the management of excavation damage and safety of personnel, but damage still occurs and personnel are injured. Techniques for modelling and monitoring have been adapted and enhanced to help us understand rock mass behaviour under high stress. Many efficacious dynamic support products have been developed, but our understanding of the demand and capacity of support systems remains uncertain.

OBJECTIVE

To create an international forum for discussing the challenges associated with deep and high stress mining and to present advances in technology.

WHO SHOULD ATTEND

- Rock engineering practitioners
- Mining engineers
- Researchers
- Academics
- Geotechnical engineers
- Hydraulic fracturing engineers
- High stress mining engineers
- Waste repository engineers
- Rock engineers
- Petroleum engineers
- Tunnelling engineers

For further information contact:

Camielah Jardine, Head of Conferencing, SAIMM, Tel: +27 11 834-1273/7, Fax: +27 11 833-8156 or +27 11 838-5923
E-mail: camielah@saimm.co.za, Website: http://www.saimm.co.za

SAIMM THE SOUTHERN AFRICAN INSTITUTE OF MINING AND METALLURGY

SANIRE SOUTH AFRICAN NATIONAL INSTITUTE OF ROCK ENGINEERING

ACG AUSTRALIAN CENTRE FOR GEOMECHANICS

CSIRO | The University of Western Australia | Joint Venture

Resilient futures for mineral processing

We would like to invite you to attend the XXX International Mineral Processing Congress in Cape Town, South Africa from 18 to 22 October 2020.

IMPC 2020 will be hosted by the Southern African Institute of Mining and Metallurgy (SAIMM).

IMPC2020

XXX INTERNATIONAL MINERAL PROCESSING CONGRESS
18 - 22 OCTOBER CAPE TOWN SOUTH AFRICA

www.impc2020.com

IMPC
INTERNATIONAL MINERAL PROCESSING COUNCIL

SAIMM
THE SOUTHERN AFRICAN INSTITUTE OF MINING AND METALLURGY

THE SAIMM

IMPC 2020 will be hosted by the Southern African Institute of Mining and Metallurgy (SAIMM). The SAIMM has been in existence for 125 years, having been established in 1894 as a 'learned society' to support mining and metallurgical professionals during the emergence and growth of the early South African minerals industry.

Mining is of great importance to Africa in general, and particularly to Southern Africa. Africa accounts for a major portion of the world's mineral reserves and more than half of gold, platinum group metals, cobalt and diamonds. Southern Africa produces over two-thirds of Africa's mineral exports by value.

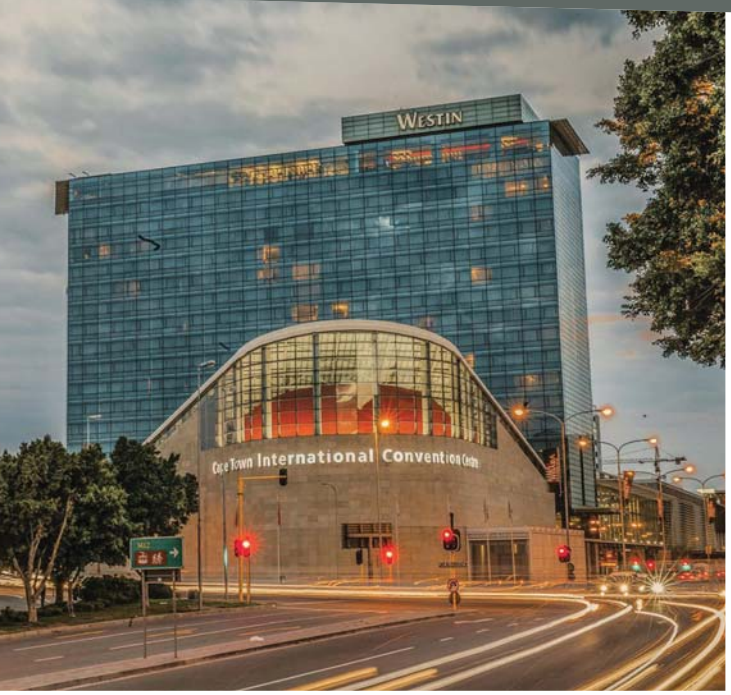

Photo courtesy CTICC

CAPE TOWN INTERNATIONAL CONVENTION SQUARE
1 LOWER LONG STREET
CAPE TOWN 8001

CAPE TOWN INTERNATIONAL CONVENTION CENTRE

IMPC 2020 will be hosted at Cape Town International Convention Centre (CTICC). Since the inception of the CTICC in 2003, Cape Town has been proudly the number one destination for conferences in Africa, according to the latest International Congress and Convention Association (ICCA) statistics.

Cape Town, the "Mother City", is the oldest city in South Africa and has a cultural heritage spanning more than 300 years. Cape Town is a modern, cosmopolitan city and is often rated as one of the premier world holiday destinations. The city has a large range of hotels & guest houses and modern transport infrastructure. The city has numerous activities & attractions, including Table Mountain, Robben Island, Cape Point, the Castle, V&A Waterfront, world class beaches, wine farms, nature reserves, scenic drives, hiking, whale watching, shark cage diving and fine dining.